The Institute for Solid State Physics
The University of Tokyo

Activity Report 2024

ISSP
Activity Report
2024

Contents

Preface

We are pleased to share the Annual Activity Report of the Institute for Solid State Physics (ISSP) for the 2024 academic year. ISSP, established in 1957 and affiliated with the University of Tokyo, functions as a joint usage/research center. Since its founding, ISSP has consistently contributed to the advancement of condensed matter physics and materials science through fundamental scientific and technological research.

This report highlights a broad range of research achievements by ISSP members, as well as by external researchers who participated in our joint research programs.

- The first section presents 30 research highlights from ISSP internal research groups.
- The second section features 13 highlights from joint research conducted by external researchers, supported by ISSP members through the joint-use program.
- The third section outlines developments of the following facilities: Supercomputer Center, Neutron Science Laboratory, International MegaGauss Science Laboratory, Center of Computational Materials Science, Laser and Synchrotron Research Center, and Synchrotron Radiation Laboratory.
- The fourth section provides overviews of the 15 conferences and workshops hosted by ISSP in 2024.
- The report concludes with listings of joint-use research subjects and publications.

These activities reflect ISSP's continued role as a global center of excellence in condensed matter physics and materials science. We are sincerely grateful for the ongoing support and collaboration of the research community, which enables us to sustain and further develop our activities.

October 2025
HIROI Zenji
Director of the Institute for Solid State Physics
The University of Tokyo

Research Highlights

Construction of a 3D Dirac Semimetal by Stacking 2D Massless Dirac Fermion Layers

Osada Group

Dirac and Weyl semimetals are three-dimensional (3D) topological semimetals in which the conduction and valence bands touch at nodal points with a linear dispersion in the 3D Brillouin zone (BZ). They exhibit characteristic magnetotransport phenomena, negative longitudinal magnetoresistance and a planar Hall effect, resulting from the chiral anomaly. Recently, a layered organic conductor, α-$(ET)_2I_3$, exhibited these phenomena at low temperatures, indicating that it is a 3D Dirac or Weyl semimetal [1]. However, it is well established that each ET layer of α-$(ET)_2I_3$ is a two-dimensional (2D) massless Dirac fermion system, where the conduction and valence bands touch at two nodes in the 2D BZ. Therefore, the question is whether and how 3D Dirac or Weyl semimetals can be formed by stacking 2D massless Dirac fermion layers.

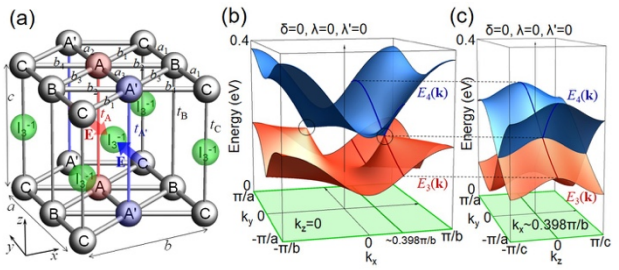

Fig. 1. (a) Schematic structure of α-$(ET)_2I_3$ or α-$(BETS)_2I_3$. (b) In-plane dispersion at $k_z = 0$ and (c) interlayer dispersion at an in-plane Dirac point in α-$(ET)_2I_3$ with no SOC.

Because the α-$(ET)_2I_3$ crystal has space inversion symmetry (SIS) and time reversal symmetry (TRS), the stacking must preserve these symmetries. Under SIS and TRS, the Weyl semimetal is never allowed, but the Dirac semimetal can be allowed because the total Berry curvature of the spin-degenerate bands is cancelled out. However, when simple interlayer hopping is introduced into the electronic structure model without breaking the SIS and TRS, the system usually becomes a 3D nodal-line semimetal, where 2D nodal points form nodal lines along the stacking direction in the 3D BZ. To realize a Dirac semimetal, we must consider spin–orbit coupling (SOC) in interlayer hopping [2]. In the α-$(ET)_2I_3$ crystal, the ET conduction layer and the I_3^- anion layer are alternately stacked. Electrons hopping from one ET layer to the neighboring ET layer must penetrate the I_3^- layer, and the I_3^- configuration is unsymmetrical around some hopping paths. In fact, the I_3^- ion is located on one side of the interlayer hopping path between the A (or A') sites of the neighboring layers and imposes a strong potential gradient on the hopping electrons, resulting in SOC. Note that SOC is relatively strong in interlayer hopping; however, it is generally considered weak in the ET layers because the ET molecule consists of light atoms. This interlayer SOC reflecting the I_3^- configuration opens a gap along the nodal line in the interlayer k_z-dispersion, leaving two Dirac points at $k_z = 0$ and π/c. Therefore, the interlayer SOC arising from the anion potential can realize the Dirac semimetal state while maintaining the SIS and TRS [2]. If the SIS is broken by the introduction of interlayer hopping, each band exhibits zero-field spin splitting, and the Weyl semimetal state, where spin degeneracy is lifted, arises instead of the Dirac semimetal state. Especially, in the case with broken SIS and no SOC, the two Weyl points with the same chirality and opposite spin degenerate, resulting in the spinless Weyl semimetal [3].

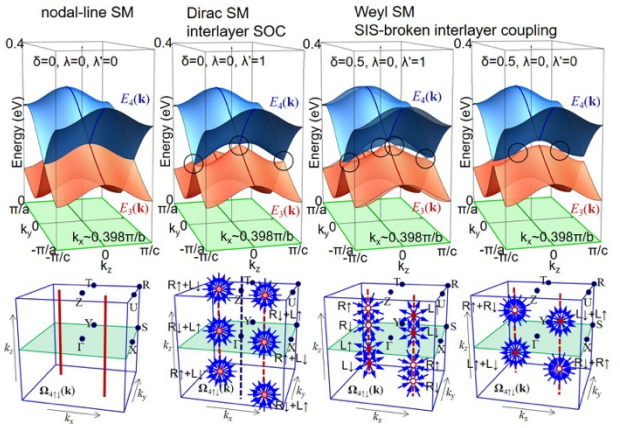

Fig. 2. (upper panels) Interlayer dispersion in the nodal-line, Dirac, Weyl, spinless Weyl semimetal states in α-$(ET)_2I_3$. (lower panels) Berry curvature configuration in the 3D BZ corresponding to each semimetal state.

In contrast to α-$(ET)_2I_3$, an iso-structural compound α-$(BETS)_2I_3$, which has non-negligible in-plane SOC, is usually considered as a 2D topological insulator (TI). When the interlayer coupling is introduced into this 2D TI, the system is expected to become a 3D weak TI with surface states only on the side surfaces. However, the surface transport over the whole surface, which is specific for 3D strong TIs, has been experimentally observed in α-$(BETS)_2I_3$ at low temperatures [4]. On the other hand, it is found that α-$(BETS)_2I_3$ still remains a weak TI under SIS [2]. The 3D strong TI state in α-$(BETS)_2I_3$ could be realized by some topological transition accompanied by the symmetry breaking which is possibly caused by electron correlation effect.

References

[1] N. Tajima, Y. Kawasugi, T. Morinari, R. Oka, T. Naito, and R. Kato, J. Phys. Soc. Jpn. **92**, 123702 (2023).
[2] T. Osada, J. Phys. Soc. Jpn. **93**, 123703 (2024).
[3] T. Osada, JPS Hot Topics **5**, 003 (2025).
[4] T. Nomoto, S. Imajo, H. Akutsu, Y. Nakazawa, and Y. Kohama, Nat. Commun. **14**, 2130 (2023).

Author

T. Osada

Orbital Hybridization of Donor and Acceptor to Enhance the Conductivity of Mixed-stack Organic Complexes

Mori and Yoshimi Groups

Despite the accumulation of abundant knowledge through structure-property correlation studies, research on organic conductors is still in the basic research stage, and there is a gap between basic research and device research. This is because organic conducting single crystals are considered to have poor solution processability and are unsuitable for large-scale synthesis. As a next-generation material that could bridge this gap, there is growing interest in charge-transfer complexes formed by electron-rich donor molecules and electron-deficient acceptor molecules. Charge-transfer complexes are classified into "mixed-stack type", where donors and acceptors are mixed-stacked, and "separated-layer type", where donor layer and acceptor sheet are alternately stacked. In separated-layer-type complexes, complexes exhibiting high conductivity, including metallic states, have been identified. However, it has been generally accepted that mixed-stack-type charge-transfer complexes, which are relatively easier to obtain, exhibit little electrical conductivity. This low conductivity was caused by the charge transfer quantity δ, which indicates the amount of electrons transferred from the donor to the acceptor, is in the neutral region (0 – 0.4) or the ionic region (δ > 0.75) (Fig. 1b), resulting in few effective carriers involved in charge transport. While there had been expectations that synthesizing charge-transfer complexes in the neutral-ionic boundary region could enhance electrical conductivity, such complexes remained elusive for decades.

Our research group has recently developed an oligomer model of doped poly(3,4-ethylenedioxythiophene) (PEDOT) as an electron-rich donor molecule [1–3]. We have found that the shortest dimer (2O, Fig. 1a) [1] and its oxygen/sulfur atom substituted derivatives (2S, Fig. 1a)

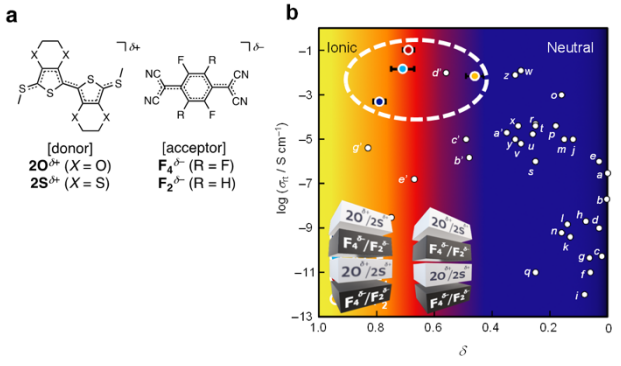

Fig. 1. The structures of donors, developed in this study, and acceptors, and room temperature conductivity vs. charge transfer quantity of the one-dimensional single crystals of the mixed-stack charge transfer complexes. Our developed high-conductive complexes are surrounded by the dotted circle.

possess an ideal electronic structure for constructing neutral-ionic boundary region complexes with electron-deficient fluorine-substituted tetracyanoquinodimethane derivatives (F4 and F2, Fig. 1a). To realize such a boundary region, it is expected that a small energy difference between the donor's highest occupied molecular orbital (HOMO) and the acceptor's lowest unoccupied molecular orbital (LUMO) is essential, and the combination of 2O/2S donors and F4/F2 acceptors well satisfies these conditions. Furthermore, the symmetry of the molecular orbital structure after charge transfer is also well matched, and it is expected that a highly conductive carrier conduction pathway with strong hybridization between the two orbitals can be realized.

By focusing on the molecular orbitals of the donor and acceptor in the design, we successfully enhanced the conductivity of the mixed-stack charge transfer complexes and achieved the highest room-temperature conductivity (σ_{RT}) in a one-dimensional single crystal as shown in the dotted surrounding circle in Fig. 1b: σ_{RT} [2S-F4, 0.10 Scm, δ = 0.69(2)] > σ_{RT} [2O-F2, 1.4×10^{-2} Scm, δ = 0.71(4)] > σ_{RT} [2S-F2, 6.9×10^{-3} Scm, δ = 0.46(3)] > σ_{RT} [2O-F4, 4.9×10^{-4} Scm, δ = 0.79(2)]. These mixed-stack charge-transfer complexes are scalable for large-scale synthesis, exhibit high solubility in organic solvents, and remain stable for extended periods without decomposition in solution, thereby demonstrating significant potential as a coating-type conductive material. It holds great promise as next-generation organic conducting materials.

References

[1] R. Kameyama *et al.*, Chemistry - A Euro. J. **27**, 6696 (2021).
[2] K. Onozuka *et al.*, J. Am. Chem. Soc. **145 (28)**, 15152 (2023).
[3] T. Fujino *et al.*, Faraday Discuss. **250**, 348 (2024).
[4] T. Fujino *et al.*, Nat. Commun. **15**, 3028 (2024).

Authors

T. Fujino, R. Kameyama, K. Onozuka, K. Matsuo, S. Dekura, T. Miyamoto, Z. Guo[a], H. Okamoto[a], T. Nakamura[b], K. Yoshimi, S. Kitou[a], T. Arima[a,c], H. Sato[d], K. Yamamoto[e], A. Takahashi[f], H. Sawa[g], Y. Nakamura[h], and H. Mori
[a]Department of Advanced Materials Science, The University of Tokyo
[b]Institute for Molecular Science
[c]RIKEN Center for Emergent Matter Science (CEMS)
[d]Rigaku Corporation
[e]Okayama University of Science
[f]Nagoya Institute of Technology
[g]Nagoya University
[h]Japan Synchrotron Radiation Research Institute (JASRI), SPring-8

Studies of Axion Insulator Candidate $EuIn_2As_2$ by NMR and Ca-doping

Yamashita Group

Magnetic topological materials provide a unique playground for exploring exotic quantum phenomena in condensed matter physics, such as the axion insulator state and the quantum anomalous Hall effect. The rare-earth Zintl compound $EuIn_2As_2$, in which topological InAs layers are sandwiched by magnetic Eu layers, is recently pointed out to be an intrinsic magnetic topological insulator by first-principles calculations. However, although the emergence of this topological state depends on the magnetic structure of Eu layers, the details of the magnetic states remain controversial.

To clarify the magnetic structure, we investigate the magnetic state of $EuIn_2As_2$ by using NMR measurements [1]. Our ^{75}As NMR measurements reveal that an incommensurate magnetic state with a non-uniform semi-circle fan structure appears by applying an in-plane magnetic field. In addition, the reorientation process in the ordered moments under the external field, in which more spins are concentrated in the direction perpendicular to the applied field, is observed as an increase of the NMR intensity. On the other hand, the magnetic structure smoothly transforms to the forced ferromagnetic state when the magnetic field is applied perpendicular to the plane. These results indicate that an incommensurate magnetic structure weakly pinned in the crystal axes appears in this compound. We conclude that a fine control of the magnetic structure by applying a chemical or physical pressure is required to realize the topological states found by the first-principles calculations.

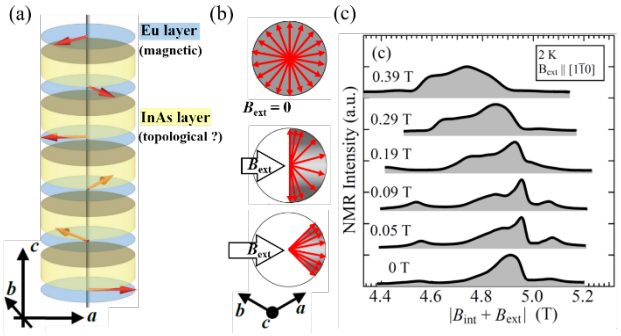

Fig. 1. (a) Illustration of the magnetic structure of Eu (red arrows) in $EuIn_2As_2$. (b) Distribution of Eu moment in the a-b plane as a function of the external field (B_{ext}). (c) ^{75}As NMR spectra at different external fields.

Furthermore, we try the carrier doping of this compound. Actually, previous transport and angle-resolved photoemission spectroscopy measurements have shown that $EuIn_2As_2$ is highly hole doped, which is needed to be compensated to realize the axion insulator nature. Chemical doping has been attempted to compensate the hole carrier, which is, however, often accompanied by unintended changes in the magnetic property. For example, P-doping in $EuIn_2As_2$ changes the AFM order into a spin glass state, as well as the disappearance of the Néel peak in the temperature dependence of the magnetic susceptibility.

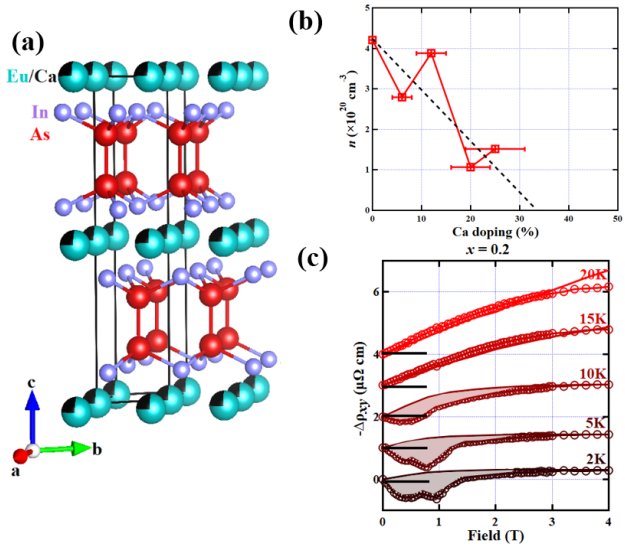

Fig. 2. (a) Schematic crystal structure of Ca-doped $(Eu_{1-x}Ca_x)In_2As_2$ (b) The doping dependence of the carrier density. (c) The magnetic field dependence of the anomalous Hall component at $x = 0.2$. The topological Hall components are marked by the gray shaded regions.

To tune the Fermi level, we dope Ca ions to Eu sites of $EuIn_2As_2$ and characterize electronic state by transport measurements [2]. Unexpectedly, we find that the hole carrier is decreased by the isovalent Ca doping due to a slight increase of the valence charge of the Ca ions, giving rise to an effective electron doping. We further find that, although the magnetic transition temperature decreases with increasing the Ca ions, both the temperature dependence of the magnetic susceptibility and the topological Hall effect are observed in all the Ca-doped samples as observed in our previous measurements done in the pristine $EuIn_2As_2$ [3], suggesting that the AFM magnetic structure remains almost the same. Our results indicate that non-magnetic Ca doping can modify the band structure without largely changing the magnetic ground state of $EuIn_2As_2$, providing an opportunity to realize the axion insulating state by only tuning the carrier density.

References

[1] H. Takeda *et al.*, npj Quantum Materials **9**, 67 (2024).
[2] J. Yan *et al.*, Phys. Rev. B **110**, 115111 (2024).
[3] J. Yan *et al.*, Phys. Rev. Research **4**, 013163 (2022).

Authors

H. Takeda, J. Yan, J. Si[a], Z. Jiang[b], H. Ma, Y. Uwatoko, B.-T. Wang[b], X. Luo[b], Y. Sun[b], and M. Yamashita
[a]Songshan Lake Materials Laboratory
[b]Chinese Academy of Sciences

Magnon Thermal Hall Effect on the Antiferromagnetic Skyrmion Lattice

Yamashita Group

Recently, transport phenomena involving quantum quasiparticles other than electrons have attracted significant interest in both fundamental and applied sciences. A prominent example is the magnon, a magnetic quasiparticle that propagates through magnetic insulators and carries heat and spin without electric charge. Due to their charge neutrality, magnons do not experience the Lorentz force and typically do not exhibit transverse transport under an external magnetic field, i.e., the thermal Hall effect in conventional insulators. However, when certain conditions are satisfied in the spin interactions or magnetic structure of a material, an emergent gauge field—a fictitious magnetic field—can arise and induce a magnon thermal Hall effect. This phenomenon has been interpreted in terms of emergent U(1) gauge fields, which can give rise to a nonzero thermal Hall conduction in materials with corner-sharing lattice geometries such as kagome and pyrochlore lattices. In contrast, for edge-sharing lattices such as square or triangular lattices, a so-called "no-go theorem" predicts the strict cancellation of the Hall conduction due to the commutative nature of the U(1) gauge field. As a result, magnon thermal Hall effects in edge-sharing lattices have long been considered unlikely, with rare exceptions such as our previous work [1] done in the ferromagnetic skyrmion lattice in GaV_4Se_8.

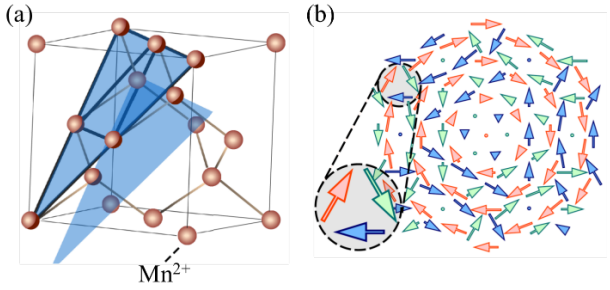

Fig. 1. (a) Diamond lattice formed by Mn^{2+} ions in $MnSc_2S_4$. The two (111) planes marked in blue include Mn^{2+} ions belonging to different sublattice of the bipartite diamond structure. (b) Schematic figure of the AFM-SkL state in $MnSc_2S_4$ viewed along [111] direction.

In this study [2], we have demonstrated that the spinel compound $MnSc_2S_4$, in which Mn atoms form a diamond lattice (Fig. 1(a)), exhibits a magnon-induced thermal Hall effect. This material undergoes antiferromagnetic ordering below approximately 2.3 K and, under magnetic fields of about 4–6 T, enters a novel magnetic phase known as an antiferromagnetic skyrmion lattice (AFM-SkL) composed of three interpenetrating sublattices (Fig. 1(b)). Each sublattice hosts a ferromagnetic skyrmion lattice, and collectively they form a 120° antiferromagnetic configuration. Thermal transport measurements reveal a sharp increase in the thermal Hall conductivity by magnons within the AFM-SkL phase region, followed by a gradual decrease while retaining a positive value above 8 T (Fig. 2).

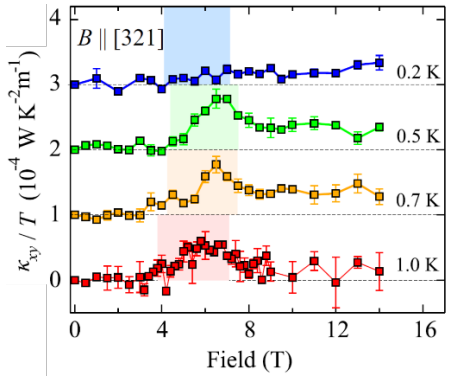

Fig. 2. Field dependence of thermal Hall conductivity divided by temperature κ_{xy}/T in the magnetically ordered phases. The shaded area represents the AFM-SkL phase.

This experimental result goes beyond conventional understanding based on U(1) gauge fields, which cannot account for a finite Hall conductivity in edge-sharing lattices. Theoretical analysis based on the spin texture of the AFM-SkL reveals that an emergent SU(3) gauge field arises from the system. The three U(1) gauge fields associated with each sublattice couple via off-diagonal spin interactions and form a non-Abelian SU(3) gauge structure. The non-commutativity of SU(3) enables a net emergent magnetic flux that does not cancel out, allowing a finite magnon thermal Hall effect even in edge-sharing lattices. This work presents the first experimental signature of an emergent SU(3) gauge field in a solid-state system and highlights how the topological nature of magnetic order can fundamentally alter magnon transport, paving the way for new functional properties in quantum magnetic materials.

References

[1] M. Akazawa *et al.*, Phys. Rev. Research **4**, 043085 (2022).
[2] H. Takeda *et al.*, Nature Commun. **15**, 566 (2024).

Authors

H. Takeda, M. Kawano[a], K. Tamura, M. Akazawa, J. Yan, T. Waki[b], H. Nakamura[b], K. Sato[c], Y. Narumi[c], M. Hagiwara[c], M. Yamashita, and C. Hotta[d]
[a]Department of Physics, Technical University of Munich
[b]Department of Materials Science and Engineering, Kyoto University
[c]Center for Advanced High Magnetic Field Science, Graduate School of Science, Osaka University
[d]Department of Basic Science, University of Tokyo

Shot Noise in Nonequilibrium Spin Dynamics Excited by Pulsed Light

Kato Group

The flow of carriers following Poissonian statistics generates current fluctuations called shot noise. The electronic shot noise is utilized to determine an effective charge in electronic transport. Similarly, the study of spin shot noise is expected to provide insight into the nature of the elementary unit of angular momentum quanta $\hbar$, and to provide information on fundamental spin transport properties [1,2]. However, spin shot noise has not yet been observed experimentally, since it is difficult to detect physically meaningful noise by separating from other noises in the method proposed in the theoretical studies [1,2].

In our study [3], we propose an all-optical approach to detect spin shot noise. The key idea is to use an ultrafast pump laser pulse to impulsively drive the uniform magnetization of a ferromagnet far from equilibrium, as shown in Fig. 1(a). To model this experimental situation, we theoretically calculate the magnon population dynamics using the Lindblad equation and the Fokker-Planck equation, considering the function of the spin component (see Fig. 1(b)). We analyze the time derivative of the autocorrelation function, which mimics the fluctuation of the spin flow, i.e., the spin current. Furthermore, we define the Fano factor as the ratio between the nonequilibrium spin current flowing out of the spin system and its nonequilibrium fluctuation.

We show the calculated temperature dependence of the Fano factor under the magnetic field of 3 T in Fig. 1(c). At low temperatures ($k_B T \ll \hbar\omega_0$, ω_0: the Larmor frequency), only the energy relaxation process predominates, resulting in the Fano factor becoming $\hbar$. Through an intuitive discussion grounded in the Poisson process, this outcome signifies the transfer of angular momentum from the spin system to the bath in units of $\hbar$. The conditions required for this experiment, —low temperature (<1 K) and high magnetic field (~3 T)—, are experimentally feasible. It is worth noting that a similar rationale has been applied in determining the unit of charge in electronic transport, derived from nonequilibrium current noise (shot noise). As the temperature increases, the energy gain process also becomes significant. Consequently, the presence of two distinct transition processes diminishes the average spin flow, although it contributes additively to its fluctuation, leading to the increase of the Fano factor with increasing temperature.

Finally, we outline a feasible experimental protocol to observe the Fano factor. We propose using a thin film of ferromagnetic permalloy as the sample. Ultrafast dynamics of the z-component of the sample's magnetization, $S_z(t)$, is measured following laser pulse irradiation (see Fig. 1(b)), employing time-resolved magneto-optical Kerr effect measurements. We can deduce the ensemble average of the spin flow from the time derivative of the average across trials of the magnetization dynamics measurements, i.e., $d\langle S_z(t)\rangle/dt$. Then, the correlation function $C(t',t)$ is obtained by calculating the covariance of S_z at different times, that is, $\langle S_z(t')S_z(t)\rangle$. From a cusp in $C(t',t)$ along the line $t'=t$, we can obtain the Fano factor, combining the time derivative of the mean magnetization value.

In summary, we investigated the nonequilibrium fluctuation arising from the ferromagnetic magnetization under pulse irradiation. We calculated the Fano factor, which is defined as the ratio between the nonequilibrium spin current flowing out of the spin system and its nonequilibrium fluctuation and observed that the Fano factor measured at low temperature offers insight into the unit of angular momentum transferred per spin relaxation process in a bulk ferromagnet. Our proposal sets the stage for nonequilibrium spin-noise spectroscopy, offering an advanced technique to access information that is inaccessible by other experimental means.

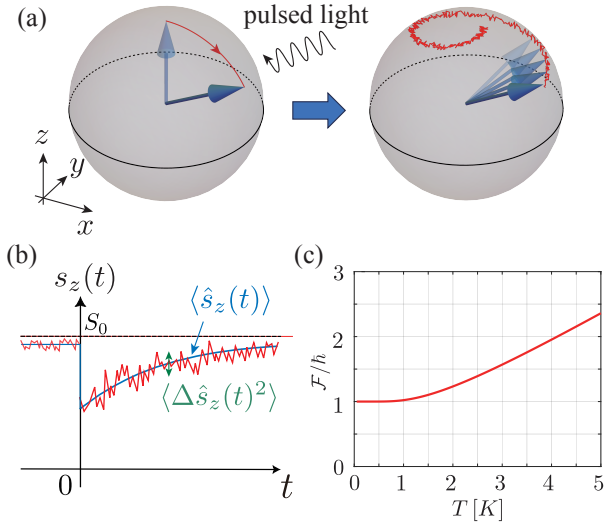

Fig. 1. (a) A schematic picture for the spin dynamics in our setup. Initially, the spin is in thermal equilibrium and distributed centering on the z axis. After the pulsed light excites the spin of the ferromagnet at $t=0$, the spin precession occurs accompanying the nonequilibrium fluctuation. (b) A schematic picture of the time evolution of S_z. The red line indicates one measurement of the time evolution of S_z. While the ensemble average with respect to a number of measurements, $\langle S_z(t)\rangle$, (the blue line) decays toward the saturated value, S_0. (c) The Fano factor F is plotted as a function of temperature. At low temperatures, the Fano factor approaches $\hbar$.

References

[1] A. Kamra and W. Belzig, Phys. Rev. Lett. **116**, 146601 (2016).
[2] M. Matsuo, Y. Ohnuma, T. Kato, and S. Maekawa, Phys. Rev. Lett. **120**, 037201 (2018).
[3] T. Sato, S. Watanabe, M. Matsuo, and T. Kato, Phys. Rev. Lett. **134**, 106702 (2025).

Authors

T. Sato, S. Watanabe[a], M. Matsuo[b], and T. Kato
[a]Keio University,
[b]University of Chinese Academy of Sciences

In situ Nanoscale Transport Measurements at Low Temperature

Hasegawa Group

Understanding electron transport in materials is key to investigating their electronic properties. However, most of the transport measurements have been performed at macroscopic scales, and thus the development of microscopic methods to measure transport is pivotal. Scanning tunneling potentiometry (STP), based on scanning tunneling microscopy (STM), reveals transport properties in nanometer spatial resolution as schematically shown in Fig. 1.

Our group has been developing STP [1,2], which enables us to visualize spatial variation of electrochemical potential across a sample surface. Assuming constant current density, the gradient of the electrochemical potential corresponds to resistance. Combined with STM, one can correlate potential features to atomic-scale surface structures and local density of states.

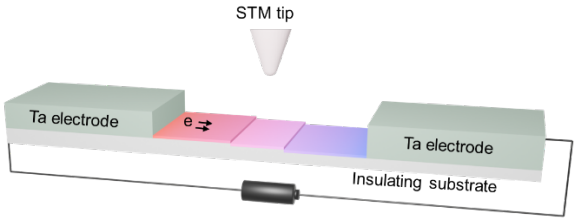

Fig. 1. Schematic of STP measurements.

Until now, STP measurements have been mostly limited to room temperature. However, many intriguing physical phenomena, such as superconductivity and electron localization, emerge only at low temperatures. Recently, we have successfully developed an STP system that operates at low temperatures (LT-STP) by optimizing all setups for the low temperature system [3, 4].

Figures 2(a) and (b) show the topographic image and the corresponding STP image taken at low temperatures, respectively. The images are obtained on a monolayer Pb film formed on a Si(111) substrate. The coverage is approximately 1.3 monolayers (1.3 Pb atoms per 1 Si unit cell). Since we performed the sample fabrication and measurements in the same chamber, we obtained extremely clean surfaces. Figure 2(c) shows the cross-sectional profiles taken along the blue and red dashed lines in Fig. 2(a) and (b), respectively. We found that the STP signal has no abrupt change at the step (indicated by the black arrow), indicating that electric current flows smoothly across atomic steps [3].

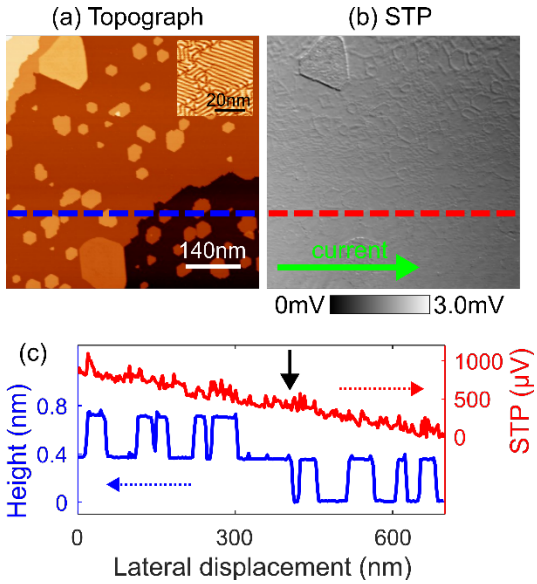

Fig. 2. (a) Topographic image of 1.3 monolayers Pb films on Si(111). The inset shows the zoomed image. (b) Corresponding potential image during current flow from left to right. (c) Cross-sectional profiles taken along the blue and red dashed lines in (a) and (b), respectively.

On the other hand, our further experiments revealed that by reducing the coverage to 1.0 monolayers, the steps act as a barrier to the transport [4]. Our findings suggest that the small difference of the coverage and structures affect their transport properties. They also open new possibilities for studying quantum effects in clean, low-temperature environments.

References

[1] M. Hamada and Y. Hasegawa, Jpn. J. Appl. Phys. **51** 125202 (2012).
[2] M. Hamada and Y. Hasegawa, Phys. Rev. B **99**, 125402 (2019).
[3] M. Hamada, M. Haze, J. Okazaki, and Y. Hasegawa, Phys. Rev. Applied **23**, 064051 (2025).
[4] M. Haze, J. Okazaki, M. Hamada, and Y. Hasegawa, submitted to Appl. Surf. Sci.

Authors

M. Haze M. Hamada, J. Okazaki, and Y. Hasegawa

CO Oxidation and CO_2 Desorption Dynamics on Pt(111) by van der Waals DFT Calculations

Yoshinobu and Sugino Groups

Heterogeneous catalysis is a key technology in modern society. To develop new catalysts, it is essential to understand chemical reactions on catalyst surfaces. Researchers have studied these interactions extensively using both experiments and theory. Among theoretical methods, density functional theory (DFT) is a powerful tool for analyzing how molecules adsorb on metal surfaces, including their structures and energies.

In the field of chemical reaction on catalysts, the role of the dispersion forces in adsorption on metal surfaces is important. The dispersion forces arise from fluctuating dipole moments of atoms and molecules, yielding the long-range attractive force of the van der Waals (vdW) interaction. The fluctuations are taken into account in the new type of the correlation functionals called van der Waals functional. Recently, the augmentation of the generalized gradient approximation (GGA) with the vdW functional (vdW correction) was found to be essential not only for physisorbed systems but also for chemisorbed molecules. In addition, ab initio molecular dynamics (AIMD) simulation enables tracking catalytic reactions on the femtosecond scale using quantum mechanical mechanics. While this method can reveal detailed reaction mechanisms and dynamics, its accuracy depends heavily on the choice of functionals. Therefore, selecting suitable functionals is increasingly important for modeling specific catalytic processes accurately.

Here, we investigated the CO oxidation and CO_2 desorption processes on Pt(111) through density functional theory (DFT) calculations employing three different exchange-correlation functionals, namely PBE, vdW-DF, and optB86b-vdW. AIMD simulation was performed to elucidate the desorption dynamics of CO_2 on Pt(111). The oxidation reaction of CO on Pt surfaces is a prototype catalytic reaction and has long been investigated both experimentally and theoretically. When the CO+O on the Pt(111) surface is heated to 200–350 K, these adsorbates are associated to desorb as β_1, β_2, and β_3 CO_2 states [1]. For the desorbed CO_2 molecules, the dynamic properties including kinetic energy, angular distribution, and vibrational states have been investigated [2-5]; a hyperthermal velocity distribution and a narrow desorption angular distribution has been reported and they are assigned to the formation and desorption of CO_2 from the Pt(111) terrace [5]. However, the previous DFT calculation could not correctly reproduce the experimental results including the kinetic energy of CO_2 (0.38 eV) and $\cos^8\theta$ desorption angular distribution [5], probably because their functional did not include the vdW corrections. Since the vdW correction is necessary for correctly calculating the adsorption energy of CO_2 on the Pt(111) surface, it would be crucial for a deeper understanding of the CO oxidation kinetics and dynamics on the Pt(111) surface.

Our calculated potential energy surfaces [7] indicate that the kinetically favorable pathway for the CO oxidation is the hexagonal close packed (HCP) pathway, where the oxidation is initiated by the movement of an O atom at the HCP site toward an adsorbed CO at the on-top site (Fig. 1).

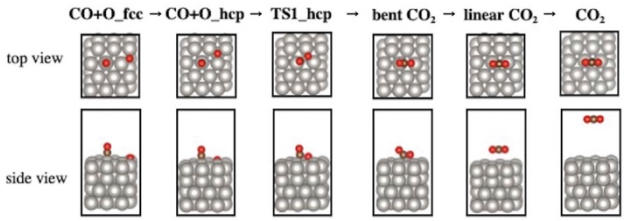

Fig. 1. The HCP pathway of CO oxidation on Pt(111).

The present AIMD simulation [7] has also revealed that "vdw-DF" functional, provides the most quantitative explanation of the experimental results regarding the distribution of the kinetic energy, the sharp desorption angle, and the OCO bending vibration of the desorbed CO_2. The good agreement is the result of an accurate description of the reactant (CO + O) and product (CO_2) in both the chemisorbed and physisorbed states on Pt(111). The present AIMD simulation also clearly shows that the CO_2 is desorbed in vibrationally excited states with the energy transfer between the bending and symmetric stretching modes (Fermi resonance).

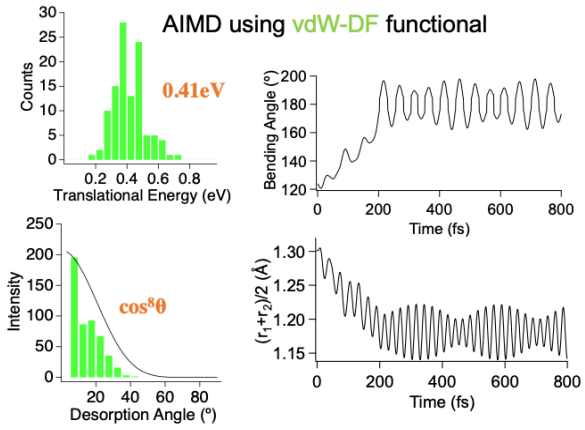

Fig. 2. Results from AIMD of the HCP pathway for the distributions of translational energy and desorption angle. and the time-evolutions of bending angle and symmetric stretching mode of CO_2 desorbed from Pt(111).

References

[1] J. Yoshinobu and M. Kawai, J. Chem. Phys. **103**, 3220 (1995).
[2] T. Matsushima, Surf. Sci. **127**, 403 (1983).
[3] K. H. Allers *et al.*, J. Chem. Phys. **100**, 3985 (1994).
[4] K. Nakao *et al.,* J. Phys. Chem. B **109**, 24002 (2005).
[5] J. Neugebohren *et al.,* Nature, **558**, 280 (2018).
[6] L. Zhou, Angew. Chem. Int. **131**, 6990 (2019).
[7] H. Li *et al.,* J. Phys. Chem. C **128**, 15393 (2024).

Authors

H. Li, Y. Kataoka, S. Tanaka, J. Haruyama, O. Sugino, and J. Yoshinobu

Autonomous Synthesis of Metastable Ferrites

Lippmaa Group

Ferrites with the structural formula $LnFeO_3$ (*Ln* = lanthanide) usually crystallize in the orthorhombic phase, forming canted antiferromagnetic crystals with a small residual magnetic moment. These well-known ferrites can also form metastable layered hexagonal structures that can be stabilized in the form of nanoparticles or epitaxial thin films. We have explored the formation of these ferrite phases by growing thin films on a hexagonal YSZ(111) substrate surface, which provides a stabilizing template for the formation of the hexagonal ferrite phase. Unfortunately, even on a hexagonal substrate, the ferrites may form orthorhombic crystallites or films with a mixed phase composition. The structures of the metastable film phases are not well known. The formation of the orthorhombic or the hexagonal phases depends on both thermodynamic (temperature, pressure) and kinetic (growth rate) process parameters, giving a very multidimensional parameter space for either mapping the phase boundaries or finding the optimal crystal growth conditions in the accessible parameter space.

We have utilized a combination of several machine learning techniques [1,2] to simplify the process-phase-space optimization task by utilizing in-situ reflection high-energy electron diffraction (RHEED) images. The workflow is illustrated in Fig. 1.

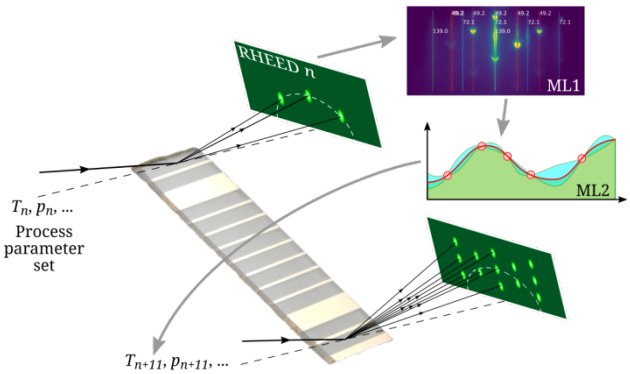

Fig. 1. Autonomous synthesis of ferrites by rapidly growing up to 12 thin films on a single substrate at different process conditions selected by a combination of a neural network (ML1) and Gaussian process (ML2) machine learning models.

The surface structure of a growing film is analyzed by real-time RHEED, which provides information on the surface crystallinity, lattice parameters, and phase purity. The image processing relies on a convolutional neural network (ML1) that is used to segment the image data and isolate diffraction features. [2] Clustering is then used to determine the phase purity of the film surface. Real-time imaging means that it is possible to combine structural quality metrics (crystallinity, phase purity) with temporal metrics (growth rate, phase stability). Examples of calculated quality metrics are shown in Fig. 2(a). At the start of an experiment, a Gaussian process (ML2) optimizer [1] is bootstrapped with quality factors determined from a small number of test films grown at process conditions selected by the operator. After that, the autonomous process starts by allowing the Gaussian process to automatically select process conditions for subsequent growth experiments.

An example of the effectiveness of the autonomous synthesis workflow is illustrated for pulsed laser deposition of $EuFeO_3$ films in Fig. 2. A shadow mask is used in the film growth chamber to fabricate up to 12 thin films on a single substrate (Fig. 1). Experiments needed for both model bootstrapping and condition optimization can thus be done quickly on a single substrate without the need for sample transfers. The operator initially guesses deposition process parameters in a four-dimensional space (temperature, oxygen pressure, ablation pulse energy, deposition rate) and the quality factors are determined for each film, as shown in Fig. 2(a). In this case, the operator did not find the conditions where a flat, high-crystallinity surface is obtained.

The Gaussian process, however, found the optimal process conditions in just four tries, as shown in Fig. 2(b), obtaining phase-pure films with a clear streak pattern, corresponding to a nanometer-scale flat surface without three-dimensional structures.

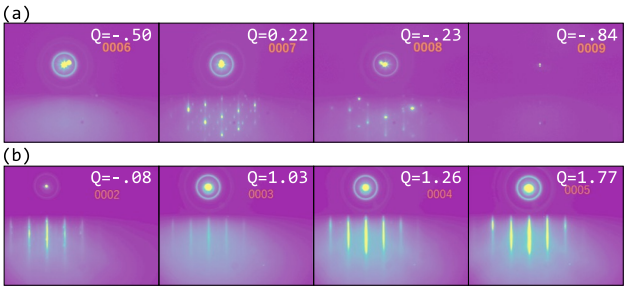

Fig. 2. Growth parameter optimization for $EuFeO_3$ films. (a) A human operator obtained films that were amorphous, not crystalline, three-dimensional, or contained multiple phases. (b) Autonomous growth reached optimal fabrication conditions in just four tries, yielding a strong and sharp streak pattern.

The main advantage of the autonomous process is to rapidly probe different regions in a multidimensional parameter space. For a human operator, it is difficult to perform optimization experiments effectively when the parameter space dimensionality is larger than two or three. The autonomous workflow greatly reduces the number of required experiments.

References

[1] I. Ohkubo *et al.*, Mater. Today Phys. **16**, 100296 (2021).
[2] H. Liang *et al.*, Phys. Rev. Materials **6**, 063805 (2022).

Authors

I. Ohkubo[a], Z. Hou[a], T. Aizawa[a], T. Chikyow[a], T. Mori[a], K. Tsuda[a], H. Liang[b], V. Stanev[b], A. G. Kusne[b], I. Takeuchi[b], Y. Tsukahara[c], K. Ito[c], R. Takahashi[c], J. N. Lee, and M. Lippmaa
[a]NIMS
[b]University of Maryland
[c]Nihon University

Oxygen Reduction Reaction at Oxide/Solution Interfaces

Sugino Group

Controlling the oxygen reduction reaction (ORR) is a pivotal challenge at the heart of energy conversion science. It's an area of extensive research across various scientific disciplines, including catalysis and biological reactions. Developing materials that maximize the efficiency of the 4-electron oxygen reduction reaction ($1/2\,O_2 + 4e^- + 4H^+ \rightarrow 2H_2O$) through their electrocatalytic properties is crucial. Industrially, platinum surfaces are commonly used. However, their high cost and limited durability necessitate the search for novel materials. This has led to the development of acid-resistant oxides. Doped TiO_2 and ZrO_xN_y, for instance, have shown activity comparable to platinum. Nevertheless, understanding their reaction mechanisms remains a pressing challenge.

First-principles calculations based on Density Functional Theory (DFT) are the most effective way to investigate reaction activity. However, we face several hurdles related to DFT accuracy and electrode-interface modeling when it comes to materials like TiO_2 and ZrO_xN_y. The ORR begins when oxygen molecules adsorb weakly. The accuracy of DFT for these weakly adsorbed oxygen systems must be carefully validated. Furthermore, oxygen must compete successfully with water molecules for absorption. To examine the content of competition, sampling of adsorption structures of water molecules is necessary. Accurately modeling the surface also demands extensive sampling of various dopant configurations. It is clear that these challenges have hindered theoretical research in this area. This report will explain how we overcame these obstacles and provide crucial insights into the activity mechanisms of these promising materials.

Accuracy of O_2 adsorption [1]: To validate the accuracy of oxygen adsorption, we compared experimental Temperature-Programmed Desorption (TPD) spectra with van der Waals-corrected DFT + U calculations on the anatase-TiO_2(101) surface. The results showed excellent agreement between the experiment-based and DFT-based simulations, both indicating weak adsorption of approximately 0.2 eV. This comparison between TPD and DFT is a novel approach.

Applying this method to the Pt(111) surface, we observed agreement for dissociative adsorption, albeit with a certain degree of correction. However, for molecular adsorption, the adsorption energy was significantly overestimated. This suggests that more advanced DFT functionals are necessary for accurate predictions on this system.

Adsorption Competition on ZrO_xN_y Surfaces [2]: To understand the competition between oxygen and water molecules for adsorption sites on the ZrO_xN_y(101) surface, we exhaustively sampled water molecule structures. By employing a machine learning force field, which allowed us to maintain DFT accuracy while achieving the computational efficiency of classical force fields, we performed approximately 1000 molecular dynamics simulations, each on the nanosecond scale, to determine average distributions. We found that on defect-free ZrO_2 (where $x = 2, y = 0$), the water molecule layer was weakly adsorbed and maintained a distance from the surface. In contrast, on the defective surface (where $x = 8/7, y = 4/7$), the distance shortened, indicating stronger adsorption. Notably, water molecules exhibited a strong tendency to adsorb away from the oxygen vacancies present on the surface (which were previously shown to be the O_2 adsorption site [3]), suggesting they do not compete with oxygen molecules for these specific adsorption sites. This finding supports the scenario where oxygen vacancies are stabilized by nitrogen impurities, thereby avoiding site competition.

Role of Surface Oxygen Vacancies: While our previous first-principles Monte Carlo calculations have shown that nitrogen impurities stabilize surface oxygen vacancies, it is not immediately obvious whether these vacancies act as active sites. This is because a simple comparison of adsorption energies for oxygen and water molecules under vacuum conditions suggested that water molecules would adsorb preferentially. Therefore, it is surprising that water molecules are stable in a vacuum yet become unstable at interfaces surrounded by other water molecules. The exact mechanism of this instability is unknown, but our simulations clearly demonstrate this tendency. The significance of our simulations lies in their ability to explain observational results by thoroughly sampling heterogeneous systems. This is a promising step forward for future research on heterogeneous catalytic reactions.

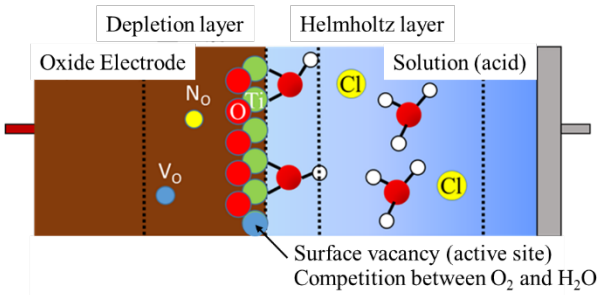

Fig. 1. *Ab initio* simulation of the electrochemical interface. This illustration, derived from comprehensive sampling within our *ab initio* molecular dynamics and Monte Carlo framework, highlights the adsorption competition between O_2 and H_2O molecules at the surface vacancy site.

References

[1] S. Muhammady *et al.*, arXiv:2506.18225.
[2] A. Nakanishi *et al.*, J. Phys. Chem. C. **129**, 2403 (2025).
[3] S. Muhammady *et al.*, J. Phys. Chem. C **126** 15662 (2022).

Authors

O. Sugino, S. Kasamatsu[a], S. Muhammady[b], A. Nakanishi[d], and J. Haruyama[b]
[a]Yamagata University
[b]RIKEN
[c]Tsukuba University

Gilbert Damping of NiFe Thin Films Grown on Two-Dimensional Chiral Hybrid Lead-Iodide Perovskites

Miwa, Ideue and Inoue Groups

Spin polarization in chiral molecules, extensively explored under the framework of chirality-induced spin selectivity (CISS), has attracted significant attention in recent research [1]. A notably perplexing issue is the observed substantial variance in CISS-induced magnetoresistance (MR) ratios between spin-polarized conductive atomic force microscopy measurements and multilayer device assessments, despite using identical material systems. This discrepancy might be linked to pinholes within multilayer film devices, though the specifics remain unresolved [2]. Our objective is to delve into CISS-related phenomena absent of electric current injection into chiral molecules. By omitting the bias electric current, we sidestep the complications associated with pinholes in chiral molecule films. Our approach involves a bilayer system composed of two-dimensional (2D) chiral hybrid lead-iodide perovskite [2] and NiFe, where spin pumping facilitates the pure spin current injection into chiral molecules [3].

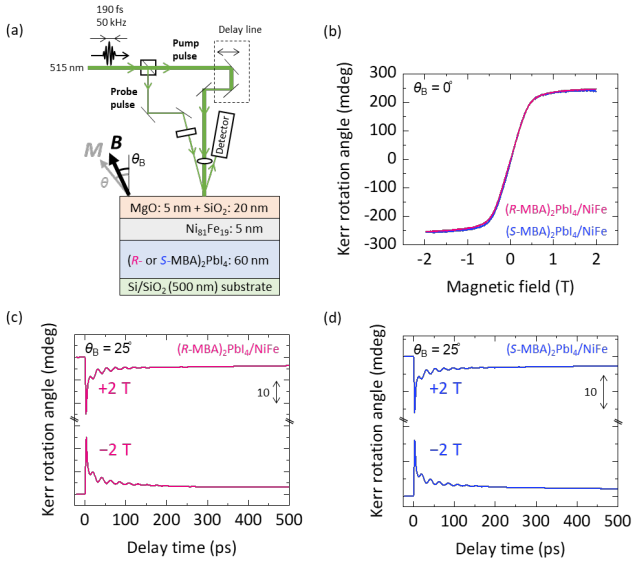

Fig. 1. (a) Schematic of the sample structure and measurement setup. (b) Magnetization hysteresis curve of NiFe. (c), (d) Results of TRMOKE measurements of NiFe grown on (R-MBA)$_2$PbI$_4$ and (S-MBA)$_2$PbI$_4$.

2D chiral hybrid lead-iodide perovskites, (R)-(+)-α-methylbenzylammonium lead iodide and (S)-(−)-α-methylbenzylammonium lead iodide ((R-MBA)$_2$PbI$_4$ and (S-MBA)$_2$PbI$_4$) [2], were synthesized and employed in this work. The spin pumping experiments involved multilayer films, comprising a 5 nm thick $Ni_{81}Fe_{19}$ layer deposited on the approximately 60 nm thick 2D chiral perovskite films, as depicted in Fig. 1(a). Time-resolved magneto-optical Kerr effect (TRMOKE) measurements were conducted employing a femtosecond pulse laser at a wavelength of 515 nm. Figure 1(b) shows the magnetization curves for NiFe films deposited on 2D chiral perovskites, (R-MBA)$_2$PbI$_4$ and (S-MBA)$_2$PbI$_4$, as measured by the magneto-optical Kerr effect with perpendicular magnetic field (θ_B = 0°). In Fig. 1(c), the TR-MOKE measurements results for the (R-MBA)$_2$PbI$_4$/NiFe are presented. These measurements, conducted under a constant magnetic field of ±2 T angled 25° from the film normal, reveal a pronounced initial drop in the Kerr rotation angle at zero delay time, followed by distinct oscillations as the Kerr rotation magnitude gradually recovers. Figure 1(d) shows similar TRMOKE measurement outcomes for the (S-MBA)$_2$PbI$_4$/NiFe, almost mirroring the results observed for (R-MBA)$_2$PbI$_4$/NiFe.

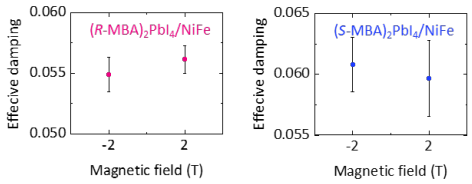

Fig. 2. The effective damping constant between positive and negative magnetic fields.

The impact of magnetic field direction on the resonant frequency and effective damping constants is shown in Fig. 2. As can be seen for (R-MBA)$_2$PbI$_4$/NiFe, the damping constant at +2 T is slightly (~0.001) higher than at −2 T. Conversely, for (S-MBA)$_2$PbI$_4$/NiFe, the damping constant at +2 T is marginally (~0.001) lower than at −2 T. Although the variations in the damping constant fall within the error range, the experiment demonstrates that the additional damping of NiFe, induced by the chirality of perovskite layer, is small. Considering the intrinsic damping constant of NiFe (5 nm) on a Si/SiO$_2$ substrate, as determined from separate measurements (not shown), to be 0.005±0.002, the increase in intrinsic damping of NiFe due to spin pumping is estimated at ~0.04. Consequently, the damping difference of ~0.001, when considered in the context of spin injection from NiFe to (R-MBA)$_2$PbI$_4$, is likely to represent at most a few percent of the difference of the spin injection. Note that this observation is not consistent with the spin filtering effect deduced from the substantial CISS-induced MR effect [2]. The minimal difference in damping constants, indicating a minor CISS, implies that the differences in CISS observed between the spin-polarized conductive atomic force microscopy and multilayer device methods may stem from fundamentally distinct physical mechanisms. The origin of the substantial CISS-induced MR using the spin-polarized conductive atomic force microscopy is unlikely to be due to spin filtering effect.

References

[1] R. Naaman *et al.*, Nat. Rev. Chem. **3**, 250-260 (2019).
[2] H. Lu *et al.*, Sci. Adv. **5**, eaay0571 (2019).
[3] T. Hatajiri *et al.*, Phys. Rev. B **110**, 054435 (2024).

Authors

T. Hatajiri, S. Sakamoto, H. Kosaki, Z. Tian, M. Tanaka, T. Ideue, K. Inoue, D. Miyajima[a,b], and S. Miwa
[a]RIKEN
[b]The Chinese University of Hong Kong

Anisotropy of the Gilbert Damping Constant in NiFe Grown on the Chiral Antiferromagnet Mn_3Sn

Miwa and Nakatsuji Groups

Spintronics is an important field of electronics that utilizes the two degrees of freedom of electrons: charge and spin angular momentum. Chiral antiferromagnets are attracting attention as spintronics materials due to their high resonant frequency and minimal stray fields. $D0_{19}$-Mn_3Sn (Fig. 1(a)) is a chiral antiferromagnet with a noncolinear spin structure. Its Mn spins form a spin structure called a cluster magnetic octupole [1]. The magnetic effects on Mn_3Sn are known to be anisotropic due to its anisotropic magnetic structure, which originates from the kagome crystal structure [2]. Utilizing Mn_3Sn as a material for spintronics devices requires Mn_3Sn/ferromagnet heterostructures because these structures produce current-induced magnetic effects. Spin current transport at a metal/metal interface is characterized by the spin mixing conductance $g^{\uparrow\downarrow}_{\mathrm{eff}}$. A previous study [3] evaluated the $g^{\uparrow\downarrow}_{\mathrm{eff}}$ at the Mn_3Sn/NiFe ($Ni_{81}Fe_{19}$, permalloy) interface using spin pumping. In this study, the anisotropy of the spin mixing conductance has been investigated.

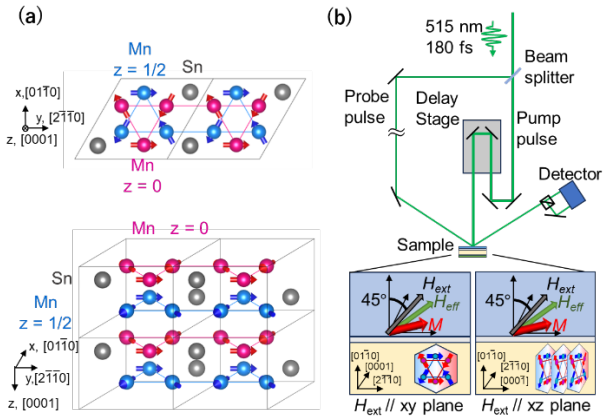

Fig. 1(a).Crystal and spin structure of $D0_{19}$-Mn_3Sn. (b) Schematic of the TRMOKE measurements.

A $Mn_3Sn(01\bar{1}0)$ (20 nm)/MgO spacer (0-3.5 nm)/NiFe (4 nm) multilayer sample was prepared by molecular beam epitaxy method. The Mn_3Sn ($01\bar{1}0$ thin film has kagome planes perpendicular to the film plane. Spin mixing conductance is characterized by the spin pumping. Spin current transport at metal/ferromagnet interface is evaluated from the damping constant of the ferromagnet. The damping of the NiFe ferromagnet is characterized using a time-resolved magneto-optical Kerr effect (TRMOKE). Figure 1(b) shows a schematic of the TRMOKE measurements, where the ferromagnetic spin in the NiFe layer, excited by the pump pulse, is detected by the probe pulse via MOKE. An external magnetic field was applied at 45° in the *xy* and *zx* planes. The TRMOKE signal is shown in Fig. 2(a). Based on the Landau-Lifshitz-Gilbert equation,

$$\frac{d\boldsymbol{M}}{dt} = -\gamma \boldsymbol{M} \times \boldsymbol{H}_{\mathrm{eff}} + \frac{\alpha}{M_s} \boldsymbol{M} \times \frac{d\boldsymbol{M}}{dt}$$

damping constant α was evaluated for each MgO spacer thickness as shown in Fig. 2(b). Here, $\boldsymbol{M}$ is magnetization of NiFe and $\boldsymbol{H}_{\mathrm{eff}}$ is the effective magnetic field.
We find that the damping was large where the MgO spacer thickness was thin because the nonmagnetic insulator MgO can cut the spin transport at Mn_3Sn/NiFe interface. The obtained damping constant was used to obtain the mixing conductance $g^{\uparrow\downarrow}_{\mathrm{eff}}$, which was found to be $g^{\uparrow\downarrow}_{\mathrm{eff}} = 3.6 \pm 0.6 \times 10^{18}$ m^{-2} when the field was applied out of the Mn_3Sn kagome plane and $g^{\uparrow\downarrow}_{\mathrm{eff}} = 1.5 \pm 0.1 \times 10^{18}$ m^{-2} when the field was applied in the Mn_3Sn kagome plane.

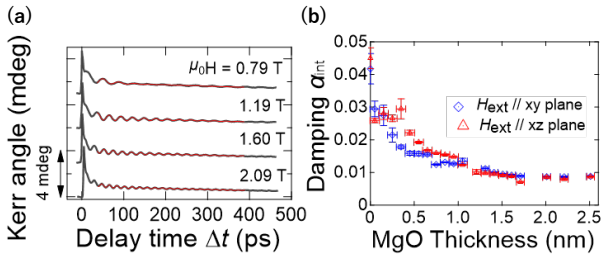

Fig. 2. (a) Time-resolved magneto-optical Kerr effect signals of Mn_3Sn/MgO(0.45 nm)/NiFe. (b) MgO spacer thickness dependence of intrinsic Gilbert damping constants of NiFe.

There are several possible reasons for the anisotropy of $g^{\uparrow\downarrow}_{\mathrm{eff}}$. One possibility is the spin transparency of conduction electrons at the NiFe/Mn_3Sn interface. The anisotropic band structure of Mn_3Sn [1] may cause anisotropy in spin transparency. However, it is difficult to explain the anisotropy in terms of spin absorption efficiency, because the spin diffusion length (~ 1 nm) of Mn_3Sn [4] is much smaller than the Mn_3Sn thickness. Furthermore, since the damping enhancement anisotropy is greater than twice as large, the anisotropy cannot be solely attributed to the spin current via conduction electrons. We believe the damping enhancement anisotropy is caused by magnetic coupling between NiFe and Mn_3Sn via the exchange spring effect [5].

References

[1] M.-T. Suzuki *et al.*, Phys. Rev. B **95**, 94406 (2017).
[2] S. Nakatsuji, N. Kiyohara, and T. Higo, Nature **527**, 212 (2015).
[3] J.-Y. Yoon *et al.*, Nature Mater. **22**, 1106 (2023)
[4] P. K. Muduli *et al.*, Phys. Rev. B **99**, 184425 (2019)
[5] H. Kosaki *et al.*, Phys. Rev. B **111**, 024418 (2025).

Authors

H. Kosaki, S. Sakamoto, T. Hatajiri, T. Higo, S.Nakatsuji, and S.Miwa

Bulk and Surface-sensitive X-ray Magnetic Circular Dichroism Study of an Epitaxial Mn_3Sn Thin Film

Miwa and Nakatsuji Groups

To move beyond modern electronics, increasing attention has turned to spintronics, which utilizes both the charge and spin degrees of freedom of electrons. Spintronics has largely focused on ferromagnets due to their strong electrical responses. Recently, however, antiferromagnetic systems have attracted significant interest for their potential to operate at much higher frequencies. Despite this promise, their typically weak electrical signals present major challenges for practical implementation.

Mn_3Sn is an antiferromagnet featuring an inverse triangular spin structure on a Mn kagome lattice. This spin arrangement breaks macroscopic time-reversal symmetry and can be described by an octupole polarization. Mn_3Sn exhibits strong ferromagnet-like responses, such as anomalous Hall effect, despite having negligible net magnetization. Recent progress in fabricating epitaxial W/Mn_3Sn bilayers has enabled electrical manipulation of this spin structure via spin-orbit torque generated by the spin Hall effect in W. This advancement makes the W/Mn_3Sn system a promising candidate for antiferromagnet-based spintronic devices. However, it remains unclear whether the observed spin-torque-induced effects are intrinsic to the W/Mn_3Sn interface or are influenced by ferromagnetic secondary phases.

To address this issue, we conducted x-ray magnetic circular dichroism (XMCD) measurements. While XMCD is conventionally used for probing ferromagnetic materials, we have recently shown that it can also detect the inverse triangular spin structure of Mn_3Sn through the magnetic dipole term [1]. In this study [2], we employed both surface-sensitive total electron yield (TEY) and bulk-sensitive partial fluorescence yield (PFY) modes to investigate the uniformity of the antiferromagnetic spin structure (or octupole polarization) throughout a W/Mn_3Sn/MgO multilayer, from the bottom to the top interface.

The epitaxial Mn_3Sn thin film was grown by molecular beam epitaxy on an MgO(110) substrate, with the final structure comprising MgO(110)/W (7 nm)/Mn_3Sn (30 nm)/MgO (3 nm). XMCD measurements were carried out at beamline BL25SU at SPring-8 at room temperature. In TEY mode, the drain current compensating for photoemitted electrons was recorded, while in PFY mode, fluorescence x-rays were detected using a silicon drift detector (SDD), as shown in Fig. 1. The probing depths of TEY and PFY are approximately a few nanometers and ~100 nm, respectively—thus, TEY probes the surface region, while PFY covers the full 30-nm-thick Mn_3Sn layer.

Figure 2 presents the Mn L_3-edge XMCD spectra acquired using TEY and PFY modes under an applied magnetic field of 50 mT. Prior to this, a field of 1.9 T was applied to saturate the octupole polarization. Both spectra show a distinct positive peak at 638.7 eV, characteristic of the inverse triangular spin structure. Notably, the TEY and PFY spectra are nearly identical, demonstrating uniform electronic and magnetic structures across the entire Mn_3Sn layer from the bottom W/Mn_3Sn and the top Mn_3Sn/MgO interfaces. Furthermore, the absence of any signatures associated with ferromagnetic secondary phases confirms the structural and magnetic purity at the W/Mn_3Sn interface. These results suggest that the spin-torque induced phenomena recently observed in W/Mn_3Sn bilayers are intrinsic in nature and originate from the direct interplay between spin currents and the octupole polarization.

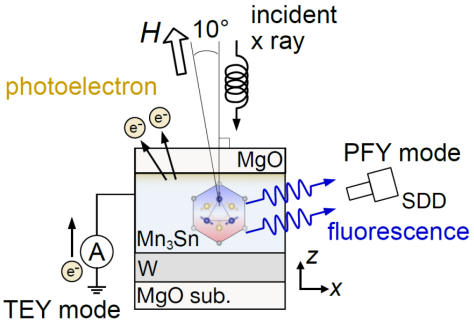

Fig. 1. Experimental setup for XMCD measurements.

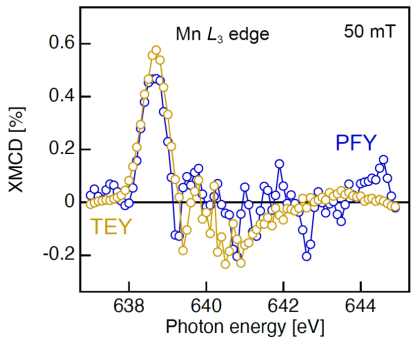

Fig. 2. XMCD spectra at the Mn L_3 absorption edge measured with surface-sensitive TEY mode and bulk-sensitive PFY mode.

References

[1] S. Sakamoto, T. Higo, M. Shiga, K. Amemiya, S. Nakatsuji, and S. Miwa, Phys. Rev. B **104**, 134431 (2021).
[2] S. Sakamoto, T. Higo, Y. Kotani, H. Kosaki, T. Nakamura, S. Nakatsuji, and S. Miwa, Phys. Rev. B **110**, L060412 (2024).

Authors

S. Sakamoto, T. Higo[a], Y. Kotani[b], H. Kosaki, T. Nakamura[b,c], S. Nakatsuji[a,d], and S. Miwa
[a]The University of Tokyo
[b]Japan Synchrotron Radiation Research Institute
[c]Tohoku University
[d]Johns Hopkins University

Observation of Antiferromagnetic Spin-torque Diode Effect

Miwa and Nakatsuji Groups

Spintronics based on ferromagnets has not only revolutionized memory technologies but also led to the development of microwave devices such as spin-torque oscillators and spin-torque diodes. These microwave spintronic devices typically operate at ferromagnetic resonance conditions, with frequencies reaching several tens of GHz. However, increasing the frequency often narrows the magnetization precession cone angle, thereby weakening the output signals. Antiferromagnets offer a promising alternative. In easy-plane antiferromagnets, when a spin current with spin polarization perpendicular to the easy plane is injected, each spin deviates out of the easy plane. Due to this deviation, the exchange interaction acts to restore the spins to the easy plane, creating an effective magnetic field. This field drives spin precession around itself, enabling operation at much higher frequencies while maintaining the precession cone angle.

In this study [1], we focused on the easy-plane non-collinear antiferromagnet Mn_3Sn. This material exhibits a strong anomalous Hall effect despite negligible magnetization, and therefore, sizeable microwave responses are expected. Recent studies have shown that spin torque can drive switching and continuous rotation—referred to as chiral spin rotation—of the non-collinear triangular spin structure. In this work, we investigate the microwave response of Mn_3Sn and demonstrate the antiferromagnetic spin-torque diode effect [1], in which the interaction between chiral spin rotation and a microwave current generates a rectified DC transverse Hall voltage.

We fabricated W/Mn_3Sn epitaxial bilayers on MgO(110) substrates using molecular beam epitaxy. Hall bar devices (Mn_3Sn: 7 nm, W: 6 nm) were patterned by standard photolithography and Ar ion etching. A DC bias current and amplitude-modulated microwave current were applied via a bias-tee, and the resulting DC Hall voltages were measured using a lock-in amplifier, as schematically shown in Fig. 1.

Figure 2 shows the observed DC Hall voltage as a function of in-plane magnetic fields under the simultaneous application of DC and microwave currents. When the DC current is lower than the threshold for initiating chiral spin rotation, the data are rather featureless. On the other hand, when the DC current exceeded the threshold, peak feature appeared at a specific magnetic field. Numerical simulations suggest that these rectification signals originate from the effective modulation of the chiral spin rotation frequency by the microwave spin-orbit torque. This antiferromagnetic spin-torque diode effect was found robust at higher frequencies, offering the potential for broadband spintronic functionality beyond the GHz limitations of ferromagnetic systems.

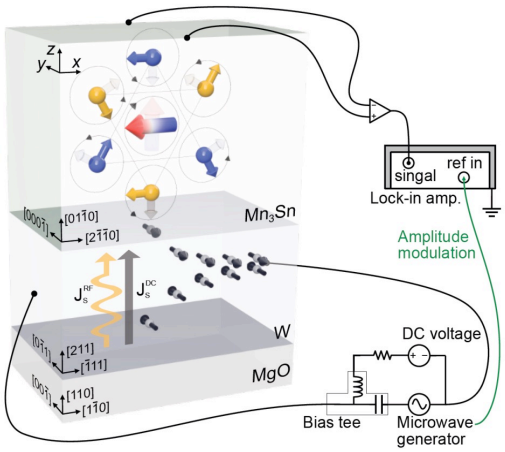

Fig. 1. Experimental setup for spin-torque diode effect measurements. DC and microwave currents were applied to the device via a bias tee, and resulting DC Hall voltages were measured using lock-in amplifier.

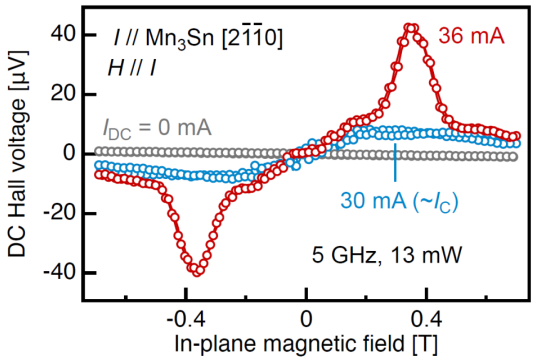

Fig. 2. Observed DC Hall voltages as a function of in-plane magnetic fields under a simultaneous application of DC and microwave current.

References

[1] S. Sakamoto, T. Nomoto, T. Higo, Y. Hibino, T. Yamamoto, S. Tamaru, Y. Kotani, H. Kosaki, M. Shiga, D. Nishio-Hamane, T. Nakamura, T. Nozaki, K. Yakushiji, R. Arita, S. Nakatsuji, and S. Miwa, Nat. Nanotechnol. **20**, 216-221 (2025).

Authors

S. Sakamoto, T. Nomoto[a,b], T. Higo[a], Y. Hibino[c], T. Yamamoto[c], S. Tamaru[c], Y. Kotani[d], H. Kosaki, M. Shiga, D. Nishio-Hamane, T. Nakamura[e,d], T. Nozaki[c], K. Yakushiji[c], R. Arita[a,f], S. Nakatsuji[a,g], and S. Miwa

[a]The University of Tokyo

[b]Tokyo Metropolitan University

[c]National Institute of Advanced Industrial Science and Technology

[d]Japan Synchrotron Radiation Research Institute

[e]Tohoku University

[f]RIKEN

[g]Johns Hopkins University

A New Promising Thermoelectric Material with Cubic and Complex Crystal Structure

Okamoto Group

Cubic materials with complex crystal structures are promising for thermoelectric conversion. The multivalley electronic structure stemming from the cubic symmetry increases Seebeck coefficient S keeping low electrical resistivity ρ, and the complex crystal structure reduces the phonon contribution of thermal conductivity κ_{lat}. When atoms are enclosed in highly symmetric and oversized cages in their crystal structures, the rattling effect can further suppress κ_{lat} while maintaining a high electrical conductivity. In fact, there are several material families with cubic and complex crystal structures that exhibit high thermoelectric performance, such as filled skutterudite and clathrate.

We report the thermoelectric properties of ReSTe with cubic and complex crystal structure. ReSTe was first synthesized by Fedorov *et al*. in powder form and was reported to crystallize in a cubic MoSBr type, as shown in Fig. 1 [1]. Their transport properties have not been reported, because the only small single crystals have been synthesized thus far. We succeeded in synthesizing undoped, W-doped, and Sb-doped ReSTe sintered samples and investigated their thermoelectric properties [2].

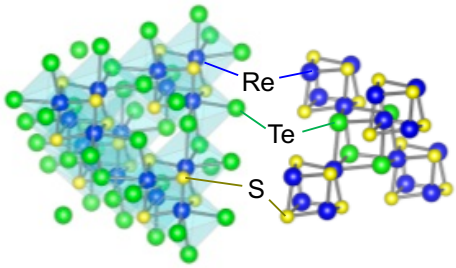

Fig. 1. Crystal structure of ReSTe.

The undoped ReSTe exhibited a positive S increasing with increasing temperature with a concave downward curve. The value of S was the largest among all the samples, exceeding 260 μV K^{-1} at 300 K, which is high enough to be a thermoelectric material. The ρ of undoped ReSTe exhibits a semiconducting temperature dependence, with ρ exponentially increasing with decreasing temperature. The value of ρ = 30 mΩ cm at 300 K is one order of magnitude higher than that of practical materials. With increasing W content x, both S and ρ systematically decrease, and the temperature dependence of ρ becomes weaker.

As shown in Fig. 2(a), the dimensionless figure of merit ZT evaluated using these physical properties ($ZT = S^2T/\rho\kappa$) increased with increasing temperature for all the samples. Over the entire temperature range below room temperature, the lightly W-doped samples showed a large ZT; the x = 0.007 sample exhibited the largest ZT = 0.055 at 300 K, whereas the undoped sample exhibited ZT = 0.04 at the same temperature. As shown in Fig. 2(b), the ZT values of the undoped and x = 0.007 samples increased significantly at higher temperature. They exhibit ZT = 0.39 and 0.36, respectively, at the highest measured temperature of 660 K, indicating they are promising p-type thermoelectric materials. This high performance is attributed to large power factor $P = S^2/\rho$ owing to the degenerate semiconducting state realized by the strong spin–orbit coupling and low lattice thermal conductivity of the sintered samples. Furthermore, the electronic band dispersion at the bottom of the conduction band of ReSTe is almost flat owing to the large band splitting in the valence band caused by the strong spin–orbit coupling. These results strongly suggest that a high thermoelectric performance far beyond that of the p-type can be realized in n-type samples, indicating the great potential of tellurides with cubic and complex crystal structures as thermoelectric materials.

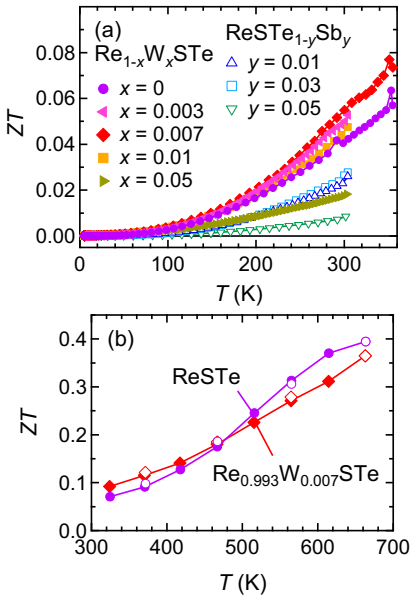

Fig. 2. Temperature dependences of the dimensionless figure of merit ZT. (a) ZT of the sintered $Re_{1-x}W_xSTe$ and $ReSTe_ySb_{1-y}$ samples below 350 K. (b) ZT of the sintered ReSTe and $Re_{0.993}W_{0.007}STe$ samples above room temperature.

References

[1] V. E. Fedorov, Y. V. Mironov, V. P. Fedin, and Y. I. Mironov. J. Struct. Chem. **35**, 146 (1994).

[2] H. Matsumoto, H. Isomura, K. Kojima, R. Okuma, H. Ohshima, C.-H. Lee, Y. Yamakawa, and Y. Okamoto, Appl. Phys. Lett. **126**, 243903 (2025).

Authors

Y. Okamoto, H. Matsumoto, H. Isomura, K. Kojima, R. Okuma, H. Ohshima[a], C.-H. Lee[a], and Y. Yamakawa[b]

[a]National Institute of Advanced Industrial Science and Technology (AIST)

[b]Nagoya University

Discovery of Zr-Based Superconductors with Hexagonal Zr_6CoAl_2-Type Crystal Structure

Okamoto and Yamaura Group

Recently, new superconductors have been discovered in A_6MX_2 compounds with the hexagonal Zr_6CoAl_2-type crystal structure. Figure 1 shows this crystal structure, which is an ordered Fe_2P type with the noncentrosymmetric space group $P\bar{6}2m$. The discovery of superconductors in the A_6MX_2 family was triggered by Sc_6MTe_2, which was found to exhibit superconductivity in the cases of seven transition metals M (M = Fe, Co, Ni, Ru, Rh, Os, and Ir) [1]. The superconducting transition temperature T_c in these compounds is approximately 2 K for M = 4*d* and 5*d* transition metals. However, for M = 3*d*, T_c increases in the order of Ni, Co, and Fe, reaching the highest value of T_c = 4.7 K for Sc_6FeTe_2. A remarkable feature of the A_6MX_2 superconductor family is its compositional flexibility, as the A, M, and X atoms can be substituted with various elements. The number of combinations of these A, M, and X atoms is considerably large, with more than 100 materials synthesized to date, raising expectations for discovering additional *d*-electron superconductors within this family.

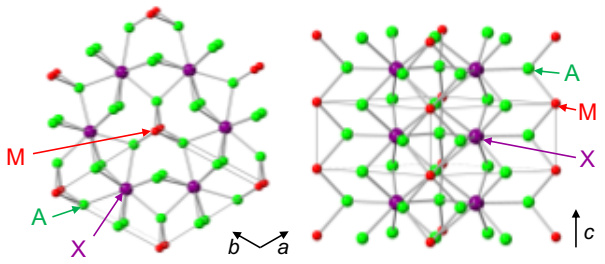

Fig. 1. Crystal structure of Zr_6CoAl_2-type A_6MX_2.

We focused on Zr_6MBi_2 crystallizing in the Zr_6CoAl_2-type structure and found that Zr_6RuBi_2 and Zr_6FeBi_2 show bulk superconductivity, based on the electrical resistivity, magnetization, and heat capacity measurements of polycrystalline samples [2]. As shown in Fig. 2, Zr_6RuBi_2 and Zr_6FeBi_2 samples exhibit zero resistivity and strong diamagnetic signals owing to superconductivity. Considering the midpoint of the resistivity drop and the onsets of the magnetization drop and heat capacity jump, T_c was determined as 4.9 and 1.4 K for M = Ru and Fe, respectively.

Superconductivity of Zr_6RuBi_2 is most likely conventional; however, its T_c is considerably higher than that of Zr_6FeBi_2. We synthesized Zr_6MBi_2 samples with other M atoms, including Rh, Ir, and Co. However, no material other than M = Ru was confirmed to exhibit bulk superconductivity above 2 K, indicating that an anomalously high T_c is present in Zr_6RuBi_2. This trend in T_c differs from that observed in Sc_6MTe_2, where Sc_6FeTe_2 displayed the highest T_c of 4.7 K [1]. The fact that Zr_6RuBi_2 showed the highest T_c among the current A_6MX_2 members suggests that M being a 3*d* transition metal element is not always favorable for superconductivity and that the combination of A, M, and X elements is crucial. Recently, Zr_6RuTe_2 is found to show bulk superconductivity below T_c = 1.1 K [3], which exceeds that of Zr_6MTe_2 with other transition metals. We hope that the exploration of new superconductors in the A_6MX_2 family will lead to the discovery of new superconductors with higher T_c or unusual properties.

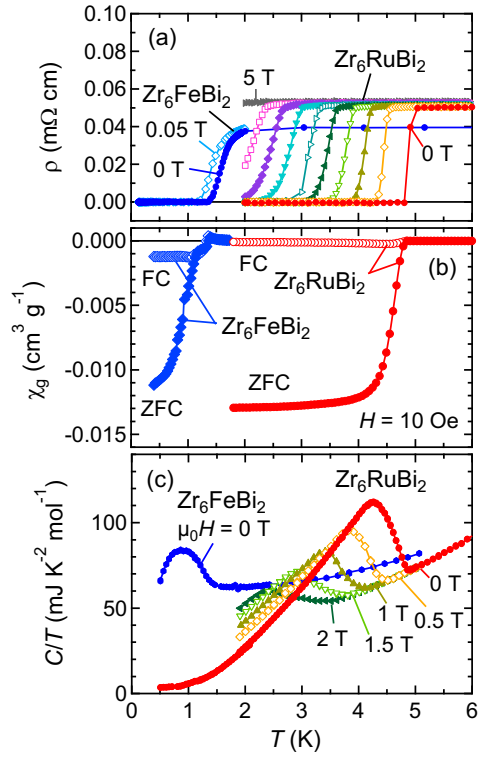

Fig. 2. Temperature dependences of (a) electrical resistivity, (b) field-cooled and zero-field-cooled magnetic susceptibility, and (c) heat capacity divided by temperature of Zr_6RuBi_2 and Zr_6FeBi_2 polycrystalline samples measured under zero magnetic field and various magnetic fields.

References

[1] Y. Shinoda, Y. Okamoto, Y. Yamakawa, H. Matsumoto, D. Hirai, and K. Takenaka, J. Phys. Soc. Jpn. **92**, 103701 (2023).

[2] K. Yuchi, D. Nishio-Hamane, K. Kojima, K. Moriyama, R. Okuma, and Y. Okamoto, J. Phys. Soc. Jpn. **94**, 013701 (2025).

[3] K. Yuchi, H. Matsumoto, D. Nishio-Hamane, K. Moriyama, K. Kojima, R. Okuma, J. Yamaura, and Y. Okamoto, J. Phys. Soc. Jpn. **94,** 085001 (2025).

Authors

Y. Okamoto, K. Yuchi, H. Matsumoto, D. Nishio-Hamane, K. Kojima, K. Moriyama, R. Okuma, and J. Yamaura

Two-Dimensional Quantum Critical Behavior of Boson Gas in $YbCl_3$

Kitagawa Group

Certain types of magnets near the saturation magnetic field can be viewed as an ensemble of dilute bosons with hard-core interactions (Fig. 1). Here, the deviation of the magnetization from its saturation value represents the number of bosons, and the ordering of the magnetic degrees of freedom perpendicular to the magnetic field (the XY component) corresponds to a Bose-Einstein condensation (BEC) [1]. What is unique here is that we can precisely tune the boson density just by changing the magnetic field and investigate the property of dilute bosons in the low temperature limit on the verge of BEC. Such bosons are governed by strong fluctuations between the two different states, namely, the BEC of finite number of bosons and a vacuum (a state with no bosons). These fluctuations, which exist even at absolute zero temperature, originate from the uncertainty principle of quantum mechanics and are called quantum critical fluctuations.

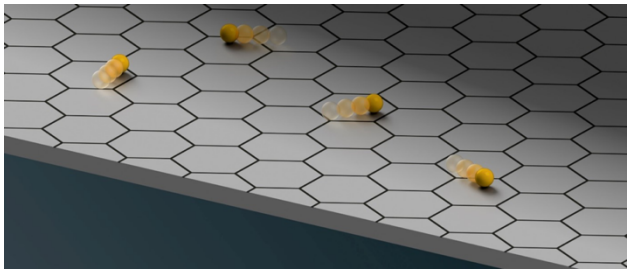

Fig. 1. Illustration of hardcore bosons confined to a two-dimensional plane.

Interestingly, the property of bosons significantly changes depending on the spatial dimension. In the pure 2D case, bosons cannot form a true condensate and, instead, turn to an exotic quasi-condensate through a topological phase transition described by the dissociation of vortex pairs, known as the Berezinskii-Kosterlitz-Thouless (BKT) transition. Moreover, the effective hard-core interaction between bosons vanishes in the dilute limit with the logarithmic correction ln <*n*> characteristic to 2D, where <*n*> is the boson density. Unfortunately, this has never been done. We need an ideal model system, a stack of ideal 2D magnets connected through extremely tiny interlayer coupling. In addition, the saturation field should be small enough to make detailed thermodynamic/thermal transport studies.

In this work, we experimentally clarified for the first time the unique 2D behavior of a dilute boson gas using the pseudospin-1/2 honeycomb Heisenberg magnetic material $YbCl_3$. This material has recently attracted much attention as a candidate for the Kitaev quantum spin liquid, but more recent studies have revealed that it is a nearly pure 2D Heisenberg magnet with in-plane interactions of 5 K and interlayer interactions about five orders of magnitude smaller than this [2]. The saturation field is relatively small, about 5.93 T in the in-plane direction, which makes high-precision thermodynamics and thermal transport measurements around this field possible.

We studied the field-induced quantum criticality of $YbCl_3$ by using magnetization, specific heat and thermal conductivity measurements (Fig. 2) [3]. We found specific heat and magnetization at the saturation magnetic field (BEC-QCP) are surprisingly well described as a 2D Bose gas in the dilute limit. Furthermore the boson-boson repulsion in the quantum critical 2D Bose gas takes a considerably small value, at least one order of magnitude smaller than those found in its 3D analogues, which evidences the presence the logarithmic correction ln <*n*> unique to 2D. With boson doping, decreasing the magnetic field from the saturation field, the quantum critical 2D Bose gas was found to experience a 3D BEC, marginally produced by an extremely small interlayer coupling (three-dimensionality). The demonstration of such a distinct 2D nature of Bose gas establishes $YbCl_3$ as a unique playground of further explorations for novel phenomena of 2D Bose gas.

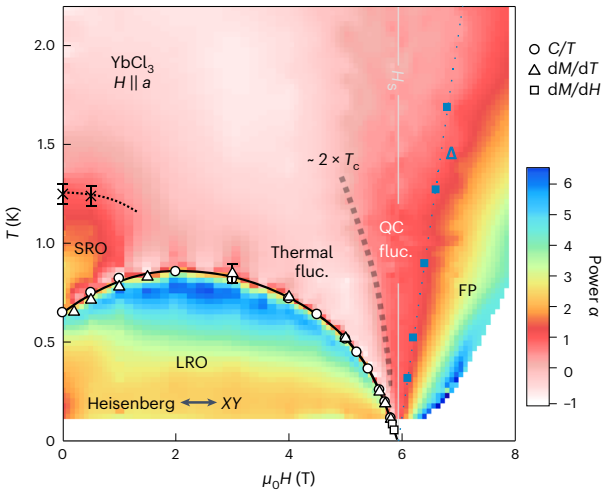

Fig. 2. Magnetic-field-induced quantum phase transition and *H*–*T* phase diagram for $YbCl_3$. The power α is determined from the *T*-dependent specific heat *C*. The open symbols indicate the long-range magnetic ordering. The crosses represent the locations of the broad SRO peaks in *C*/*T*. Filled squares indicate the gap size Δ determined by *C*/*T*. The grey broken line indicates the onset of the 2D thermal fluctuations.

References

[1] V. Zapf, M. Jaime, and C.D. Batista, Rev. Mod. Phys. **86**, 563 (2014).
[2] G. Sala *et al.*, Phys. Rev. B **100**, 180406 (2019).
[3] Y. Matsumoto *et al.*, Nat. Phys. **20**, 1131 (2024).

Authors

Y. Matsumoto[a], S. Schnierer[a], J.A.N. Bruin[a], J. Nuss[a], P. Reiss[a], G. Jackeli[a], K. Kitagawa, H. Takagi[a]
[a]MPI-FKF

Bulk High-Temperature Superconductivity Achieved in $La_2PrNi_2O_7$ under High Pressure

Kitagawa Group

In 2023, signatures of high-temperature superconductivity (HTSC) with $T_c \approx$ 80K were reported at pressures above 14 GPa in $La_3Ni_2O_7$ [1]. This discovery has immediately attracted tremendous research interest for a new family of HTSC. $La_3Ni_2O_7$ is a bilayer member (n = 2) of the Ruddlesden-Popper (R-P) perovskite nickelates denoted as $La_{n+1}Ni_nO_{3n+1}$. In contrast to well-known cuprate HTSCs, and to infinite-layer $Nd_{1-x}Sr_xNiO_2$ thin films superconductros with $T_c \approx$ 9-15 K (2019), $La_3Ni_2O_7$ exhibits an exceptionally unique electronic valence state with the nominal oxidation state of $Ni^{2.5+}$ ($3d^{7.5}$) instead of $3d^9$. The $3d^{7.5}$ electronic configuration sitting on bilayers with moderate interlayer exchange has been theoretically proposed as an alternative HTSC playground to that of cuprate. The prediction was reported prior to the discovery in real materials. However, HTSC in $La_3Ni_2O_7$ has not been experimentally established yet, because Meissner diamagnetic shielding effect, inherent to a genuine superconductor, was not confirmed in any of bilayer nickelate HTSC candidates.

Subsequent high-pressure studies on $La_3Ni_2O_7$ crystals confirmed the presence of a zero-resistance state under better hydrostatic pressure conditions, but issues related to sample-dependent behaviors remain unclear so far. ISSP Activity Report 2023 12 successfully reproduced zero-resistivity using high-quality $La_3Ni_2O_{7-\delta}$ ($\delta \approx 0.07$) polycrystalline samples by using the sol-gel method and under hydrostatic pressure condition up to 18 GPa [2]. Although diamagnetic response was not detected during ac-susceptibility measurement, the report constructed pressure-temperature (P-T) phase diagram and intimate relationship between superconductivity, density-wave-like order, and the strange-metal-like behaviors. However, again, still HTSC as bulk was not obtained even with the high-quality sample, and identification of the exact superconductivity phase/structure is the most prominent task at present.

$La_3Ni_2O_7$ is known to include considerable amount of intergrowths of other R-P phases, La_2NiO_4 (monolayer) and $La_4Ni_3O_{10}$ (trilayer), resulting in stacking faults against the bilayer-bilayer stacking sequence. To overcome this problem, we synthesized the polycrystalline samples of bilayer nickelates $La_{3-x}Pr_xNi_2O_{7-\delta}$ via sol-gel method [3]. In this work, we found that the above-mentioned sample-quality issues of $La_3Ni_2O_7$ can be effectively resolved via substitution of smaller Pr ions for La, leading to the successful synthesis of high-purity $La_2PrNi_2O_7$ with nearly an ideal bilayer R-P structure. Combined resistivity and ac magnetic susceptibility measurements under hydrostatic pressures provided the key evidence of bulk HTSC, including the zero resistance with high T_c^{onset} = 82.5 K and T_c^{zero} = 60 K, along with a clear diamagnetic response correspondinZg to a superconducting shielding volume fraction of 97% (Fig. 1,2). The key parts of the measurements were carried out by a two-stage 6/8 multianvil apparatus of the high-pressure measurement section in ISSP. These results provide critical experimental evidence for bulk HTSC in the pressurized $La_2PrNi_2O_7$, confirming the bilayer R-P phase as the source of HTSC for the first time.

References

[1] H.L. Sun *et al*., Nature **621**, 493 (2023).
[2] G. Wang *et al*., Phys. Rev. X **14**, 011040 (2024).
[3] N. Wang *et al*., Nature **634**, 579 (2024).

Authors

N. Wang[a], G. Wang[a], X. Shen[b], J. Hou[a], J. Luo[a], X. Ma[a], H. Yang[a], L. Shi[a], J. Dou[a], J. Feng[a], J. Yang[a], Y. Shi[a], Z. Ren[a], H. Ma[a], P. Yang[a], Z. Liu[a], Y. Liu[a], H. Zhang[a], X. Dong[a], Y. Wang[a], K. Jiang[a], J. Hu[a,c], S. Nagasaki, K. Kitagawa, S. Calder[d], J. Yan[d], J. Sun[a], B. Wang[a], R. Zhou[a], Y. Uwatoko & J. Cheng[a]
[a]Chinese Academy of Sciences
[b]Shanghai Jiao Tong University
[c]New Cornerstone Science Laboratory
[d]Oak Ridge National Laboratory

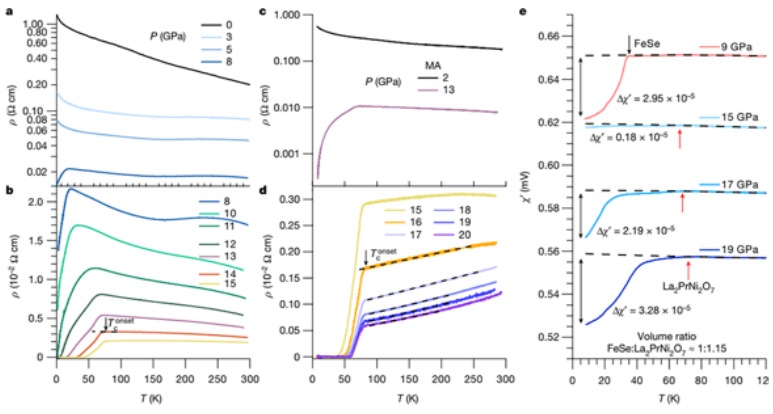

Fig. 1. The resistivity and ac-susceptibility measurements using the multianvil apparatus in ISSP, showing pressure-induced HTSC in $La_2PrNi_2O_7$.

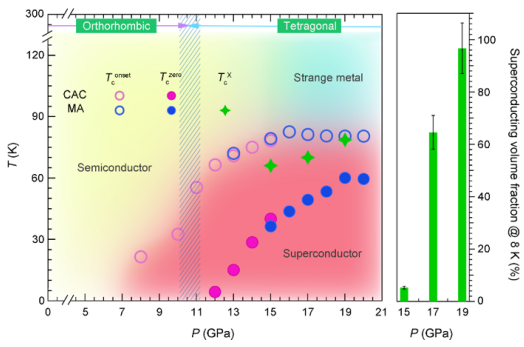

Fig. 2. The P-T phase diagram of $La_2PrNi_2O_7$.

Novel Electronic Instability in Topological Semimetal KAlGe

Yamaura, Okamoto, and Hiroi Groups

This study focuses on the compound KAlGe, which has an anti-PbFCl crystal structure with two-dimensional electronic states that exhibit various electronic instabilities and physical properties (inset of Fig. 1). NaAlSi and NaAlGe, analogous compounds exhibit distinct properties: NaAlSi is a superconductor with a transition temperature of 6.8 K [1, 2], while NaAlGe is an insulator featuring a pseudogap around 100 K [3, 4] (Fig. 1). These three compounds have structural features, including layered geometries composed of Al-Ge/Si tetrahedra and alkali metal sheets, yet their low-temperature behaviors differ markedly.

Employing a potassium–indium flux method, we successfully synthesized single crystals of KAlGe. First-principles electronic structure calculations revealed that KAlGe is isoelectronic with NaAlSi and NaAlGe, suggesting related underlying electronic characteristics. Notably, KAlGe demonstrates a metal-to-metal transition at 89 K (Fig. 1), accompanied by substantial changes in electrical resistivity, heat capacity, and X-ray diffraction patterns [5]. The transition entails structural symmetry-breaking, resulting in the loss of four-fold rotational symmetry (Fig. 2) [5].

The low-temperature phase of KAlGe exhibits markedly decreased carrier density with extremely very high electron mobility (Fig. 1), akin to Dirac electron systems. Dirac points exist in the high-temperature phase, and some may persist near the Fermi level following the transition. These features make KAlGe a topological semimetal with a "hidden" Dirac point in its high-temperature tetragonal phase which becomes more pronounced in the low-temperature phase. The manifestation of these phenomena suggests the potential influence of excitonic electron-hole interactions on the transition—an assertion corroborated by the lack of superconductivity and similarities to other topological materials.

In contrast to NaAlSi, which shows superconductivity potentially mediated by electron-phonon interactions [1], KAlGe exhibits no superconductivity above 1.8 K despite its high mobility [3]. Instead, its low-temperature properties seem to stem from strong electron-electron interactions that trigger structural and electronic transitions. The nature of the transition remains unclear, but it is thought to involve excitonic instability, a phenomenon wherein electron-hole pairs are generated, hence destabilizing the initial metallic phase.

These findings emphasize the importance of understanding such interactions and structural changes, since they are key to unveiling new physics in topological materials. Through this work, KAlGe emerges as a novel platform for studying interplay between topology, electron correlations, and structural instabilities. It bridges the gap between conventional semimetals and correlated topological phases, offering potential insights into the mechanisms behind electronic phase transitions in the layered topological materials.

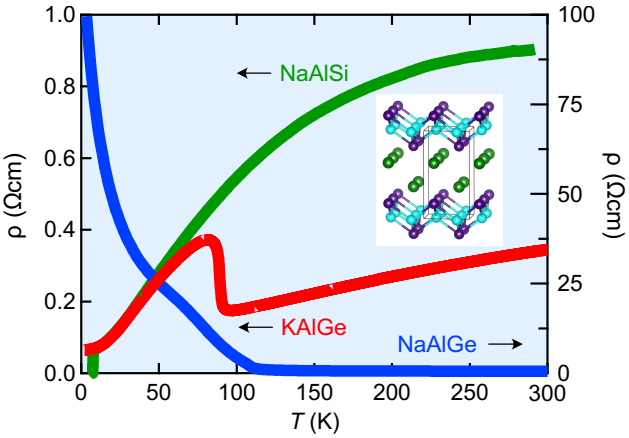

Fig. 1. Temperature dependence of the in-plane electrical resistivity for KAlGe (red line), NaAlGe (blue line), and NaAlSi (green line) single crystals. The inset shows the representative crystal structure of this series, which consists of the alternate stacking of edge-shared Al-(Si, Ge)$_4$ tetrahedra and alkali metal sheets.

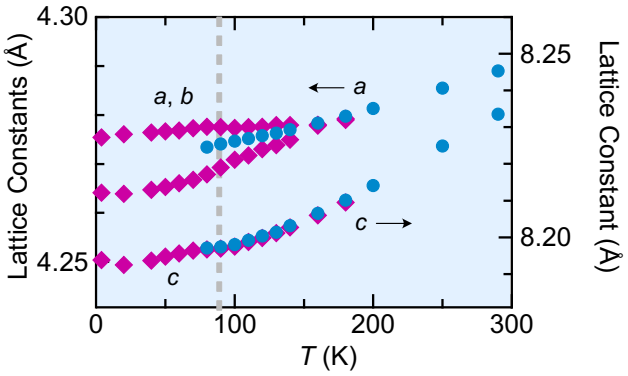

Fig. 2. Temperature dependence of lattice constants analyzed by the Rietveld method on the basis of a tetragonal system (sky blue solid circles) and an orthorhombic system (magenta solid diamonds).

References

[1] T. Yamada *et al.*, J. Phys. Soc. Jpn. **90**, 034710 (2021).
[2] D. Hirai *et al.*, J. Phys. Soc. Jpn. **91**, 024702 (2022).
[3] T. Yamada *et al.*, J. Phys. Soc. Jpn. **91**, 074801 (2022).
[4] T. Ikenobe *et al.*, Phys. Rev. Mater. **7**, 104801 (2023).
[5] T. Ikenobe *et al.*, Chem. Mater. **37**, 189 (2025).

Authors

T. Ikenobe, T. Yamada[a], J. Yamaura, T. Oguchi[b], R. Okuma, D. Hirai[c], H. Sagayama[d], Y. Okamoto, and Z. Hiroi

[a]Tohoku University
[b]The University of Osaka
[c]Nagoya University
[d]High Energy Accelerator Research Organization (KEK)

Stroboscopic Time-of-Flight Neutron Diffraction in Pulsed Magnetic Fields

Nakajima and Kohama Groups

Exploring new quantum states of matter in high magnetic fields is one of the central topics in condensed matter physics. In fact, novel field-induced phases, such as spin-lattice-coupled magnetization plateaus in frustrated spin systems [1], have been extensively investigated to this date. Neutron scattering is one of the most powerful techniques to study magnetic materials because it can probe Fourier-transformed time-space correlation functions of magnetic moments; specifically magnetic structures are determined by the elastic scattering and magnons are measured by the inelastic scatterings. However, the highest magnetic field for neutron scattering instruments is limited to approximately 15 T even for state-of-the-art superconducting magnets.

To enhance the capability of high-field neutron scattering, we recently developed a long-pulsed magnet for time-of-flight (TOF) neutron diffraction measurements [2]. Figure 1 shows a typical temporal profile of the long-pulsed magnetic field. The full-width at half-maximum of the field pulse exceeds 100 ms, which is much longer than the timescale for TOF neutron diffraction measurements. Specifically, the temporal pulse width of a polychromatic neutron pulse, which normally contains wavelengths ranging from 0.5 to 5 Å, will reach approximately 10 ms after flying a typical source-to-sample distance of the existing neutron diffractometers. The pulse width of our long-pulsed magnet is sufficiently longer than this timescale, and therefore all the wavelengths included in a polychromatic neutron pulse can satisfy the high-field condition. In other words, our long-pulsed magnetic field can be regarded as a quasistatic magnetic field for a neutron pulse.

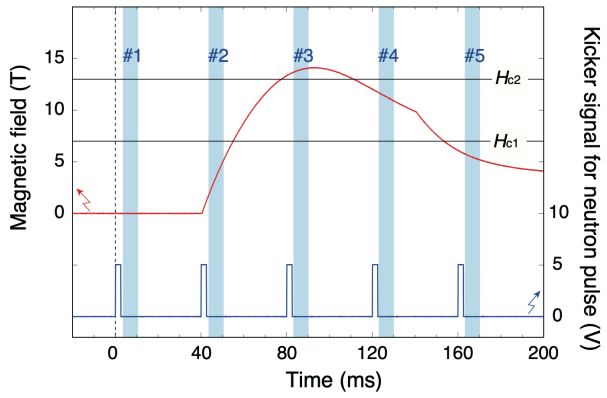

Fig. 1. The temporal profile of the long pulsed magnetic field, and the kicker signals for neutron pulse generation. The neutron pulses are triggered by the rising edges of the kicker signals. The vertical blue bars show the time range in which the sample is exposed to the neutrons with wavelengths ranging from 1 to 3 Å. H_{c1} and H_{c2} are critical fields for magnetic phase transitions in $CuFeO_2$ at 4 K.

We performed TOF neutron diffraction measurements on a frustrated triangular lattice magnet $CuFeO_2$ with this long-pulsed magnet at the small and wide-angle neutron diffractometer TAIKAN in the Materials and Life-science experimental Facility (MLF) of Japan Proton Accelerator Research Complex (J-PARC). The application of the pulsed magnetic field was synchronized with the pulsed neutron beam and repeated about 100 times. As a result, we obtained neutron diffraction intensity maps with varying magnetic field. Figure 2 shows the typical intensity maps at selected magnetic fields. We successfully observed magnetic phase transition from the four-sublattice antiferromagnetic state with the magnetic modulation wavevector of q=(1/4,1/4,0) to the 1/5-magnetization plateau phase with q=(1/5,1/5,0) [2].

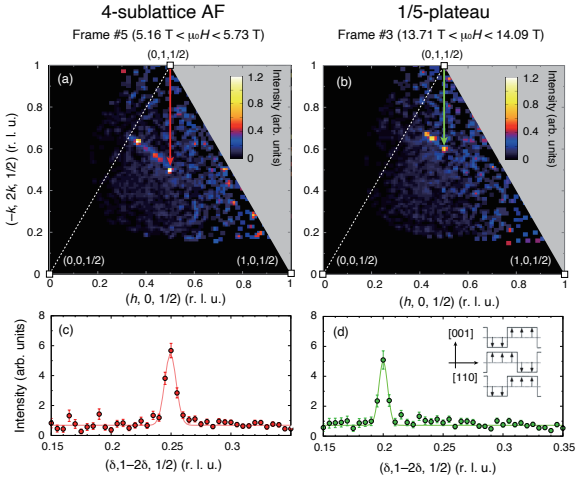

Fig. 2. Intensity maps of the (H,K,1/2) plane in (a) the 4-sublattice phase and (b) the 1/5-plateaus phase of $CuFeO_2$. [(c),(d)] 1D line-cut profiles along the (-k, 2k, 1/2) direction measured in the (c) 4-sublattice and (d) 1/5-plateau phases.

We note that the combination of short pulsed-magnetic fields and a pulsed neutron beam has been already established in previous studies [3]. The advantage of our long-pulsed magnetic field is that we can utilize much wider wavelength range in high magnetic fields as compared to the short-pulsed magnet. Although the highest magnetic field for our setup is still below 15 T, we are going to improve the magnet to generate magnetic fields more than 20 T in the future.

References

[1] H. Ueda *et al.*, Phys. Rev. Lett. **94**, 047202 (2005).
[2] T. Nakajima *et al.*, Phys Rev. Res. **6**, 023109 (2024).
[3] H. Nojiri *et al.*, Phys. Rev. Lett. **106**, 237202 (2011).

Authors

T. Nakajima, M. Watanabe[a], Y. Inamura[a], K. Matsui, T. Kanda, T. Nomoto, K. Ohishi[b], Y. Kawamura[b], H. Saito, H. Tamatsukuri[a], N. Terada[c], and Y. Kohama
[a]J-PARC center/JAEA
[b]CROSS
[c]NIMS

Dirac Magnons in Honeycomb-Lattice $NiTiO_3$

Masuda Group

Since the discovery of topological insulators, the concept of topology has become widely recognized as an important aspect of condensed-matter physics. These materials host massless Dirac fermions on their edges or surfaces, giving rise to phenomena such as the quantum Hall effect. Recently, potential applications for highly efficient spintronic devices that exploit spin currents along these edges or surfaces have attracted significant attention. Moreover, the notion of topology has been extended from fermionic to magnonic systems, as evidenced by phenomena such as the thermal Hall effect.

Inelastic neutron scattering (INS) experiments have confirmed the existence of topological magnons in several materials. For example, in layered honeycomb-lattice ferromagnet CrI_3 [1] and three-dimensional ferromagnet Mn_5Ge_3 [2], bulk magnon dispersions exhibit gaps at the K point, and theoretical calculations predict the presence of edge states—Dirac magnons—within these gaps. Dirac magnons have also been observed in the three-dimensional antiferromagnet Cu_3TeO_6 [3] and in the ilmenite-type antiferromagnet $CoTiO_3$ [4], where linear band crossings at the K point create Dirac cones for both bulk and edge modes. These findings underscore the rapid expansion of topological motifs in magnonic systems that mirror those long explored in electronic counterparts.

In this study, we investigate $NiTiO_3$ [5], which has the same crystal structure and magnetic ordering as $CoTiO_3$. Magnetic-susceptibility measurements reveal that $NiTiO_3$ exhibits stronger interlayer interactions, whereas $CoTiO_3$ is dominated by intralayer coupling. To determine the spin Hamiltonian and examine the presence of Dirac magnons in $NiTiO_3$, we conducted single-crystal INS experiments.

Measurements were performed using the multiplex spectrometer HODACA at JRR-3 and the triple-axis spectrometer CTAX at ORNL/HFIR [6]. Figure 1(a) shows the INS spectrum measured by HODACA along the (0, 0, *l*) direction, revealing spin-wave excitations with a band energy of 3.7 meV. Using linear spin-wave theory (LSWT), experimental data were accurately reproduced (Fig. 1(b)) by a model incorporating exchange interactions and easy-plane anisotropy. This model confirmed $NiTiO_3$ as a three-dimensional magnet in which interlayer coupling outweighs intralayer coupling. Moreover, whereas nearest-neighbor interactions suffice to describe $CoTiO_3$, modeling $NiTiO_3$ demands exchange paths extending to third-nearest neighbors within the *ab* plane.

Figure 1(c) shows the INS spectra measured by CTAX along the high-symmetry path Γ_1-M-K-Γ_2. Near the K point, considering the instrumental energy resolution, the spectra were fitted by single Gaussian at the K point and two Gaussians near the K point. The dispersion relations calculated using the best fit parameters, shown in Fig. 1(d), reveal two modes that intersect linearly at the K point, confirming the formation of Dirac cones in $NiTiO_3$, just as in $CoTiO_3$. Previous work [4] argued that Dirac magnons remain stable against anisotropy and further-neighbor interactions. Our study experimentally demonstrates that Dirac magnons persist even with significant interlayer coupling and second- and third-neighbor interactions within the honeycomb layer.

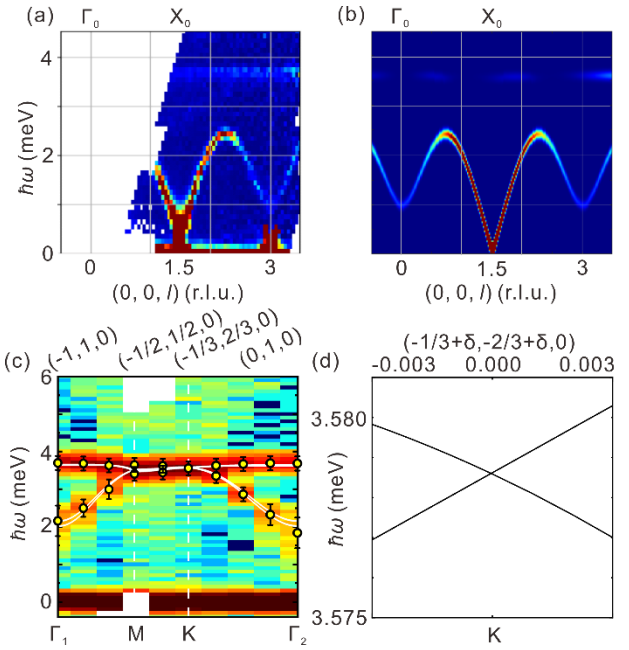

Fig. 1. (a, b) (a) INS spectra along the (0, 0, *l*) direction measured by HODACA, and (b) calculated INS spectra using linear spin-wave theory. (c) Pseudocolor plot of INS spectra measured by CTAX along the reciprocal lattice points Γ_1-M-K-Γ_2. White lines represent dispersion relations calculated using LSWT, yellow dots indicate peak positions obtained by Gaussian fitting, and error bars correspond to the full width at half maximum (FWHM) from the Gaussian fitting. (d) Enlarged view of the calculated dispersion relations near the K point.

References

[1] L. Chen *et al.*, Phys. Rev. X **8**, 041028 (2018).
[2] M. dos Santos Dias *et al.*, Nat. Commun. **14**, 7321 (2023).
[3] W. Yao *et al.*, Nat. Phys. **14**, 1011 (2018).
[4] B. Yuan *et al.*, Phys. Rev. X **10**, 011062 (2020).
[5] K. Dey *et al.*, Phys. Rev. B **103**, 134438 (2021).
[6] H. Kikuchi *et al.*, J. Phys. Soc. Jpn. **94**, 024703 (2025).

Authors

H. Kikuchi, M. Ozeki, N. Kurita[a], S. Asai, T. J. Williams[b], T. Hong[b], and T. Masuda
[a]Institute of Science Tokyo
[b]Oak Ridge National Laboratory

A New Inelastic Neutron Spectrometer HODACA

Masuda Group

Neutron scattering is an indispensable experimental technique in a wide range of fields including physics, chemistry, and engineering. In 1949, Nobel Laureate C.G. Shull demonstrated its usefulness by elucidating the magnetic structure of the antiferromagnet MnO using neutron scattering [1]. Particularly, inelastic neutron scattering (INS) has proven to be a powerful tool for observing collective excitations of atoms and spins in condensed matter. These collective modes are characterized by a wavevector $\boldsymbol{Q}$ and energy E, thus measuring them allows for the determination of the system's Hamiltonian. The dynamics of crystals [2], magnetic materials [3], and other systems have been actively studied using this technique.

The neutron triple-axis spectrometer (TAS) has been widely used in both inelastic and elastic scattering experiments since its development in the 1950s, establishing its position as a versatile and important spectrometer [4]. By using a single analyzer and detector along with a focused neutron beam, TAS allows for high signal-to-noise (S/N) ratio measurements at specific $\boldsymbol{Q}$-E points. On the other hand, chopper spectrometers employ an array of detectors surrounding the sample, combined with time-of-flight energy analysis, enabling efficient measurements across a wide $\boldsymbol{Q}$-E space. Recently, there has been a global trend in the design, construction, and operation of multiplex-type spectrometers, which combine high S/N measurements with efficient $\boldsymbol{Q}$-E space coverage [5]. In this study, we constructed a multiplex spectrometer called HODACA (HOrizontally Defocusing Analyzer Concurrent data Acquisition) based on the inverse Rowland inelastic spectrometer (IRIS) concept proposed by Harriger and Zaliznyak [6]. The instrument was installed at the C11 beam port of the research reactor JRR-3 [7].

As shown in Fig. 1, the HODACA spectrometer employs an array of analyzers arranged on a Rowland circle to refocus scattered neutrons. Due to the inscribed angle theorem, the reflection angles of all analyzers remain constant, and the trajectories of the neutrons form a pattern as if they are diffused from a sample image. Neutrons are then detected by an array of detectors positioned on a circle centered on the sample image. The use of radial collimators before and after the analyzers is expected to effectively reduce background noise. This spectrometer enables efficient and high-S/N measurements across a wide $\boldsymbol{Q}$-space at constant energy. As a result, HODACA became a spectrometer capable of measuring spectra from −1 meV to 7 meV by fixing the scattered neutron energy Ef at 3.635 meV. It consists of 24 analyzers and 24 detectors spaced at 2◦ intervals, covering a scattering angle A2 of 46◦. Each analyzer is composed of 3 to 7 PG crystals mounted in a vertically focusing configuration. The vertical size of each analyzer (number of PG crystals) is determined to ensure that the solid angles spanned by the analyzer viewed from the sample position are the same. Radial collimators with divergence angle of 2° are installed between the sample-analyzer and analyzer-detector to minimize cross-talk of scattered neutrons from neighboring analyzers.

For the standard sample to measure INS spectra, we selected the frustrated magnetic compound $CsFeCl_3$. Its dispersion relation at ambient pressure is well described by the Extended Spin Wave Theory (ESWT) [8]. The INS spectrum measured by the HODACA spectrometer is shown in Fig. 1(b), where $\boldsymbol{Q}$ = (1/3, 1/3, l) direction. The white lines in the figure represent the dispersion curves calculated using ESWT parameters from previous studies. The experimental results are well reproduced by the calculations using the previously reported parameters. An ideal spectrometer for measuring dynamics in the energy range of cold neutrons is now ready for users.

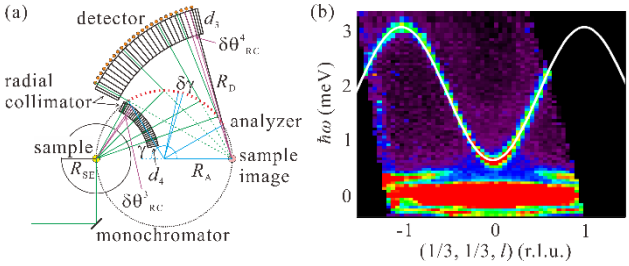

Fig. 1. (a) Representative figure of HODACA spectrometer. Green lines indicate the neutron paths. (b) False color plots for the (1/3, 1/3, l) direction. The integration ranges are (1/3 ± 0.05, 1/3 ± 0.05, l). The white curves represent the dispersion curves obtained from ESWT.

References

[1] C. G. Shull and J. S. Smart, Phys. Rev. **76**, 1256 (1949).
[2] R. Pynn and G. L. Squires, Proc. R. Soc. A **326**, 347 (1972).
[3] M. F. Collins et al., Phys. Rev. **179**, 417 (1969).
[4] G. Shirane, S. M. Shapiro, and J. M. Tranquada, Neutron Scattering with a Triple-Axis Spectrometer (Cambridge University Press, Cambridge, U.K., 2008).
[5] F. Groitl *et al.,* Rev. Sci. Instrum. **87**, 035109 (2016).
[6] L. Harriger and I. Zaliznyak, 2015 NCNR Annual Report (2015) p. 46
[7] H. Kikuchi *et al.,* J. Phys. Soc. Jpn. **93**, 091004 (2024).
[8] S. Hayashida, M. Matsumoto, M. Hagihala, N. Kurita, H. Tanaka *et al.,* Sci. Adv. **5**, eaaw5639 (2019).

Authors

H. Kikuchi, S. Asai, T. J. Sato[a], T. Nakajima, L. Harriger[b], I. Zaliznyak[c] and T. Masuda
[a]Tohoku University
[b]National Institute of Standards and Technology
[c]Brookhaven National Laboratory

Experimental Verification of a New Magnetic Concept—Observation of Altermagnetic Materials via Neutron Scattering Experiments—

Masuda Group

Background of the Research: Magnetic materials have traditionally been classified into two categories based on their microscopic spin structure: ferromagnetic materials, where spins align parallel, and antiferromagnetic materials, where spins align antiparallel. Recently, a third type of magnetic material, known as "altermagnetic materials," has been proposed [1]. This new classification is based on the symmetry of not only the spins but also the surrounding crystal structure. In antiferromagnetic materials, the crystal structure around adjacent spins is identical. However, in altermagnetic materials the crystal structures around up-spins and down-spin do not overlap without a 90-degree rotation. Thus, these materials are classified as altermagnetic when the spins are arranged antiparallel with distinct crystal symmetries.

The altermagnetic materials predicted the existence of chiral magnons, which are quasiparticles that can carry spin current [2]. While the chiral magnons in ferromagnetic materials have been studied, their application in spintronics devices is limited due to low-frequency (GHz) operation and undesirable stray magnetic fields due to non-zero magnetization. On the other hand, antiferromagnetic materials promise high-frequency (THz) operation, but their magnons' chirality cancels out, preventing spin current. Altermagnetic materials combine the advantages of both. Their magnons are theoretically predicted to exhibit large chiral splitting at high frequencies, capable of generating spin current. Despite having zero magnetization like antiferromagnetic materials (eliminating stray fields), they possess chiral magnons similar to ferromagnetic materials, making them ideal for device applications. Observing the magnons in altermagnetic materials is crucial both for verifying their properties and exploring their application potential. Until now, no successful observation had been made.

Content of the Research: The observed neutron spectra are shown in Figs. 1(a) and 1(c). In Fig. 1(a), at high energies above E = 30 meV, a magnon splitting of approximately 2 meV, indicated by white circles, was observed. On the other hand, the magnon dispersion in the low-energy, small-momentum region rises linearly, similar to that of an antiferromagnet. These are crucial pieces of evidence for the existence of alternating magnets.

Figure 1(c) shows the high-energy spectrum in a different momentum region, where the alternating propagation of the split magnon dispersion along the momentum axis was clearly observed. The calculated magnon dispersion is shown in Figs. 1(b) and 1(d) by black solid and dashed lines. The calculations perfectly reproduced the observed neutron spectra. Furthermore, when counterclockwise chirality is represented in red and clockwise chirality in blue, at low energies, the two chiralities cancel each other out, resulting in a colorless region. However, at higher energies, the two magnons have different chiralities, clearly appearing in blue and red. In Fig. 1(d), it was confirmed that the chirality alternates. From these results, it became clear that the observed magnons are chiral magnons that carry spin current.

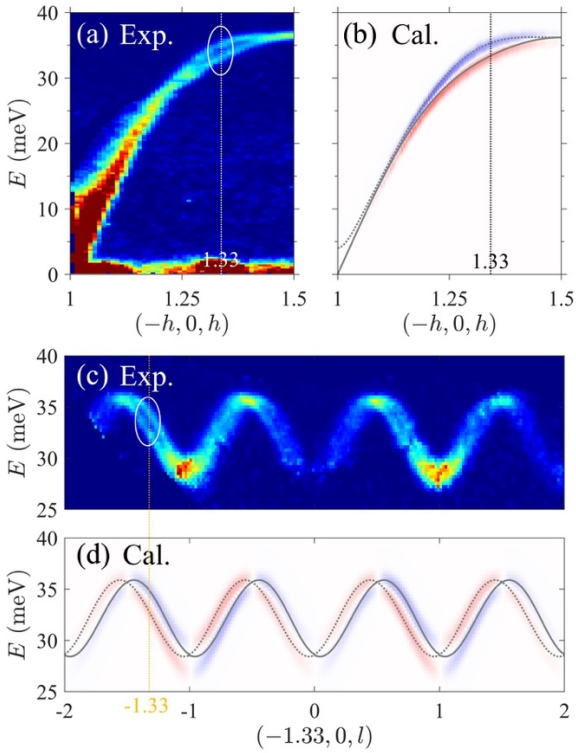

Fig. 1. (a) & (c) Neutron spectra of MnTe. These show different momentum regions, but h = 1.33 in (a) and l = -1.33 in (c) represent the same momentum (-1.33, 0, -1.33). At this momentum, a magnon splitting of approximately 2 meV was observed. (b) & (d) Calculated magnon chirality. Red and blue represent magnons with different chiralities. The gray solid and dashed lines indicate the calculated magnon dispersion.

Future Prospects: Altermagnetic materials represent a new concept in magnetism. The experimental verification of chiral magnons in this study reveals their potential to generate spin current. This discovery paves the way for future advancements in high-speed, efficient electronic devices, potentially revolutionizing everyday life.

References

[1] L. Šmejkal, J. Sinova, and T. Jungwirth, Phys. Rev. X **12**, 040501 (2022).
[2] M. Naka, S. Hayami, H. Kusunose, Y. Yanagi, Y. Motome, and H. Seo, Nat. Commun. **10**, 4305 (2019).

Authors

L. Zheyuan, M. Ozeki, S. Asai, S. Itoh[a], T. Masuda,
[a]KEK

Nano Structure and Rheological Properties of Carrageenan Gels

Mayumi Group

Carrageenans are polysaccharides used in food and biotechnological applications. In our study, we focus on three types of carrageenans, κ-(KC), ι-(IC), and λ-(LC) carrageenans with different numbers and positions of sulfate groups. By decreasing temperature, carrageenan aqueous solutions become gels in which carrageenan chains are cross-linked by aggregated domains of helical chains (Fig. 1). We investigated the hierarchical structure of the carrageenan gels by SANS to understand the microscopic origin of their mechanical properties [1].

Figure 2 shows the temperature dependence of elastic modulus *G*' and loss modulus *G*'' of KC, IC, and their mixtures, KCIC gels. For KC and IC gels, *G*' increases drastically at a certain temperature, where sol-gel transition occurs. *G*' of KC gel is larger than that of IC gel, indicating that KC gel is stiffer than IC gel. KCIC gel exhibits a two-step increase of *G*', corresponding to independent aggregation of KC and IC chains in KCIC gel.

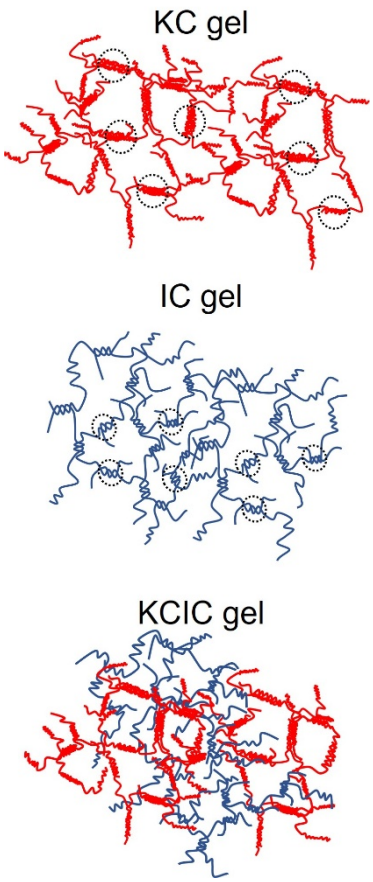

Fig. 1. Network structure of carrageenan gels.

To study the microscopic structure of KC, IC and KCIC gels, we performed SANS measurements at SANS-U. The SANS profiles are converted to Kratky plots in Fig. 3. In the Kratky plots, a peak was observed at 0.06 Å^{-1} for KC gel, 0.07 Å^{-1} for KCIC gel, and 0.09 Å^{-1} for IC gel, respectively. This suggests that the chain aggregate in KC gel is larger than that in IC gel, which results in the higher elastic modulus of KC gel.

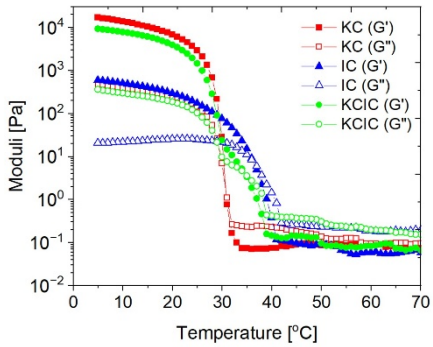

Fig. 2. Temperature dependence of elastic modulus G' (solid symbols) and loss modulus G" (open symbols) of KC (red, square), IC (blue, triangle), and KCIC (green, circle).

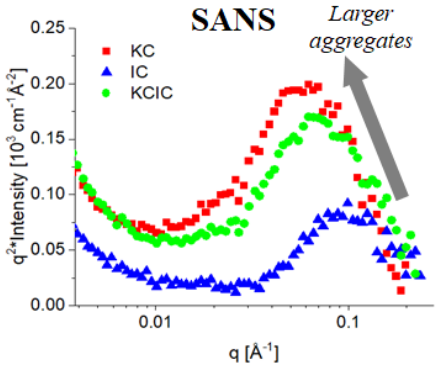

Fig. 3. Krathky plot of SANS profiles for different types of carrageenan gels.

References

[1] L. Geonzon, K. Hashimoto, T. Oda, S. Matsukawa and K. Mayumi, Macromolecules, **56**, 8676 (2023).

Authors

K. Mayumi, and L. C. Geonzon

Boson Peaks of Simple Molecular Glasses Studied by Adiabatic Calorimetry and Inelastic Neutron Scattering

Yamamuro Group

The boson peak is one of the important unresolved problems of glass, along with glass transition. This excitation peak universally exists around an energy (E) range of 2-5 meV for most of glasses with quite different hardness from oxide glasses to molecular glasses. Although it is known that the temperature variation of the peak intensity can be scaled by the Bose factor (harmonic oscillator approximation) and that the peak energy does not change with respect to the momentum transfer Q (suggesting local excitation), the origin of the peak is still unclear.

Our group has been studying the boson peak for many years, mainly focusing on simple molecular glasses [1-3]. Molecular glasses aggregate through simple van der Waals interactions and so suitable for the collaboration with theoretical and molecular dynamics works. Although simple molecules crystallize readily upon cooling, we have prepared glasses at low temperatures (< 5 K) by using a vapor-deposition (VD) method, whose cooling rate is faster than 10^7 K/s. The most effective experimental tool to study boson peaks is inelastic neutron scattering (INS), which provides vibrational density of states. Another effective method is heat capacity (C_p) measurement. We use an adiabatic method to obtain absolute C_p values accurately.

We have examined three VD glasses with different molecular structures; CCl_4 (tetrahedral, van der Waals), CS_2 (linear molecule, van der Waals) and water (dog-leg-shape, hydrogen bond). They are vitrified at 5 K with custom-made cryostats for VD samples [2,3] and measured in situ with BL14, AMATERAS at J-PARC, MLF and an adiabatic calorimeter at our laboratory.

Figure 1 shows the INS data for the three samples. For CCl_4 and CS_2, $S(Q,E)$ of the glassy sample was clearly larger than that of the crystalline states. As known in the previous studies, there was no Q dependence of the peak energy and the peak intensity was enhanced at the second and third peaks of $S(Q)$. Figure 2 shows the heat capacities

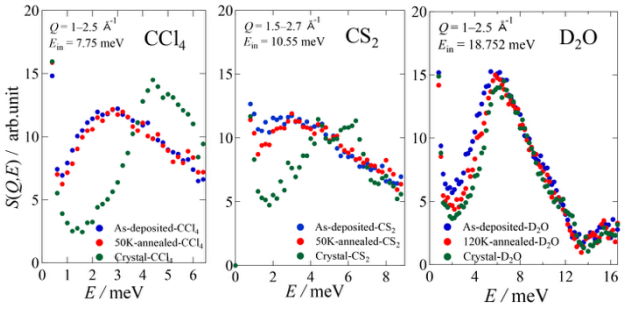

Fig. 1. Dynamic structure factors of glassy and crystalline CCl_4, CS_2 and D_2O.

of the three samples. Apparently, excess heat capacities were observed in CCl_4 and CS_2. The curve in Fig. 2 was calculated through the density of states $G(E)$ which was calculated from $S(Q,E)$ by the established method [1-3]. During this calculation, the scale factor to link the neutron and calorimetric data was determined. The agreement between the experimental and calculated data was satisfactory except high temperature region where anharmonic effects become important. Figure 3 gives the "absolute value" of the density of states divided by squared energy. It should be noted that this value is obtained by combining the data of the INS and adiabatic calorimetry. The gray-shaded area, corresponding to the degrees of freedom related to the boson peak, is 0.48 for CCl_4 and 0.22 for CS_2. We have integrated $G(E)$ up to 15 meV to discuss the origin of the boson peak. Interestingly, there is no difference between the glassy and crystalline states, and the integrated $G(E)$ was about 6 for CCl_4 and 5 for CS_2, both corresponding to the sum of the translation and rotation degrees of freedom. The present result has indicated an important fact that there is no extra degrees of freedom for the boson peaks of molecular glasses.

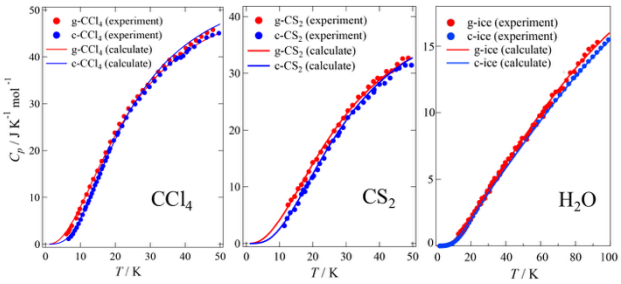

Fig. 2. Heat capacities of glassy and crystalline CCl_4, CS_2 and H_2O. The curves are calculated from the INS data.

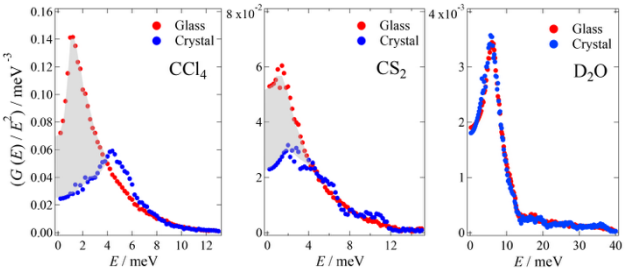

Fig. 3. Absolute density of states divided by squared energy for glassy and crystalline CCl_4, CS_2 and D_2O. The excess parts due to the boson peaks are shaded.

References

[1] O. Yamamuro *et al.*, J. Chem. Phys. **105**, 732 (1996).
[2] O. Yamamuro *et al.*, J. Chem. Phys. **106**, 2997 (1997).
[3] O. Yamamuro *et al.*, J. Chem. Phys. **115**, 9808 (2001).

Authors

X. Wu, Y. Zhao, H. Akiba, Y. Ohmasa, M. Kofu, and O. Yamamuro

Large Thermodynamic Signatures of In-gap Fermionic Quasiparticle states in YbB_{12}

Kohama Group

YbB_{12} is a 3D mixed-valence Kondo insulator with a well-developed charge gap. Intriguingly, previous studies found quantum oscillations in resistivity and magnetic torque—signatures associated with metallic Fermi surfaces. More recently, metallic-like thermal conductivity has been reported in its insulating regime, violating the Wiedemann–Franz law by orders of magnitude and suggesting the presence of charge-neutral mobile excitations. However, related thermodynamic signatures—particularly in bulk probes like specific heat (C) and magnetocaloric effect (MCE)—had been elusive. The present study fills that gap by identifying sharp anomalies in C and MCE under high magnetic fields, offering evidence of emergent in-gap fermionic quasiparticles.

In this study, we carried out high-resolution measurements of C, MCE, magneto-resistance (ρ_{xx}) and Hall resistivity (ρ_{xy}) in pulsed (up to 60 T) and static (up to 35 T) magnetic fields [1]. We found a sequence of distinct double-peak features in C/T at 11, 16, 19.6 and 30 T, as shown in Fig. 1(d). The double-peak structure displays a characteristic temperature-dependent splitting, which becomes more pronounced at higher temperatures, as shown in Fig. 2. The MCE exhibits a single peak feature at corresponding field regions (Fig.1(c)). On the other hand, the ρ_{xy} and ρ_{xx} show smooth features across these low-field thermodynamic anomalies (Fig. 1(a)-(b)), suggesting they are not due to conventional electronic excitation.

The double-peak structure in C/T, whose separation scales linearly with 4.8 k_BT, aligns with theoretical expectations for fermionic DoS singularities passing over the Fermi level, akin to Landau level crossings [2]. The magnitude and bulk nature of the anomalies rule out trivial sources (e.g., Schottky contributions, phonons, impurity spins). Compared with narrow-gap electronic models, the features in YbB_{12} do not exhibit thermally activated behavior, implying the formation of Fermi surface. Angular measurements revealed a four-fold rotational symmetry in the field positions of the thermodynamic anomalies, further confirming their bulk origin, as opposed to surface states [1]. Our tentative calculation supports a strong interaction-induced fractionalization of the electron, leading to the emergence of electrically neutral fermionic excitations [1].

Further theoretical work is needed to unravel the microscopic origin of peak structures—whether neutral spinon, composite excitons, or other emergent quasiparticles. Future experimental avenues include spectroscopic probes and exploring related correlated insulators to generalize the findings. Through high-field and low-temperature measurements, the present study reveals pronounced thermodynamic anomalies indicative of in-gap fermionic quasiparticles in YbB_{12}. This marks a major advance in understanding Kondo insulators and sets the stage for deeper explorations into electron fractionalization in strongly correlated materials.

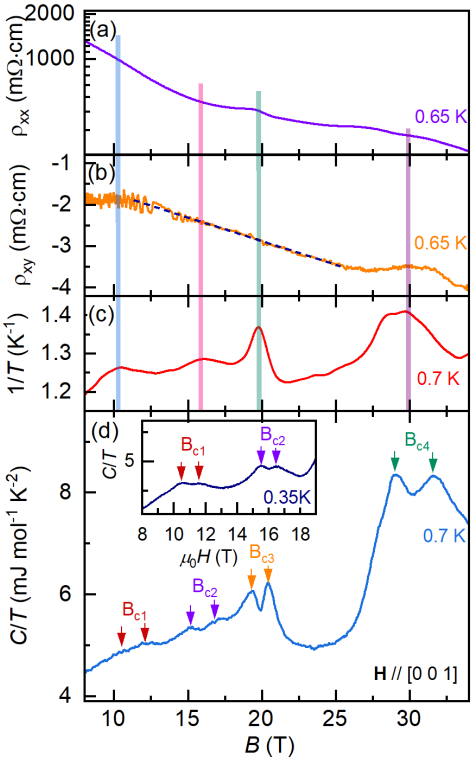

Fig. 1. Comparison of magnetoresistance (ρ_{xx}), Hall resistivity (ρ_{xy}), MCE and specific heat (C) of YbB_{12} as a function of magnetic field.

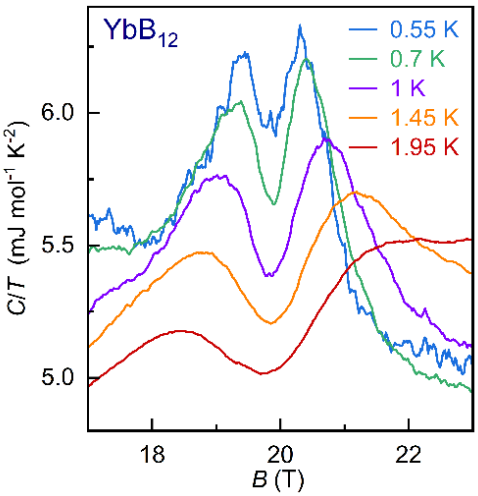

Fig. 2. Specific heat divided by temperature (C/T) as a function of the magnetic field at indicated temperature.

References

[1] Z. Yang *et al.*, Nature Communications **15** (1), 7801 (2024).

[2] Z. Yang *et al.*, Nature Communications **14** (1), 7006 (2023). **Editor's highlights**

Authors

Z. Yang and Y. Kohama

Ultrahigh Magnetic Field Effect on the Dielectric Constant in the Nonmagnetic Archetypal Ferroelectric $BaTiO_3$

Y. H. Matsuda Group

The magnetic field effect of the covalent bond between atoms is generally small because the magnetic field available in a laboratory is typically around 10 T, and its Zeeman energy is much smaller than the bonding energy. However, the covalency of a specific chemical bond in ferroelectric is affected by a temperature change near the transition temperature (T_c). Namely, the ion position shifts, and electrical polarization appears, which can be regarded as a phenomenon that occurs by changing the covalency of a specific chemical bond. Since the chemical bond generally becomes soft in the vicinity of the T_c, we may have a chance to observe a significant magnetic field effect on the covalency in ferroelectrics if the magnetic field is strong enough.

Recently, several new techniques for measurements in ultrahigh magnetic fields exceeding 100 T have been developed [1-7]. One of them is on the measurement of the dielectric constant [7]. Here, we introduce the technique for the dielectric measurement and a preliminary result on the dielectric constant of an archetypal ferroelectric $BaTiO_3$.

Figure 1 shows the schematic diagram of the dielectric constant measurement in ultrahigh magnetic fields exceeding 100 T. The single-turn coil magnetic field generator at ISSP, UTokyo, was used to generate a magnetic field of up to 120 T for the present work. The radio frequency (RF) modulated electromagnetic wave (34 MHz) is introduced to the sample, and the transmission signal is recorded by the oscilloscope. The recorded RF data is modulated by the change in the sample dielectric constant. The sample temperature is controlled by a hand-made heater and is measured by a thermocouple placed near the sample.

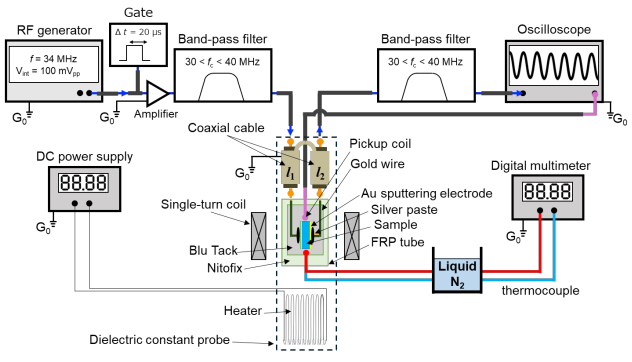

Fig. 1. Schematic diagram of the RF dielectric constant measurement setup.

The single crystal of $BaTiO_3$ was used for the experiment. The T_c was found to be near 393 K. Before the high magnetic field experiment, the electrical polarization (P) direction was forced to be aligned by the poling process with the application of high voltage.

The result of the magnetic field dependence of the dielectric constant (ε) is shown in Fig. 2. The RF signal detected is converted to ε through the calibration curve that is obtained by the temperature dependence of the dielectric constant of the sample.

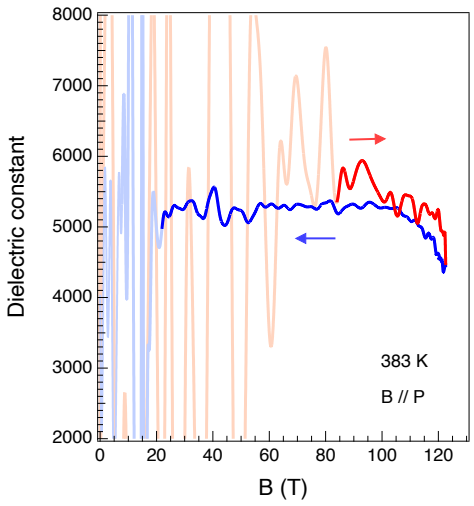

Fig. 2. The magnetic field dependence of the dielectric constant [7].

The dielectric constant decreases by a magnetic field (B) when the field exceeds near 100 T. We confirmed that similar results are obtained whenever the B is parallel to the P and the temperature is close to T_c. However, there appears to be no reduction of the ε appears in high magnetic fields when $B \perp P$ or the temperature is far from T_c [7]. Currently, one of the possible explanations is an enhancement of the covalency and resultant stabilization of the ferroelectric phase by a magnetic field. Further studies in the future will elucidate the origin of the field-induced change in ε.

References

[1] S. Takeyama, R. Sakakura, Y. H. Matsuda, A. Miyata, and M. Tokunaga., J. Phys. Soc. Jpn. **81**, 014702 (2012).
[2] A. Ikeda T. Nomura, Y. H. Matsuda, S. Tani, Y. Kobayashi *et al.,* Rev. Sci. Instrum. **88**, 083906 (2017).
[3] T. Nomura, A. Hauspurg, D. I. Gorbunov, A. Miyata, E. Schulze *et al.,* Rev. Sci. Instrum. **92**, 063902 (2021).
[4] D. Nakamura, M. M. Altarawneh, and S. Takeyama, Meas. Sci. Technol. **29**, 035901 (2018).
[5] T. Shitaokoshi S. Kawachi, T. Nomura *et al.*, Rev. Sci. Instrum. **94**, 094706 (2023).
[6] S. Peng X-G. Zhou, Y. H Matsuda, Q. Chen *et al.*, Supercond. Sci. Technol. **38**, 075012 (2025).
[7] P. Chiu Y. Ishii, and Y. H. Matsuda, J. Appl. Phys. **137**, 155903 (2025).

Authors

P. Chiu, Y Ishii, and Y. H. Matsuda

Unveiling van Hove Singularity Modulation and Fluctuated Charge Order in Kagome Superconductor CsV_3Sb_5

Okazaki Group

The kagome lattice, characterized by its corner-sharing triangle geometry, hosts distinctive electronic structures such as topological flat bands, Dirac bands, and van Hove singularities (VHS) [Fig. 1(a)]. These features enable kagome materials to support exotic electronic phases. Recently, the kagome metals AV_3Sb_5 (A = K, Rb, Cs) have attracted intense interest due to diverse phenomena [1] including superconductivity, charge-density wave (CDW), pair density wave, and giant anomalous Hall effects. The suppression of CDW by pressure or doping in AV_3Sb_5 enhances superconductivity, illustrating a strong interplay between these two states.

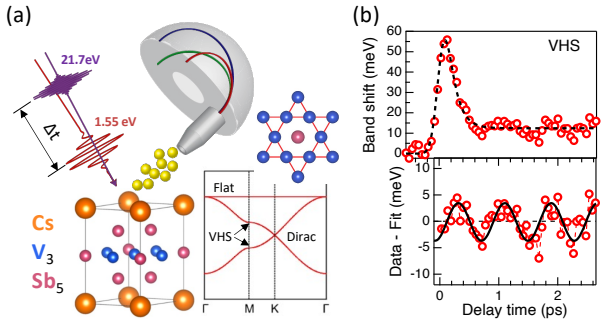

Fig. 1. (a) Schematic plots for kagome-lattice's band structure, time-resolved ARPES experimental setup, and the crystal structure of CsV_3Sb_5. (b) Temporal energy shift of the van Hove singularity and its coherent oscillation.

Despite significant research efforts [1], the microscopic origin of CDW remains under active debate. Angle-resolved photoemission spectroscopy (ARPES) experiments suggest an electronic instability mechanism, highlighting VHS near the Fermi level (E_F) with favorable nesting conditions. This is further supported by the absence of the acoustic phonon anomalies. Conversely, density functional theory calculations indicate lattice instabilities via unstable phonon modes, corroborated by lattice distortions observed in scanning tunneling microscopy and x-ray diffraction experiments. Due to the complex interplay between electrons and phonons, static experimental methods face limitations in conclusively identifying the primary driving force behind the CDW.

To address these challenges, we conducted comprehensive time-resolved ARPES measurements on CsV_3Sb_5 [2], providing direct insights into the dynamic interplay of electrons and phonons. We demonstrate an ultrafast response of the VHS to laser excitation [Fig. 1(b)]. Remarkably, upon ultrafast optical pumping, the VHS immediately shifts closer to E_F, altering the electronic density of states. Moreover, these energy shifts exhibit coherent oscillations at a frequency of approximately 1.3 THz, matching a previously reported phonon mode strongly associated with the CDW.

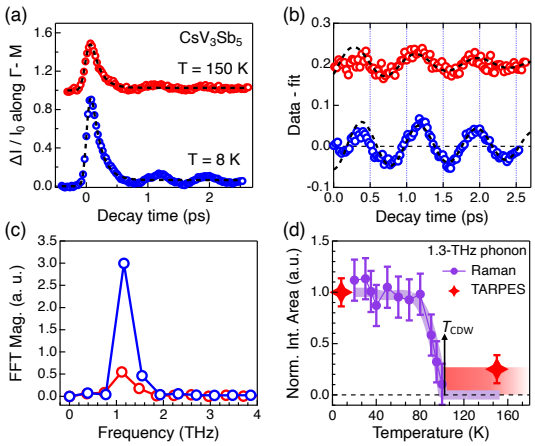

Fig. 2. (a) Intensity dynamics along Γ-M direction below and above $T_{CDW} \sim 94$ K. (b) Extracted coherent oscillation components. (c) Fast Fourier transform (FFT) spectra for the oscillations. (d) Comparison between the normalized intensity of 1.3-THz phonon mode in Raman spectra [3] and FFT spectra in (c), with the red shade highlighting fluctuated phonon spectral weight above T_{CDW}.

Another striking experimental finding is the persistence of the 1.3-THz phonon mode above the CDW transition temperature, suggesting the existence of fluctuating CDW orders [Fig. 2]. These fluctuations, normally undetectable under equilibrium conditions [3], become observable through the intense, ultrafast optical excitations utilized in time-resolved ARPES, providing new insights into transient quantum states that may be relevant for manipulating superconductivity.

These findings have important implications for understanding the CDW in CsV_3Sb_5. The observed VHS-phonon coupling indicates a synergistic effect between electron-phonon interactions and electronic correlations, together generating the CDW with exotic time-reversal symmetry-breaking behavior. Furthermore, ultrafast laser excitation can dynamically tune the VHS closer to the Fermi level, hinting at potential mechanisms for enhancing superconductivity through nonequilibrium conditions.

References

[1] S. Wilson and B. Ortiz, Nat. Rev. Mater. **9**, 420 (2024).
[2] Y. Zhong *et al.*, Phys. Rev. Res. **6**, 043328 (2024)
[3] S. Wu *et al.*, Phys. Rev. B **105**, 155106 (2022)

Authors

Y. Zhong, T. Suzuki, H. Liu[a], K. Liu, Z. Nie[a], Y. Shi[a], S. Meng[a], B. Lv[b], H. Ding[b], T. Kanai, J. Itatani, S. Shin, and K. Okazaki
[a]Chinese Academy of Science
[b]Shanghai Jiao Tong University

Time- and Angle-Resolved Photoemission Spectroscopy with Wavelength-Tunable Pump and Extreme Ultraviolet Probe Enabled by Twin Synchronized Amplifiers

Okazaki Group

Angle-resolved photoemission spectroscopy (ARPES) reveals band structures [1], and its time-resolved variant (TARPES) enables observation of nonequilibrium states using femtosecond lasers [2]. While ~6 eV light from BBO crystals limits energy access, high harmonic generation (HHG) extends reach up to 70 eV, allowing studies of large momentum space as well as valence and core levels. Yet, NIR pump pulses cause broad excitations and heating, obscuring pure electronic dynamics. To address this, we developed a wavelength-tunable TARPES system as shown in Fig. 1.

Our setup employs twin Ti:sapphire amplifiers (800 nm, 35 fs, 0.7 mJ, 10 kHz) seeded by a shared oscillator to minimize timing jitter. One drives the pump, the other the probe. SHG at 3.1 eV is used to generate HHG in Ar gas (4 mm, 3–5 Torr), with a stabilizer maintaining beam alignment. The 7th harmonic (21.7 eV) is filtered and directed via MLM mirrors with differential pumping (10^{-3} Torr → 10^{-8} Torr), yielding ~10^{9} photons/s. A He lamp checks sample quality.

The pump beam is wavelength-tunable (1160–2580 nm) via OPA, with pulse profile monitored by autocorrelator and fluence/polarization adjusted using waveplates and attenuator. An optional 800 nm source is also available. Photoelectrons are analyzed with a Scienta Omicron R4000 under 2×10^{-11} Torr vacuum, and temperature controlled down to 7 K via cryostat.

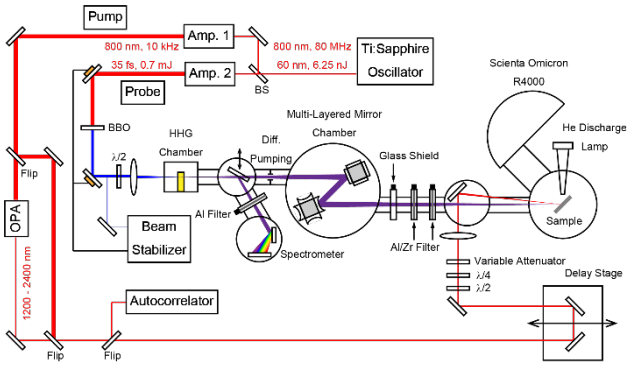

Fig. 1. Schematic illustration of the twin laser-based time- and angle-resolved photoemission spectroscopy (TARPES) system composed of two Ti:sapphire amplification systems, an optical parametric amplifier (OPA), a beam stabilizer, a high harmonic generation (HHG) chamber, a spectrometer, a multi-layered mirror chamber, and a hemispherical electron analyzer.

We validated our system using highly oriented pyrolytic graphite crystals with a fixed probe energy of 21.7 eV and pump photons ranging from 0.52 eV (2400 nm) to 1.03 eV (1200 nm), plus an 800 nm reference.

Figures 2(a) and 2(b) show the differential TARPES images excited by 0.52 and 1.03 eV pulses, respectively, by subtracting the image before the arrival of the pump. The delay time is set to be the largest change, corresponding to 160 and 80 fs for Figs. 2(a) and 2(b), respectively. Since the Dirac band has a linear dispersion symmetric about the Dirac point ($E = E_D$), the electrons are excited from $E_D - 1/2\ \hbar\omega$ to $E_D + 1/2\ \hbar\omega$ by a pump with energy $\hbar\omega$. To track the initial dynamics after photoexcitation, we highlight the photoexcited electrons at $E = E_D + 1/2\ \hbar\omega$, which correspond to the $E - E_F = 0.25$ and 0.5 eV for 0.52 and 1.03 eV pumps, respectively.

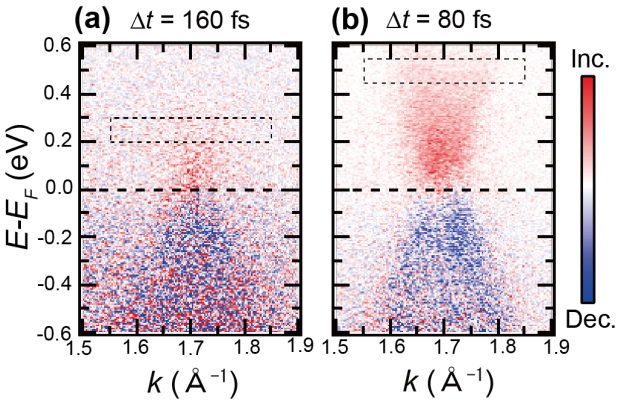

Fig. 2. Differential TARPES images for highly oriented pyrolytic graphite at the delay times of 160 and 80 fs excited by the (a) 0.52 and (b) 1.03 eV pulse, respectively.

By employing wavelength-tunable excitation, it becomes possible to achieve resonant and non-resonant excitations in intriguing quantum materials. Consequently, our developed system opens up the potential for discovering novel non-equilibrium phenomena in the future.

References

[1] A. Damascelli, A. Hussain, and Z. -X. When, Rev. Mod. Phys. **75**, 473 (2003).

[2] T. Suzuki, S. Shin, and K. Okazaki, J. Electron Spectrosc. Relat. Phenom. **251**, 1474105 (2021).

Authors

T. Susuzki, Y. Zhong, K. Liu, T. Kanai, J. Itatani, and K. Okazaki

Layer-Selectively Enhanced Superconductivity in the Highest-Temperature Superconductor

Iwao Matsuda Group

The material dependence of superconducting transition temperature (T_c) provides useful clues to the mechanism of high-temperature superconductivity. In cuprate high-temperature superconductors, it is known that T_c depends on the number of CuO_2 planes in a unit cell, n, and is generally maximized at $n = 3$. On the other hand, even within the $n = 3$, trilayer cuprate family, there exist substantial T_c variations, ranging from 110 K in $Bi_2Sr_2Ca_2Cu_3O_{10+\delta}$ (Bi2223) to 134 K in $HgBa_2Ca_2Cu_3O_{8+\delta}$ (Hg1223), which is also known as the highest record of T_c at ambient pressure among any superconductors. In this context, comparative studies on such trilayer cuprates are desired to understand key elements governing their T_cs and to explore possible paths to realize superconductivity at higher temperatures.

One powerful experimental probe of electronic structure is angle-resolved photoemission spectroscopy (ARPES). ARPES is particularly effective for the study of trilayer cuprates as it is capable of observing the electronic states of two inequivalent CuO_2 planes [inner plane (IP) and outer plane (OP), see Fig. 1(a)] separately. ARPES is a momentum-resolved technique and thus requires single-crystalline samples. Furthermore, due to high surface sensitivity of the technique, crystals should be cleaved under ultra-high vacuum to expose a fresh surface. Bi2223 is easy to cleave and hence has been intensively studied by ARPES. Previous ARPES works [1] revealed an imbalance between the electronic states of IP and OP; larger superconducting gap for the IP by a factor of ~1.5. Thus, it has been conjectured that strong superconductivity at the IP is responsible for high T_c of trilayer cuprates. However, that alone does not account for the T_c variation within the trilayer cuprates and significantly higher T_c of Hg1223, necessitating direct ARPES investigations into Hg1223.

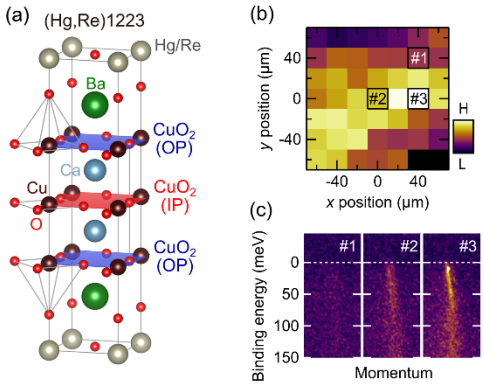

Fig. 1. Properties of (Hg,Re)1223. (a) Crystal structure. (b) Spatial distribution of ARPES intensity. (c) ARPES spectra at positions indicated in (b)

Although it has been challenging to synthesize high-quality single crystals of Hg1223, Mino *et al.* [2] solved the problem by making partial Re substitution for Hg. They succeeded in growing sizable single crystals of $(Hg,Re)Ba_2Ca_2Cu_3O_{8+\delta}$ [(Hg,Re)1223)] with T_cs exceeding 130 K. Since (Hg,Re)1223 lacks natural cleavage plane unlike Bi2223 and thus cleaved surface is expected to be highly disordered, we utilized tightly focused (10μm × 10μm) beam available at the Bloch beamline of MAX IV to target a flat region out of rough surfaces.

We initiated our ARPES investigation by making a spatial map of spectral intensity [3]. As can be seen in Fig. 1(b), the intensity varies drastically over space, reflecting the disordered cleaved surface. However, after careful examination, we found that it is possible to obtain ARPES spectra with decent intensity and sharpness at the optimal position [Fig. 1(c)]. Fixing the sample position, we quantitatively evaluated the magnitude of spectral gaps at various momentum positions separately for the IP and OP. The obtained gap values are plotted as a function of d-wave order parameter in Fig. 2. While the proportionality breaks down at larger d-wave parameters due to pseudogap opening, superconducting properties can be evaluated by extrapolating the linear dependence to d-wave parameter = 1 and defining gap Δ_0. Comparing the values of Δ_0 to those of Bi2223 [1] (Fig. 2), Δ_0 (IP) was virtually identical. On the other hand, Δ_0 (OP) was found to be significantly larger for (Hg,Re)1223. While large Δ_0 (IP) has been highlighted as the key characteristic of trilayer cuprates, the present results imply that Δ_0 (OP) is a significant factor governing the T_c variations within trilayer cuprates. The outcome of this work [3] may provide useful information to establish a designing principle of higher T_c compounds at ambient pressure.

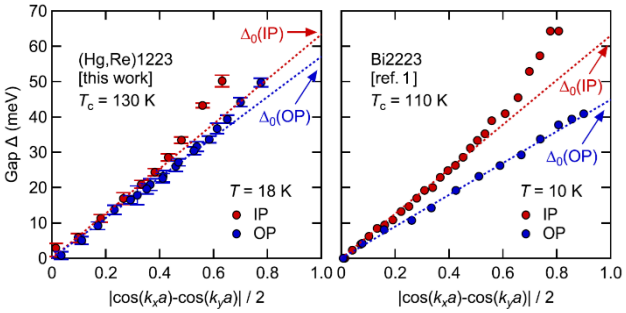

Fig. 2. The magnitude of spectral gap plotted as a function of d-wave order parameter for (Hg,Re)1223 (left) and Bi2223 (right) [1].

References

[1] S. Ideta *et al.*, Phys. Rev. Lett. **104**, 227001 (2010).
[2] Y. Mino *et al.*, J. Phys. Soc. Jpn. **93**, 044707 (2024).
[3] M. Horio *et al.*, Phys. Rev. Lett. **135**, 046501 (2025).

Authors

M. Horio, M. Miyamoto, Y. Mino[a,b], S. Ishida[b], B. Thiagarajan[c], C. M. Polley[c], C. H. Lee[b], T. Nishio[a], H. Eisaki[b], and I. Matsuda
[a]Tokyo University of Science
[b]National Institute of Advanced Industrial Science and Technology (AIST)
[c]MAX IV Laboratory

Realizing Soft X-Ray Photoelectron Spectroscopy Under Ambient Pressure

Iwao Matsuda Group

Soft X-ray photoelectron spectroscopy (XPS) is a surface-sensitive probe of the chemical state of materials. A prime example where the characteristic of surface sensitivity is utilized is chemical reactions on catalyst surfaces. For improving the performance of catalysts, it is essential to understand the chemical reaction processes on their surfaces, where analysis using XPS provides valuable information. However, performing XPS measurements in a gas environment presents challenges. First, soft X rays are easily absorbed by gas molecules in the air, causing a significant reduction in their intensity before reaching the sample. Second, photoelectrons emitted from the sample also undergo strong scattering by gas molecules, making it difficult to guide them to the detector. Vacuum environments solve both problems, and hence XPS measurements have typically been performed under ultra-high vacuum.

In recent years, advances in photoelectron measurement technique and synchrotron X-ray technology have led to the development of XPS in gas environments. Such XPS instruments are now installed at synchrotron facilities around the world and are used for research of surface chemistry. However, the gas pressure is limited to 0.13 bar at maximum [1], and many chemical reactions that occur at atmospheric pressure have not been covered. To address this problem, we developed an ambient-pressure soft X-ray photoelectron spectroscopy (APXPS) instrument that operates at atmospheric pressure [2] at NanoTerasu, a synchrotron radiation facility recently constructed on the Tohoku University campus (Fig. 1).

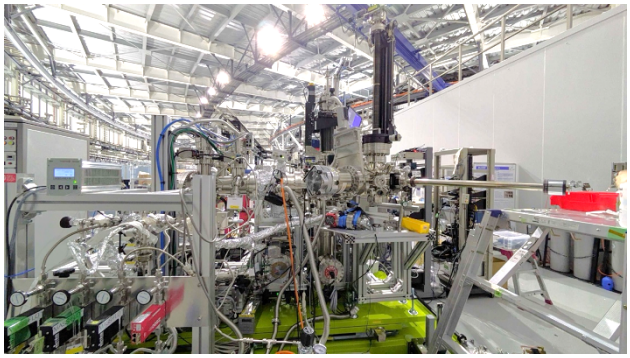

Fig. 1. Photo of the APXPS apparatus developed at NanoTerasu BL08U.

The key to realize XPS at ambient pressure is to suppress the attenuation of soft X-rays and photoelectrons by gas. To achieve this, it is important to bring the soft X-ray outlet and photoelectron entry as close to the sample as possible, thereby minimizing the distance that soft X rays and photoelectrons travel through the gas. We first prepared a soft X-ray introduction path consisting of a vacuum tube to avoid soft X-ray attenuation [Fig. 2(a)]. At the tip, we attached a SiN thin film (200 nm thick) with high transmittance in the soft X-ray region. By combining this soft X-ray introduction path with a movable stage, we created an environment where the SiN film could be brought very close to the sample (~5 mm). On the other hand, to suppress the scattering of photoelectrons by gas, an aperture cone [Fig. 2(b)] was attached to the tip of the analyzer. We used focused ion beam processing to create an aperture with a diameter of as small as 24 μm, which considerably reduces the conductance and makes it possible to introduce ambient-pressure gas to the analysis chamber while maintaining high vacuum inside the electron analyzer. By bringing the sample very close (comparable to the aperture-cone diameter) to the tip of the aperture cone during measurement, the distance that photoelectrons travel in the gas can be reduced.

Combining these elements [Fig. 2(c)], and owing to high photon flux available at NanoTerasu BL08U, we succeeded in observing Au 4*f* photoelectron peaks under H_2 atmosphere even at 1.0 bar [Figs. 2(d),(e)]. The time spent to acquire the spectrum in Fig. 2(e) is only 8 minutes, which is quick enough to trace chemical reactions in a real-time fashion. The developed APXPS system [2] dramatically expands the capability of XPS and opens up new applications to real functional materials under operation.

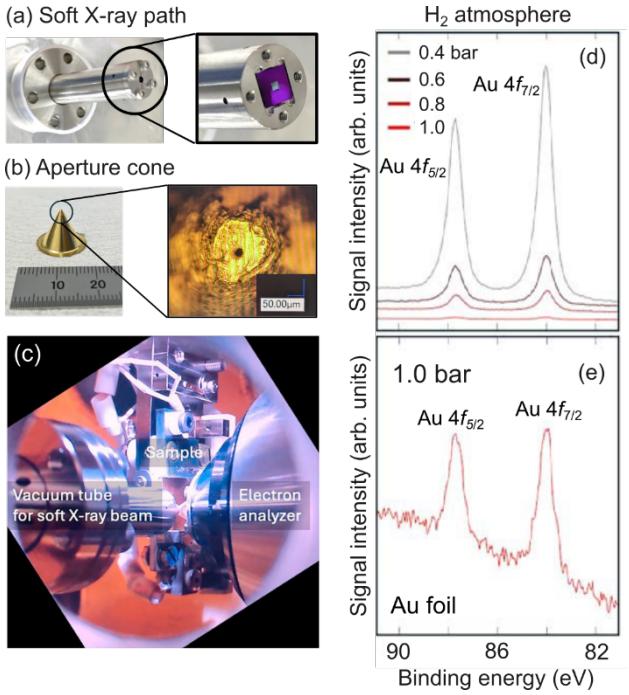

Fig. 2. Photos of (a) Vacuum tube for soft X-ray introduction, (b) aperture cone, and (c) components in the analysis chamber. (d) Au 4*f* spectra of a Au foil sample measured under H_2 atmosphere with varying pressure. The spectrum acquired at 1.0 bar is magnified in (e).

References

[1] S. Kaya *et al.*, Catal. Today **205**, 101 (2013).
[2] T. Wada *et al.*, Appl. Phys. Express **18**, 036504 (2025).

Authors

M. Horio, T. Wada, Y. Liu, Y. Murano, H. Sakurai, T. Sumi[a], M. Miyamoto, S. Yamamoto[a], and I. Matsuda
[a]Tohoku University

Joint Research Highlights

Conductivity Switching by Reversible Electric-Field-Induced Proton Transfer for a Hydrogen-Bonding Heterobilayer Film

Heteromolecular interactions are responsible for a variety of functions. We reported the first observation of reversible tunneling conductivity switching induced by external electric field (EEF) for a proton (H^+) donor/acceptor bilayer film on Au substrates under ambient conditions at room temperature [1].

Depending on the H^+-transferred sites, the molecular orbitals of the H^+-donor and -acceptor molecules are modified. Thus, the H^+-transfer in the heteromolecular pair is able to control molecular properties and to function as a switch. To achieve this function in molecular systems, catechol-fused tetrathiafulvalene (Cat-TTF) derivatives were introduced, which were designed to exhibit H^+-electron-correlated properties [2-4]. We fabricated the bilayer films containing Cat-TTF derivatives as a H^+-donor and imidazole-terminated undecanethiolate self-assembled monolayer (Im-SAM) as a H^+-acceptor on Au substrates (Fig. 1a), through a two-step immersion procedure. The bilayer film topographies, molecular adsorption states, and physical properties were characterized using several spectroscopic and microscopic methods.

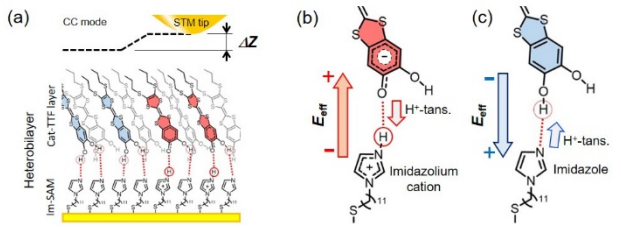

Fig. 1. Schematic of Cat-TTF/Im-SAM bilayer film and EEF response in STM measurements under CC mode (a), H^+-transfer from a catechol moiety to an imidazole group (b), and its reverse H^+-transfer (c), depending on EEF.

In particular, scanning tunneling microscope (STM) revealed reversible changes in the tunneling conductivity of the bilayer film depending on EEF stimulation. Figure 2a shows a typical STM image of the bilayer film, obtained in constant current (CC) mode. The observed atomically flat terraces and steps imply that the bilayer film is uniform in terms of structurally and quantum tunneling properties. Figures 2b–2d show STM images of the bilayer film after EEF stimulation at various stimulation sample-bias V_{SS}. At negative V_{SS} (-1.5 V), the stimulated area surrounded by red corners in Fig. 2b increased in height change ($\Delta Z > 0$), implying increase of tunneling conductivity. This applied EEF may transfer H^+ from the catechol moiety to the imidazole group in the bilayer film (Fig. 1b). In contrast, at the stimulation by positive V_{SS} (+2.0 V) to a part of high conductivity area, surrounded by light-blue corners in Fig. 2c, the area returned to original height ($\Delta Z \approx 0$). This EEF may transfer H^+ from the imidazole group back to the catechol moiety (Fig. 1c). Moreover, the area surrounded by red corners in Fig. 2d increased in height again by negative V_{SS} (-1.5 V). We confirmed that this height change in the CC mode is corresponding to the conductivity change by a *di/dv* mapping method. The mechanism of reversible conductivity switching is considered to be H^+-transfer by applied EEF. The ability of H^+-transfer under EEF was theoretically expected in molecular cluster calculations.

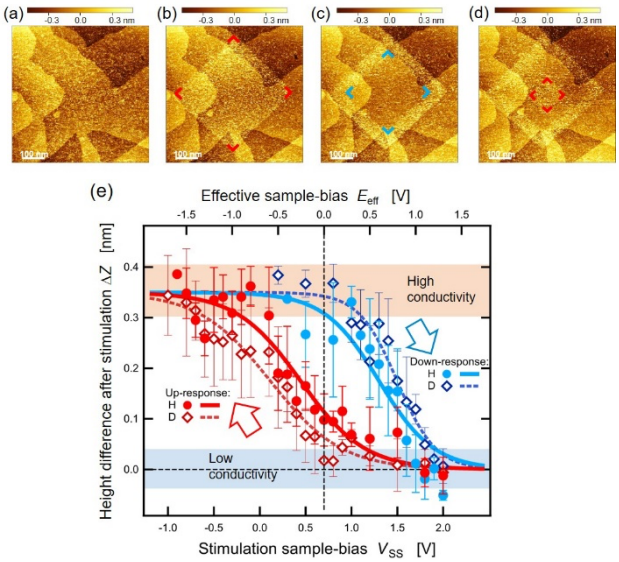

Fig. 2. STM topographies of the bilayer film before (a) and after EEF stimulation at sample bias V_{SS} = -1.5 V (b), +2.0 V (c), and -1.5 V (d). The height change ΔZ against V_{SS} is shown in (e) including its H/D isotope dependence. All measurements were performed in air at room temperature.

Figure 2e shows the EEF-induced height change ΔZ against V_{SS}. These results clearly demonstrate two important features: the threshold of the EEF response exhibits hysteresis and H/D isotope dependence. The isotope dependence is crucial evidence of the EEF response due to H^+-transfer. In addition, the hysteresis in the EEF response indicates that the bilayer film can function as a molecular memory device driven by the H^+-transfer.

References

[1] H. S. Kato *et al.*, Nano. Lett. **25**, 11116 (2025).
[2] T. Isono *et al.*, Nat. Commun. **4**, 1344 (2013).
[3] A. Ueda *et al.*, J. Am. Chem. Soc. **136**, 12184 (2014).
[4] H. Mori *et al.*, Chem. Commun. **22**, 5668 (2022).

Authors

H. S. Kato[a], R. Muneyasu[a], T. Fujino[b], A. Ueda[c], Y. Kanematsu[d], M. Tachikawa[e], J. Yoshinobu, and H. Mori
[a]Osaka University
[b]Yokohama National University
[c]Kumamoto University
[d]Hiroshima University
[e]Yokohama City University

PI of Joint-use project: H. S. Kato
Host labs: Mori and Yoshinobu Groups

Rotational Grüneisen Ratio as a Novel Probe for Quantum Criticality in Anisotropic Systems

Quantum criticality, a phenomenon driven by quantum fluctuations near absolute zero, plays a pivotal role in understanding exotic states in condensed matter systems. In this study [1], we introduce a novel thermodynamic quantity, the rotational Grüneisen ratio Γ_ϕ, as a highly sensitive probe for detecting quantum critical behavior in anisotropic systems.

The rotational Grüneisen ratio Γ_ϕ is defined as $\Gamma_\phi = (1/T)(\partial T/\partial\phi)_S$, where ϕ is the angle of the external field. In contrast to conventional Grüneisen parameters, which employ the *magnitude* of the magnetic field or pressure as control parameters, the rotational Grüneisen ratio utilizes the *angle* ϕ of the external field as a tuning parameter. This method enables the detection of quantum phase transitions with higher angular resolution by measuring the rotational magnetocaloric effect, $(\partial T/\partial\phi)_S$ [2].

We applied this method to two highly anisotropic paramagnets, CeRhSn and CeIrSn, both of which possess a quasi-kagome lattice and exhibit strong geometrical frustration and Kondo effect. By measuring the rotational magnetocaloric effect under varying a magnetic field angle within the ac plane, we investigated Γ_ϕ over a wide range of temperatures, magnetic fields, and field orientations.

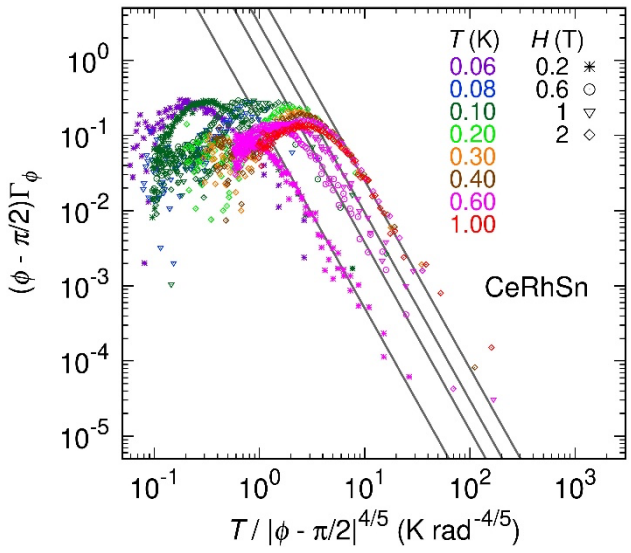

Fig. 1. Scaling plot of the rotational Grüneisen ratio Γ_ϕ for CeRhSn for various temperatures and several selected magnetic fields. Solid lines indicate the scaling functions.

Remarkably, for both compounds, the $(\phi - \phi_{cr})\Gamma_\phi$ data at each magnetic field collapse onto a universal scaling function $f(T/(\phi - \phi_{cr})^n)$, with identical critical exponents $n = 4/5$ and a critical field angle $\phi_{cr} = \pi/2$, as exemplified in Fig. 1 for CeRhSn. These results indicate the existence of a quantum critical line along the hard-magnetization axis (the a axis), where the c-axis component of the magnetic field, $H_\parallel$, governs the critical behavior. The scaling behavior of the rotational magnetic Grüneisen ratio, $\tilde{\Gamma}_\phi = -\Gamma_\phi/H_\perp$, further supports the universality of the quantum criticality, where $H_\perp$ denotes the a-axis component of the magnetic field. The constant $H_\parallel\tilde{\Gamma}_\phi$ supports the presence of a quantum critical point at $H_\parallel = 0$. The small value of the critical exponent implies relatively long correlation length and time, potentially reflecting a characteristic feature of quantum criticality driven by geometrical frustration in these compounds.

These findings highlight that the rotational Grüneisen ratio as a powerful and versatile tool for investigating quantum criticality in strongly anisotropic systems, such as Ising magnets. This method enables high-resolution, field-angle-resolved measurements, providing a novel approach to exploring quantum phase transitions in anisotropic materials.

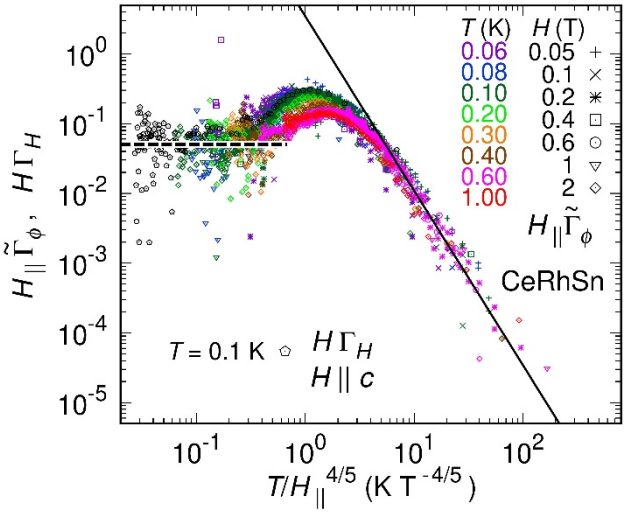

Fig. 2. Scaling plots of the rotational magnetic Grüneisen ratio $\tilde{\Gamma}_\phi$ and magnetic Grüneisen ratio Γ_H for CeRhSn. The solid line indicates the universal scaling function $\tilde{\Gamma}_\phi \sim H_\parallel T^{-5/2}$. The dashed line represents $H_\parallel\tilde{\Gamma}_\phi = 0.05$.

References

[1] S. Yuasa *et al.*, Phys. Rev. B **111**, 045123 (2025).
[2] S. Kittaka *et al.*, J. Phys. Soc. Jpn. **87**, 073601 (2018).

Authors

S. Yuasa[a], Y. Kono[a], Y. Ozaki[a], M. Yamashita, Y. Shimura[b], T. Takabatake[b], and S. Kittaka[a,c]
[a]Chuo University
[b]Hiroshima University
[c]Department of Basic Science, The University of Tokyo

PI of Joint-use project: S. Kittaka
Host lab: Yamashita Group

Polarity of Homoepitaxial ZnO Films

ZnO is an oxide semiconductor that has been shown to be a useful optoelectronic material due to the wide tunability of the direct band gap from 3 to 4.4 eV by Mg or Cd doping. In practical device applications, the device characteristics are strongly influenced by the polarity direction of the crystal, i.e., whether the wurtzite-type crystal is terminated by a zinc face or an oxygen face. For perfect epitaxial thin film layers, the crystal polarity is determined by the termination of the underlying layer. In practical films, however, the film termination can change, depending on the film growth conditions. When grown on an $Al_2O_3(0001)$ surface, ZnO films tend to be terminated by the zinc face when grown at a slow rate at high temperature. The termination switches to the oxygen face at high growth rates or low growth temperatures.

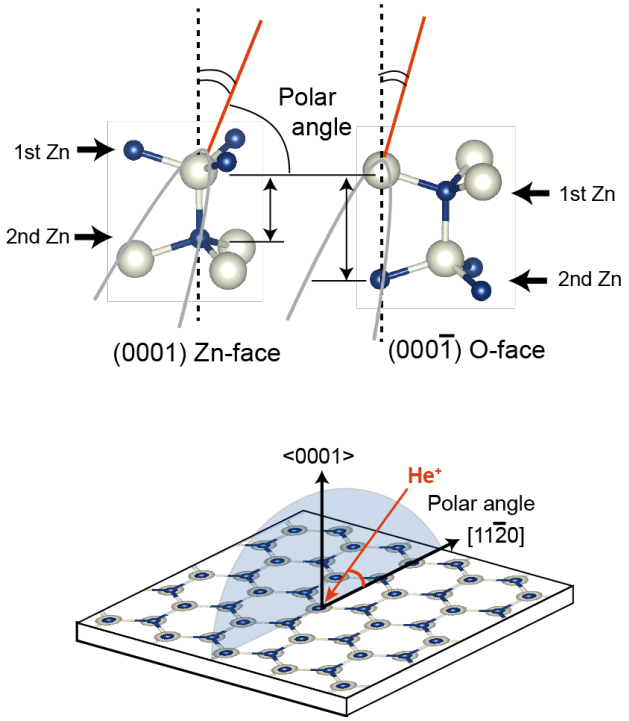

Fig. 1. He ion backscattering geometries for the two ZnO terminations and the CAICISS measurement geometry.

In this work [1], we have used co-axial impact-collision ion scattering spectroscopy (CAICISS) to determine the termination type of homoepitaxial ZnO films grown by Nd:YAG laser ablation at various growth conditions. CAICISS can be used to determine the crystal polarity by measuring the angle dependence of backscattered He ions from a crystal surface. The measurement geometry and the crystal polarity models are shown in Fig. 1. For ZnO structure analysis, the time-of-flight window is set at He ion backscattering from Zn atoms. The scattering is angle dependent, mostly due to He ion focusing and shadowing that occurs in the two topmost atomic layers. High backscattering intensity is observed at slightly different polar angles for the Zn- and O-face crystal terminations.

Homoepitaxial Mg:ZnO films were grown at several temperatures to verify if a termination change occurs similarly to growth on $Al_2O_3(0001)$. Although there were significant surface morphology differences, the CAICISS polar scans were essentially unchanged. The optimal growth temperature for surface flatness was found to be 550 °C at an oxygen pressure of 10^{-5} Torr. The films were grown by pulsed laser deposition (PLD) with a fourth-harmonic Nd:YAG laser operating at 10 Hz and an ablation fluence of 2.3 J/cm^2.

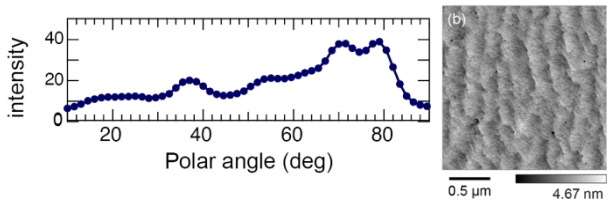

Fig. 2. Polar angle dependence of He ion scattering intensity from Zn atoms (left) and an AFM image of the film surface morphology (right).

The polar angle ion scattering scan is shown in Fig. 2 together with an atomic force microscope (AFM) topography image. The double peak structure in the ion scattering intensity between 70 and 80 degrees indicates the presence of the ZnO oxygen face, same as the substrate surface.

These results show that it is possible to use solid-state laser pulsed laser deposition to fabricate ZnO films with a clear step-and-terrace morphology while maintaining a constant ZnO layer termination.

References

[1] T. Masuda, T. Sato, M. Lippmaa, T. Dazai, N. Sekine, I. Hosako, H. Koinuma and R. Takahashi, J. Appl. Phys. 136, 095303 (2024).

Authors

T. Masuda[a], T. Sato[b], M. Lippmaa, T. Dazai[c], N. Sekine[d], I. Hosako[d], H. Koinuma[a], and R. Takahashi[c]
[a]Smart Combinatorial Technology, Inc.
[b]Vacuum Products, Inc.
[c]Nihon University
[d]NICT

PI of Joint-use project: R. Takahashi
Host lab: Lippmaa Group

Observation of Current-Induced Lattice Distortion in Spin–Orbit Coupled Iridium Oxide $Ca_5Ir_3O_{12}$

Recently, a nonlinear electrical conductivity has been reported in single crystals of 4*d* and 5*d* transition metal (TM) oxides. In the layered perovskite oxides Ca_2RuO_4 and Sr_2IrO_4, conductivity is increased when current is applied and nonlinear electrical conductivity is observed [1–3]. In the layered structure, the TM–O–TM bond angle, which is important for conductivity, is changed by the application of current. It has been reported that the crystal structure of these materials under the application of current is in a non-equilibrium state, which is different from the thermal equilibrium state. Spin–orbit coupling is thought to play an important role in the nonlinear electrical conductivity of these 4*d* and 5*d* transition metal oxides. Therefore, such spin–orbit coupled materials are expected to have applications in devices based on a new mechanism.

We have reported that $Ca_5Ir_3O_{12}$ exhibits nonlinear electrical conductivity along the *c*-axis [4,5]. $Ca_5Ir_3O_{12}$ has a hexagonal crystal structure without centrosymmetry, in which one-dimensional chains of edge-sharing IrO_6 octahedra along the *c*-axis form triangular lattices in the *c*-plane (Fig. 1). Recently, to investigate the effect of current application on the crystal structure, Raman scattering experiments on $Ca_5Ir_3O_{12}$ were performed under the application of DC current [6]. Changes in the Raman spectrum caused by the application of DC current, which are different from the effect of self-heating due to DC current, were also observed. These results indicate that the oxygen bonds in the edge-sharing IrO_6 chain along the *c*-axis are strengthened by applying a DC current.

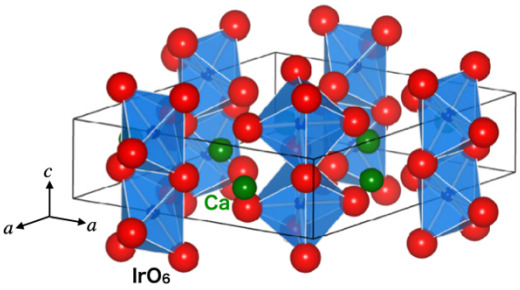

Fig. 1. Crystal structure of $Ca_5Ir_3O_{12}$.

In this study, we report current-induced lattice distortion in iridium oxide $Ca_5Ir_3O_{12}$ with a hexagonal structure that exhibits nonlinear conductivity along the *c*-axis [7]. Using the synchrotron radiation X-ray diffraction experiments on the single crystal, the change in the lattice constant due to thermal expansion at temperatures above room temperature and the change in the lattice constant due to the application of current along the *c*-axis were investigated. We found that the current application along the *c*-axis caused anisotropic lattice distortion that expanded within the *c*-plane direction. The observed distortion due to the electric current is not caused by the piezoelectric effect that would be expected given the symmetry of the crystal structure of this material; the evaluated piezoelectric constant is a very large value compared to typical piezoelectric materials. These results show that the change in the lattice constant ratio *a*/*c* due to the application of current is greater than the change in thermal expansion caused by self-heating. In spin–orbit coupled oxides, this result reveals the possibility of significant current-induced distortion based on a mechanism different from the conventional piezoelectric effect.

References

[1] G. Cao, J. Phys.: Condens. Matter **32**, 423001 (2020).
[2] R. Okazaki, Y. Nishina, Y. Yasui, F. Nakamura, T. Suzuki, and I. Terasaki, J. Phys. Soc. Jpn. **82**, 103702 (2013).
[3] G. Cao, J. Terzic, H. D. Zhao, H. Zheng, L. E. De Long, and P. S. Riseborough, Phys. Rev. Lett. **120**, 017201 (2018).
[4] K. Matsuhira, K. Nakamura, Y. Yasukuni, Y. Yoshimoto, D. Hirai, and Z. Hiroi, J. Phys. Soc. Jpn. **87**, 013703 (2018).
[5] H. Hanate, K. Nakamura, and K. Matsuhira, J. Magn. Magn. Mater. **498**, 166203 (2020).
[6] M. Hayashida, T. Hasegawa, K. Kadohiro, H. Hanate, S. Kawano, and K. Matsuhira, J. Phys. Soc. Jpn. **93**, 104704 (2024).
[7] K. Kadohiro, H. Hanate, M. Hayashida, T. Hasegawa, H. Nakao, Y. Okamoto, K. Miyazaki, S. Tsutsui, and K. Matsuhira, J. Phys. Soc. Jpn. **94**, 023601 (2025).

Authors

K. Matsuhira[a] and Y. Okamoto
[a]Kyushu Institute of Technology

PI of Joint-use project: K. Matsuhira
Host lab: Okamoto Group, Materials Synthesis Section

Development of Open Data Analysis Tool for Science and Engineering (ODAT-SE)

We developed open-source software Open Data Analysis Tool for Science and Engineering (ODAT-SE) [1], by the PASUMS project in FY2024 as a major upgrade of 2DMAT [2, 3]. ODAT-SE solves an inverse problem, when one gives a direct or forward model, a physical or statistical model representing the system under investigation. Currently, ODAT-SE offers five analysis methods: (i) grid search, (ii) Nelder-Mead optimization, (iii) Bayesian optimization, (iv) replica exchange Monte Carlo method, and (v) population-annealing Monte Carlo (PAMC) method.

The code structure of ODAT-SE is drawn schematically in Fig. 1. The original architecture in 2DMAT was tightly coupled with specific experimental techniques, limiting its flexibility and reusability across other scientific fields. In ODAT-SE, the architecture explicitly separates direct problems from the optimization or search algorithms. This modular approach enables researchers to apply ODAT-SE to diverse fields; users can easily add their own direct problem solvers or search algorithms tailored to their research needs.

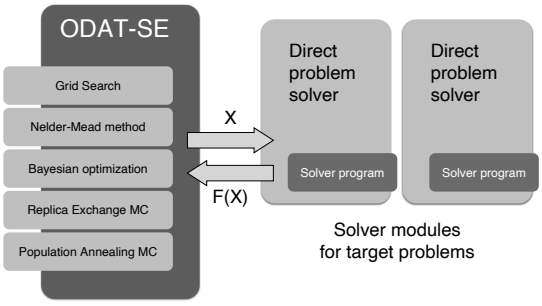

Fig. 1. Schematic diagram of the code structure of ODAT-SE.

Hereafter, we focus on the PAMC method, a massively parallel Bayesian inference. In general, the Bayesian inference gives the posterior probability distribution $P(X|Y)$, as histogram, where X is the target quantity (vector), the quantity that we would like to know, and Y is the experimentally observed quantity (vector). The PAMC method is suitable to supercomputers. Since the PAMC method is a global search algorithm, one can find the global solution and local solutions in the data space of X. The PAMC method was used to determine the surface structure of the 3×3-Si phase on the Al (111) surface by total reflection high-energy positron diffraction experiment (https://www2.kek.jp/imss/spf/eng/, Fig. 2(a)) and core-level photoemission spectroscopy [4]. The analysis finds the global solution as a flat surface structure shown in Fig. 2(b) and local solutions, which indicates the crucial importance of global search algorithm.

In future outlook, ODAT-SE will be developed further and used both in plasma and material science, for example, through our project launched recently in the Moonshot R&D Program [5]. Notably, a recent study [6] using 2DMAT have successfully demonstrated efficient fitting of high-dimensional experimental parameters. With the modular architecture of ODAT-SE, similar complex analyses can now be performed more easily, enabling broader applicability across various scientific fields.

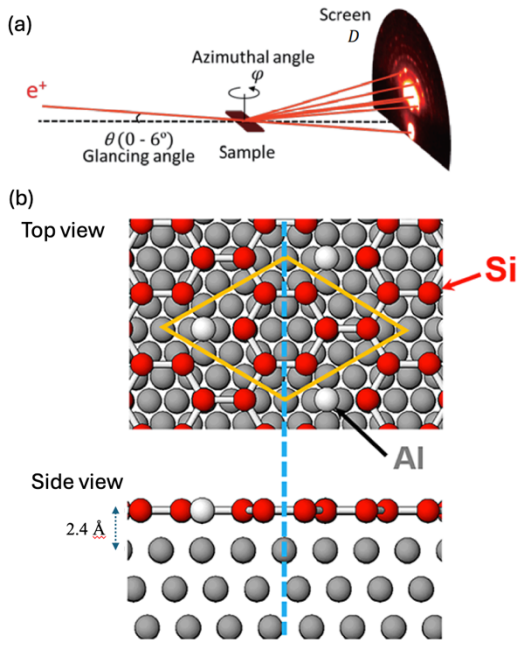

Fig. 2. (a) Schematic diagram of total reflection high-energy positron diffraction experiment (b) Top view (upper panel) and side view (lower panel) for the surface structure of the 3×3-Si phase on the Al (111) surface [4].

References

[1] https://www.pasums.issp.u-tokyo.ac.jp/odat-se/
[2] Y. Motoyama *et al*., Comp. Phys. Commun. **280**, 108465 (2022).
[3] https://www.pasums.issp.u-tokyo.ac.jp/2dmat/
[4] Y. Sato *et al*., Phys. Rev. Materials **9**, 014002 (2025).
[5] https://www.jst.go.jp/moonshot/en/program/goal10/A3_hoshi.html
[6] S. Liu *et al*., Phys. Rev. Lett. **135**, 056502 (2025).

Authors

T. Hoshi[a,b], A. Nakano[a,b], T. Aoyama, Y. Motoyama, and K. Yoshimi
[a] National Institute for Fusion Science
[b] The Graduate University for Advanced Studies, SOKENDAI

PI of Joint-use project: Takeo Hoshi
Host lab: supercomputer center

Temperature-Dependent Magnetic, Electronic, and Structural Properties of $Ba_2Fe_{14}O_{22}$: Effects of Fe^{2+} Localization

In this study, we conducted a comprehensive investigation of the magnetic, electronic, and structural properties of high-quality polycrystalline Y-type ferrite $Ba_2Fe_{14}O_{22}$ throughout a wide temperature range [1]. This compound with a mixed valence state of Fe^{2+} and Fe^{3+} is expected to display a rich variety of physical phenomena because of the interplay of charge, spin, and orbital degrees of freedom. Previous studies have been impeded by the difficulties in synthesizing phase-pure samples since ferrimagnetic impurities like $BaFe_2O_4$ and Fe_3O_4 can contaminate $Ba_2Fe_{14}O_{22}$. We were able to synthesize high-purity polycrystalline samples that are ideal for studying the material's intrinsic characteristics by fine-tuning solid-state reaction conditions.

A ferrimagnetic transition was detected at 662 K, which is somewhat higher than the values reported in previous literature [2,3], according to magnetic measurements. Dissimilarities in oxygen stoichiometry are probably to blame for this disparity. The finding of a precipitous decrease in magnetization at 160 K points to the existence of a phase transition. The magnetic moment per formula unit drops from 9.4 μ_B before of the transition to 8.8 μ_B below it. Magnetization curves above the transition and below 160 K are also significantly different.

Above the transition, the magnetization curve indicates planar-type collinear ferrimagnetism with saturation occurring at around 20 kOe. In contrast, the magnetization grows ferromagnetically at lower temperatures; it keeps growing linearly all the way up to 70 kOe, though. We can infer a non-collinear magnetic structure from this unsaturated field-linear behavior near high fields.

Electrical conductivity measurements indicate semiconducting behavior with moderate conductivity at room temperature ($\rho \approx 33\ \Omega\cdot$cm). On cooling, conductivity gradually diminishes and shows a drop near 160 K, suggesting carrier localization. The conductivity exhibits Arrhenius-type behavior at lower temperatures, with two distinct activation energies: 98 meV between 105–125 K, and 50 meV below 105 K. This implies a reduction in carrier population and mobility at low temperatures.

Figure 1 illustrates the powder X-ray diffraction pattern obtained using Cu-$K\alpha_1$ radiation on a SmartLab diffractometer with a He closed-cycle refrigerator system. The results revealed a structural phase transition at 160 K from a high-temperature rhombohedral to a low-temperature triclinic crystal system. The site-selective localization of Fe^{2+} ions is thought to be the cause of this structural change. Owing to the larger ionic radius compared to Fe^{3+}, Fe^{2+} ions preferentially occupy octahedral sites, particularly those with an up-spin alignment in the magnetic structure. The magnetic moment per formula unit decreases from 9.4 μ_B above the transition to 8.8 μ_B below it, consistent with the theoretical value assuming Fe^{2+} localization among specific octahedral sites.

In summary, this study elucidates the intrinsic temperature-dependent properties of $Ba_2Fe_{14}O_{22}$ by combining structural, magnetic, and electronic measurements. The first order structural transition at 160 K, linked to Fe^{2+} site-selective localization, leads to a reduction in magnetic moment and a marked change in magnetic anisotropy. These findings highlight the intricate coupling between charge, spin, and lattice degrees of freedom in mixed valence hexaferrites.

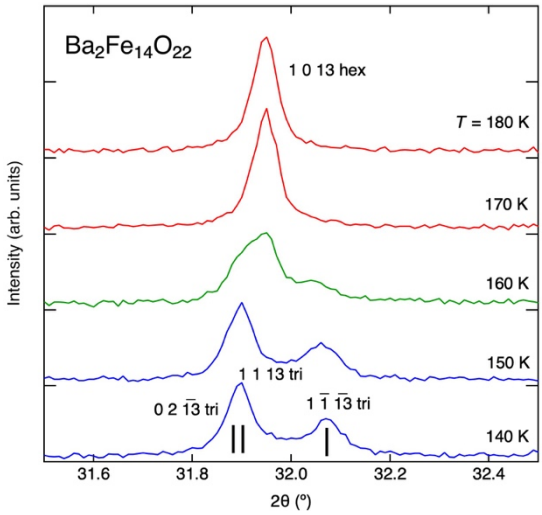

Fig. 1. X-ray diffraction pattern of 1 0 13 reflection (indexed by high-temperature phase manner) near the phase transition at 160 K. The reflection splits into three with the 0 2 -13, 1 1 13, 1 -1 -13 reflections (indexed by low-temperature phase manner).

References

[1] T. Waki *et al.*, J. Phys. Soc. Jpn. **94** (in press).
[2] M. A. H. Farhat and J. C. Joubert, J. Magn. Magn. Mater. **62**, 353 (1986).
[3] X. Zhang and J. Zhang, Mater. Lett. **269**, 127642 (2020).

Authors

T. Waki[a], R. Sobajima[a], J. Yamaura, Y. Tabata[a], and H. Nakamura[a]
[a]Department of Materials Science and Engineering, Kyoto University

PI of Joint-use project: Takeshi Waki
Host lab: Yamaura group and X-Ray Diffraction Section

Neutron Scattering Studies on the Room-Temperature Altermagnet FeS

Antiferromagnets with broken time-reversal symmetry, which are also termed altermagnets, have been attracting marked attention in condensed matter physics in recent years [1], because they potentially show emergent phenomena, such as large anomalous Hall effect or spin-current generation, which would be applicable to novel spintronics devices in the future. We have recently discovered a new altermagnet FeS, which exhibits antiferromagnetic (AFM) order and spontaneous Hall effect at room temperature [2]. This system is known to exhibit a spin reorientation transition at around 190 K. We found that the spontaneous Hall effect disappears at this transition. To investigate the magnetic structures above and below the transition temperature, we performed unpolarized and polarized neutron scattering measurements with a single crystal of FeS.

Unpolarized neutron diffraction measurements were carried out at High-Resolution Spectrometer HRC(BL12) in the Materials and Life-science experimental Facility (MLF) in Japan Accelerator Research Complex (J-PARC). A single crystal of FeS was mounted in a closed-cycle ^{4}He refrigerator with the (*H*,*H*,*L*) horizontal scattering plane. The sample was exposed to a pulsed polychromatic incident neutron beam. Bragg reflections from the sample were detected by the ^{3}He position sensitive detectors. Figures 1(a) and 1(b) show the comparison between the temperature variations of magnetic susceptibilities and the integrated intensity of the 002 Bragg reflection, at which nuclear scattering is expected to be very weak. Since the neutron scattering cross section of a magnetic peak is proportional to a square of Fourier-transformed magnetization projected onto the plane perpendicular to the scattering vector, the intensity of the 002 reflection at high temperatures is attributed to the easy-plane type q=0 AFM structure as illustrated in the inset on the right side of Fig. 1b. At around 190 K, the intensity of the 002 reflection was abruptly reduced, which is exactly coincides with the sharp drop of the magnetic susceptibility along the *c* axis. These changes can be interpreted that the system undergoes the spin-reorientation transition from the easy-plane type AFM to the easy-axis type AFM shown in the inset on the left side of Fig. 1(b).

To further corroborate the easy-axis type AFM order at low temperatures, we also performed polarized neutron scattering measurement at the POlarized Neutron Triple-Axis spectrometer PONTA installed at Japan Research Reactor 3. Similarly to the experiment at HRC, the (*H*,*H*,*L*) horizontal scattering plane was selected. We measured polarized neutron scattering profile of the 112 reflection at 100 K. The polarization direction of the incident neutron beam was set to be parallel to the vertical direction. As shown in Fig. 2, we observed a strong spin-flip (SF) scattering, which arises from the Fourier-transformed magnetization perpendicular to both the scattering vector and the vertical direction, in addition to a non-spin-flip (NSF) scattering, which includes the nuclear scattering. By combining the results from HRC and PONTA, we confirmed that the system exhibits the q=0 AFM structure with magnetic moments parallel to the *c* axis at low temperature.

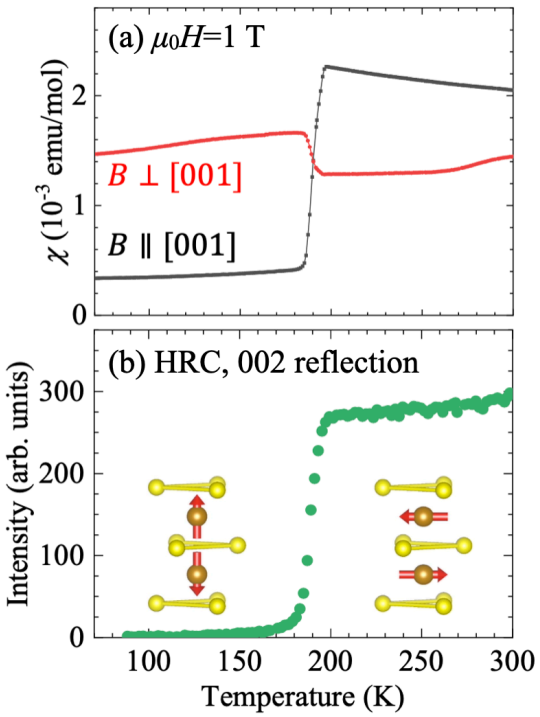

Fig. 1. (a) Temperature variations of magnetic susceptibility parallel and perpendicular to the c axis in FeS. (b) Temperature dependence of the integrated intensity of the 002 reflection measured at HRC in MLF of J-PARC.

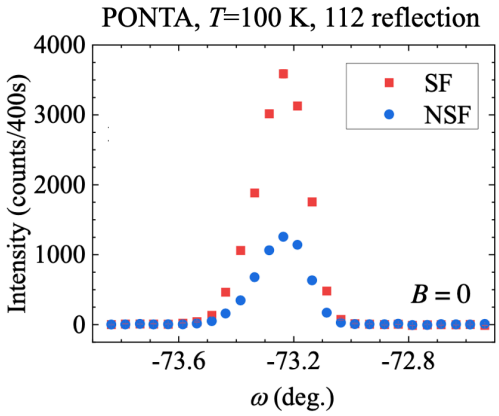

Fig. 2. Polarized neutron scattering profile of 112 reflection of FeS measured at 100 K.

References

[1] L. Šmejkal *et al*., Phys. Rev. X 12, 031042 (2022).
[2] R. Takagi *et al*., Nat. Mater. **24**, 63-68 (2024).

Authors

S. Seki[a], R. Takagi, A. Kitaori[a], H. Saito and T. Nakajima
[a]The University of Tokyo

PI of Joint-use project: S. Seki
Host lab: Neutron Science Laboratory

Gapless Magnon-Driven Anomalous Hall Conductivity in the Collinear Kagome Antiferromagnet $YbFe_6Ge_6$

$YbFe_6Ge_6$ is a kagome-lattice intermetallic whose Fe^{3+} moments order antiferromagnetically below $T_N \approx 500$ K. Neutron diffraction shows an A-type structure with spins along the c axis above the spin-reorientation temperature $T_{SR} \approx 63$ K; on cooling the moments rotate into the kagome plane while the propagation vector remains $\mathbf{k} = (0, 0, 0)$, preserving inversion–time-reversal symmetry and eliminating static scalar chirality [1]. Magnetotransport reveals that this reorientation generates an anomalous Hall conductivity $\Delta\sigma_{xy} \approx 30\ \Omega^{-1}\,cm^{-1}$ at 10 K for in-plane fields, whereas no signal appears for out-of-plane fields or $T > T_{SR}$, confirming its anisotropy dependence rather than any coupling to net magnetization [1].

Low-energy spin dynamics were resolved by inelastic neutron scattering. As shown in Fig. 1(a) [1], magnetic intensity at $\mathbf{Q} = (0, 0, 1)$ in the spin-reoriented phase is continuous up to ≈ 0.6 meV, defining a gapless magnon branch above the 0.14 meV resolution. The temperature evolution of intensities at 0.55 meV and 2.55 meV, plotted in Fig. 1(b) [1], demonstrates that the gap remains closed throughout the easy-plane phase and reopens abruptly at TSR, growing to 1.34 meV by 80 K. The concomitant loss of $\Delta\sigma_{xy}$, reproduced in Fig. 1(c) [1], shows a one-to-one correspondence between gapless magnons and Hall response: whenever the sub-meV continuum vanishes, the transverse conductivity collapses. A 7 T field also quenches $\Delta\sigma_{xy}$; its Zeeman energy for the 1.5 μ_B Fe moment is 0.6 meV, matching the upper edge of the gapless band and reinforcing the causal link.

Because the combined space inversion and time-reversal (*IT*) symmetry eliminates equilibrium Berry curvature and the magnetization never exceeds 0.3 μ_B/Fe even at 50 T, conventional intrinsic or skew-scattering mechanisms are excluded. Instead, propagating magnons transiently cant neighboring Fe moments; coupling to partially polarized Yb^{3+} spins biases the distribution of local scalar chiralities, creating a net dynamic Berry phase that deflects itinerant electrons. When the magnon gap opens thermally or via Zeeman splitting these fluctuations are suppressed and the Hall signal disappears [2]. Comparable fluctuation-driven Hall effects in kagome ferromagnets AMn_6Sn_6 [3] and in Fe_3Sn_2 [4] require non-collinear ground states, yet $YbFe_6Ge_6$ shows that collinear antiferromagnets can host the same physics provided that low-energy magnons are gapless. The absence of any Hall signal in FeSn, whose gap stays near 2 meV at all temperatures, underscores the necessity of near-zero-energy modes [5]. Only the quasi-acoustic branch softens across TSR; higher-energy magnons up to 40 meV remain unchanged, indicating that anisotropy rather than exchange drives the soft mode. Integrating the inelastic intensity yields a fluctuating Fe moment of $\approx 1.5\ \mu_B$, consistent with diffraction and validating the local-moment picture.

These results demonstrate that centrosymmetric, magnetically compensated antiferromagnets can exhibit field-controllable topological transport when anisotropy collapses the magnon gap to zero, extending antiferromagnetic spintronics beyond systems with static chirality and suggesting that engineered soft-mode transitions could enable chirality-mediated charge–spin conversion at terahertz frequencies [6].

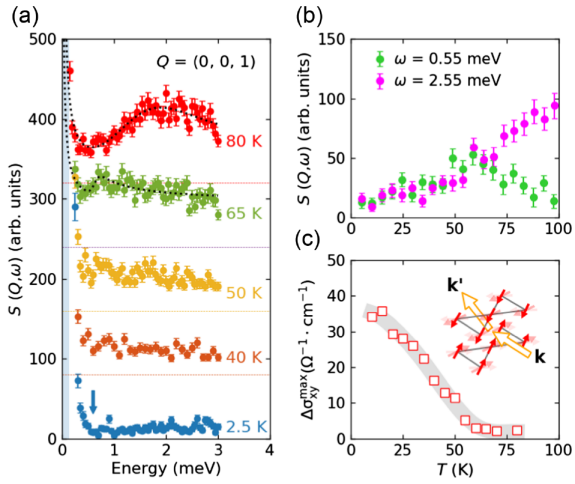

Fig. 1. (a) Low-energy spin excitations at (0, 0, 1) at selected temperatures, offset for clarity. Horizontal dashed lines indicate the zero intensity for the data above 2.5 K. Dashed curves are the fits to 65 K and 80 K data [36]. The light blue region shows energy resolution, and the arrow marks 0.6 meV, below which gapless excitations emerge. (b) Temperature dependence of the intensities at (0, 0, 1) at 0.55 meV and 2.55 meV. (c) Temperature dependence of the maximum magnitudes of $\Delta\sigma_{xy}$. The bold gray curve is a guide to the eyes. Inset illustrates electron scattering by the spin fluctuations.

References

[1] W. Yao *et al.*, Phys. Rev. Lett. **134**, 186501 (2025).
[2] W. Wang *et al.*, Nat. Mater. **18**, 1054 (2019).
[3] N. Ghimire *et al.*, Sci. Adv. **6**, eabe2680 (2020).
[4] M. Kang *et al.*, Nat. Mater. **19**, 163 (2020).
[5] S.-H. Do *et al.*, Phys. Rev. B **105**, L180403 (2022).
[6] Y. Fujishiro *et al.*, Nat. Commun. **12**, 317 (2021).

Authors

W. Yao[a,b], S. Liu[b] H. Kikuchi, H. Ishikawa, Ø. S. Fjellvåg[c,d], D. W. Tam[c], F. Ye[e], D. L. Abernathy[e], G. D. A. Wood[f], D. Adroja[f,g], C-M. Wu[h], C-L. Huang[i], B. Gao[a], Y. Xie[a], Y. Gao[a], K. Rao[a], E. Morosan[a], K. Kindo, T. Masuda, K. Hashimoto[b], T. Shibauchi[b], and P. Dai[a]

[a]Rice University, [b]The University of Tokyo, [c]Paul Scherrer Institut, [d]Institute for Energy Technology, [e]Oak Ridge National Laboratory, [f]Rutherford Appleton Laboratory, [g]University of Johannesburg, [h]National Synchrotron Radiation Research Center, [i]National Cheng Kung University

PI of Joint-use project: P. Dai
Host lab: Masuda Group and Kindo Group

Visualization of Electrically Controllable Magnetic Domains in a Quasi-One-Dimensional Quantum Antiferromagnet $BaCu_2Si_2O_7$

Quasi-one-dimensional quantum antiferromagnets (q1D-QAFMs) consist of chains of magnetic ions with a small spin quantum number (S = 1/2 and 1), where intrachain antiferromagnetic (AF) interactions dominate over interchain ones. They have attracted attention for their potential to exhibit exotic phenomena and their possible application in quantum spintronic technology. Like other AFMs, q1D-QAFMs will form a pair of domain states when undergoing an AF transition due to interchain interactions, typically represented by an "up-down-up-down" state and a "down-up-down-up" state. These domains are randomly distributed in a single crystal sample, and their observation and control are critical for device applications. However, observing domain patterns in q1D-QAFMs appears to be challenging because of the absence of net magnetization and strong quantum fluctuations reducing the ordered spin components. Indeed, there has been no experimental observation of the domain pattern in q1D-QAFMs.

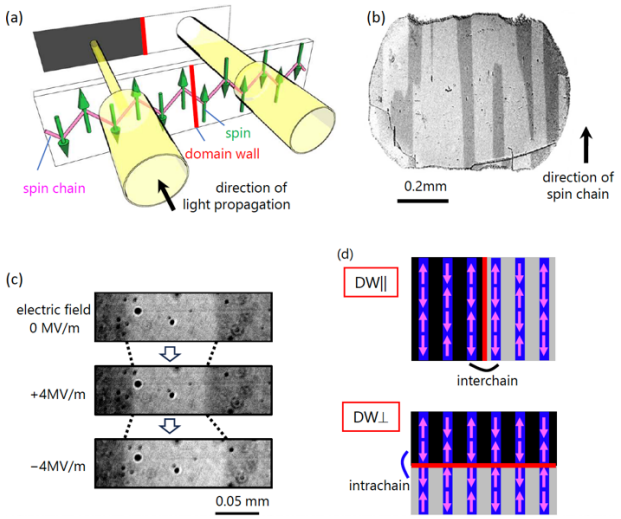

Fig. 1. (a) Schematic illustration of visualizing AF domains in a q1D-QAFM via NDD. Yellow transparent cylinders denote light beams along the thick black arrow, with diameter indicating intensity. In the AF phase, spins or magnetic moments (green arrows) are antiparallel, though parallel alignment can appear as a defect called a domain wall (red line). (b) Optical microscopy image of a sample at 5 K. (c) Visualization of electric-field-driven displacement of AF domain walls. (d) Schematics of a domain wall parallel (DW||) and perpendicular (DW⊥) to the spin chains.

In this study [1], we successfully visualize AF domains in one of the most representative spin-1/2 q1D-QAFMs, $BaCu_2Si_2O_7$, which orders antiferromagnetically below T_N = 9.2 K with reduced moments of only 0.1 μ_B per Cu^{2+} ion [2]. We use a recently developed optical imaging technique based on nonreciprocal directional dichroism (NDD) [3], a change in optical absorption upon reversing the light propagation direction or the sign of magnetic order parameters. Thus, AF domain patterns appear as differences in transmitted light intensity, as illustrated in Fig. 1(a). NDD requires breaking both space-inversion and time-reversal symmetries, which in $BaCu_2Si_2O_7$ arises from AF order combined with the zigzag chain arrangement of Cu^{2+} ions. We used single crystals of $BaCu_2Si_2O_7$ grown by the Masuda group using a floating zone method.

Figure 1(b) shows an optical microscopy image of a thin plate sample at 5 K below T_N. A clear two-level contrast appears in the AF phase, indicating the coexistence of the opposite AF domains. The image reveals that the domain walls (DWs) separating opposite AF domains run predominantly along the spin chains. After heating above T_N and cooling, the domain pattern was changed but the DW orientation was maintained, indicating the robust DW anisotropy in $BaCu_2Si_2O_7$. Furthermore, the AF domains can be controlled by an applied electric field with a small bias magnetic field. As highlighted by the dotted lines in Fig. 1(c), positive and negative electric fields shift the DWs in opposite directions. This displacement can be explained by a magnetoelectric coupling allowed by broken space-inversion and time-reversal symmetries. Importantly, the direction of the DWs is maintained during the displacement. Thus, the DW anisotropy also governs the electric-field driven DW motion in $BaCu_2Si_2O_7$.

Qualitatively, the observed DW anisotropy can be attributed to the anisotropic magnetic interactions. Figure 1(d) schematically shows spin arrangements near DWs parallel (DW||) and perpendicular (DW⊥) to the spin chains. The formation of DW⊥ costs the energy from strong intrachain interaction, which is two orders of magnitude larger than the interchain interactions governing DW||, making DW|| favorable, consistent with experiment. However, the interaction anisotropy greatly exceeds the DW anisotropy estimated by the ratio their lengths: $L_{DW||}/L_{DW\perp} \sim 10$. This suggests another factor contributes to the DW formation. To our knowledge, no relevant theory exists, and future work is required to clarify the microscopic origin of the DW anisotropy in the q1D-QAFMs.
In conclusion, this study advances understanding of domain physics of q1D-QAFMs and raises the interesting question of whether the domain pattern in $BaCu_2Si_2O_7$ is material-specific or intrinsic to q1D-QAFMs.

References

[1] M. Moromizato T. Miyake, T. Masuda, T. Kimura, and K. Kimura, Phys. Rev. Lett. **133**, 086701 (2024).
[2] M. Kenzelmann *et al*., Phys. Rev. B **64**, 054422 (2001).
[3] K. Kimura *et al*., APL Mater. **11**, 100902 (2023).

Authors

K. Kimura[a]
[a]Osaka Metropolitan University

PI of Joint-use project: Kenta Kimura
Host lab: Masuda Group

Tough and Elastic Ion Gels Reinforced by Strain-Induced Crystallization

Ion gels, containing a polymer network and an ionic liquid as their solvent, are deemed one of the most promising soft materials for stretchable electronics, which may supersede incumbent rigid wearable devices in the future. Developing tough ion gels is indispensable for applications, including, but not limited to, conformal wearables or soft actuators. One of the mainstream strategies for materializing tough gels is introducing a sacrificial polymer network. Therein, noteworthy work includes that of double-network (DN) hydrogels [1], and successful fabrication of tough DN or self-healing ion gels followed. However, the very nature of the "sacrificial" network in those gels deteriorates their instantaneous mechanical reversibility. Aiming to overcome this shortcoming, we turned to strain-induced crystallization (SIC, Fig. 1) in gels. Although SIC itself is a long-renowned reinforcement mechanism within vulcanized natural rubber or certain types of polymers, it proved equally valid in polymer gels, which was found in slide-ring (SR) hydrogels of a high polymer concentration and a high molecular weight between cross-links [2]. We implemented this SIC strategy for fabricating tough ion gels. In this presentation, we will overview scattering patterns of in-situ wide-angle X-ray scattering (WAXS), small-angle X-ray scattering (SAXS), and small-angle neutron scattering (SANS) obtained from the ion gels being stretched, and discuss what is inferred about the structural deformation of the polymer network therein. We will also discuss the paths to designing an ion gel of better mechanical performance, from the results of the complementary scattering experiments.

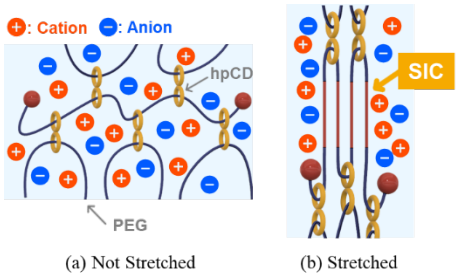

Fig. 1. SIC of highly exposed and oriented PEG chain(s) in an SR ion gel. SIC is formed when the gel is stretched beyond its threshold strain, and it disappears as soon as the load is removed.

We fabricated SR ion gels, in which polyrotaxane (PR) supramolecules possess dynamic crosslinking points via their ring-shaped molecules. The PR was comprised of the axial component, polyethylene glycol (PEG), and the annular ones, (2-hydroxypropyl)-α-cyclodextrin (hpCD). We used an imidazolium-based ionic liquid, 1-ethyl-3-methylimidazolium bis(trifluoromethanesulfonyl)imide ([C2mim][NTf2]), as their solvent. Since [C2mim][NTf2] has an X-ray scattering length density close to that of hpCD, the SAXS patterns reflected the contrast derived from PEG, suppressing the one from hpCD. On the other hand, no contrast matching was realized in the gels for in-situ SANS between the three constituents: deuterated [C2mim][NTf2]-d_8, PEG, and hpCD. SANS measurements were performed at SANS-U, JRR-3.

At a large strain (λ = 10, λ represents the extension ratio), as shown in Fig. 2, scattering spots corresponding to the planar zigzag crystalline structure of PEG were confirmed in the WAXS patterns, and a vertical streak perpendicular to the stretching direction was identified in SAXS, which we concluded as an indication of highly oriented PEG. The SANS patterns suggests that hpCDs form aggregations and that the aggregates are deformed by stretching [3].

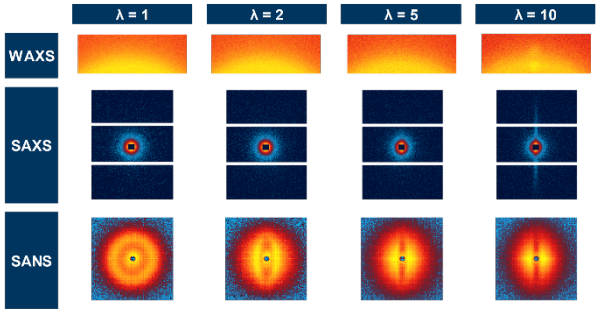

Fig. 2. In-situ WAXS, SAXS, and SANS patterns from SR ion gels being stretched in the horizontal direction.

References

[1] J.P. Gong, Y. Katsuyama, T. Kurokawa, Y. Osada., Adv. Mater., **15**, 1155 (2003).
[2] C. Liu, N. Morimoto, L. Jiang, S. Kawahara, T. Noritomi, H. Yokoyama, K. Mayumi, and K. Ito., Science, **372**, 1078 (2021).
[3] T. Enoki, K. Hashimoto, T. Oda, K. Ito, and K. Mayumi, Macromolecules, **57**, 11498 (2024).

Authors

K. Mayumi, T. Enoki, and K. Hashimoto[a]
[a]Gifu University

PI of Joint-use project: K. Hashimoto
Host lab: Neutron Science Laboratory

Observation of The Mexican Hat–Shaped Valence Band of ferroelectric α-In_2Se_3

This study investigates the electronic band structure of the van der Waals ferroelectric semiconductor α-In_2Se_3 using nanoscale angle-resolved photoemission spectroscopy (ARPES), magneto-optical transmission under high magnetic fields up to ~60 T, and Density Functional Theory (DFT) [1]. These experiments reveal that α-In_2Se_3 hosts an indirect band gap and a distinctive inverted Mexican hat–shaped (IMH) valence band - featuring a nearly flat central region surrounded by a hexagonal ring of maxima and saddle points. This topology results in van Hove singularities and large hole effective masses, validating long-standing theoretical predictions.

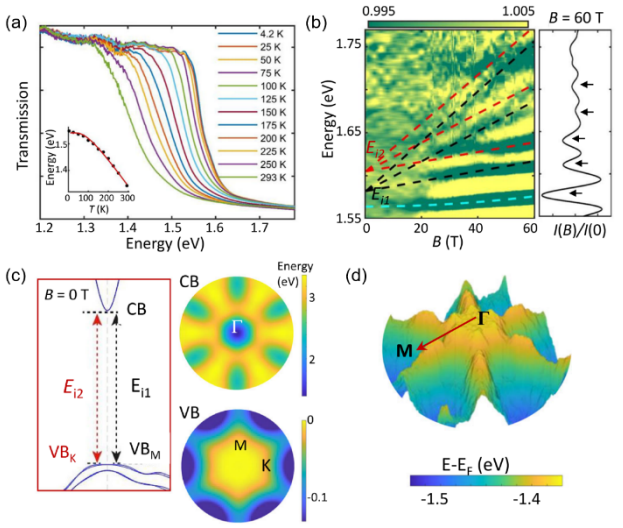

Fig. 1 (a) Temperature-dependent transmission spectra of α-In_2Se_3. Insert: band gap energy as a function of temperature fitted by an empirical model. (b) Color plot of magneto-transmission spectra of α-In_2Se_3 with magnetic field up to 60 T. (b) Electronic band structure of α-In_2Se_3 calculated from DFT. (d) Energy dispersion of α-In_2Se_3 as measured by ARPES for the uppermost valence band.

Figure 1 highlights the temperature and magnetic field dependent optical properties of α-In_2Se_3. At zero magnetic field, the transmission spectra (Fig. 1(a)) exhibit a clear blue shift in the indirect absorption edge from 1.35 eV at 293 K to 1.54 eV at 4.2 K. These values align well with previous reports [2-3] despite prior claims that α-In_2Se_3 exhibits a direct band gap [3-4]. An inset in Fig. 1(a) shows the temperature dependence of the band gap energy, fitted by an empirical model that commonly applies to indirect band gap semiconductors. This excellent agreement reinforces the assignment of α-In_2Se_3 to an indirect band gap semiconductor.

Figure 1(c) presents the magneto-transmission spectra at $T = 4.2$ K, normalized to zero field spectrum ($I(B)/I(0)$). At high field (~60 T), five distinct absorption features emerge. The lowest-energy feature is attributed to an excitonic transition, whose diamagnetic shift is well described using a binding energy of 18 meV and a shift coefficient σ = 3.3 μeV/T². The higher-energy features correspond to two sets of interband Landau level transitions: one from the valence band maximum located at the M-point, and another from a saddle point in the K-point of the valence band, denoted as E_{i1} (black) and E_{i2} (red) in Fig. 1(c). The extracted effective reduced masses ($\mu \approx 0.11\ m_e$) and energy separations (ΔE_i = 23 meV) are in excellent agreement with ARPES (Fig. 1(d)) and DFT results, confirming the IMH-like valence band structure.

The evolution of the interband optical transitions with magnetic field provides direct experimental access to the effective mass and band-edge topology, consistent with the features predicted by DFT calculations. These optical signatures serve as a fingerprint of the complex valence band landscape and illustrate the power of magneto-optical spectroscopy in mapping electronic structures in layered van der Waals semiconductors.

These results validate theoretical predictions about IMH bands in layered semiconductors. The combination of ferroelectric behavior and tunable electronic structure opens possibilities for engineering van der Waals devices—such as low-power, memory, and neuromorphic systems—by tailoring band topology, carrier mass, and density of states.

References

[1] J. Felton *et al.*, Nature Communications **16**, 922 (2025).
[2] J. Quereda *et al.*, Adv. Optical Mater. **4**, 1939 (2016).
[3] M. Emziane *et al.*, Mater. Chem. Phys. **62**, 84 (2000).
[4] G. Kremer *et al.*, ACS nano **17**, 18924 (2023).

Authors

Z. Yang, A. Patanè[a], and Y. Kohama
[a]University of Nottingham

PI of Joint-use project: A. Patanè
Host lab: Kohama Group

Magnetic Shape Memory Effect in a Heavy-Fermion System $CeSb_2$

"Magnetic shape memory effect", the phenomenon that deformed materials returning to their original shape upon exceeding a certain magnetic field, can be adopted for applications such as field-tuned actuators, as it offers much faster controllability than the temperature-driven shape memory effect. The magnetic shape memory effect has been studied predominantly in Heusler alloys composed of transition metals using magnetic and structural properties of martensitic and parent phases. Similar effects are well studied for the *f*-electron compounds RCu_2 (*R*: rare-earth elements) [1]. Applying a magnetic field along the hard magnetization axis causes a rapid increase in magnetization that results in the direction of the field becoming the easy magnetization axis. However, such memory effects in RCu_2 are stable only at low temperatures, and no *f*-electron compounds that maintain memory at room temperature have been identified. This study revealed that the heavy-fermion compound $CeSb_2$ exhibited easy-axis switching accompanied by crystal-axis conversion under a magnetic field. Remarkably, this magnetic shape memory effect remains stable, even at room temperature.

As shown in Fig. 1(a), $CeSb_2$ exhibits a sharp metamagnetic-like increase in magnetization near 34 T, and significant hysteresis is observed during demagnetization when a magnetic field is applied along one of the in-plane principal axes [2]. Subsequent measurements revealed a memory effect, that is, the magnetization approached its previous maximum. The measurements obtained by applying fields along the other in-plane axis revealed a reduction in magnetization, indicating that the direction perpendicular to the field becomes the hard axis. These observations were surprising because the applied field direction was changed by rotating the sample by 90° after heating the sample to room temperature. Moreover, the change from the hard to easy axis is reproducibly observed through the higher-field magnetization measurements. These findings demonstrate that the "magnetic memory effect" remains stable up to at least room temperature. This easy-axis switching accompanies crystallographic axis conversion, which can be confirmed as a domain rearrangement through a polarizing light microscope. Thus, this phenomenon constitutes a "magnetic shape memory effect" that is remarkably stable at room temperature.

$CeSb_2$ crystallizes in a nearly tetragonal orthorhombic lattice that consists of Sb layers and Ce-Sb layers stacked along the orthorhombic *c*-axis. Ce atoms in the *ab*-plane form a distinctive "pantograph" structure [Fig. 2]. Adjusting the pantograph angles allows the lattice constants to be swapped between the *a*- and *b*-axes. The Sb_2 sandwiched between the Ce pantographs forms dimers and acts as hinges during axis transformations. The magnetic anisotropy inherent in the pantograph structure is a key to the magnetic shape memory effect of $CeSb_2$.

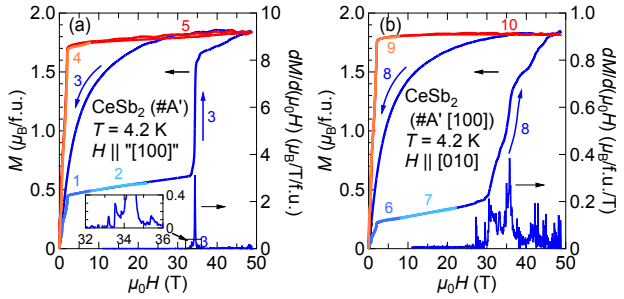

Fig. 1. (a) Magnetization [M (H)] curves of the as-cast $CeSb_2$ (#A') at 4.2 K by applying the fields along one of the in-plane axes. (b) M (H) curves measured at 4.2 K after rotating the same sample 90° at room temperature to change the applied field direction. The number indicates the order of measurements.

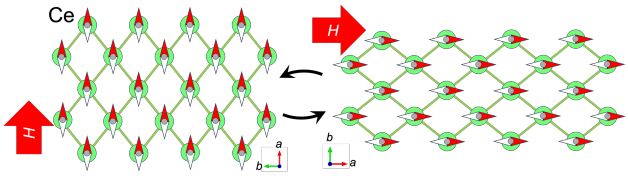

Fig. 2. Schematic drawing of the Ce-pantograph network. By changing the field direction, the pantograph angles change accompanied by the easy-axis switch.

Although the relationships between the magnetic shape memory effect and heavy electron states remain unclear, the characteristic feature of $CeSb_2$, which memorizes the magnetization values corresponding to the maximum applied field, indicates its potential as a magnetic memory material. This discovery opens new avenues for exploring materials for practical applications under moderate magnetic fields and temperatures.

References

[1] see for example, K. Sugiyama *et al.*, J. Magn. Magn. Mater. **262**, 389 (2003).
[2] A. Miyake *et al.*, J. Phys. Soc. Jpn. **94**, 043702 (2025).

Authors

A. Miyake[a], R. Hayasaka[a], H. Fukuda[a], M. Kondo, Y. Kinoshita, D. Li[a], A. Nakamura[a], Y. Shimizu[a], Y. Homma[a], F. Honda[b], M. Tokunaga, and D. Aoki[a]
[a]IMR, Tohoku University
[b]RI center, Kyushu University

PI of Joint-use project: A. Miyake
Host lab: Tokunaga Group

Photo-Induced Nonlinear Band Shift and Valence Transition in SmS

Strongly correlated materials near quantum criticality show unique phase transitions—metal-insulator, magnetic to nonmagnetic—when pressure or magnetic fields are applied. Recently, photo-excitation has emerged as a tool to create nonequilibrium states, including transient metallic [1] and superconducting phases [2], with potential applications in ultrafast electronics. SmS, a black semiconductor at ambient conditions, transitions to a golden semimetallic state above 0.65 GPa via a Sm^{2+} to Sm^{3+} valence change. Optical excitation may mimic this phase by generating electron–hole pairs, offering a new pathway to study valence dynamics. Time-resolved ARPES (TrARPES) enables visualization of such transient states, having revealed phenomena like Floquet–Bloch states [3] and excitonic transitions [4].

Figures 1(a) and 1(b) show an angle-resolved photoelectron spectroscopy (ARPES) image and the corresponding angle-integrated photoelectron (AIPE) spectrum. The three peaks at approximately 1, 1.7, and 2.5 eV indicated by dashed lines in Fig. 1(d) are the Sm 4f multiplets of bulk-6H [6H(b)], the overlap of bulk-6F [6F(b)] and surface-6H [6H(s)], and surface-6F [6F(s)], respectively.

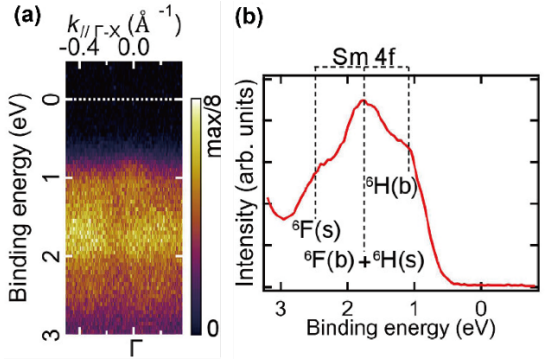

Fig. 1. (a) Band mappings of SmS with ARPES without the photo-irradiation of a pump laser. (b) Angle-integrated-photoelectron spectrum of (a). The multiplet structures of the Sm^{2+} $4f^5$ final state are visible. The peak positions of Sm $4f^5$ multiplets are indicated by the dashed lines

The colored solid lines in Fig. 2(a) labeled as different fluences show the AIPE spectra of the multiplet structure of the Sm^{2+} $4f^5$ final state, obtained immediately after the arrival of the pump pulse. Meanwhile, the spectrum obtained immediately before the arrival of the pump pulse is shown as a black dashed line. After photo-irradiation, the spectrum shifts toward low binding energies but in the opposite direction to the shift at $\Delta t < 0$, that is, a nonlinear shift in time. To investigate the time development of the energy shift after photo-irradiation, the spectra were fitted by the same procedure mentioned above, and the peak shift was plotted as a function of delay time, as shown in Fig. 2(b). The AIPE spectrum shifts towards the Fermi level within 0.1 ps and then gradually shifts back in the following several picoseconds to the position before pumping.

To obtain a more quantitative understanding, we fitted the time-dependent energy shift to a single-exponential decay function convoluted with a Gaussian function, as shown in Fig. 2(b). The fitting parameters, that is, the maximum energy shift (E_{smax}), recovery time τ, and rise time τ_r at different pump fluences, are plotted as functions of the pump fluence in Figs. 2(c)–2(e). Figure 2(c) shows the pump fluence dependency of E_{smax}. E_{smax} initially increases as fluence increases up to a pump fluence of approximately 1.2 mJ/cm^2 and then saturates at a certain value. The saturation value of E_{smax} was evaluated as 58 ± 4 meV by assuming a single-exponential function. The recovery time τ and rise time τ_r are shown in Figs. 2(d) and 2(e), respectively. Both parameters remained constant at each fluence; τ was as long as 1 ps, and τ_r was several tens of femtoseconds, which is comparable to the time resolution.

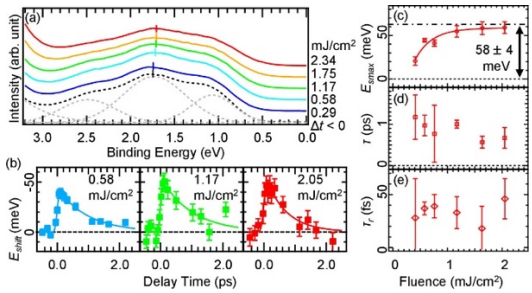

Fig. 2. (a) AIPE spectra of the multiplet structure of SmS 4f final state before the arrival of the pump pulse ($\Delta t < 0$) (black dashed line) and just after the arrival of the pump pulse (less than 0.1 ps) under irradiation of the pump laser with a fluence. (b) Time structure of the energy shift of the three 4f multiplet peaks at various pump fluences. (c) Pump fluence dependence of the maximum energy shift of the 4f multiplet structure at $\Delta t > 0$. (d) Relaxation time of the fitting function in (b) as a function of pump fluence. (e) Energy shift time after photo-irradiation as a function of pump fluence.

The Sm 4f band shifts upward rapidly and soon shifts back within several ps. Photo-induced band narrowing, SPV shift, or heating effect of the pump pulse are possible candidates to explain this ultra-fast band shift. However, this band shift happens in ps, which is much faster than the excitation of the thermal phonons. Therefore, the photo-induced band shift seems to be the most possible scenario.

References

[1] K. Miyano *et al*., Phys. Rev. Lett. **78**, 4257 (1997).
[2] A. Cavalleri, Contemp. Phys. **59**, 31 (2018).
[3] Y. H. Wange *et al*., Science **342**, 453 (2013).
[4] K. Okazaki *et al*., Nat. Commun. **9**, 4322 (2018).

Authors

Y. Chen[a], T. Nakamura[a], H. Watanabe[a], T. Suzuki, Q. Ren, K. Liu, Y. Zhong, T. Kanai, J. Itatani, K. Okazaki, H. S. Suzuki, S. Shin[b], K. Imura[c], N. K. Sato[d], and S. Kimura[a]
[a]The University of Osaka
[b]The University of Tokyo
[c]Nagoya University
[d]Aichi Institute of Technology

PI of Joint-use project: T. Nakamura
Host lab: Okazaki Group

Progress of Facilities

Supercomputer Center

The Supercomputer Center (SCC) is a part of the Materials Design and Characterization Laboratory (MDCL) of ISSP. Its mission is to serve the whole community of computational condensed-matter physics of Japan, providing it with high performance computing environment. In particular, the SCC selectively promotes and supports large-scale computations. For this purpose, the SCC invites proposals for supercomputer-aided research projects and hosts the Steering Committee, as mentioned below, that evaluates the proposals.

The ISSP supercomputer system consists of two subsystems: System B, which was last replaced in Oct. 2020, is intended for larger total computational power and has more nodes with relatively loose connections whereas System C is intended for higher communication speed among nodes. System B (ohtaka) consists of 1680 CPU nodes of AMD EPYC 7702 (64 cores) and 8 FAT nodes of Intel Xeon Platinum 8280 (28 cores) with total theoretical performance of 6.881 PFlops. System C was replaced in June 2022 and the current system (kugui) consists of 128 nodes of AMD EPYC 7763 (128 cores) and 8 nodes of AMD EPYC 7763 (64 cores) with total theoretical performance of 0.973 PFLOPS.

In addition to the hardware administration, the SCC puts increasing effort on the software support. Since 2015, the SCC has been conducting “Project for advancement of software usability in materials science (PASUMS).”In this project, for enhancing the usability of the ISSP supercomputer system, we conduct several software-advancement activities: developing new application software that runs efficiently on the ISSP supercomputer system, adding new functions to existing codes, help releasing private codes for public use, creating/improving manuals for public codes, etc. Two target programs were selected for fiscal year 2024: (1) Addition of dynamical susceptibility calculation function to the dynamical mean-field method program DCore (Proposer: Junya Otsuki (Okayama University)), and (2) Generalizing a data analysis framework for advanced measurement (Proposer: Takeo Hoshi (National Institute for Fusion Science)). In addition, since 2021, we have been maintaining the data repository service for secure storage and enhanced usability of results of numerical calculation.

All staff members of university faculties or public research institutes in Japan are invited to propose research projects (called User Program). The proposals are evaluated by the Steering Committee of SCC. Pre-reviewing is done by the Supercomputer Project Advisory Committee. In fiscal year 2024, totally 374 projects were approved including the ones under the framework of Supercomputing Consortium for Computational Materials Science (SCCMS), which specially supports FUGAKU and other major projects in computational materials science. The total points applied and approved are listed on Table. 1 below.

The research projects are roughly classified into the following three (the number of projects approved, not including SCCMS):

First-Principles Calculation of Materials Properties (190)
Strongly Correlated Quantum Systems (34)
Cooperative Phenomena in Complex, Macroscopic Systems (141)

In all the three categories, most proposals involve both methodology and applications. The results of the projects are reported in 'Activity Report 2024' of the SCC. Every year 3-4 projects are selected for “invited papers” and published at the beginning of the Activity Report. In the SCC Activity Report 2024, the following three invited papers are included:

1. “Surface Structure Analysis and Atomic Force Microscopy Simulation Using DFT”, Masahiro FUKUDA (ISSP)
2. “Magnetic-Field Control of Visons in Kitaev Quantum Spin Liquids under Energy Dissipation”, Chihiro HARADA, Atsushi ONO, and Joji NASU (Tohoku Univ.)
3. “Development of Open Data Analysis Tool for Science and Engineering (ODAT-SE)”, Takeo HOSHI, Akito NAKANO (National Institute for Fusion Science), Tatsumi AOYAMA, Yuichi MOTOYAMA, and Kazuyoshi YOSHIMI (ISSP)

Class	Max Points		Application	Number of Projects	Total Points			
					Applied		Approved	
	System B	System C			System B	System C	System B	System C
A	100	50	any time	28	2.8k	1.4k	2.8k	1.4k
B	650	100	twice a year	116	68.7k	7.7k	45.0k	6.2k
C	6.5k	500	twice a year	189	968.4k	57.7k	524.2k	41.5k
D	10k	500	any time	10	50.5k	3.3k	38.6k	2.4k
E	20k	1.5k	twice a year	22	401.0k	28.1k	209.0k	19.2k
S			twice a year	0	0	0	0	0
SCCMS				9	21.0k	1.7k	21.0k	1.7k
Total				374	1512.4k	99.9k	840.6k	72.4k

Table 1: Research projects approved in Academic Year 2024.
The maximum points allotted to the project of each class are the sum of the points for the two systems; Computation of one node for 24 hours corresponds to one point for the CPU nodes of System B and System C. The FAT nodes require four points for a 1-node 24-hours use. The ACC nodes require two points for a 1-node 24-hours use.

Neutron Science Laboratory

The Neutron Science Laboratory (NSL) has been playing a central role in neutron scattering activities in Japan since 1961 by performing its own research programs as well as providing a strong General User Program (GUP) for the university-owned various neutron scattering spectrometers installed at JRR-3 (20 MW) operated by Japan Atomic Energy Agency (JAEA) in Tokai, Ibaraki (Fig. 1).

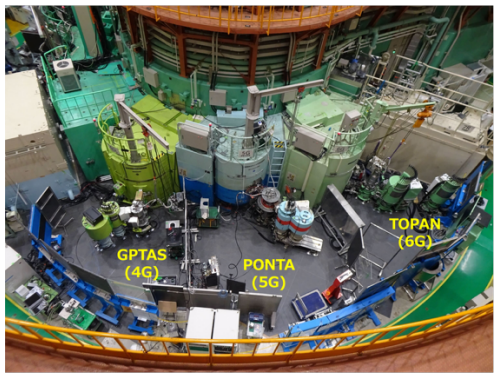

Fig. 1. Three triple axis spectrometers in the reactor hall of JRR-3.

In 2003, the Neutron Scattering Laboratory was reorganized as the Neutron Science Laboratory to further promote the neutron science with use of the instruments at JRR-3. Under GUP supported by NSL, 12 university-group-owned spectrometers at the JRR-3 reactor are available for a wide scope of research on material science. The submitted proposals were about 300 and the visiting users reached over 6000 person-day in FY2010. In 2009, NSL and Neutron Science Division (KENS), High Energy Accelerator Research Organization (KEK) built a chopper spectrometer, High Resolution Chopper Spectrometer, HRC, at the beam line BL12 of MLF/J-PARC (Materials and Life Science Experimental Facility, J-PARC) (Fig. 2). HRC covers wide energy transfer (100 μeV < ħω < 0.5 eV) and momentum transfer (0.03 Å-1 < Q < 30 Å-1) ranges and therefore becomes complementary to the existing inelastic spectrometers at JRR-3. HRC has accepted general users through the J-PARC proposal system since FY2011.

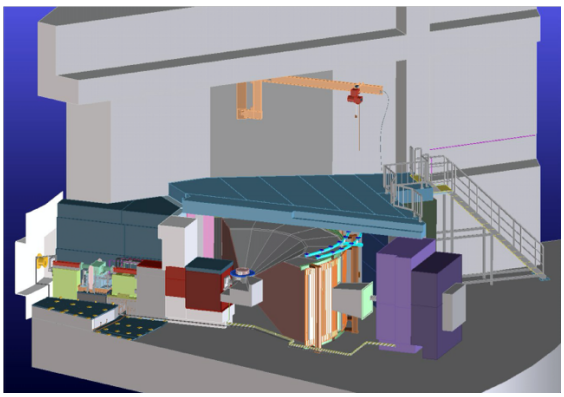

Fig. 2. Schematic view of HRC.

Triple axis spectrometers, HRC, a four-circle diffractometer, and a high resolution powder diffractometer are utilized mainly for a conventional solid state physics and a variety of research fields on hard-condensed matter, while in the field of soft-condensed matter science, researches are mostly carried out by using a small angle neutron scattering (SANS-U) and/or neutron spin echo (iNSE) instruments. The upgraded time-of-flight (TOF) inelastic scattering spectrometer, AGNES, is available both for hard- and soft-matter science. Our GUP has produced approximately 2000 publications and approximately 350 dissertations as of July, 2024. Their lists for the last 10 years are given in Activity Report on Neutron Scattering Research which is available in ISSP and NSL web pages.

As for international cooperative programs, NSL operates the U.S.-Japan Cooperative Program on neutron scattering, providing further research opportunities to material scientists who utilize the neutron scattering technique for their research interests. In 2010, relocation of the U.S.-Japan triple-axis spectrometer, CTAX, was completed, and it is now open to Japanese users. In March 2024, we had an international review for the renewal of the cooperative program which is mandated by the MEXT every 10 years. The review and contract renewal were successfully completed, and the cooperation program is now entering a new phase. Here, as proposed by the review committee, we plan to further revitalize soft matter science.

After the resumption of JRR-3 operation in 2021, many instrumental advances have been made. First, improvements to the instruments and guide tubes during the beam shutdown period (2011-2021) resulted in a 10-fold increase in the intensity of GPTAS (4G) and an 8-fold increase in AGNES (C3-1-1). Next, a new multiplex-type triple-axis spectrometer HODACA was constructed at C1-1. This spectrometer is 40 times more efficient than the conventional spectrometer (HER). The development and improvement of these instruments and the latest status of the other university spectrometers at JRR-3 are described in detail in a special topic of the Journal of the Physical Society of Japan (JPSJ) (Vol. 93(9)). Some improvements have also been made to the proposal adoption system: multibeam proposals (in cooperation with PF at KEK) were launched in 2022, student proposals (doctor-course students can apply as PIs) in 2023, international proposals (researchers from overseas institutions can apply as PIs) in 2024, and industrial proposals (in which researchers from industry can apply as PIs) in 2025.
We had conducted 84 experiments for 155 approved proposals in 2021 (reactor operation: 4 cycles, 92 days), 123 experiments for 166 approved proposals in 2022 (reactor operation: 7 cycles, 152 days), 122 experiments for 154 approved proposals in 2023 (reactor operation: 6 cycles, 143 days), and 115 experiments for 140 approved proposals in 2024 (reactor operation: 7 cycles, 139 days). For these experiments, about 110 papers have been published as of July, 2025.

International MegaGauss Science Laboratory

The objective of this laboratory (Fig. 1) is to study the physical properties of solid-state materials (such as metals, semiconductors, insulators, superconductors, and magnetic materials) in a high magnetic field of 100 T or even higher. Such a high magnetic field can control material phases and functions. Our pulsed magnets, at the moment, can generate up to 88.6 Tesla (T) in a non-destructive manner and up to 1200 T in a destructive manner. The world record for an indoor magnetic field of 1200 T was achieved in 2018. The laboratory is open for scientists both domestic and overseas. Lots of fruitful results have come out from the collaborative researches and our in-house activities.

Fig. 1. The building C of the IMGSL.

Our interests cover the studies on quantum phase transitions (QPT) induced by high magnetic fields. Field-induced QPT has been explored in various materials, such as quantum spin systems, strongly correlated electron systems, and other magnetic materials. One of our ultimate goals is to provide joint-research users with a 100 T millisecond-long pulse using a non-destructive magnet and to offer versatile high-precision physical measurements. Measurable physical quantities or properties are magneto-optical spectra, magnetization, magnetostriction, electrical transport, specific heat, nuclear magnetic resonance, and ultrasound propagation. They can be carried out with sufficiently high accuracy. Another ultimate goal is to extend the magnetic field region and discover novel phenomena happening only in extremely strong magnetic fields exceeding 100 T. Recent technical developments allow us to even measure magnetostriction and ultrasound propagation in destructive magnetic fields over 100 T, which can directly reach potential structural changes in the ultrahigh magnetic fields. The recent discovery of magnetic field-induced insulator-metal transitions of strongly correlated materials in 500 T would open a new direction of the megagauss field research, namely the exploration of field-induced novel phases in materials with strong interactions comparable to the thermal energy at room temperature.

A set of supercapacitor power supplies with a total accumulation energy of 150 MJ (Fig. 2) was installed in 2023 and used as an energy source for super-long pulse magnets.

The magnet technologies are intensively devoted to the quasi-steady long pulse magnet (an order of 1-10 sec) energized by the giant DC power supply. The giant DC power source will also be used for the giant outer magnet coil to realize a 100 T nondestructive magnet by inserting a conventional pulse magnet coil in its center bore. Recently, the super-long pulsed magnet has been intensively used to investigate thermal properties such as specific heat and magnetocaloric effects.

Fig. 2. Upper: The K-building for the supercapacitor power supply (left-hand side) and a long pulse magnet station (right-hand side). Lower: The supercapacitors have a total accumulation energy of 150 MJ installed in 2023 and are planned to drive the long pulse 60 T magnet and the first stage of the dual-coil 100 T non-destructive magnet.

Magnetic fields exceeding 100 T can only be obtained with the destruction of a magnet coil. The ultrahigh magnetic fields are obtained in a microsecond time scale. The project, financed by the Ministry of Education, Culture, Sports, Science and Technology aiming to generate 1000 T with the electromagnetic flux compression (EMFC) system (Fig. 3), has been completed.

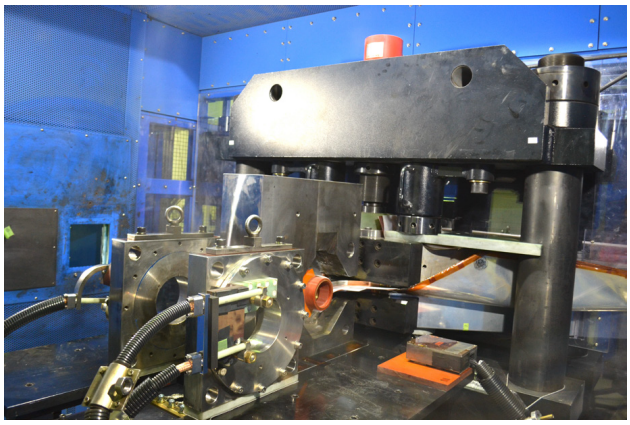

Fig. 3. A view of the coil setup of the electromagnetic flux compression inside of an anti-explosive house. The world's strongest indoor magnetic field of 1200 T was achieved in 2018.

Our experimental techniques using the destructive magnetic fields have intensively been developed. The system, which is unique to ISSP on the world scale, is comprised of a power source of 5 MJ main condenser bank and 2 MJ condenser bank. Two magnet stations are constructed, and both are energized by each power source. Both systems are fed with another 2 MJ condenser bank used for a seed-field coil, the magnetic flux of which is to be compressed. The 2 MJ EMFC system can generate 450 T. The 5 MJ system is used for the generation of a 1000 T-class magnetic field. For the research in the magnetic field range of 100 - 300 T, we have two single-turn coil (STC) systems that have a fast-capacitor bank system of 200 kJ for each. One is the horizontal type (H-type), and the other is a vertical type (V-type, Fig. 4). Various kinds of laser spectroscopy experiments, such as the cyclotron resonance and the Faraday rotation, are possible using the H-type STC, while a stable low-temperature condition of 2 K is available for the V-type STC.

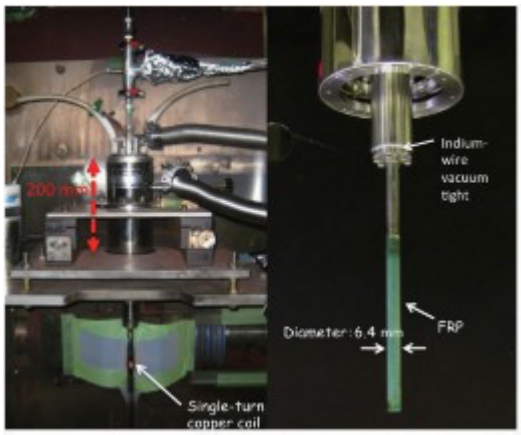

Fig. 4. Schematic picture of the V-type single-turn coil equipped with a 40 kV, 200 kJ fast capacitor bank system. The liquid-helium-bath cryostat with a plastic tail is also shown.

Available Magnets, Specifications

	Magnet	Type	B_{max}	Pulse width Bore	Power source	Applications	Others
Building C Room 101-113	Electromagnetic Flux Compression	Destructive	1200 T	3μs (100–1200 T) 10 mm	5 MJ, 50kV 2 MJ, 50kV	Magneto-Optics Magnetization Magneto-Striction Magneto-Transport	5 K - room temperature
	Horizontal Single-turn Coil	Destructive	300 T 200 T	6μs 5 mm 10 mm	0.2 MJ, 50 kV	Magneto-Optics Magnetization Magneto-Striction Magneto-Transport Ultrasound	5 K - room temperature
	Vertical Single-turn Coil	Destructive	300 T 200 T	8μs 5 mm 10 mm	0.2 MJ, 40 kV	Magneto-Optics Magnetization Magneto-Striction Magneto-Transport Ultrasound	2 K - room temperature
Building C Room 114-120	Mid-pulse Magnet	Non-de-structive	60 T 70 T	40 ms 18 mm 40 ms 10 mm	0.9 MJ, 10 kV	Magneto-Optics Magnetization Magneto-Transport Electric-Polariza-tion Magneto-Striction Magneto-Imaging Torque Magneto- Calorim-etry Heat Capacity Ultrasound	Independent Experiment in 5 sites Lowest tem-perature 0.1 K
Building C Room 121	PPMS	Steady	14 T			Resistance Heat Capacity	Down to 0.3 K
	MPMS	Steady	7 T			Magnetization	Down to 2 K
Building K	Short-pulse magnet	Non-de-structive	88.6 T	2.5 ms 12 mm	0.5 MJ, 20 kV	Magnetization Magneto-Transport	1.4 K - Room tem-perature
	Long-pulse magnet	Non-de-structive	40 T	1 s 30 mm	150 MJ, 2.4 kV	Resistance Magneto-Calorime-try	0.5 K - Room tem-perature

Center of Computational Materials Science

With the advancement of hardware and software technologies, large-scale numerical calculations have been making important contributions to materials science and will have even greater impact on the field in the near future. CCMS is a specialized research center established in 2011 for promoting computer-aided materials science with massively parallel computers, such as the Fugaku supercomputer, which has been developed in Kobe as the core of a billiondollar national project. Activities of CCMS are divided into the following three categories: (1) highly efficient and largescale use of the Fugaku supercomputer and its application to grand-challenge problems in computational materials science, (2) activities as the center for the community of computational condensed matter physics and materials science, and (3) computational physics research aiming to solve intriguing physics emerged from strongly correlated systems.

For the first category, each group in CCMS is carrying out various individual research projects in its own expertise to efficiently utilize large-scale parallel computers. For example, the Ozaki group has been developing efficient and accurate methods and software packages to extend the applicability of DFT to more realistic systems and investigated the structural and electronic properties of various 2D materials in successful collaboration with experimental groups and industrial companies. There are other activities such as development of Tensor Network (TN) based numerical methods and Markov-chain Monte Carlo methods by the Kawashima group and the Todo group.

As for the activities in the second category, apart from major annual conferences and formal international meetings, the CCMS provided a series of lectures and training sessions at Kashiwa. For example, training sessions "Kashiwa Hands On" for getting accustomed to various application programs, such as OpenMX, HΦ, mVMC, AkaiKKR, and MateriApps LIVE!, as shown in Fig. 1, have been held monthly. Each session is designed for more than 10 trainees and takes 4-5 hours. We also coordinate the use of the computational resources available to our community, and

Fig. 1. Software in the CCMS community

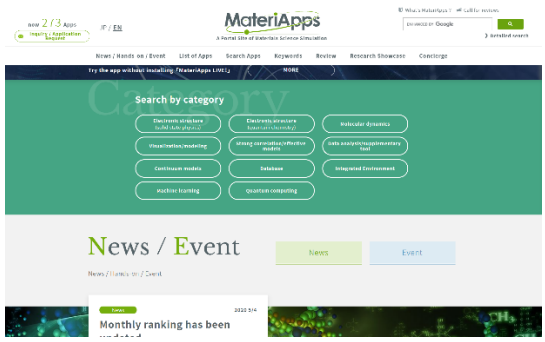

Fig. 2. MateriApps Website

support community members through various activities such as administrating the website "MateriApps" for information on application software in computational science as shown in Fig. 2.

For the third category, the Misawa group addressed searching for topological insulators in solids which is one of the main issues of modern condensed-matter physics since robust gapless edge or surface states of the topological insulators can be used as building blocks of next-generation devices, and showed a way to realize a topological state characterized by the quantized Zak phase, termed the Zak insulator with spin-polarized edges in organic antiferromagnetic Mott insulators without relying on the spin-orbit coupling. The finding provides an unprecedented way to realize a topological state in strongly correlated electron systems. Prof. Misawa was also involved in the Data generation and utilisation materials Research and development projects (DxMT).

These activities are supported by funds for various governmental projects including the DxMT project and the Program for Promoting Researches on the Supercomputer Fugaku.

The following is the selected list of meetings organized by CCMS in recent years:

- 2024/4/3-4 ISSP joint workshop for ISSP Supercomputer Co-use and CCMS.
- 2024/6/5 Matching Workshop for industries & graduate students/ postdocs.
- 2024/7/24-26 DxMT AIM Hack2024.
- 2024/11/22 11/29,12/6, 12/13 MP-CoMS lecture series: Fundamentals and Practice of Materials Informatics.

In addition to the events listed above, we organize regular hands-on programs for various applications, such as 2DMAT, ALAMODE and moller.

Laser and Synchrotron Research Center (LASOR Center)

The Laser and Synchrotron Research Centre (LASOR Center) was established in October 2012 to advance photon and materials science research. With 10 groups in 2024, LASOR is the largest division in ISSP. Most of the research activities on the development of new high-power lasers and their application to materials science are conducted in specially designed buildings D and E with large clean rooms and vibration-isolated floors at the Kashiwa campus. We also have a clean room for a laser processing platform at the Kashiwa II campus. On the other hand, experiments using synchrotron radiation are conducted at Nano Terasu (Miyagi), SPring-8 and SACLA (Hyogo).

The development of new laser light sources in the vacuum ultraviolet to soft X-ray range has revolutionized materials research. This is represented by high-energy-resolution photoelectron spectroscopy, ultrafast time-domain spectroscopy, and ultrafast nonlinear spectroscopy. Materials science research using lasers has entered a new era. Ultrashort, high-power lasers are becoming an increasingly attractive light source for both basic research and industry. State-of-the-art laser sources and spectroscopy are being explored in great detail.

Synchrotron-based research is another area of activity at the ISSP. The dramatic increase in the brilliance of synchrotron radiation has also opened up a new field of photon science. In 2018, the Japanese government has announced the construction of a new synchrotron facility in Tohoku (Nano Terasu). LASOR has decided to subjectively contribute to this facility from design to operation, and Nano Terrace is currently in operation.

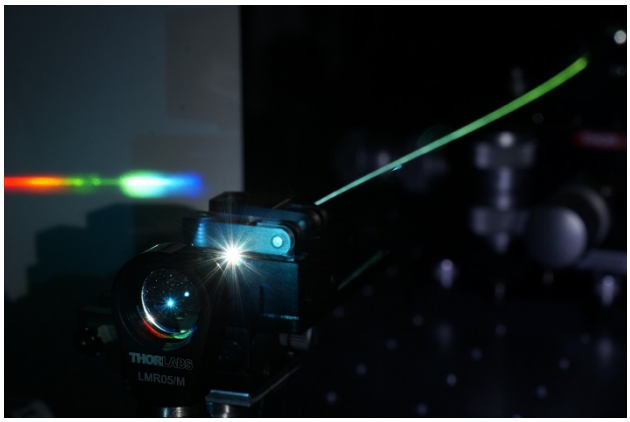

Fig. 1. Optical frequency comb

Lasers and synchrotrons evolved independently, and today both types of light source cover a wide range of photon energies, overlapping in the vacuum ultraviolet to soft X-ray regions. Recognising their shared research interests and technologies, ISSP has brought together the fields of extreme lasers and synchrotron radiation on a single platform. By facilitating interaction between these two fields, LASOR will become a global hub for innovation in light and materials science, fostering collaborative research and close cooperation with other ISSP divisions such as New Materials Science, Nanoscale Science, and Condensed Matter Theory.

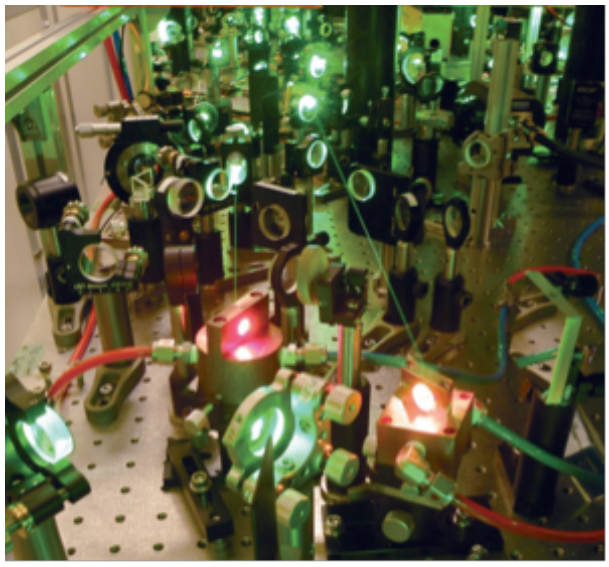

Fig. 2. Close look of a high-peak-power ultrashort-pulse laser

The mission of LASOR is to cultivate and advance the following three scientific fields:

1. Laser Science,
2. Synchrotron radiation science,
3. Extreme Spectroscopy,

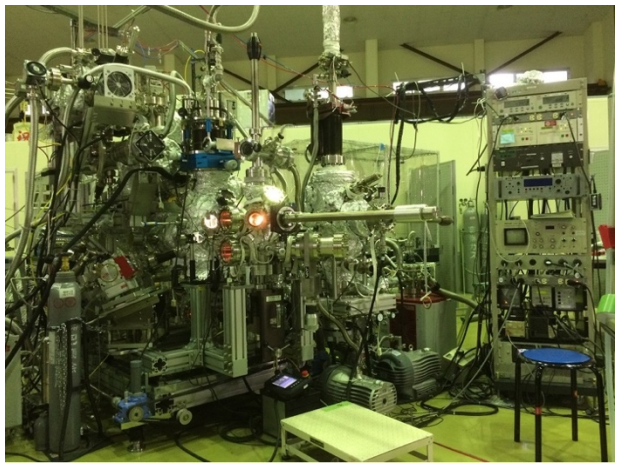

Fig. 3. Spin-resolved photo-emission spectroscopy.

Laser science group

We have continued to develop various state-of-the-art laser systems, such as high-power solid-state lasers, high-intensity lasers, ultra-short pulse lasers down to the attosecond time scale (peta-Hz linewidth), ultra-stable 1-Hz linewidth lasers, optical frequency combs, mid-infrared lasers, THz light sources, and semiconductor lasers. The technology of high-power and ultrashort pulse lasers has progressed

during these 10 years. It has opened two research directions. One is a coherent extreme ultraviolet light source realized by a high harmonic generation (HHG) scheme. The average power of HHG became high enough to be used for photoemission spectroscopy. Photon energies from 7 eV to 60 eV are now available. They can be either very narrow bandwidth or ultrashort pulse. The other is an industrial science such as laser processing. Variable pulse duration, 100 W average power, femtosecond laser is now available at LASOR for any collaborative research, including companies. We have a laser processing platform for both industrial and scientific applications.

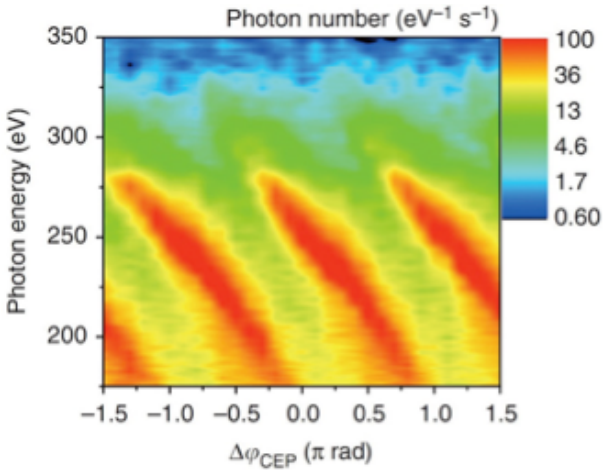

Fig. 4. Phase-dependence of high harmonic spectra in soft X-rays.

We also aim to develop novel laser spectroscopy and coherent nonlinear optical physics enabled by emerging lasers and optical science/technology, and to comprehensively study fundamental light-matter physics, optical materials science, and applied photonics. Such research includes ultrafast spectroscopy for excited state dynamics, terahertz magnetic field spectroscopy for spin dynamics, quantitative microspectroscopy of semiconductor lasers, and nanostructured photonic devices such as quantum wire lasers, gain-switched semiconductor lasers, multi-junction solar cells, and bioluminescent systems.

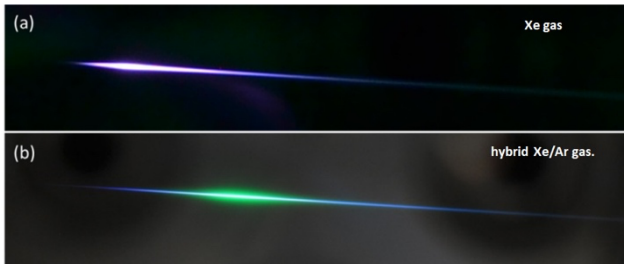

Fig. 5. Generation of 7-eV, femtosecond light with (a) Xe and (b) Xe/Ar gases.

Synchrotron radiation science group

By inheriting and developing the synchrotron techniques cultivated for more than 20 years, we are continuously developing world-class spectroscopies such as time-resolved photoemission/diffraction, ultra-high-resolution soft X-ray emission, 3D (depth + 2D microscopy) nano-ESCA, and X-ray magneto-optical effect, and providing these techniques for both basic materials science and applied science that contributes to the instrument applications in collaboration with outside researchers. In order to pioneer new spectroscopies for next-generation light sources, we are improving the fast polarization switching of the undulator light source in collaboration with SPring-8. In addition, we are promoting frontier work on the use of X-ray free-electron lasers, SACLA, with high spatial and temporal coherence comparable to optical lasers in collaboration with scientists of laser light sources and spectroscopy.

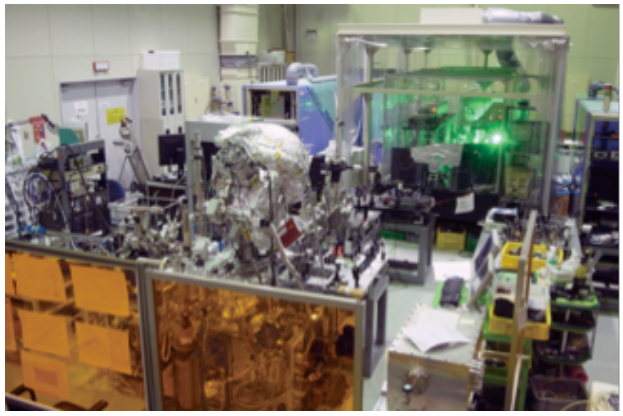

Fig. 6. Pump-probed photoemission system using 60-eV laser

Extreme spectroscopy group

The advent of laser-based light sources in the soft X-ray region opens a new stage in the field cultivated by synchrotron radiation. One of the milestones was the development of a laser-based light source of ~7 eV for sub-meV resolution photoemission spectroscopy. In the last five years, the available photon energy has been increased to 11 eV using Yb fiber laser technology. It has high photon flux(10^{14} photons/sec) with sub-picosecond time resolution. Laser-based spin-resolved ARPES is realized in LASOR with 11 eV laser. This technology would open up a whole new field of spectroscopy. High-harmonic-generation based photoemission spectroscopy in the 20-60 eV region is another direction to be pursued. Femtosecond time domain spectroscopy has been achieved. Combined with picosecond time-domain spectroscopy using the pulsed light delivered by synchrotrons, we are investigating the electronic structures and dynamics of matter in the bulk, on the surface, and down to the nanoscale. The ultimate goal is to extend soft x-ray operando methods to lasers. Diffractions, magneto-optical effects, and inelastic scattering now performed at synchrotrons will be performed by lasers to access the real-time dynamics of chemical reactions and phase transitions down to femtoseconds.

State-of-the-art laser-based organismal spectroscopy is a new direction in LASOR. The ISSP research field is

shifting from simple materials and science to a complex one involving living bodies and functional materials with excited state physics.

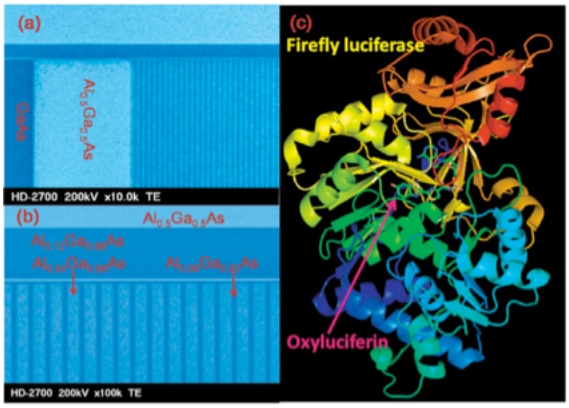

Fig. 7. Photonics devices under study: (left panel) semiconductor quantum wires and (right panel) firefly-bioluminescence system consisting of light emitter (oxyluciferin) and enzyme (luciferase)

Synchrotron Radiation Laboratory

The Synchrotron Radiation Laboratory (SRL) was established in 1975 as a research division dedicated to solid state physics using synchrotron radiation. Currently, SRL is composed of three research sites, the Sendai office, the Harima office and the E-building of the Institute for Solid State Physics.

Synchrotron soft X-ray experimental stations at Sendai office and Harima office

In 2009 SRL established the Harima branch laboratory in SPring-8 and operated a high brilliant and polarization-controlled 25-m long soft X-ray undulator beamline, BL07LSU until August 2022 in collaboration with Synchrotron Radiation Research Organization (SRRO) of the University of Tokyo. The management of the beamline was transferred to the RIKEN SPring-8 Center in September 2022. In November 2022, the Sendai office was formed on the Aobayama campus of Tohoku University under the auspices of a new SRRO launched in April 2022 and includes six departments of the University of Tokyo. At the end of FY2022, three endstations, ambient pressure X-ray photoemission (APXPS) (Fig. 1a), nanoESCA (Fig. 1c), and high resolution soft X-ray emission spectroscopy (HORNET-II) (Fig. 1d) stations were relocated to the new 3GeV synchrotron facility NanoTerasu in Sendai, which started commissioning of the storage ring in early 2023. In 2024, the Sendai Office witnessed significant progress following the official launch of NanoTerasu, which commenced its user operation on April 9, 2024. At the initial stage of operation, two beamlines—BL07U and BL08U—were fully equipped and opened to coalition users. During the first half of 2024, more than 30 user proposals were accepted, and in the second half, the number exceeded 40 users. The storage ring current has reached 200 mA in routine operation—surpassing that of SPring-8—enabling remarkably bright soft X-ray radiation that dramatically expands the scope of advanced spectroscopy experiments. Both BL07U and BL08U beamlines have achieved a spectral resolving power of $E/\Delta E > 15{,}000$ under standard conditions. In RIXS (Resonant Inelastic X-ray Scattering) experiments at HORNET-II station, energy resolutions around $E/\Delta E \approx 10{,}000$ have been realized in the photon energy range from N 1s (400 eV) to Fe 2p (710 eV). The APXPS station has reached a maximum operating pressure of 1 atm, successfully enabling in situ studies of surface reaction dynamics under true ambient conditions, which marks a significant technical achievement. In 2024, three research papers utilizing BL07U and BL08U have been published, accompanied by one press release and one news release. Continuous efforts are being made to further optimize beamline performance, including enhancements in beam stability, polarization control, and energy range extension. These developments indicate steady progress toward full-scale user operation and advanced experimental capabilities in the coming years.

At the Harima Office, research and development efforts have been actively pursued in collaboration with the RIKEN SPring-8 Center and the Japan Synchrotron Radiation Research Institute (JASRI), focusing on the development and application of next-generation X-ray imaging technologies utilizing both the soft X-ray beamline BL07LSU and the X-ray Free Electron Laser facility SACLA.

At BL07LSU, six undulators transferred to RIKEN have been reconfigured as an R&D beamline aimed at achieving higher stability and resolution. Advanced X-ray optical components such as mirrors, diffraction gratings, and polarization elements have been developed, achieving a spatial resolution of 50 nm in experimental imaging. Particular emphasis has been placed on ptychography in combination with total-reflection mirror optics (Fig. 1c) and high-intensity pink-beam illumination to establish an ultrafast spectro-microscopy method. This system is being extended toward a four-dimensional analytical framework integrating spatial, temporal, and energy domains.

At SACLA, ultrafast imaging experiments with femtosecond time resolution are underway to simultaneously observe the dynamics of electrons, spins, and lattice vibrations in materials. Exploratory studies of nonlinear optical phenomena, coherent phonons, and X-ray-induced magnetic transitions have also been initiated.

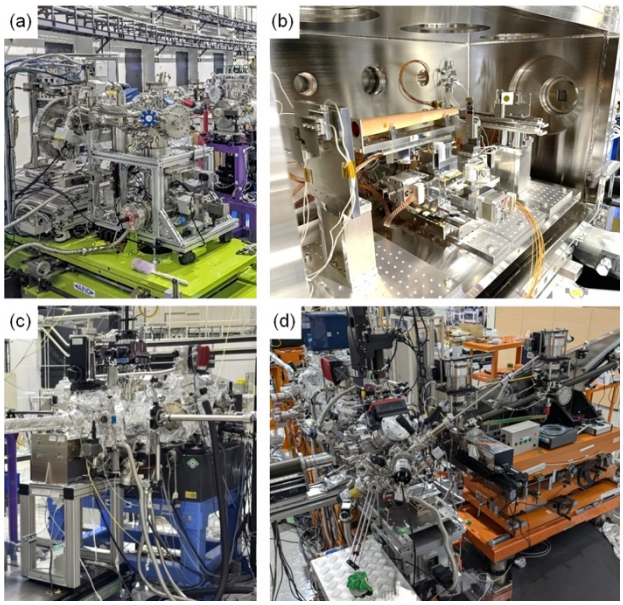

Fig. 1. Soft X-ray advanced experimental stations (a) Ambient pressure photoemission (APXPS) (b) Soft X-ray imaging (c) NanoESCA (d) Soft X-ray emission (HORNET-II). APXPS, NanoESCA and HORNET-II stations were transferred to the new 3GeV synchrotron facility NanoTerasu at the end of FY2022 and installed in BL07U (NanoESCA, HORNET-II) and BL08U (APXPS) at the end of FY2023.

High-resolution Laser SARPES and ARTOF system at E-building

High-resolution Laser Spin- and Angle-Resolved Photoemission Spectroscopy (SARPES) is a powerful technique

to investigate the spin-dependent electronic states in solids. In FY2014, LASOR and SRL staffs constructed a new SARPES apparatus (Fig. 2a), which was designed to provide high-energy and -angular resolutions and high efficiency of spin detection using a laser light at E-building. The achieved energy resolution of 1.7 meV in SARPES spectra is the highest in the world at present. From FY2015, the new SARPES system has been opened the joint-research program. The Laser-SARPES system consists of an analysis chamber, a carousel chamber connected to a load-lock chamber, and a molecular beam epitaxy chamber, which are kept ultra-high vacuum (UHV) environment and are connected to UHV gate valves. The electrons are excited with 6.994 eV photons, yielded by 6th harmonic of a Nd:YVO4 quasi-continuous wave laser with a repetition rate of 120 MHz, and 10.7 eV photons, driven by the third harmonic radiation at 347 nm of an Yb:fiber chirped pulse amplifier laser, which was developed by Kobayashi's lab in LASOR. The hemispherical electron analyzer is a custom-made Scienta Omicron DA30-L, modified for installing the spin detectors. The spectrometer is equipped with two high-efficient spin detectors orthogonally placed each other, associating very low energy electron diffraction, which allows us to analyze the three-dimensional spin polarization of electrons. At the exit of the hemispherical analyzer, a multi-channel plate and a CCD camera are also installed, which enables us to perform the angle-resolved photoelectron spectroscopy with two-dimensional (energy-momentum) detection. The laser-SARPES with 7 eV laser can provide both high-resolution spin-integrated and spin-resolved photo-emission spectra in various types of solids, such as spin-orbit coupled materials and ferromagnetic materials. In addition, using the 10.7 eV makes it possible to follow their ultrafast spin dynamics in the time domain by pump-probe scheme. A spectroscopy system using a dichroic mirror (SiO_2/HfO_2 multilayer) was introduced for a stable switching of the 7 eV and 10.7 eV lasers. A major experimental challenge lies in achieving both efficient spin detection and long-term stability in pump–probe measurements. In 2024, the team successfully improved the beam profile by introducing the fundamental wave into the optical path to compensate for deterioration in the laser amplifier over time. This modification has led to significant improvements in beam focus and intensity stability, resulting in enhanced reproducibility and higher-quality band dispersion images. With the energy resolution of 1.7 meV, the system now allows for precise spin-resolved analysis of electronic band structures.

Looking ahead, further advancements are planned through the implementation of a high-power optical parametric amplifier (OPA) to generate tunable pump pulses, enabling studies of nonlinear optical responses and photoinduced phase transitions under strong excitation conditions. Improvements to real-time laser diagnostics using FROG and related tools are also underway to enhance the accuracy of time-resolved measurements. Through these developments, we aim to strengthen its role as a national and international hub for spin dynamics research.

The time-resolved soft X-ray spectroscopy (TR-SX) station was moved from SPring-8 BL07LSU to the E-building in 2020. The measurement chamber is equipped with a unique electron spectrometer, the two-dimensional (2D) angle-resolved time-of-flight (ARTOF) analyzer (Fig. 2b). The system is currently operational for measurements of 2D angle-resolved photoemission spectroscopy with pulsed laser of 6 eV photon energy supplied by Itatani's lab in LASOR. Time-resolved measurements can also be conducted with temporal resolution of 600 fs. An ultra high-speed reading and visualization program is currently in development to enhance usability.

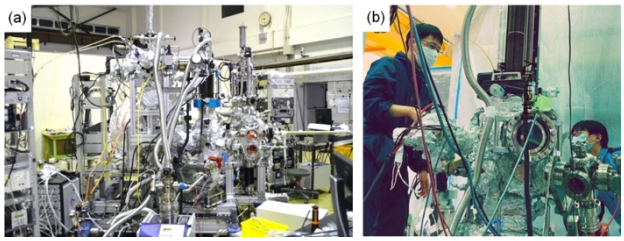

Fig. 2. (a) Laser-SARPES system and (b) ARTOF system at E-building.

Conferences and Workshops

Focus Week on Non-Equilibrium Quantum Dynamics

September 30 - October 4, 2024
H. Katsura, Y. Miao, M. Oshikawa, and M. Yamazaki

Nonequilibrium dynamics in quantum many-body systems is a fundamentally important yet notoriously difficult problem in statistical physics. Recent theoretical progress—much of it rooted in modern quantum field theory—has significantly deepened our understanding, and the subject has become central in high-energy theory as well. A characteristic example is the Sachdev–Ye–Kitaev (SYK) model. Originally conceived as a model for strongly correlated electrons, the SYK model features fermions with random, infinite-range interactions and is exactly solvable in the large-N limit. It exhibits maximally chaotic, fast-scrambling quantum dynamics saturating a bound on the Lyapunov exponent, and it connects in surprising ways to quantum gravity and gauge/gravity duality. With rapid advances in controllable quantum platforms and growing relevance to quantum devices and computation, there is a clear opportunity for breakthroughs by combining insights across disciplines.

To catalyze such cross-fertilization, we organized an international workshop bringing together leading researchers with diverse backgrounds. The meeting was held at the neighboring Kavli Institute for the Physics and Mathematics of the Universe (Kavli IPMU) as a Focus Week, co-hosted by ISSP. Topics covered included non-Hermitian systems, violations and breakdown mechanisms of the Eigenstate Thermalization Hypothesis (ETH), applications of generalized symmetry concepts, and holographic approaches to quantum dynamics. We had 15 invited talks by:

Masayuki Hashisaka (ISSP, Japan), Yunfeng Jiang (Yau Center, Southeast Univ., China),
Gyu-Boong Jo (HKUST, Hong Kong), Kohei Kawabata (ISSP, Japan),
Jong Yeon Lee (UIUC, USA), Chihiro Matsui (The University of Tokyo, Japan),
Pratik Nandy (RIKEN & YITP, Japan), Takashi Oka (ISSP, Japan), Pedram Roushan (Google, USA),
Kareljan Schoutens (University of Amsterdam, the Netherlands), Krishnendu Sengupta (IACS, India),
Hal Tasaki (Gakushuin University, Japan), Takafumi Tomita (IMS, Japan),
Frank Verstraete (Cambridge & Ghent, UK/Belgium), Derek S. Wang (IBM, USA).

We reserved ample time for discussion, leading to many questions during and after the talks. Most talks were recorded and have been uploaded to YouTube (https://youtube.com/playlist?list=PLqgD11rbhHmkEyc-_epjUw39g3lQuqSah&si=96m1hU_MeMlacA-p), which should be useful to colleagues who could not attend, as well as to participants for reviewing. In addition, we held poster sessions on Tuesday and Thursday with 25 contributions; the sessions were lively and continued well beyond the scheduled time. We subsidized travel for early-career participants based in Japan, which helped boost attendance among young researchers. The joint hosting by Kavli IPMU and ISSP successfully attracted participants from both the high-energy and condensed-matter communities; for many condensed-matter participants, this was their first visit to Kavli IPMU. In total, we had 82 participants, including 25 from abroad.

Overall, the workshop was a great success. We thank Kavli IPMU and ISSP for hosting, and JST for financial support (PRESTO Grant No. JPMJPR225A).

ISSP International Workshop “Materials Science of Solids and Surfaces using Radiation Field Controlled in Time and Space Domain”

October 28-31, 2024

K. Watanabe, T. Kumagai, R. Shiotari, O. Sugino,
Y. Hasegawa, I. Matsuda, R. Matsunaga, and J. Yoshinobu.

This ISSP International Workshop was held from October 28 to October 31, 2024. A total of 120 participants attended in person (including 10 international participants), and the cumulative number of participants over the four-day workshop was 293 (including 31 international participants).

In recent years, the interdisciplinary fields of radiation fields, nanoscale solid-state physics and surface science have rapidly developed. This field encompasses topics such as carrier-envelope-phase (CEP) controlled terahertz (THz) pulses using ultrashort pulse lasers, tip-enhanced Raman spectroscopy, local plasmons in metal nanoparticles, electric fields and scattered light at electrodes and interfaces, and novel optical properties of low-dimensional materials. Furthermore, experimental studies on local electronic properties and surface/interface reactions using *operando* spectroscopy with lasers and synchrotron radiation are expanding. ISSP has conducted these cutting-edge studies by the members in LASOR Center, Division of Nanoscale Science, and Division of Condensed Matter Theory. In this workshop, leading researchers were invited from the world and Japan. The workshop program consisted of one tutorial lecture, six oral presentation sessions (25 invited lectures and 4 contributed talks), and 34 poster presentations.

Researchers from different fields engaged in lively discussion. The posters mainly presented by young researchers and graduate students were of a high standard and featured active discussions. It was also impressive to see prominent overseas scientists taking notes during the lectures and asking questions. After the workshop, we received an email from an overseas invited speaker saying that “I would like to thank you from the bottom of my heart for the invitation to the workshop and the excellent organization. I learned a lot and enjoyed the talks and discussions tremendously!” Many participants were greatly inspired by learning cutting-edge research from different fields.

This workshop was supported by “ISSP International Workshop”, JST-CREST “Innovative Reactions”, and NINS “2024 Advanced Optical Science Research Project.” These supports enabled us to invite many researchers from both Japan and abroad. Finally, we would like to express our gratitude to Director Prof. Hiroi for his opening remarks and introduction of ISSP, as well as to the staffs (faculty members, administrative assistants) and graduate students of ISSP who made significant contributions to the workshop's organization.

The workshop program and abstracts can be downloaded from the following URL.
https://yoshinobu.issp.u-tokyo.ac.jp/2024Oct_ISSP_WS_Abstract_v4.pdf

Group photo at the workshop (October 30, 2024)

Correlated Quantum Materials + *beyond* (CQM+*b*2024)

November 18-29, 2024
H. Tsunetsugu, Y. Motome, and C. Batista

Following the tradition of the annual international theory workshops that began in 2006, this year's workshop was held over two weeks in late November with focusing on the discussion of cutting-edge theoretical research on strongly correlated systems. While the main themes centered on novel quantum magnetism and superconductivity, particular emphasis was placed on dynamics and nonequilibrium phenomena in strongly correlated quantum systems as well as the application of data science techniques such as machine learning and quantum information approaches.

Presentations about nonequilibrium and dynamical properties included topics such as the nonlinear optical response of spin liquids and the non-Hermitian Kondo effect. Regarding equilibrium properties, in-depth discussions were held on multipole degrees of freedom formed by spin and orbital moments in transition metal compounds. Topics also covered recent developments on altermagnets – a newly emerging class of antiferromagnets garnering rapid research interest – alongside kagome antiferromagnets and Kitaev materials related to spin liquids.

During the eight non-symposium days of the workshop, a total of 23 oral presentations were delivered, including 10 by invited speakers from overseas and 7 by invited speakers from Japan. Over the two-day symposium, there were 28 oral presentations (7 international invited speakers and 15 domestic invited speakers) and 52 poster presentations, of which 9 were from general international participants. In total, the workshop – including the symposium – had 151 registered participants, 33 of whom were from overseas. The total number of individual entries (i.e., attendance counts) was 178 during the two-day symposium and 224 during the remaining eight days, reaching an impressive total of 402.

To promote future international collaboration and joint research, we made a special effort to invite early-career researchers. In addition, 15 general participants from abroad – including graduate students and postdocs affiliated with the invited speakers – joined and actively interacted with domestic researchers, especially during and after the presentations. We believe that this workshop has laid the groundwork for multiple future collaborations.

11th Annual Ambient Pressure X-ray Photoelectron Spectroscopy Workshop(APXPS 2024）

December 3-6, 2024
I. Matsuda

This workshop was held as the international conference 11th Annual Ambient Pressure X-ray Photoelectron Spectroscopy Workshop (APXPS 2024) from December 3rd to 6th, 2024. This international workshop (APXPS Workshop), which specializes in the technology and application research of this method, has been held every year since 2014, but this was the first time it was held in Japan. The workshop was held face-to-face at Katahira Sakura Hall in the Tohoku University campus, where the University of Tokyo's Sendai office is located, and those affiliated with the Institute for Solid State Physics could also join online. Speakers and participants came from all over the world, with a total of 123 participants from 19 countries, including Japan.

Recently, *operando* measurements that directly observe actual materials in their operating environment have become indispensable. Our institute has been developing and jointly using the ambient pressure X-ray photoelectron spectroscopy (APXPS) system, which allows for real-time tracking of chemical reaction processes, at the SPring-8 synchrotron radiation facility. On the occasion of the construction of a new synchrotron radiation facility, NanoTerasu, our institute has updated a cutting-edge APXPS instrument at the soft X-ray beamline. The facility began the user operation in April of the year the symposium is held (2024). Thus, the institute took this opportunity to introduce our APXPS instrument to overseas experts, to become an international hub in the *operando* measurement research community, and to build a network of researchers.

The workshop program consisted of two keynote lectures, 13 oral presentation sessions (invited and general presentations), and a poster presentation session. The sessions were "Technical Innovations in *Operando* Spectroscopy", "Technical Update Session I", "Technical Update Session II", "*In Situ* Observations at Gas- Solid Interfaces I", "*In Situ* Observations at Gas- Solid Interfaces II", "*In Situ* Observations on Metals and Alloys", "*In Situ* Observations on Functional Materials", "*In Situ* Observations at Liquid- Solid Interfaces", "*In Situ* Observations on Electrocatalyst Surfaces and Interfaces", "*In Situ* Observations during Reactions with Oxygen", "*In Situ* Observations on Catalysts and Electrodes", "Real Applications in Environmental Science", and "*In Situ* Observations on Metal Oxides".

The technology of APXPS equipments has progressed rapidly with the development of synchrotron radiation, and many presentations on technological developments at the frontiers were given at the workshop. There were also many presentations on research into its use in the fields of catalytic chemistry, electrochemistry, and atmospheric chemistry. It was apparent that the APXPS method is being used around the world and is making a significant contribution to the development of science and technology in each country.

After the workshop, on December 9th, we invited one of the invited speakers to the University of Tokyo Kashiwa Campus to hold a face-to-face seminar. The seminar room was packed with an audience of nearly 30 participants. Lively discussions were held, making it a very successful event.

Finally, I would like to express our deep gratitude to the organizing members, Dr. S. Yamamoto, Dr. T. Abukawa, Dr. H. Kondoh, Dr. Y. Takagi, Dr. T. Koitaya, Dr. R. Yukawa, Dr. R. Toyoshima, and Dr. M. Horio. I am also thankful to the administrative staff at the Institute for Solid State Physics and the graduate students who supported the workshop.

The group photo of APXPS 2024 (Dec. 4, 2024)

Annual Meeting of MDCL Supercomputer Center and CCMS
－The Present and Future of Computational Materials Science－

April 3-4, 2024
T. Ozaki, N. Kawashima, O. Sugino, H. Noguchi, T. Misawa,
K. Ido, H. Nakano, J. Haruyama, M. Fukuda, and K. Yoshimi

This annual meeting brings together ISSP joint-use supercomputer users and CCMS members to share research progress. Organized in rotation by ISSP's computer-related staff, the event reflects advances in both supercomputing such as "Fugaku" and simulation methods, which have enabled more precise and large-scale studies. These developments support fundamental understanding of physical phenomena and collaborative work with experiments. The rise of machine learning and AI has further expanded computational materials science. Since FY2022, ISSP's system "kugui" (8 PF performance) has served as a national platform for simulation-based research. Held fully on-site, the workshop had 66 registrants, with 53 and 52 attendees on April 3rd and 4th, respectively. It featured 16 invited talks, including two by Yasuhiro Hatsugai (University of Tsukuba) and Masaaki Kondo (Keio University), and 31 poster presentations. Speakers from OIST, Hiroshima University, Ehime University, and NAIST were invited to enhance regional exchange. Topics ranged from strongly correlated systems and first-principles calculations to machine learning and soft matter simulations. The workshop highlighted emerging perspectives through data-driven approaches and provided insight into the future of the field. Kondo's special lecture introduced prospects for next-generation supercomputing and software development over the coming five years. Two posters, by Yasumasa Arakawa (Yamagata University) and Tetsuya Yamamoto (Keio University), were selected for the Excellent Poster Award by participant vote. Throughout the sessions, active discussion, particularly among students and early-career researchers, fostered community engagement and exchange.



Frontier of Neutron Science in Research Reactor
～Future Perspective of US-Japan Cooperative Program on Neutron Scattering～

September 4-5, 2024
T. Masuda, T.J. Sato, K. Kaneko, A. Aczel, and M. Frontzek

Three years have passed since the research reactor JRR-3 resumed operation, resulting in numerous scientific achievements and significant advancements in the development and upgrade of instrumentation. For example, the cold-neutron multiplex triple-axis spectrometer HODACA, constructed under the US-Japan Cooperative Program on Neutron Scattering, completed its commissioning phase last year and became available for user experiments this year. Meanwhile, Oak Ridge National Laboratory is planning the construction of the next-generation triple-axis spectrometer MANTA and rearranging existing instruments, timed with the replacement of the beryllium reflector. Additionally, in western Japan, construction plans for a new research reactor, led by JAEA, Kyoto University, and Fukui University, are advancing steadily. Given this rapidly evolving environment in neutron research, sharing expertise and know-how regarding instrument development is increasingly important.

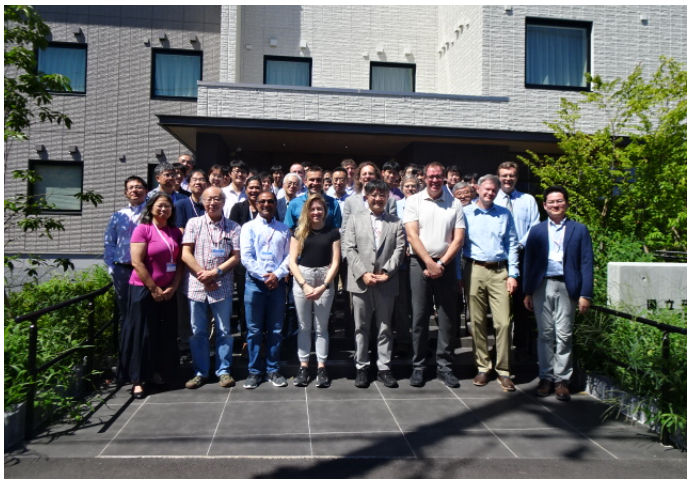

Against this background, this workshop invited 21 speakers (11 from the US and 10 from Japan) to discuss solid-state physics and soft matter research using neutron scattering, as well as neutron instrumentation development. The presentations covered cutting-edge topics from each field and stimulated active discussion. A poster session was also held, featuring 33 presentations primarily by early-career researchers (9 from the US and 24 from Japan).

ISSP Joint Research Results Presentation Meeting 2024

September 10, 2024
Joint Research Program Office (Kyodo Riyou Gakari)

The Joint Research Program is one of the most crucial functions of the Institute for Solid State Physics (ISSP). This symposium was organized to share the results obtained through the Joint Research Program at ISSP and to promote future collaborations. The program included four invited lectures: one by an external speaker and three by speakers within ISSP. From outside ISSP, Prof. Hiyama from Gunma University presented her theoretical and experimental research on the biological luminescence of firefly luciferase, conducted in collaboration with the Laser and Synchrotron Research Center (LASOR). From within ISSP, Dr. Kinoshita from the International MegaGauss Science Laboratory gave a talk on direct observation under strong magnetic fields using polarized light microscopy. Prof. Mayumi from the Neutron Science Laboratory presented recent studies on multicomponent soft matter using neutron scattering methods, while Dr. Okawa from LASOR reported on investigation of the electronic structures of thermoelectric material candidates and excitonic insulator candidates using time-resolved ARPES with high-harmonic lasers.

Frontier of New Materials and Systems Research: Physical Properties and Functionalities Based on Molecules and Atomic Clusters

October 2-4, 2024
Y. Okamoto, T. Akutagawa, T. Kusamoto, K. Takimiya, H. Yamamoto, T. Ideue, R. Takagi, S. Miwa, H. Mori, and J. Yamaura

This workshop was organized to facilitate the exchange of recent findings on the development of new materials and systems composed of molecules and atomic clusters with a focus on their physical properties and functionalities. Recently, various physical properties and functionalities, such as non-reciprocal superconductivity, chirality-induced spin selectivity, ferroelectrics based on molecular rotators, anisotropic circularly polarized luminescence, and exotic excitonic properties, have been discovered in new molecular compounds, metal complexes, metal-organic frameworks (MOFs), and van der Waals crystals, characterized by features such as chirality, polarization, nontrivial topology, molecular mobility, and luminescence. However, it remains challenging to get comprehensive overview of which studies are driving innovation within the broad field of molecular and cluster compounds. We organized a hybrid-style workshop from October 2nd to 4th, highlighting recent developments in materials and systems composed of molecules and atomic clusters with a view to their physical properties and functionalities. The workshop attracted 110 registered participants, with more than half attending on-site. It featured 34 invited talks and 17 poster presentations, fostering lively discussions and interdisciplinary exchange among researchers from a variety of fields.

Forefront Research in Glass and Related Fields

October 30-Novempber 1, 2024
S. Tatsumi, M. Kofu, O. Yamamuro, A. Ikeda, M. Saito, T. Kawasaki, and H. Akiba

This workshop, held at the Institute for Solid State Physics, is conducted every 3 to 4 years to share cutting-edge research with glass researchers from all around Japan. Lively discussions were held throughout the workshop, focusing on researchers in experiments, theories, and numerical calculations, as well as peripheral fields such as proteins, granular materials, pharmaceutics, and other related areas. Additionally, new trends were explored, including active glass and electronic glass. In addition to 42 oral presentations and 28 poster presentations, we have featured three special lectures by Osamu Yamamuro, Takeshi Kawasaki, and Kazushi Kanoda. Finally, we found very stimulating discussions that went beyond the boundaries of academic societies, involving participants from different academic fields who shared their daily research experiences.

Correlated Quantum Materials + *beyond*: Symposium

November 25-26, 2024
H. Tsunetsugu, Y. Motome, Y. Yanase, J. Otsuki, Y. Nomura, Y. Okamoto

This was a two-day symposium in the two-week theory workshop starting on Nov. 18 and provided a valuable platform for international participants and domestic researchers, both experimentalists and theorists, to engage in focused discussions. While the symposium's main theme centered novel quantum magnetism and superconductivity, two emerging directions were particularly emphasized.

The first was the study of dynamics and non-equilibrium phenomena. Presentations in this area featured several exciting developments, including nonlinear optics in cavity systems, spin switching in antiferromagnets using terahertz radiation, and high-harmonic spectroscopy. The second is the application of data-driven approaches, such as machine learning. The symposium also featured promising theoretical work on quantum many-body dynamics, eigenvalue optimization, and experimental data interpretation using Bayesian inference, demonstrating the growing potential of data science in condensed matter physics.

ISSP Women's Week 2024

December 3-4, 2024
T. Nakajima, T. Ideue, K. Kawabata, Y. Hasegawa, I. Matsuda, A. Miyata, J. Yamaura
A. Shirai, L. Watakabe, R. Watanabe, M. Hara, and R. Yamaoka

ISSP Women's week started from 2021 to encourage female scientists studying and working in condensed matter science. In the fiscal year of 2024, we organized "ISSP Women's Week(s) 2024" from November 22 to December 6 in 2024. During this period, regular ISSP seminars were held with female invited speakers. This period also included a talking event for female graduate students, in which female researchers working in universities, academic institutes or companies gave enlightening talks regarding their work careers. As the main event in this period, we organized ISSP women's week workshop 2024 on Dec. 3rd and 4th in the large lecture room of ISSP. We invited seven invited speakers, ranging from company researchers to university professors. In addition to their valuable talks, we held discussion sessions facilitated by graduate students of ISSP. The students brought up questions regarding gender equality, diversity in Japanese society, life-work balance etc., which leads to fruitful discussions between the students, invited speakers and the audience. There were more than 30 participants on each day. The week was supported by KIOXIA Holdings Corporation and by the MEXT Academic Transformative Research (A) project "Chemical Catastrophe in Ultra-Strong Magnetic Fields of 1000 Tesla: Science of Chemical Bonding in Non-Perturbative Magnetic Fields".

100th anniversary of pulsed magnets

December 16-18, 2024
A. Miyata, Y. Kohama, M. Tokunaga, Y. H. Matsuda, and K. Kindo

The concept of pulsed-field magnets dates back to the early 20th century. In 1924, Pyotr Kapitza first demonstrated the possibility of a pulsed magnet to generate magnetic fields up to 50 Tesla. To commemorate this milestone, we organized a workshop to review the development of pulsed magnets and to discuss recent advances and future directions in high-field research. In the workshop, a wide range of topics including quantum oscillations, topological materials, superconductors, magnetic materials, and experimental techniques under high magnetic fields were actively discussed. A total of 114 participants joined the workshop (102 onsite and 12 online). Many early-career researchers also gave oral and poster presentations, and the workshop provided a valuable opportunity for them to connect and build networks for future collaboration.

New trends in condensed matter theory 2024

December 9-11, 2024
T. Oka, T. Kato, M. Oshikawa, and K. Kawabata

The workshop New Trends in Quantum Condensed Matter Theory 2024 was held in December 2024, bringing together a wide range of topics in condensed matter physics. The field continues to evolve around quantum materials that exhibit remarkable quantum phenomena driven by strong interactions and unique electronic structures. Recent years have also seen rapid developments in nonequilibrium phenomena, active matter, artificial materials, and interdisciplinary areas involving quantum information science. Theoretical advances have been supported by progress in numerical methods and mathematical approaches.

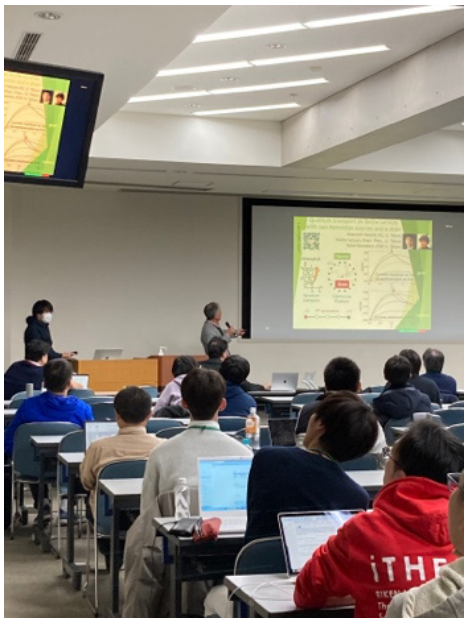

This workshop was organized to highlight these broad and dynamic developments, with a particular focus on early-career researchers who have made notable contributions in recent years. The program featured 18 invited talks and 36 poster presentations, stimulating lively discussions across disciplines and generations.

Topological Nonlinear Optics in Quantum Materials

February 19-21, 2025
T. Oka, R. Shimano, T. Morimoto, and M. Hayashi

The ISSP workshop Topological Nonlinear Optics in Quantum Materials was held from February 19 to 21, 2025, at the Institute for Solid State Physics, University of Tokyo. The workshop brought together researchers aiming to deepen the understanding of exotic optical responses in topological materials and explore future applications in quantum devices and novel functional materials. With a strong focus on fostering early-career researchers and enhancing ISSP's international role, the event provided a valuable platform for interdisciplinary exchange.

The program featured 23 invited talks covering a wide range of topics including Floquet theory, nonlinear optics, spin control with terahertz fields, and topological phenomena in quantum materials. Both theoretical and experimental perspectives were represented, with contributions from leading researchers across Japan and abroad. Notably, themes such as Berry-phase-driven shift currents, circular photogalvanic effects, and ultrafast control of quantum states highlighted the frontier of nonlinear optical studies.

The workshop gathered approximately 85 participants, both in person and online, enabling vibrant discussions across disciplines. By bridging topics from strong correlations and spintronics to quantum information and light–matter interactions, the event offered insight into the future of topological quantum photonics and reinforced ISSP's position as a hub for cutting-edge condensed matter research.

Advances of Frustrated Magnetism in Kagome Antiferromagnets

March 10-11, 2025
Y. Okamoto, Y. Kohama, C. Hotta, H. Yoshida and M. Yamashita

In magnetic systems with geometric frustration, including a kagome lattice, a quantum spin liquid state with no long-range order may appear with elementary excitations different from those in conventional magnetic materials, such as spinon excitations and Majorana quasiparticles. Among frustrated systems, kagome materials have been extensively studied because an emergence of a quantum spin liquid state is theoretically predicted even in the simplest Heisenberg model. Recently, the successful syntheses of new kagome materials have led to new discoveries, including the 1/9 magnetization plateau in $YCu_3(OH)_{6.5}Br_{2.5}$ and the 1/3 plateau at low magnetic fields in In-kapellasite. We thus had a workshop at ISSP to share advances of these new studies, as well as to review previous experimental and theoretical studies on kagome antiferromagnets. We also had many presentations reporting progresses in research on frustrated magnetism done in frustrated magnetism not limited in kagome materials. The workshop began with review lectures on kagome materials by Prof. Yoshida from Hokkaido Univ. and Prof. Hotta from University of Tokyo focusing on the experimental and theoretical perspectives, respectively. We also had 16 oral presentations and 17 poster presentations. This meeting was found to be very successful and meaningful with nearly 60 participants for lively hot discussions that include progresses in research on magnetization plateaus in kagome lattice antiferromagnets, as well as advancements in studies of other frustrated magnets.

Publications

ISSP publications

Division of Condensed Matter Science

Mori group

We have successfully developed and unveiled unprecedented functional properties for the molecular materials and systems. The major achievements in 2024 are to develop (1) the high conductive EDOT [(3,4-ethylenedioxythiophene)] -based oligomer conductors by the introduction of Se atoms and (2) the Ni dithiolene-based flexible capsules with uniaxial magnetic anistoropy in water.

1. オリゴマー型有機電子材料の高伝導化: 藤野 智子, 小野塚 洸太, 森初 果, 応用物理 **93**, 490-493 (2024).
2. †*Orbital hybridization of donor and acceptor to enhance the conductivity of mixed-stack complexes: T. Fujino, R. Kameyama, K. Onozuka, K. Matsuo, S. Dekura, T. Miyamoto, Z. Guo, H. Okamoto, T. Nakamura, K. Yoshimi, S. Kitou, T.-H. Arima, H. Sato, K. Yamamoto, A. Takahashi, H. Sawa, Y. Nakamura and H. Mori, Nat Commun **15**, 3028 (2024).
3. †*Combined x-ray diffraction, electrical resistivity, and *ab initio* study of $(TMTTF)_2PF_6$ under pressure: Implications for the unified phase diagram: M. Itoi, K. Yoshimi, H. Ma, T. Misawa, T. Tsumuraya, D. Bhoi, T. Komatsu, H. Mori, Y. Uwatoko and H. Seo, Phys. Rev. Research **6**, 043308 (1-14) (2024).
4. *Higher conductivity in doped ethylenedioxythiophene (EDOT) dimers with chalcogen-substituted end groups: K. Onozuka, T. Fujino, T. Miyamoto, T. Yamakawa, H. Okamoto, H. Akiba, O. Yamamuro, E. Kayahara, S. Yamago, H. Oike and H. Mori, J. Mater. Chem. C **12**, 13956 (2024).
5. Single-crystalline oligomer-based conductors modeling the doped poly(3,4-ethylenedioxythiophene) family: T. Fujino, R. Kameyama, K. Onozuka, K. Matsuo, S. Dekura, K. Yoshimi and H. Mori, Faraday Discuss. **250**, 348 (2024).
6. *Discovery of bicyclic borane molecule $B_{14}H_{26}$: X. Zhang, T. Fujino, Y. Ando, Y. Tsujikawa, T. Wang, T. Nakashima, H. Sakurai, K. Yamaguchi, M. Horio, H. Mori, J. Yoshinobu, T. Kondo and I. Matsuda, Commun Chem **8**, 14 (2025).
7. *Macroscopic Structural Transition of Nickel Dithiolate Capsule with Uniaxial Magnetic Anisotropy in Water: T. Fujino, M. Hishida, M. Ito, T. Nakamura, M. Asada, N. Kurahashi, H. Kiuchi, Y. Harada, K. Harano, R. Makiura, K. J. Takeno, S. Yokomori, H. Oike and H. Mori, Adv. Science (2025), accepted for publication.
8. 高性能かつ大気安定なアンバイポーラ型分子性半導体材料の開発: 藤野 智子, 伊藤 雅聡, 森 初果, 「有機半導体の開発と最新動向」, 監修： 安達千波矢, (シーエムシー出版, 2024), 154-163.

Osada group

We have studied the tight-binding model for the α-type layered organic conductors, α-$(ET)_2I_3$ and α-$(BETS)_2I_3$, with a uniform interlayer coupling accompanied by spin-orbit interaction originating from the I_3^- anion potential. The model preserves the time reversal and inversion symmetries. In α-$(ET)_2I_3$, the interlayer spin-orbit coupling realizes the experimentally suggested Dirac semimetal state with inversion symmetry. In contrast, the inversion breaking in interlayer hoppings realizes the Weyl semimetal state without spin-orbit coupling. In α-$(BETS)_2I_3$, the proposed strong topological insulator is hardly realized with inversion symmetry.

1. Hofstadter Butterfly and Broken-Symmetry Quantum Hall States in α-Type Organic Dirac Fermion Systems: T. Osada, J. Phys. Soc. Jpn. **93**, 034711(1-6) (2024).
2. Three-Dimensional Topological Semimetal/Insulator States in α-Type Organic Conductors with Interlayer Spin-Orbit Interaction: T. Osada, J. Phys. Soc. Jpn. **93**, 123703(1-4) (2024).

Yamashita group

We have been studying (1) quantum criticality in heavy-fermion materials by ultralow temperature cryostat, (2) thermal-Hall conductivity of exotic excitations in frustrated magnets and (3) a new technique for the study of strongly-correlated electron systems. In this year, we have performed (1) low-temperature magnetostriction measurements of a quantum spin ice candidate $Ce_2Hf_2O_7$ (2) spontaneous thermal Hall measurements of candidate materials of chiral superconductivity, and (3) thermal Hall measurements of kagome antiferromagnets.

1. Doping-tunable Fermi surface with persistent topological Hall effect in the axion candidate $EuIn_2As_2$: J. Yan, J. Si, Z. Jiang, H. Ma, Y. Uwatoko, B.-T. Wang, X. Luo, Y. Sun and M. Yamashita, Phys. Rev. B **110**, 115111 (2024).
2. Magnetic structure of polar magnet GaV_4Se_8 with Ne´el-type skyrmion lattice probed by ^{51}V NMR: H. Takeda, M. Ishikawa, M. Takigawa, M. Yamashita, Y. Fujima and T.-H. Arima, Phys. Rev. B **110**, 224430 (2024).
3. $*\mathbf{J}_{eff}$ = 1/2 Hyperoctagon Lattice in Cobalt Oxalate Metal-Organic Framework: H. Ishikawa, S. Imajo, H. Takeda, M. Kakegawa, M. Yamashita, J.-I. Yamaura and K. Kindo, Phys. Rev. Lett. **132**, 156702 (2024).
4. Incommensurate magnetic order in an axion insulator candidate $EuIn_2As_2$ investigated by NMR measurement: H. Takeda, J. Yan, Z. Jiang, X. Luo, Y. Sun and M. Yamashita, npj Quantum Mater. **9**, 67 (2024).
5. Magnon thermal Hall effect via emergent SU(3) flux on the antiferromagnetic skyrmion lattice: H. Takeda, M. Kawano, K. Tamura, M. Akazawa, J. Yan, T. Waki, H. Nakamura, K. Sato, Y. Narumi, M. Hagiwara, M. Yamashita and C. Hotta, Nature Communications **15**, 566 (2024).
6. †Rotational Gru¨neisen ratio: A probe for quantum criticality in anisotropic systems: S. Yuasa, Y. Kono, Y. Ozaki, M. Yamashita, Y. Shimura, T. Takabatake and S. Kittaka, Phys. Rev. B **111**, 045123 (2025).

Ideue group

We have explored novel transport and optical properties reflecting symmetry breaking in two-dimensional materials. We found that symmetry-reduced uniaxial-strained trigonal superconductor exhibits a superconducting diode effect. We also investigated nonlinear optical properties of symmetry-controlled van der Waals magnets. In particular, we revealed that complex magnetic symmetry and the resulting unique second harmonic generation can be realized at the heterointerface of two-dimensional magnets with different magnetic anisotropies.

1. ∗Gilbert damping of NiFe thin films grown on two-dimensional chiral hybrid lead-iodide perovskites: T. Hatajiri, S. Sakamoto, H. Kosaki, Z. Tian, M. Tanaka, T. Ideue, K. Inoue, D. Miyajima and S. Miwa, Phys. Rev. B **110**, 054435 (1-6) (2024).
2. Superconducting diode effect under time reversal symmetry: F. Liu, Y. M. Itahashi, S. Aoki1, Y. Dong, Z. Wang, N. Ogawa, T. Ideue and Y. Iwasa, Science Advances **10**, eado1502 (2024).
3. Gate-Controlled Potassium Intercalation and Superconductivity in Molybdenum Disulfide: R. D. Septianto, A. P. Romagosa, Y. Dong, H. Matsuoka, T. Ideue, Y. Majima and Y. Iwasa, Nano Letters **24**, 13790-13795 (2024).
4. Giant Modulation of the Second Harmonic Generation by Magnetoelectricity in Two-Dimensional Multiferroic $CuCrP_2S_6$: S. Aoki, Y. Dong, Z. Wang, X. S. W. Huang, Y. M. Itahashi, N. Ogawa, T. Ideue and Y. Iwasa, Advanced Materials **36**, 2312781 (2024).

Takagi group

This year we have reported spontaneous topological Hall effect induced by collinear antiferromagnetic order in altermagnet FeS. We also revealed multistep topological transitions in a tetragonal magnet $GdRu_2Ge_2$ and spin excitations for skyrmionin states in a polar magnet $VOSe_2O_5$.

1. SP-STM study of the multi-Q phases in $GdRu_2Si_2$: J. Spethmann, N. D. Khanh, H. Yoshimochi, R. Takagi, S. Hayami, Y. Motome, R. Wiesendanger, S. Seki and K. von Bergmann, Phys. Rev. Materials **8**, 064404 (2024).
2. ∗Multistep topological transitions among meron and skyrmion crystals in a centrosymmetric magnet: H. Yoshimochi, R. Takagi, J. Ju, N. D. Khanh, H. Saito, H. Sagayama, H. Nakao, S. Itoh, Y. Tokura, T. Arima, S. Hayami, T. Nakajima and S. Seki, Nature Physics **20**, 1001-1008 (2024).
3. Exotic Spin Excitations in a Polar Magnet $VOSe_2O_5$: T. Araki, R. Takagi, T. Kurumaji, Y. Tokura, M. Mochizuki and S. Seki, Physical Review Letters **133**, 136702 (2024).
4. *Spontaneous Hall effect induced by collinear antiferromagnetic order at room temperature: R. Takagi, R. Hirakida, Y. Settai, R. Oiwa, H. Takagi, A. Kitaori, K. Yamauchi, H. Inoue, J.-I. Yamaura, D. Nishio-Hamane, S. Itoh, S. Aji, H. Saito, T. Nakajima, T. Nomoto and R. A. &. S. Seki, Nature Materials **24**, 63-68 (2025).

Division of Condensed Matter Theory

Tsunetsugu group

We have worked on a theoretical proposal for realizing long-period modulated structures of electronic degrees of freedom with even parity under time reversal operation. This includes various incommensurate orders of electric quadrupoles using electron's orbital degrees of freedom. We have demonstrated the presence of such an incommensurate phase realized on a triangular lattice. We have performed Monte Carlo simulations to investigate long range correlations based on its classical effective model, and found that it is a critical phase characterized by a Kosterlitz-Thouless type transition. We have also continued a study on basic properties of chiral phonons and now the target system is a three dimensional lattice with cubic symmetry.

1. Numerical Renormalization Group Study of Quadrupole Kondo Effect with the Crystal-Field Excited State: Y. Kaneko and H. Tsunetsugu, J. Phys. Soc. Jpn. **93**, 033705 (2024).
2. Orbital moire´ and quadrupolar triple-q physics in a triangular lattice: K. Hattori, T. Ishitobi and H. Tsunetsugu, Phys. Rev. Research **6**, L042068-1-7 (2024).
3. Proof of Completeness of the Local Conserved Quantities in the One-Dimensional Hubbard Model: K. Fukai, J Stat Phys **191**, 70 (2024).
4. On correlation functions in models related to the Temperley-Lieb algebra: K. Fukai, R. Kleinemu¨hl, B. Pozsgay and E. Vernier, SciPost Phys. **16**, 003 (2024).

Kato group

The main research subject of Kato Lab. is transport properties in mesoscopic and spintronic devices. We theoretically studied nonequilibrium spin transport in the context of chiral phonons, material curvature, spin noises, thermal transport, and spin pumping.

1. Spin pumping into quantum spin chains: S. C. Furuya, M. Matsuo and T. Kato, Phys. Rev. B **110**, 165129(1-13) (2024).
2. Theory of the inverse Rashba-Edelstein effect induced by thermal spin injection: K. Hosokawa, M. Yama, M. Matsuo and T. Kato, Phys. Rev. B **110**, 035309(1-12) (2024).
3. Chirality-Induced Phonon-Spin Conversion at an Interface: T. Funato, M. Matsuo and T. Kato, Phys. Rev. Lett. **132**, 236201(1-7) (2024).
4. †*Observation of Terahertz Spin Hall Conductivity Spectrum in GaAs with Optical Spin Injection: T. Fujimoto, T. Kurihara, Y. Murotani, T. Tamaya, N. Kanda, C. Kim, J. Yoshinobu, H. Akiyama, T. Kato and R. Matsunaga, Phys. Rev. Lett. **132**, 016301(1-7) (2024).
5. †*Sub-photon accuracy noise reduction of a single shot coherent diffraction pattern with an atomic model trained autoencoder: T. Ishikawa, Y. Takeo, K. Sakurai, K. Yoshinaga, N. Furuya, Y. Inubushi, K. Tono, Y. Joti, M. Yabashi, T. Kimura and K. Yoshimi, Opt. Express **32**, 18301 (2024).
6. †*H-wave – A Python package for the Hartree-Fock approximation and the random phase approximation: T. Aoyama, K. Yoshimi, K. Ido, Y. Motoyama, T. Kawamura, T. Misawa, T. Kato and A. Kobayashi, Computer Physics Communications **298**, 109087(1-10) (2024).
7. 国際物理オリンピック 2023 日本大会　理論問題作成の舞台裏: 加藤 岳生, 大学の物理教育 **30**, 10-13 (2024).
8. Curvature-induced valley-dependent spin-orbit interaction: A. Yamakage, T. Sato, R. Okuyama, T. Funato, W. Izumida, K. Sato, T. Kato and M. Matsuo, Phys. Rev. B **111**, 045121(1-12) (2025).
9. *Light-induced inverse spin Hall effect and field-induced circular photogalvanic effect in GaAs revealed by two-dimensional terahertz Fourier analysis: T. Fujimoto, Y. Murotani, T. Tamaya, T. Kurihara, N. Kanda, C. Kim, J. Yoshinobu, H. Akiyama, T. Kato and R. Matsunaga, Phys. Rev. B **111**, L201201 (2025).
10. Microscopic theory of Rashba-Edelstein magnetoresistance: M. Yama, M. Matsuo and T. Kato, Phys. Rev. B **111**, 144416(1-20) (2025).
11. Fluctuations in Spin Dynamics Excited by Pulsed Light: T. Sato, S. Watanabe, M. Matsuo and T. Kato, Phys. Rev. Lett. **134**, 106702(1-7) (2025).
12. Theory of spin pumping and inverse Rashba-Edelstein effect in a two-dimensional electron gas: M. Yama, M. Matsuo and T. Kato, in: *Proceedings Volume 13119, Spintronics XVII* (SPIE, 2024), 105.

Kawabata group

Recent years have seen remarkable progress in the physics of open quantum systems. In view of the recent rapid development of quantum information science and technology, it seems urgent to develop a general theory of open quantum systems. In our group, we are broadly interested in theoretical condensed matter physics, with a particular focus on nonequilibrium physics, to establish new foundations and principles in contemporary physics. Our recent research highlights topological phases of open quantum systems, as well as dissipative quantum chaos and lack thereof. On the basis of fundamental concepts such as symmetry and topology, we aim to uncover new physics intrinsic to far from equilibrium.

1. Topological enhancement of nonnormality in non-Hermitian skin effects: Y. O. Nakai, N. Okuma, D. Nakamura, K. Shimomura and M. Sato, Phys. Rev. B **109**, 144203 (2024).
2. Lieb-Schultz-Mattis Theorem in Open Quantum Systems: K. Kawabata, R. Sohal and S. Ryu, Phys. Rev. Lett. **132**, 070402 (2024).
3. Non-Hermitian Topology in Hermitian Topological Matter: S. Hamanaka, T. Yoshida and K. Kawabata, Phys. Rev. Lett. **133**, 266604 (2024).
4. Universal hard-edge statistics of non-Hermitian random matrices: Z. Xiao, R. Shindou and K. Kawabata, Phys. Rev. Research **6**, 023303 (2024).
5. Field theory of non-Hermitian disordered systems: Z. Chen, K. Kawabata, A. Kulkarni and S. Ryu, Phys. Rev. B **111**, 054203 (2025).
6. Multifractality of the many-body non-Hermitian skin effect: S. Hamanaka and K. Kawabata, Phys. Rev. B **111**, 035144 (2025).
7. Universal Stochastic Equations of Monitored Quantum Dynamics: Z. Xiao, T. Ohtsuki and K. Kawabata, Phys. Rev. Lett. **134**, 140401 (2025).
8. Non-linear sigma models for non-Hermitian random matrices in symmetry classes AI† and AII†: A. Kulkarni, K. Kawabata and S. Ryu, J. Phys. A **58**, 225202 (2025).
9. Topological Order Intrinsic to Mixed Quantum States: K. Kawabata, Physics **18**, 9 (2025).

Division of Nanoscale Science

Otani group

In 2024, we made significant progress in spintronics, magnonics, and antiferromagnetic systems by developing new methods to control and detect spin, orbital, and phononic dynamics. We demonstrated enhanced magnetoacoustic coupling via spin current. We studied spin relaxation in monolayers and generated out-of-plane spin currents at ferromagnet/EuS interfaces. In antiferromagnets, we controlled chiral and octupole domain walls, observed fast domain-wall motion, and imaged cluster magnetic octupole moments in MnSn nanowires. We also achieved perpendicular magnetization in noncollinear systems. In magnonics, we demonstrated strong spin wave–SAW coupling, nonreciprocal magnetoacoustic waves, and hybrid magnon-phonon crystals. We tuned magnon-magnon interactions and examined underlayer effects in heterostructures. We applied these insights to high-sensitivity SAW magnetic sensors and contributed to broader perspectives through the 2024 magnonics roadmap and a chapter on voltage-controlled anisotropy. Together, we advanced low-power spintronic technologies through collaborative, cross-disciplinary research.

1. The 2024 magnonics roadmap: B. Flebus, D. Grundler, B. Rana, Y. Otani, I. Barsukov, A. Barman, G. Gubbiotti, P. Landeros, J. Akerman, U. Ebels, P. Pirro, V. E. Demidov, K. Schultheiss, G. Csaba, Q. Wang, F. Ciubotaru, D. E. Nikonov, P. Che, R. Hertel, T. Ono, D. Afanasiev, J. Mentink, T. Rasing, B. Hillebrands, S. V. Kusminskiy, W. Zhang, C. R. Du, A. Finco, T. van der Sar, Y. K. Luo, Y. Shiota, J. Sklenar, T. Yu and J. Rao, J. Phys.: Condens. Matter **36**, 363501 (2024).
2. Generation of out-of-plane polarized spin current in (permalloy, Cu)/EuS interfaces: P. Gupta, N. Chowdhury, M. Xu, P. K. Muduli, A. Kumar, K. Kondou, Y. Otani and P. K. Muduli, Phys. Rev. B **109**, L060405 (2024).
3. Role of the nonmagnetic underlayer in controlling the electronic structure of ferromagnet/nonmagnetic-metal heterostructures: D. Panda, K. K. Behera, S. Madhur, B. Rana, A. Gloskovskii, Y. Otani, A. Barman and I. Sarkar, Phys. Rev. B **110**, 094424 (2024).
4. Spin relaxation of localized electrons in monolayer $MoSe_2$: Importance of random effective magnetic fields: E. Yalcin, I. V. Kalitukha, I. A. Akimov, V. L. Korenev, O. S. Ken, J. Puebla, Y. Otani, O. M. Hutchings, D. J. Gillard, A. I. Tartakovskii and M. Bayer, Phys. Rev. B **110**, L161405 (2024).

5. Observation of Cluster Magnetic Octupole Domains in the Antiferromagnetic Weyl Semimetal Mn_3Sn Nanowire: H. Isshiki, N. Budai, A. Kobayashi, R. Uesugi, T. Higo, S. Nakatsuji and Y. Otani, Phys. Rev. Lett. **132**, 216702 (2024).

6. Strongly Coupled Spin Waves and Surface Acoustic Waves at Room Temperature: Y. Hwang, J. Puebla, K. Kondou, C. Gonzalez-Ballestero, H. Isshiki, C. S. Mun˜oz, L. Liao, F. Chen, W. Luo, S. Maekawa and Y. Otani, Phys. Rev. Lett. **132**, 056704 (2024).

7. Nonreciprocal magnetoacoustic waves with out-of-plane phononic angular momenta: L. Liao, F. Chen, J. Puebla, J.-I. Kishine, K. Kondou, W. Luo, D. Zhao, Y. Zhang, Y. Ba and Y. Otani, Sci. Adv. **10**, eado2504 (2024).

8. Current-driven fast magnetic octupole domain-wall motion in noncollinear antiferromagnets: M. Wu, T. Chen, T. Nomoto, Y. Tserkovnyak, H. Isshiki, Y. Nakatani, T. Higo, T. Tomita, K. Kondou, R. Arita, S. Nakatsuji and Y. Otani, Nat Commun **15**, 4305 (2024).

9. Widen-dynamic-range surface acoustic wave magnetic sensors with high sensitivity: F. Chen, J. Lu, S. Liang, Y. Otani, X. Yang, Y. Zhang and W. Luo, Journal of Alloys and Compounds **980**, 173635 (2024).

10. Effect of the underlayer on the elastic parameters of the CoFeB/MgO heterostructures: S. Shekhar, S. Mielcarek, Y. Otani, B. Rana and A. Trzaskowska, Scientific Reports **14**, 20259 (2024).

11. Tunable strong magnon-magnon coupling in two-dimensional array of diamond shaped ferromagnetic nanodots: S. Majumder, S. Choudhury, S. Barman, Y. Otani and A. Barman, Phys. Scr. **99**, 025935 (2024).

12. Hybrid magnon-phonon crystals: L. Liao, J. Liu, J. Puebla and Q. S. &. Y. Otani, npj Spintronics **3**, 6 (2024).

13. Selective Data Writing in IrMn-Based Perpendicular Magnetic Tunnel Junction Array Through Voltage-Gated Spin-Orbit Torque: W. Li, Z. Liu, S. Peng, J. Lu, J. Liu, X. Li, S. Lu, Y. Otani and W. Zhao, IEEE Electron Device Lett. **45**, 921 (2024).

14. Nonreciprocal resonant surface acoustic wave absorption in $Y_3Fe_5O_{12}$: Y. Ba, J. Puebla, K. Yamamoto, Y. Hwang, L. Liao, S. Maekawa, O. Klein and Y. Otani, Phys. Rev. B **111**, 104401 (2025).

Hasegawa group

It is known that the vortices of monolayer superconductors formed on a substrate vary in shape at substrate steps because of the disruption of the electronic states. Vortices trapped at the steps on the striped incommensurate (SIC) phase of the Pb monolayer (ML) formed on a Si(111) substrate exhibited a round shape like those on the terraces. In contrast, the step-trapped vortices on the $\sqrt{3} \times \sqrt{7}$ Pb ML phase are elongated along the step direction, which are called Josephson-Abrikosov vortices. From the different vortex shapes, one can expect different strengths of electronic decoupling in the steps. To directly observe the different decoupling, we performed scanning tunnelling potentiometry (STP), which enables us to obtain the electrochemical potential distribution with the same spatial resolution as scanning tunneling microscopy (STM). We performed STP on the two Pb ML phases and found clear potential drops at the $\sqrt{3} \times \sqrt{7}$ Pb ML phase steps, whereas there was almost no drop in the SIC phase steps. This is the first quantitative demonstration of the resistivity of steps and their influence on superconductivity as a single disorder.

1. †*Quasi-Periodic Growth of One-Dimensional Copper Boride on Cu(110): Y. Tsujikawa, X. Zhang, K. Yamaguchi, M. Haze, T. Nakashima, A. Varadwaj, Y. Sato, M. Horio, Y. Hasegawa, F. Komori, M. Oshikawa, M. Kotsugi, Y. Ando, T. Kondo and I. Matsuda, Nano Lett. **24**, 1160 (2024).

2. †*Dimensional crossover and chirality of boron adsorbates on copper (110) surfaces: Y. Tsujikawa, T. Nakashima, X. Zhang, K. Yamaguchi, M. Horio, M. Haze, Y. Hasegawa, F. Komori, T. Kondo, Y. Ando and I. Matsuda, Phys. Rev. Materials **8**, 084003 1-7 (2024).

3. †Bound states in the core of ordered vortices in stoichiometric iron-based superconductor $CaKFe_4As_4$: W. Wu, W. Li, Y. Chen, M. Haze, T. Tamegai and Y. Hasegawa, Phys. Rev. B **111**, 054510 1-9 (2025).

4. Simple Model for Striped-incommensurate Phase Formed by Pb Adsorption on Si(111): M. Yamada, Y. Sato, M. Haze and Y. Hasegawa, e-J. Surf. Sci. Nanotechnol. **23**, 2025-019 1-8 (2025).

5. †Localized creation of bubble domains in Fe_3GaTe_2 by conductive atomic force microscopy: C.-M. Liu, Y.-J. Liu, P.-C. Chang, P.-W. Chen, M. Haze, M.-H. Hsu, N. N. Gopakumar, Y. Zhou, Y.-H. Tung, S. Hammouda, C.-H. Du, Y. Hasegawa, Y. Su, H.-C. Chiu and W.-C. Lin, Applied Surface Science Advances **26**, 100718 1-8 (2025).

Lippmaa group

Slightly canted, non-collinear antiferromagnets have very fast spin dynamics and the small residual magnetic moment can be used to probe the spin orientation and the domain structure that are normally difficult to quantify in antiferromagnetic materials. We are developing fabrication methods for obtaining high-quality antiferromagnetic films. The starting point is the orthoferrite $YFeO_3$, for which the magnetic domain structure can be controlled by the use of an orthorhombic substrate as an epitaxial template. This technique has allowed us to fabricate films large magnetic domains that have similar switching behavior to bulk single crystals, opening a path to developing thin-film-based magnetic switching devices.

1. *Fabrication of single-crystalline $YFeO_3$ films with large antiferromagnetic domains: C. Wang, M. Lippmaa and S. Nakatsuji, J. Appl. Phys. **135**, 113901 (1-8) (2024).
2. Polarity of homoepitaxial ZnO films grown by Nd:YAG pulsed laser deposition: T. Masuda, T. Sato, M. Lippmaa, T. Dazai, N. Sekine, I. Hosako, H. Koinuma and R. Takahashi, J. Appl. Phys. **136**, 095303 (1-8) (2024).
3. †The use of He buffer gas for moderating the plume kinetic energy during Nd:YAG-PLD growth of $Eu_xY_{2-x}O_3$ phosphor films: S. Suzuki, T. Dazai, T. Tokunaga, T. Yamamoto, R. Katoh, M. Lippmaa and R. Takahashi, J. Appl. Phys. **135**, 195302 (2024).
4. *Broken Screw Rotational Symmetry in the Near-Surface Electronic Structure of *AB*-Stacked Crystals: H. Tanaka, S. Okazaki, M. Kobayashi, Y. Fukushima, Y. Arai, T. Iimori, M. Lippmaa, K. Yamagami, Y. Kotani, F. Komori, K. Kuroda, T. Sasagawa and T. Kondo, Phys. Rev. Lett. **132**, 136402 (1-6) (2024).

Hashisaka group

We have continued setting up our experimental equipment, including introducing a dilution refrigerator. Alongside this, we conducted joint research on the on-chip transport of graphene plasmons and published review papers reporting on quantum transport in fractional quantum Hall systems. We also worked on developing nano-fabrication technology for quantum materials and creating nano-devices from candidate materials for quantum spin liquids, and we have already obtained some experimental results.

1. Gate-tunable giant superconducting nonreciprocal transport in few-layer Td-$MoTe_2$: T. Wakamura, M. Hashisaka, S. Hoshino, M. Bard, S. Okazaki, T. Sasagawa, T. Taniguchi, K. Watanabe, K. Muraki and N. Kumada, Phys. Rev. Research **6**, 013132 (2024).
2. エッジ状態のダイナミクスとエニオン統計: 橋坂 昌幸, 物性若手夏の学校テキスト **68**, 240 (2024).
3. On-chip transfer of ultrashort graphene plasmon wave packets using terahertz electronics: K. Yoshioka, G. Bernard, T. Wakamura, M. Hashisaka, K.-I. Sasaki, S. Sasaki, K. Watanabe, T. Taniguchi and N. Kumada, Nat Electron **7**, 537 (2024).
4. Coherent electron splitting in interacting chiral edge channels: E. Iyoda, T. Shimizu and M. Hashisaka, Phys. Rev. B **111**, 165414 (2025).
5. Mach-Zehnder interference of fractionalized electron-spin excitations: T. Shimizu, E. Iyoda, S. Sasaki, A. Endo, S. Katsumoto, N. Kumada and M. Hashisaka, Phys. Rev. B **111**, L161406 (2025).
6. 分数/整数量子ホール接合から紐解く分散エッジ状態の量子相: 橋坂 昌幸, 村木 康二, 固体物理 **60**, 171 (2025).

Yoshinobu group

We conducted several research projects in the fiscal year 2024: (1) The hydrogenation of formate and formaldehyde species on the H-Cu(997) surface was studied by HREELS and TPD. Several species were observed as desorption products by TPD, and intermediate species were identified. (2) The adsorption and decomposition of methanol on the Cu(977) and Pd-Cu(977) surfaces were studied by TPD, IRAS and SR-XPS, and selective dehydrogenation into formaldehyde was observed without oxygen. (3) The reactive desorption of CO + O -> CO_2 on Pt(111) was studied using ab-initio molecular dynamics (AIMD) with van der Waals DFT functionals. The desorption dynamics of CO_2 including kinetic energy, angular distribution and vibrational excitation were quantitatively elucidated. In addition, multidimensional neural network potential have been investigated. (4) The chemical states and reactions on the basal plane and the edge plane of MoS_2 and HOPG were studied by SR-XPS. (5) SFG spectroscopy was developed using ultra-broadband terahertz and visible ultra-short pulse laser and applied to polymer films.

1. †Element-specific cluster growth on the two-dimensional metal–organic network: N. Tsukahara, R. Arafune and J. Yoshinobu, Jpn. J. Appl. Phys. **63**, 065504 (2024).

2. †*Observation of Terahertz Spin Hall Conductivity Spectrum in GaAs with Optical Spin Injection: T. Fujimoto, T. Kurihara, Y. Murotani, T. Tamaya, N. Kanda, C. Kim, J. Yoshinobu, H. Akiyama, T. Kato and R. Matsunaga, Phys. Rev. Lett. **132**, 016301(1-7) (2024).

3. *Ultra-broadband detection of coherent infrared pulses by sum-frequency generation spectroscopy in reflection geometry: R. Kameyama, S. Tanaka, Y. Murotani, T. Matsuda, N. Kanda, R. Matsunaga and J. Yoshinobu, Opt. Lett. **49**, 3978 (2024).

4. *Anomalous Hall Transport by Optically Injected Isospin Degree of Freedom in Dirac Semimetal Thin Film: Y. Murotani, N. Kanda, T. Fujimoto, T. Matsuda, M. Goyal, J. Yoshinobu, Y. Kobayashi, T. Oka, S. Stemmer and R. Matsunaga, Nano Lett. **24**, 222 (2024).

5. Low-temperature dissociation of CO_2 molecules on vicinal Cu surfaces: T. Koitaya, Y. Shiozawa, Y. Yoshikura, K. Mukai, S. Yoshimoto and J. Yoshinobu, Phys. Chem. Chem. Phys. **26**, 9226-9233 (2024).

6. †*Operando* Observation of Hydrogenation of Carbon Dioxide by Near Ambient Pressure X-ray Photoelectron Spectroscopy: T. KOITAYA, S. YAMAMOTO, I. MATSUDA, J. YOSHINOBU and T. YOKOYAMA, Vac. Surf. Sci. **67**, 117-122 (2024).

7. *Light-induced inverse spin Hall effect and field-induced circular photogalvanic effect in GaAs revealed by two-dimensional terahertz Fourier analysis: T. Fujimoto, Y. Murotani, T. Tamaya, T. Kurihara, N. Kanda, C. Kim, J. Yoshinobu, H. Akiyama, T. Kato and R. Matsunaga, Phys. Rev. B **111**, L201201 (2025).

8. *Valley polarization dynamics of photoinjected carriers at the band edge in room-temperature silicon studied by terahertz polarimetry: A. M. Shirai, Y. Murotani, T. Fujimoto, N. Kanda, J. Yoshinobu and R. Matsunaga, Phys. Rev. B **111**, L121201 (2025).

9. *Chemical process of hydrogen and formic acid on a Pd-deposited Cu(111) surface studied by high-resolution X-ray photoelectron spectroscopy and density functional theory calculations: W. Osada, M. Hasegawa, Y. Shiozawa, K. Mukai, S. Yoshimoto, S. Tanaka, M. Kawamura, T. Ozaki and J. Yoshinobu, Phys. Chem. Chem. Phys. **27**, 1978 (2025).

10. *Emergence of high-mobility carriers in topological kagome bad metal Mn_3Sn by intense photoexcitation: T. Matsuda, T. Higo, K. Kuroda, T. Koretsune, N. Kanda, Y. Hirai, H. Peng, T. Matsuo, C. Bareille, A. Varykhalov, N. Yoshikawa, J. Yoshinobu, T. Kondo, R. Shimano, S. Nakatsuji and R. Matsunaga, Phys. Rev. Materials **9**, 014202 (2025).

11. *Discovery of bicyclic borane molecule B14H26: X. Zhang, T. Fujino, Y. Ando, Y. Tsujikawa, T. Wang, T. Nakashima, H. Sakurai, K. Yamaguchi, M. Horio, H. Mori, J. Yoshinobu, T. Kondo and I. Matsuda, Commun Chem **8**, 14 (2025).

12. Direct Observation of Dioxymethylene and Formaldehyde as Hydrogenation Products of Formate Species on the Hydrogen-Adsorbed Cu(997) Surface: H. Yoshioka, W. Osada, K. Mukai, S. Tanaka and J. Yoshinobu, ChemCatChem **17**, e202401758 (2025).

13. 表面科学的アプローチによるモデル触媒表面での二酸化炭素の吸着と化学変換: 吉信淳, 小板谷貴典, 触媒 **66**, 60-65 (2024).

14. 巻頭言「悪魔の作品を観ようではないか！」: 吉信 淳, 表面と真空 **67**, 99 (2024).

15. 準大気圧光電子分光法による二酸化炭素水素化のオペランド観測: 小板谷 貴典, 山本 達, 松田 巌, 吉信 淳, 横山 利彦, 表面と真空 **67**, 117-122 (2024).

Functional Materials Group

Akiyama group

In 2024, we demonstrated low power consumption of 0.5W and high output pulse-energy stability within 1% in our original ps gain-switched-LD seed-pulse prototype modules. In collaboration with Katayama-team in Yokohama National University, we started fs single-shot characterization of gain-switched pulses from the module. We analytically studied criteria of output gain in photovoltaic-thermoelectric tandems. Collaboration work and papers with Hiyama-team in Gunma University clarified inhibition sensitivity of in vitro firefly bioluminescence quantum yields to bivalent metal ion concentrations in aqueous solutions, and bioluminescence quantum yield of new luciferin analogs.

1. †*Observation of Terahertz Spin Hall Conductivity Spectrum in GaAs with Optical Spin Injection: T. Fujimoto, T. Kurihara, Y. Murotani, T. Tamaya, N. Kanda, C. Kim, J. Yoshinobu, H. Akiyama, T. Kato and R. Matsunaga, Phys. Rev. Lett. **132**, 016301(1-7) (2024).

2. Continuous-wave quasi-single-mode random lasing in $CH_3NH_3PbBr_3$ perovskite films on patterned sapphire substrates: G. Weng, Z. Su, S. Ye, X. Sun, F. Cao, C. Wang, D. Jiang, X. Hu, J. Tao, H. Akiyama, J. Chu and S. Chen, Opt. Lett. **49**, 3713 (2024).

3. Electrically smoothing gain-switched optical pulses from a semiconductor laser diode: C. Wang, F. Cao, Y. Liu, H. Nakamae, M. Kobayashi, D. Jiang, Y. Qi, G. Weng, X. Hu, H. Akiyama and S. Chen, Opt. Lett. **49**, 6285 (2024).

4. Regulating the crystal orientation of vapor-transport-deposited GeSe thin films by a post-annealing treatment: S. Zheng, D. Qin, R. Wang, Y. Pan, G. Weng, X. Hu, J. Chu, H. Akiyama and S. Chen, Appl. Opt. **63**, 2752 (2024).

5. ∗Light-driven Anion-Pumping Rhodopsin with Unique Cytoplasmic Anion-release Mechanism: T. Ishizuka, K. Suzuki, M. Konno, K. Shibata, Y. Kawasaki, H. Akiyama, T. Murata and K. Inoue, J. Biol. Chem. **300**, 107797 (2024).

6. Effects of localized tensile stress on GaAs solar cells revealed by absolute electroluminescence imaging and distributed circuit modeling: Q. Huang, Y. Wang, X. Hu, P. Yang, W. Zhou, G. Weng, H. Akiyama, J. Chu and S. Chen, Solar Energy **274**, 112541 (2024).

7. Subnanosecond Marx Generators for Picosecond Gain-Switched Laser Diodes: F. Cao, D. Jiang, Y. Liu, Y. Tian, X. Ran, Y. Long, T. Ito, X. Hu, G. Weng, H. Akiyama and S. Chen, IEEE Photonics J. **16**, 1 (2024).

8. Carrier tunneling and transport in coupled quantum wells: Modeling and experimental verification: F. Cao, Z. Su, C. Wang, Y. Chen, G. Weng, C. Wang, X. Hu, H. Akiyama, J. Chu and S. Chen, Appl. Phys. Lett **124**, 161106 (2024).

9. Electrical Characterization of Solar Array Panels by Absolute Electroluminescence Intensity: T. Nakamura, H. Akiyama, S. Kanaya, Y. Miyazawa, H. Toyota and S.-I. Sakai, Journal of Evolving Space Activities **2**, 161-166 (2024).

10. ∗Light-induced inverse spin Hall effect and field-induced circular photogalvanic effect in GaAs revealed by two-dimensional terahertz Fourier analysis: T. Fujimoto, Y. Murotani, T. Tamaya, T. Kurihara, N. Kanda, C. Kim, J. Yoshinobu, H. Akiyama, T. Kato and R. Matsunaga, Phys. Rev. B **111**, L201201 (2025).

11. ∗Portable laser diode module of sub-10 ps gain-switched pulse source at 1030 nm wavelength: M. Kobayashi, H. Nakamae, C. Kim, T. Nakamura, T. Ito, S. Chen, Y. Kobayashi and H. Akiyama, Jpn. J. Appl. Phys. **64**, 038004 (2025).

12. Nonlinear beam conversion with multi-spectral components: K.-H. Chang, C.-C. Fan, T.-F. Pan, J.-H. Lai, M.-S. Tsai, A. Boudrioua, C.-M. Lai, H. Yokoyama, E. Higurashi, H. Akiyama, K. Paschke and L.-H. Peng, Opt. Lett. **50**, 1313 (2025).

13. Automated quantitative diagnosis of GaAs solar cells using the CBAM-MS-1DCNN model on absolute electroluminescence imaging and distributed circuit modeling: W. Zhou, P. Yang, Y. Wang, M. Zha, D. Qin, Q. Huang, G. Weng, X. Hu, H. Akiyama, J. Chu and S. Chen, Appl. Opt. **64**, 3617 (2025).

14. Analytical evaluation of output gain in photovoltaic-thermoelectric tandems: J. Sakuma, K. Kamide and H. Akiyama, Appl. Phys. Express **18**, 034001 (2025).

15. ∗Robust asynchronous optical sampling terahertz spectroscopy using commercially available free-running lasers: M. Nakagawa, N. Kanda, H. Nakamae, H. Akiyama and R. Matsunaga, Opt. Express **33**, 23145 (2025).

16. ∗Structural Changes in the Retinal Chromophore and Ion-Conducting Pathway of an Anion Channelrhodopsin *Gt*ACR1: K. Shibata, Y. Kawasaki, S. Takaramoto, M. Watanabe, M. Fukuda, R. Ono, H. E. Kato, H. Akiyama and K. Inoue, J. Phys. Chem. Lett. **16**, published on the web (2025).

17. Non-Cadmium $TiO_2/Sb_2(Se, S)_3$ Heterojunction Solar Cells with Improved Efficiency by NaCl-Treated Interface Engineering: D. Qin, P. Yang, Y. Pan, Y. Wang, Y. Pan, G. Weng, X. Hu, J. Tao, J. Chu, H. Akiyama and S. Chen, ACS Appl. Mater. Interfaces **17**, 22050 (2025).

18. Degradations of Multijunction Solar Cell Revealed by Absolute Electroluminescence Imaging: P. Yang, Y. Wang, Q. Huang, D. Qin, J. Zhang, W. Zhou, G. Weng, X. Hu, J. Chu, H. Akiyama and S. Chen, IEEE Trans. Electron Devices **72**, 1857 (2025).

19. High efficiency $Sb_2(S, Se)_3$ thin-film solar cells by substrate-temperature-controlled vapor transport deposition method: D. Qin, P. Yang, Y. Pan, Y. Wang, Y. Pan, G. Weng, X. Hu, J. Tao, J. Chu, H. Akiyama and S. Chen, Solar Energy Materials and Solar Cells **280**, 113232 (2025).

20. †Inhibition sensitivity of *in vitro* firefly bioluminescence quantum yields to Zn^{2+} and Cd^{2+} concentrations in aqueous solutions: R. Ono, K. Saito, D. Tezuka, S. Yoshii, M. Kobayashi, H. Akiyama, N. Koga, H. Itabashi and M. Hiyama, Photochem & Photobiology **00**, php.14024 (2025).

21. Low threshold lasing of GaN-based vertical-cavity surface-emitting lasers with thin InGaN/GaN quantum well active region: R. Xu, K. Shibata, H. Akiyama, J. Zhang, L. Ying and B. Zhang, Optics & Laser Technology **182**, 112117 (2025).

Sugino group

The activity of this fiscal year includes computational study of materials using the first-principles density functional methods. Design of an electrochemical catalyst, elucidation of hydrogen diffusion on a metal surface, and analysis of magnetic properties of a cuprate. This group is also involved with cooperative work with experimental group, such as elucidation of CO dynamics on a metal surface, and analysis of muon in a Li-ion cathode material.

1. Magnetic phases of electron-doped infinite-layer $Sr_{1-x}La_xCuO_2$ from first-principles density functional calculations: A. N. Tatan, J. Haruyama and O. Sugino, Phys. Rev. B **109**, 165134 (2024).
2. Time-dependent electron transfer and energy dissipation in condensed media: E. F. Arguelles and O. Sugino, J. Chem. Phys. **160**, 144102 (2024).
3. †Correction to "Effect of Nitrogen Doping and Oxygen Vacancy on the Oxygen Reduction Reaction on the Tetragonal Zirconia(101) Surface": S. Muhammady, J. Haruyama, S. Kasamatsu and O. Sugino, J. Phys. Chem. C **128**, 10248 (2024).
4. †Elucidation of CO Oxidation and CO $_2$ Desorption Dynamics on Pt(111) by van der Waals DFT Calculations: Hyperthermal Kinetic Energy, Sharp Desorption Angle, and Excited Vibrational States: H. Li, Y. Kataoka, S. Tanaka, J. Haruyama, O. Sugino and J. Yoshinobu, J. Phys. Chem. C **128**, 15393 (2024).
5. †Predictive evaluation of hydrogen diffusion coefficient on Pd(111) surface by path integral simulations using neural network potential: Y. Kataoka, J. Haruyama, O. Sugino and M. Shiga, Phys. Rev. Research **6**, 043224 (2024).
6. †Defect Segregation, Water Layering, and Proton Transfer at Zirconium Oxynitride/Water Interface Examined Using Neural Network Potential: A. Nakanishi, S. Kasamatsu, J. Haruyama and O. Sugino, J. Phys. Chem. C **129**, 2403 (2025).

Oka group

Oka group has worked on Nonequilibrium quantum materials including Floquet engineering of Dirac semimetals, spin systems, and many-body systems.

1. Chiral Gauge Field in Fully Spin-Polarized Magnetic Weyl Semimetal with Magnetic Domain Walls: A. Ozawa, Y. Araki and K. Nomura, J. Phys. Soc. Jpn. **93**, 094704 (2024).
2. Measurement-only dynamical phase transition of topological and boundary order in toric code and gauge Higgs models: T. Orito, Y. Kuno and I. Ichinose, Phys. Rev. B **109**, 224306 (2024).
3. ∗Anomalous Hall Transport by Optically Injected Isospin Degree of Freedom in Dirac Semimetal Thin Film: Y. Murotani, N. Kanda, T. Fujimoto, T. Matsuda, M. Goyal, J. Yoshinobu, Y. Kobayashi, T. Oka, S. Stemmer and R. Matsunaga, Nano Lett. **24**, 222 (2024).
4. Extracting correlation length in Mott insulators by strong-field driving: A. AlShafey, X.-Y. Jia, Y.-M. Lu, S.-S. Gong, G. McCaul, D. Bondar, M. Randeria, T. Oka and A. S. Landsman, Journal of the Optical Society of America B **41**, B26-B31 (2024).
5. Floquet Weyl states at one-photon resonance: An origin of nonperturbative optical responses in three-dimensional materials: Y. Hirai, S. Okumura, N. Yoshikawa, T. Oka and R. Shimano, Phys. Rev. Research **6**, L012027-1-6 (2024).
6. Origin of Large Effective Phonon Magnetic Moments in Monolayer MoS_2: H. Mustafa, C. Nnokwe, G. Ye, M. Fang, S. Chaudhary, J.-A. Yan, K. Wu, C. J. Cunningham, C. M. Hemesath, A. J. Stollenwerk, P. M. Shand, E.-H. Yang, G. A. Fiete, R. He and W. Jin, ACS Nano **19**, 11241 (2025).

Inoue group

In 2024, we identified a new family of anion-pumping rhodopsins, Glycyclhalorhodopsin (GHR), from soil bacteria. This family is distinct from other anion-pumping rhodopsins and features a novel DTG motif in the third transmembrane helix, which includes a characteristic cytoplasmic glycine residue. X-ray crystallographic analysis revealed large cytoplasmic cavities formed due to the small size of this glycine residue. Time-resolved spectroscopic measurements demonstrated that the chloride release process through these cavities is distinct from that of canonical anion-pumping

rhodopsin from haloarchaea. Additionally, a new class of cation channel rhodopsin, HulaCCR, was identified through metatranscriptome analyses in Lake Hula in Israel. One member, HulaCCR1 exhibited non-specific cation transport, including the permeation of large cesium ions. Interestingly, truncation of either the N- or C-term extensions of HulaCCR1 altered its plasma membrane localization, indicating that the N- and C-termini play essential roles in determining cellular localization. Furthermore, we investigated the isomerization process of the retinal chromophore in inward proton-pumping schizorhodopsins, the quantum mechanical principles underlying the circular dichroic spectra of retinal chromophores in dimeric rhodopsins, and the ultrafast isomerization process in Archaerhodopsin-3 and its fluorescent variants, which hold promise for the development of genetically encoded voltage indicators.

1. ∗Gilbert damping of NiFe thin films grown on two-dimensional chiral hybrid lead-iodide perovskites: T. Hatajiri, S. Sakamoto, H. Kosaki, Z. Tian, M. Tanaka, T. Ideue, K. Inoue, D. Miyajima and S. Miwa, Phys. Rev. B **110**, 054435 (1-6) (2024).
2. Chromophore–Protein Interactions Affecting the Polyene Twist and π–π^* Energy Gap of the Retinal Chromophore in Schizorhodopsins: T. Urui, T. Shionoya, M. Mizuno, K. Inoue, H. Kandori and Y. Mizutani, J. Phys. Chem. B **128**, 2389-2397 (2024).
3. Hydrogen-Bonding and Hydrophobic Interaction Networks as Structural Determinants of Microbial Rhodopsin Function: E. Bertalan, M. Konno, M. D. C. Mar´ın, R. Bagherzadeh, T. Nagata, L. Brown, K. Inoue and A.-N. Bondar, J. Phys. Chem. B **128**, 7407-7426 (2024).
4. *Cis – Trans* Reisomerization Preceding Reprotonation of the Retinal Chromophore Is Common to the Schizorhodopsin Family: A Simple and Rational Mechanism for Inward Proton Pumping: T. Urui, K. Hayashi, M. Mizuno, K. Inoue, H. Kandori and Y. Mizutani, J. Phys. Chem. B **128**, 744-754 (2024).
5. Molecular Mechanisms behind Circular Dichroism Spectral Variations between Channelrhodopsin and Heliorhodopsin Dimers: K. J. Fujimoto, Y. A. Tsuzuki, K. Inoue and T. Yanai, J. Phys. Chem. Lett. **15**, 5788-5794 (2024).
6. ∗Light-driven Anion-Pumping Rhodopsin with Unique Cytoplasmic Anion-release Mechanism: T. Ishizuka, K. Suzuki, M. Konno, K. Shibata, Y. Kawasaki, H. Akiyama, T. Murata and K. Inoue, J. Biol. Chem. **300**, 107797 (2024).
7. Archaerhodopsin 3 is an Ideal Template for the Engineering of Highly Fluorescent Optogenetic Reporters: K. Herasymenko, D. Walisinghe, M. Konno, L. Barneschi, I. D. Waele, M. silwa, K. Inoue, M. Olivucci and S. Haacke, Chem. Sci. **16**, 761-774 (2024).
8. †∗Chemical-state imaging of a mammalian cell through multi-elemental soft x-ray spectro-ptychography: K. Sakurai, Y. Takeo, S. Takaramoto, N. Furuya, K. Yoshinaga, T. Shimamura, J. T. O'Neal, Y. Nakata, S. Egawa, K. Yoshimi, H. Ohashi, H. Mimura, Y. Harada, K. Inoue, M. Shimura and T. Kimura, Appl. Phys. Lett. **126**, 043702(1-7) (2025).
9. Weak Organic Acid Effect of Bacterial Light-Driven Proton-Pumping Rhodopsin: Z. Lyu, S. Takaramoto and K. Inoue, J. Phys. Chem. B **129**, 3198-3206 (2025).
10. ∗Structural Changes in the Retinal Chromophore and Ion-Conducting Pathway of an Anion Channelrhodopsin *Gt*ACR1: K. Shibata, Y. Kawasaki, S. Takaramoto, M. Watanabe, M. Fukuda, R. Ono, H. E. Kato, H. Akiyama and K. Inoue, J. Phys. Chem. Lett. **16**, published on the web (2025).
11. Structural insights into light harvesting by antenna-containing rhodopsins in marine Asgard archaea: G. Tzlil, M. D. C. Marin, Y. Matsuzaki, P. Nag, S. Itakura, Y. Mizuno, S. Murakoshi, T. Tanaka, S. Larom, M. Konno, R. Abe-Yoshizumi, A. Molina-Ma´rquez, D. Barcenas-Perez, J. Cheel, M. Koblizek, R. Leon, K. Katayama, H. Kandori, I. Schapiro, W. Shihoya, O. Nureki, K. Inoue, A. Rozenberg, A. Chazan and O. Beja, Nat Microbiol **10**, 1484 (2025).
12. 磁場による生体操作：Magnetogenetics への挑戦: 寶本 俊輝, 八尾 寛, 井上 圭一, 「日本磁気学会 第 249 回研究会資料」 (日本磁気学会, 2024), 19-22.

Hayashi group

In 2023, I moved to the Institute for Solid State Physics, and in 2024, three students participated in my lab. Together with a student, we wrote a review article on the application of extreme value analysis to axonal transport in neurons [Hayashi *et al.*, Biophys Rev 2024], based on our original research article published last year [Naoi *et al.*, Commun Phys 2024]. Regarding extreme value statistics, I also continued academic exchange with the Institute of Statistical Mathematic, and contributed to the joint research report "Applications of Extreme Value Theory to Engineering", published by the Institute [Hayashi, the Institute of Statistical Mathematic Report 478, 2024].

Apart from extreme value analysis research activities, a particularly significant event in 2024 was the 21st Congress of the International Union for Pure and Applied Biophysics (IUPAB) held in Kyoto. I contributed as a member of the Executive Committee. I had been involved with the committee since 2017, when Japan successfully won the bid to host the congress, and thus completed a major responsibility. At the IUPAB Congress, I also served as the chair of the ”Application of Non-equilibrium Physics” session [Hayashi and Li, Biophys Rev 2024]. As a member of the Executive Committee, I was in charge of the IUPAB Hands-on Training Program, and in collaboration with six universities and research institutes across Japan, we hosted approximately 70 early-career researchers from both Japan and abroad, who participated in the congress [Hayashi, BPPB 2024]. In addition, I participated in a roundtable discussion at IUPAB with promising researchers from Japan and abroad who had come to Japan for the congress, where we discussed the theme: ”Dreaming the Next 50 Years in Our Biophysics” [Hayashi *et al.*, BPPB 2025]. In 2024, I was actively involved in various initiatives related to the organization of IUPAB. Through these efforts, I believe I was able to enhance the presence of the Institute for Solid State Physics in the Biophysical Society of Japan.

In addition, I was invited as a lecturer to the 69th Condensed Matter Physics Summer School for Young Researchers, where I led a seminar and interacted with Japanese students who study soft matter and non-equilibrium statistical mechanics. Since the Institute for Solid State Physics has supported this summer school, I was glad to have had the opportunity to contribute [Hayashi, Lecture notes for the 69th Condensed Matter Physics Summer School, 2025].

1. Extreme Value Analysis of Intracellular Cargo Transport by Motor Proteins: T. Naoi, Y. Kagawai, K. Nagino, S. Niwa and K. Hayashi, Communications Physics **7**, Article number: 50 (2024).
2. Commentary to “Application of Non-equilibrium Physics”: a session of the 21st IUPAB Congress 2024, Kyoto, Japan: K. Hayashi and C.-B. Li, Biophys Rev **NA**, NA (2024).
3. Editorial: Hands-on Training Program: K. Hayashi, Biophysics and Physicobiology **21**, NA (2024).
4. IUPAB 京都 2024 年会議における座談会：我々の生物物理学の次の 50 年を夢見て（前半）: 林 久美子, G. HUMMER, J. A. JOSEPH, R. LI, 永井 健治, 大浪 修一, F. ZHANG, 北村 朗, 冨樫 祐一, 角五 彰, 藤原 郁子, 小松崎 民樹, 生物物理 **65**, 35-46 (2025).
5. A round table at IUPAB Congress in Kyoto 2024: Dreaming the next 50 years in our biophysics: K. Hayashi, G. Hummer, J. A. Joseph, R. Li, T. Nagai, S. Onami, F. Zhang, A. Kitamura, Y. Togashi, A. Kakugo, I. Fujiwara and T. Komatsuzaki, Biophysics and Physicobiology **21**, NA (2025).
6. 極値統計解析の神経細胞軸索輸送への応用: 林久美子, 「統計数理研究所共同研究リポート 478　極値理論の工学への応用」 (統計数理研究所, 2025), 36-40.
7. Extreme-value analysis in nano-biological systems: applications and implications: K. Hayashi, N. Takamatsu and S. Takaramoto, Biophys. Rev. **16**, 571-579 (2024).
8. モータータンパク質の生物医学物理: 林 久美子, 物性若手夏の学校テキスト 第 **69** 回, 188-200 (2025).

Quantum Materials Group

Oshikawa group

We developed the finite-size scaling theory of one-dimensional quantum critical systems in the presence of boundaries. While the finite-size spectrum in the conformal limit, namely of a conformal field theory with conformally invariant boundary conditions, is related to the dimensions of boundary operators by Cardy, the actual spectra of lattice models are affected by both bulk and boundary perturbations and contain non-universal boundary energies. We obtain a general expression of the finite-size energy levels in the presence of bulk and boundary perturbations. In particular, a generic boundary perturbation related to the energy-momentum tensor gives rise to a renormalization of the effective system size. We verify our field-theory formulation by comparing the results with the exact solution of the critical transverse-field Ising chain and with accurate numerical results on the critical three-state Potts chain obtained by Density-Matrix Renormalization Group. Our study greatly improves the precision, and will serve as a basis of future numerical and analytical studies of boundary critical phenomena.

1. †Boundary conditions and anomalies of conformal field theories in 1+1 dimensions: L. Li, C.-T. Hsieh, Y. Yao and M. Oshikawa, Phys. Rev. B **110**, 045118 (2024).
2. †Intrinsic symmetry-protected topological mixed state from modulated symmetries and hierarchical structure of boundary anomaly: Y. You and M. Oshikawa, Phys. Rev. B **110**, 165160 (2024).
3. †Magnetization oscillations in a periodically driven transverse field Ising chain: X. Wang, M. Oshikawa, M. Kormos and J. Wu, Phys. Rev. B **110**, 195101 (2024).

4. †Spontaneous strong symmetry breaking in open systems: Purification perspective: P. Sala, S. Gopalakrishnan, M. Oshikawa and Y. You, Phys. Rev. B **110**, 155150 (2024).
5. †System-environment entanglement phase transitions: Y. Ashida, S. Furukawa and M. Oshikawa, Phys. Rev. B **110**, 094404 (2024).
6. †Lieb-Schultz-Mattis Theorem for 1D Quantum Magnets with Antiunitary Translation and Inversion Symmetries: Y. Yao, L. Li, M. Oshikawa and C.-T. Hsieh, Phys. Rev. Lett. **133**, 136705 (2024).
7. †∗Quasi-Periodic Growth of One-Dimensional Copper Boride on Cu(110): Y. Tsujikawa, X. Zhang, K. Yamaguchi, M. Haze, T. Nakashima, A. Varadwaj, Y. Sato, M. Horio, Y. Hasegawa, F. Komori, M. Oshikawa, M. Kotsugi, Y. Ando, T. Kondo and I. Matsuda, Nano Lett. **24**, 1160 (2024).
8. †Decorated defect construction of gapless-SPT states: L. Li, M. Oshikawa and Y. Zheng, SciPost Phys. **17**, 013 (2024).
9. Finite-size corrections to the energy spectra of gapless one-dimensional systems in the presence of boundaries: Y. Liu, H. Shimizu, A. Ueda and M. Oshikawa, SciPost Phys. **17**, 099 (2024).
10. †Entanglement swapping in critical quantum spin chains: M. Hoshino, M. Oshikawa and Y. Ashida, Phys. Rev. B **111**, 155143 (2025).
11. Self-congruent point in critical matrix product states: An effective field theory for finite-entanglement scaling: J. T. Schneider, A. Ueda, Y. Liu, A. La¨uchli, M. Oshikawa and L. Tagliacozzo, SciPost Phys. **18**, 142 (2025).

Nakatsuji group

Our research group is advancing a new phase in quantum materials science, where fundamental discoveries are increasingly connected with emerging quantum technologies through interdisciplinary collaboration. We focus on designing, synthesizing, and characterizing quantum materials that exhibit novel macroscopic properties. These materials are integrated into thin-film-based devices, enabling us to probe novel quantum functionalities and assess their technological potential. By forging direct links between quantum phenomena and practical applications, our mission is to lead the creation of material platforms that drive both scientific discovery and innovation in computing, sensing, and energy-saving technologies. Our major research themes are: 1. Quantum transport in magnetic topological materials 2. Coherent quantum spin transport in antiferromagnetic spintronics 3. Strange metal and exotic superconductivity in strongly correlated electron systems

1. ∗Fabrication of single-crystalline $YFeO_3$ films with large antiferromagnetic domains: C. Wang, M. Lippmaa and S. Nakatsuji, J. Appl. Phys. **135**, 113901 (1-8) (2024).
2. ∗Bulk and surface uniformity of magnetic and electronic structures in epitaxial W/Mn_3Sn/MgO films revealed by fluorescence- and electron-yield x-ray magnetic circular dichroism: S. Sakamoto, T. Higo, Y. Kotani, H. Kosaki, T. Nakamura, S. Nakatsuji and S. Miwa, Phys. Rev. B **110**, L060412 (2024).
3. †∗Crystal field magnetostriction of spin ice under ultrahigh magnetic fields: N. Tang, M. Gen, M. Rotter, H. Man, K. Matsuhira, A. Matsuo, K. Kindo, A. Ikeda, Y. H. Matsuda, P. Gegenwart, S. Nakatsuji and Y. Kohama, Phys. Rev. B **110**, 214414 (1-10) (2024).
4. ∗Anisotropy of the Gilbert damping constant in NiFe grown on the chiral antiferromagnet Mn_3Sn: H. Kosaki, S. Sakamoto, T. Hatajiri, T. Higo, S. Nakatsuji and S. Miwa, Phys. Rev. B **111**, 024418 (2025).
5. ∗Tunneling magnetoresistance and spin-orbit torque magnetization switching in ferrimagnetic Gd-Fe-Co based magnetic tunnel junction: M. Yunokizaki, Y. Hibino, H. Idzuchi, H. Tsai, M. Ishibashi, S. Miwa, M. Hayashi and S. Nakatsuji, Jpn. J. Appl. Phys. **64**, 010904 (2025).
6. ∗Emergence of high-mobility carriers in topological kagome bad metal Mn_3Sn by intense photoexcitation: T. Matsuda, T. Higo, K. Kuroda, T. Koretsune, N. Kanda, Y. Hirai, H. Peng, T. Matsuo, C. Bareille, A. Varykhalov, N. Yoshikawa, J. Yoshinobu, T. Kondo, R. Shimano, S. Nakatsuji and R. Matsunaga, Phys. Rev. Materials **9**, 014202 (2025).
7. ∗Zero-field Hall effect emerging from a non-Fermi liquid in a collinear antiferromagnet $V_{1/3}NbS_2$: M. K. Ray, M. Fu, Y. Chen, T. Chen, T. Nomoto, S. Sakai, M. Kitatani, M. Hirayama, S. Imajo, T. Tomita, A. Sakai, D. Nishio-Hamane, G. T. McCandless, M.-T. Suzuki, Z. Xu, Y. Zhao, T. Fennell, Y. Kohama, J. Y. Chan, R. Arita, C. Broholm and S. Nakatsuji, Nat Commun **16**, 3532 (2025).
8. ∗Antiferromagnetic spin-torque diode effect in a kagome Weyl semimetal: S. Sakamoto, T. Nomoto, T. Higo, Y. Hibino, T. Yamamoto, S. Tamaru, Y. Kotani, H. Kosaki, M. Shiga, D. Nishio-Hamane, T. Nakamura, T. Nozaki, K. Yakushiji, R. Arita, S. Nakatsuji and S. Miwa, Nat. Nanotechnol. **20**, 216-221 (2025).

Miwa group

This year we worked on the following topics: (1) chirality-induced spin selectivity (CISS) in the absence of charge current, (2) X-ray spectroscopy on the chiral antiferromagnet Mn_3Sn thin film, and (3) interfacial magnetic anisotropy of the Fe/LiF/MgO system. In topic (1), we have applied the spin-pumping method to the CISS experimental system and find that the CISS-induced magnetoresistance does not originate from the spin-dependent transport (Phys. Rev. B **110**, 054435). In topic (2), we find that our expitaxial Mn_3Sn thin film exhibits uniformity of magnetic and electronic states throughout the thickness region. This is a collaboration with the groups of Nakatsuji (Phys. Rev. B **110**, L060412). In topic (3) we find that alkali fluoride with good crystallinity is effective to enhance the perpendicular magnetic anisotropy of the Fe/MgO system (Phys. Rev. B **109**, 064413).

1. ∗Bulk and surface uniformity of magnetic and electronic structures in epitaxial W/Mn_3Sn/MgO films revealed by fluorescence- and electron-yield x-ray magnetic circular dichroism: S. Sakamoto, T. Higo, Y. Kotani, H. Kosaki, T. Nakamura, S. Nakatsuji and S. Miwa, Phys. Rev. B **110**, L060412 (2024).
2. ∗Gilbert damping of NiFe thin films grown on two-dimensional chiral hybrid lead-iodide perovskites: T. Hatajiri, S. Sakamoto, H. Kosaki, Z. Tian, M. Tanaka, T. Ideue, K. Inoue, D. Miyajima and S. Miwa, Phys. Rev. B **110**, 054435 (1-6) (2024).
3. Influence of alkali-fluoride insertion layers on the perpendicular magnetic anisotropy at the Fe/MgO interface: J. Chen, S. Sakamoto and S. Miwa, Phys. Rev. B **109**, 064413 (2024).
4. ∗Anisotropy of the Gilbert damping constant in NiFe grown on the chiral antiferromagnet Mn_3Sn: H. Kosaki, S. Sakamoto, T. Hatajiri, T. Higo, S. Nakatsuji and S. Miwa, Phys. Rev. B **111**, 024418 (2025).
5. ∗Tunneling magnetoresistance and spin-orbit torque magnetization switching in ferrimagnetic Gd-Fe-Co based magnetic tunnel junction: M. Yunokizaki, Y. Hibino, H. Idzuchi, H. Tsai, M. Ishibashi, S. Miwa, M. Hayashi and S. Nakatsuji, Jpn. J. Appl. Phys. **64**, 010904 (2025).
6. ∗Antiferromagnetic spin-torque diode effect in a kagome Weyl semimetal: S. Sakamoto, T. Nomoto, T. Higo, Y. Hibino, T. Yamamoto, S. Tamaru, Y. Kotani, H. Kosaki, M. Shiga, D. Nishio-Hamane, T. Nakamura, T. Nozaki, K. Yakushiji, R. Arita, S. Nakatsuji and S. Miwa, Nat. Nanotechnol. **20**, 216-221 (2025).

Materials Design and Characterization Laboratory

Hiroi group

We concentrate on the layered polyanionic material MAlX (M = K, Na, X = Si, Ge). This material is a type of intermetallic compound known as the Zintl phase, which has an unusual bonding state between ions and metals. Its electronic structure is distinguished by its nordal-line semimetal composition. This is a topological semimetal, consisting of a linear chain of Dirac points with linearly intersecting bands in wavenumber space (upper right in the figure), and is thought to have a nontrivial quantum state.We conducted various measurements on these materials and discovered that NaAlSi is a superconductor at 6.8 K, NaAlGe is an insulator with a pseudogap of approximately 100 K, and KAlGe undergoes a metal-metal transition at 89 K. Thus, elemental substitution produces a wide range of ground states, including the low-temperature phase of KAlGe, which has a remarkably low carrier density and extremely high mobility. Synchrotron X-ray diffraction experiments have revealed that microstructural changes accompanying the superlattice occur during this transition, resulting in the formation of Al-Ge tetramer ”molecule formation”. He has recently observed Fermi surfaces using angle-resolved photoemission spectroscopy, quasiparticle interferograms and topological edge states with STM, and structural phase transitions under high pressure.

1. Nonmagnetic Ground State in RuO_2 Revealed by Muon Spin Rotation: M. Hiraishi, H. Okabe, A. Koda, R. Kadono, T. Muroi, D. Hirai and Z. Hiroi, Phys. Rev. Lett. **132**, 166702 (2024).
2. ∗Superconductivity in Hexagonal Zr_6CoAl_2-Type Zr_6RuBi_2 and Zr_6FeBi_2: K. Yuchi, D. Nishio-Hamane, K. Kojima, K. Moriyama, R. Okuma and Y. Okamoto, J. Phys. Soc. Jpn. **94**, 013701(1-5) (2025).
3. ∗Topological Semimetal KAlGe with Novel Electronic Instability: T. Ikenobe, T. Yamada, J.-I. Yamaura, T. Oguchi, R. Okuma, D. Hirai, H. Sagayama, Y. Okamoto and Z. Hiroi, Chem. Mater. **37**, 189-197 (2025).

Kawashima group

We developed efficient methods, algorithms, parallelized programs, and sometimes new concepts, based on novel numerical techniques such as the tensor network (TN) method and quantum Monte Carlo (QMC). We then applied them to relevant physical problems. To list subjects of our research in 2024: (1) Classical spin systems and novel phase transitions

and excitations [Akamatsu and Kawashima, JStatPhys191; Wu. et al. Phys. Rev. Res. 6], (2) Dynamics of quantum spin systems [Tu et al. PRXQuantum5], (3) Development of new tensor network methods [Homma, et al. Phys. Rev. Res. 6], and (4) Development of open-source software for condensed matter calculations [Ido, et al., Comp.Phys.Commun.298; Aoyama et al., Comp. Phys. Commun. 298]

1. †*H-wave – A Python package for the Hartree-Fock approximation and the random phase approximation: T. Aoyama, K. Yoshimi, K. Ido, Y. Motoyama, T. Kawamura, T. Misawa, T. Kato and A. Kobayashi, Computer Physics Communications **298**, 109087(1-10) (2024).
2. Nuclear norm regularized loop optimization for tensor network: K. Homma, T. Okubo and N. Kawashima, Phys. Rev. Research **6**, 043102（1-9） (2024).
3. Programmable order by disorder effect and underlying phases through dipolar quantum simulators: H.-K. Wu, T. Suzuki, N. Kawashima and W.-L. Tu, Phys. Rev. Research **6**, 023297(1-15) (2024).
4. Faithfulness of Real-Space Renormalization Group Maps: K. O. Akamatsu and N. Kawashima, J Stat Phys **191**, 109 (2024).
5. Generating Function for Projected Entangled-Pair States: W.-L. Tu, L. Vanderstraeten, N. Schuch, H.-Y. Lee, N. Kawashima and J.-Y. Chen, PRX Quantum **5**, 010335(1-15) (2024).
6. †*Update of HΦ : Newly added functions and methods in versions 2 and 3: K. Ido, M. Kawamura, Y. Motoyama, K. Yoshimi, Y. Yamaji, S. Todo, N. Kawashima and T. Misawa, Comp. Phys. Commun. **298**, 109093(1-15) (2024).
7. Emergent intermediate phase in the J_1-J_2 XY model from tensor network approaches: F.-F. Song, H. Nuomin and N. Kawashima, Phys. Rev. B **111**, 104428(1-13) (2025).
8. Multi-impurity method for the bond-weighted tensor renormalization group: S. Morita and N. Kawashima, Phys. Rev. B **111**, 054433 (2025).
9. Tensor network renormalization approach to antiferromagnetic 6-state clock model on the Union Jack lattice: K. Homma, S. Morita and N. Kawashima, Phys. Rev. B **111**, 134427(1-12) (2025).

Uwatoko group

1. Field-Induced Criticality in $YbCu_4Au$: T. Taniguchi, K. Osato, H. Okabe, T. Kitazawa, M. Kawamata, S. Hashimoto, Y. Ikeda, Y. Nambu, D. P. Sari, I. Watanabe, J. G. Nakamura, A. Koda, J. Gouchi, Y. Uwatoko, S. Kittaka, T. Sakakibara, M. Mizumaki, N. Kawamura, T. Yamanaka, K. Hiraki, T. Sasaki and M. Fujita, J. Phys. Soc. Jpn. **93**, 124706(1-8) (2024).
2. *Field-Induced Quantum Phase Transitions in the Pressure-Tuned Triangular-Lattice Antiferromagnet $CsCuCl_3$: K. Nihongi, T. Kida, D. Yamamoto, Y. Narumi, J. Zaccaro, Y. Kousaka, K. Inoue, Y. Uwatoko, K. Kindo and M. Hagiwara, J. Phys. Soc. Jpn. **93**, 084704(1-7) (2024).
3. Pressure-induced Superconductivity in BiS_2-based Superconductors $Eu_2SrBi_2S_{2.5}Se_{1.5}F_4$: K. Ishigaki, J. Gouchi, K. Torizuka, S. Arumugam, A. K. Ganguli, Z. Haque, K. Ganesan, G. S. Thakur and Y. Uwatoko, J. Phys. Soc. Jpn. **93**, 024706(1-4) (2024).
4. Absence of Ni^{2+}/Ni^{3+} charge disproportionation and possible roles of O 2*p* holes in $La_3Ni_2O_{7-\delta}$ revealed by hard x-ray photoemission spectroscopy: D. Takegami, K. Fujinuma, R. Nakamura, M. Yoshimura, K. -D. Tsuei, G. Wang, N. N. Wang, J. -G. Cheng, Y. Uwatoko and T. Mizokawa, Phys. Rev. B **109**, 125119(1-5) (2024).
5. Competitive multiple phase transitions and distinct superconducting states in a Re_3Ge_7 single crystal under hydrostatic pressure: C. Li, B. Ruan, Q. Dong, P. Yang, G. Xiao, T. Shi, Z. Tian, J. Sun, Y. Uwatoko, G. Chen, Z. Ren, G. Wang, Z. Ren, B. Wang and J. Cheng, Phys. Rev. B **110**, 184507(1-9) (2024).
6. Emergence of strong-coupling superconductivity and quantum criticality correlated with Lifshitz transitions in the alternate stacking compound $4H_b$–TaS_2: S. Xu, J. Deng, J. Gao, F. Meng, L. Shi, P. Yang, N. Wang, Z. Liu, J. Sun, Y. Uwatoko, H. Lei, X. Luo, Y. Sun, N. Wang, Z. Wang, B. Wang and J. Cheng, Phys. Rev. B **109**, 144522(1-10) (2024).
7. From semiconductor to Fermi metal and emergent density-wave-like transition in the quasi-one-dimensional *n*-type $Bi_{19}S_{27}I_3$ under hydrostatic pressure: S. Xu, Z. Liu, P. Yang, B. Ruan, Z. Ren, J. Sun, Y. Uwatoko, B. Wang and J. Cheng, Phys. Rev. B **109**, 144107(1-10) (2024).
8. Quantum criticality in $YbCu_4Ni$: K. Osato, T. Taniguchi, H. Okabe, T. Kitazawa, M. Kawamata, Z. Hongfei, Y. Ikeda, Y. Nambu, D. P. Sari, I. Watanabe, J. G. Nakamura, A. Koda, J. Gouchi, Y. Uwatoko and M. Fujita, Phys. Rev. B **109**, 024435(1-6) (2024).

9. ∗Bulk high-temperature superconductivity in pressurized tetragonal $La_2PrNi_2O_7$: N. Wang, G. Wang, X. Shen, J. Hou, J. Luo, X. Ma, H. Yang, L. Shi, J. Dou, J. Feng, J. Yang, Y. Shi, Z. Ren, H. Ma, P. Yang, Z. Liu, Y. Liu, H. Zhang, X. Dong, Y. Wang, K. Jiang, J. Hu, S. Nagasaki, K. Kitagawa, S. Calder, J. Yan, J. Sun, B. Wang, R. Zhou, Y. Uwatoko and J. Cheng, Nature **634**, 579-584 (2024).

10. Pressure Effect on the Magnetic Properties of the Heusler Alloy Co_2NbGa: Y. Adachi, Y. Ogi, T. Osaki, T. Eto, T. Kihara, H. Nishihara, T. Sakon, J. Gouchi, Y. Uwatoko and T. Kanomata, J. Supercond. Nov. Magn. **37**, 249-254 (2024).

11. Pressure-Induced Superconductivity In Polycrystalline $La_3Ni_2O_{7-\delta}$: G. Wang, N. N. Wang, X. L. Shen, J. Hou, L. Ma, L. F. Shi, Z. A. Ren, Y. D. Gu, H. M. Ma, P. T. Yang, Z. Y. Liu, H. Z. Guo, J. P. Sun, G. M. Zhang, S. Calder, J. Q. Yan, B. S. Wang, Y. Uwatoko and J. -G. Cheng, Phys. Rev. X **14**, 011040(1-8) (2024).

12. †∗Combined x-ray diffraction, electrical resistivity, and *ab initio* study of $(TMTTF)_2PF_6$ under pressure: Implications for the unified phase diagram: M. Itoi, K. Yoshimi, H. Ma, T. Misawa, T. Tsumuraya, D. Bhoi, T. Komatsu, H. Mori, Y. Uwatoko and H. Seo, Phys. Rev. Research **6**, 043308 (1-14) (2024).

13. Extremely large magnetoresistance with coexistence of a nontrivial Berry phase in $Nb_{0.5}Ta_{0.5}P$: an experimental and theoretical study: V. K. Gangwar, S. Singh, S. Ghosh, S. Dixit, S. Kumar, P. Shahi, Y. Uwatoko and S. Chatterjee, J. Mater. Chem. C **12**, 16375-16388 (2024).

14. First-order transition under a magnetic ordered state in $SmPtSi_2$: T. Nakano, E. Takahashi, S. Yamaguchi, N. Takeda, K. Uhlirova´, J. Prokleˇska, J. Pospˇ´ısˇil, V. Sechovsky´, K. Matusbayashi, H. Ma and Y. Uwatoko, Phys. Scr. **99**, 085923(1-7) (2024).

15. Development of a new Bridgman-type high-pressure cell by using built-in gasket up to 9.4 GPa and evaluation of deformation: A. Hisada, S. Hirota, K. Magishi, N. Fujiwara and Y. Uwatoko, Rev Sci Instrum **95**, 123905(1-7) (2024).

16. ∗High-Field Magnetism of the Spin-1/2 Two-Leg-Ladder Antiferromagnet $Cu(DEP)Cl_2$ under High Pressure: T. Morimoto, E. Morikawa, K. Nihongi, T. Kida, Y. Narumi, Z. Honda, S. Furukawa, Y. Uwatoko, K. Kindo and M. Hagiwara, J. Phys. Soc. Jpn. **94**, 024701 (2025).

17. Pressure Variation of Magnetism in Chromium and Manganese Mono-Pnictide Superconductors: M. Matsuda, J. Cheng and Y. Uwatoko, J. Phys. Soc. Jpn. **94**, 032001(1-16) (2025).

18. A Review on the Magnetovolume Effect of the Full Heusler Alloys Ni_2MnZ (Z = In, Sn, Sb): T. Kanomata, X. Xu, T. Sakon, Y. Nagata, S. Imada, T. Omori, R. Kainuma, T. Eto, Y. Adachi, T. Kihara, Y. Amako, M. Doi and Y. Uwatoko, Metals **15**, 215(1-31) (2025).

19. ∗Pressure-induced topological changes in the Fermi surface of a two-dimensional molecular conductor: T. Kobayashi, K. Yoshimi, H. Ma, S. Sekine, H. Taniguchi, N. Matsunaga, A. Kawamoto and Y. Uwatoko, Phys. Rev. Materials **9**, L021801(1-8) (2025).

20. Pressure-induced charge amorphisation in $BiNiO_3$: W.-T. Chen, T. Nishikubo, Y. Sakai, H. Das, M. Fukuda, Z. Pan, N. Ishimatsu, M. Mizumaki, N. Kawamura, S. I. Kawaguchi, O. Smirnova, M. G. Tucker, T. Watanuki, A. Machida, S. Takajo, Y. Uwatoko, Y. Shimakawa, M. Takano, M. Azuma and J. Paul Attfield, Nat Commun **16**, 2128(1-7) (2025).

Ozaki group

A noniterative method is presented to calculate the closest Wannier functions (CWFs) to a given set of localized guiding functions, such as atomic orbitals, hybrid atomic orbitals, and molecular orbitals, based on minimization of a distance measure function. It is shown that the minimization is directly achieved by a polar decomposition of a projection matrix via singular value decomposition, making iterative calculations and complications arising from the choice of the gauge irrelevant. The disentanglement of bands is inherently addressed by introducing a smoothly varying window function and a greater number of Bloch functions, even for isolated bands. In addition to atomic and hybrid atomic orbitals, we introduce embedded molecular orbitals in molecules and bulks as the guiding functions, and demonstrate that the Wannier interpolated bands accurately reproduce the targeted conventional bands of a wide variety of systems including Si, Cu, the TTF-TCNQ molecular crystal, and a topological insulator of Bi_2Se_3. We further show the usefulness of the proposed method for calculating effective atomic charges. These numerical results not only establish our proposed method as an efficient alternative for calculating WFs, but also suggest that the concept of CWF can serve as a foundation for developing novel methods to analyze electronic structures and calculate physical properties.

1. Closest Wannier functions to a given set of localized orbitals: T. Ozaki, Phys. Rev. B **110**, 125115 (2024).

2. 物性研の計算物性科学コミュニティ支援活動（その 2：最終回）: 尾崎 泰助, 加藤 岳生, 井戸 康太, 福田 将大, 藤堂 眞治, 固体物理 **59(7)**, 381-387 (2024).
3. Electronic band structure change with structural transition of buckled Au_2X monolayers induced by strain: M. Fukuda and T. Ozaki, Phys. Chem. Chem. Phys. **26**, 3367 (2024).
4. Mathematical crystal chemistry: A mathematical programming approach to crystal structures of inorganic compounds: R. Koshoji and T. Ozaki, Phys. Rev. Materials **8**, 113801 (2024).
5. Revealing the Charge Density Wave Caused by Peierls Instability in Two-Dimensional $NbSe_2$: Y.-T. Lee, P.-T. Chen, Z.-H. Li, J.-Y. Wu, C.-N. Kuo, C. S. Lue, C.-T. Wu, C.-C. Kuo, C.-T. Chiang, T. Ozaki, C.-L. Lin, C.-C. Lee, H.-C. Hsueh and M.-C. Chung, ACS Materials Lett. **6**, 2941 (2024).
6. Mechanochemical Synthesis of Non-Solvated Dialkylalumanyl Anion and XPS Characterization of Al(I) and Al(II) Species**: S. Kurumada, R. Yamanashi, K. Sugita, K. Kubota, H. Ito, S. Ikemoto, C. Chen, T. Moriyama, S. Muratsugu, M. Tada, T. Koitaya, T. Ozaki and M. Yamashita, Chemistry A European J **30**, e202303073 (2024).
7. Atomic Observation on Diamond (001) Surfaces with Near-Contact Atomic Force Microscopy: R. Zhang, Y. Yasui, M. Fukuda, T. Ozaki, M. Ogura, T. Makino, D. Takeuchi and Y. Sugimoto, Nano Lett. **25**, 1101 (2025).
8. *Chemical process of hydrogen and formic acid on a Pd-deposited Cu(111) surface studied by high-resolution X-ray photoelectron spectroscopy and density functional theory calculations: W. Osada, M. Hasegawa, Y. Shiozawa, K. Mukai, S. Yoshimoto, S. Tanaka, M. Kawamura, T. Ozaki and J. Yoshinobu, Phys. Chem. Chem. Phys. **27**, 1978 (2025).
9. *Surface structure of the 3x3-Si phase on Al(111), studied by the multiple usages of positron diffraction and core-level photoemission spectroscopy: Y. Sato, Y. Fukaya, A. Nakano, T. Hoshi, C.-C. Lee, K. Yoshimi, T. Ozaki, T. Nakashima, Y. Ando, H. Aoyama, T. Abukawa, Y. Tsujikawa, M. Horio, M. Niibe, F. Komori and I. Matsuda, Phys. Rev. Materials **9**, 014002 (2025).
10. Dimer ribbon structures on diamond (001) surfaces revealed with atomic force microscopy: R. Zhang, Y. Yasui, M. Fukuda, M. Ogura, T. Makino, D. Takeuchi, T. Ozaki and Y. Sugimoto, Phys. Rev. Research **7**, 023036 (2025).

Noguchi group

We have studied (1) spatiotemporal patterns in active Potts models, (2) curvature sensing of asymmetric proteins and rotationally symmetric proteins, and (3) dynamics of tissue sheets on substrates.

1. Cycling and spiral-wave modes in an active cyclic Potts model: H. Noguchi, F. van Wijland and J.-B. Fournier, J. Chem. Phys. **161**, 025101 (2024).
2. Curvature sensing of curvature-inducing proteins with internal structure: H. Noguchi, Phys. Rev. E **109**, 024403/1-10 (2024).
3. Growth and shrinkage of tissue sheets on substrates: buds, buckles, and pores: H. Noguchi and J. Elgeti, New J. Phys. **26**, 103027 (2024).
4. Spatiotemporal patterns in the active cyclic Potts model: H. Noguchi and J.-B. Fournier, New J. Phys. **26**, 093043 (2024).
5. Spontaneous symmetry breaking in two dimensions under non-equilibrium laminar flows: Y. Minami and H. Nakano, J. Stat. Mech. **2024**, 113205 (2024).
6. Computer Simulations of Responsive Nanogels at Lipid Membrane: A. S. Sorokina, R. A. Gumerov, H. Noguchi and I. I. Potemkin, Macromol. Rapid Commun. **45**, 2400406 (2024).
7. Power-law correlation in the homogeneous disordered state of anisotropically self-propelled systems: K. Adachi and H. Nakano, Phys. Rev. Research **6**, 033234 (2024).
8. Universal properties of repulsive self-propelled particles and attractive driven particles: H. Nakano and K. Adachi, Phys. Rev. Research **6**, 013074 (2024).
9. Curvature-sensing and generation by membrane proteins: a review: H. Noguchi, Soft Matter **21**, 3922-3940 (2025).
10. Spatiotemporal pattern formation of membranes induced by surface molecular binding/unbinding: H. Noguchi, Soft Matter **21**, 1113 (2025).
11. Spatiotemporal patterns in active four-state Potts models: H. Noguchi, Sci Rep **15**, 674 (2025).
12. Nonequilibrium Membrane Dynamics Induced by Active Protein Interactions and Chemical Reactions: A Review: H. Noguchi, ChemSystemsChem **7**, e202400042 (2025).

Yoshimi group

In 2024, we continued our contributions to the Project for Advancement of Software Usability in Materials Science (PASUMS) by developing and maintaining research software tools. One of our main developments was ODAT-SE (Open Data Analysis Tool for Science and Engineering), a general-purpose data analysis platform that integrates forward problem solvers with inverse problem-solving algorithms for optimization tasks. Formerly known as 2DMAT, ODAT-SE was restructured in version 3 with a modular architecture to enhance applicability across various scientific domains. We also extended the capabilities of DCore and developed ChiQ, a new tool for computing two-particle spectra from DMFT results. In parallel with software development, we conducted theoretical studies on pressure-induced electronic structure changes in organic conductors, including investigations of Fermi surface topology, phase transitions, and orbital hybridization effects on conductivity. Furthermore, we collaborated on experimental data analysis projects involving coherent X-ray diffraction and spectro-ptychography, applying machine learning techniques.

1. †Multipolar ordering from dynamical mean field theory with application to CeB_6: J. Otsuki, K. Yoshimi, H. Shinaoka and H. O. Jeschke, Phys. Rev. B **110**, 035104 (2024).
2. †*Compensated Ferrimagnets with Colossal Spin Splitting in Organic Compounds: T. Kawamura, K. Yoshimi, K. Hashimoto, A. Kobayashi and T. Misawa, Phys. Rev. Lett. **132**, 156502(1-6) (2024).
3. †*Sub-photon accuracy noise reduction of a single shot coherent diffraction pattern with an atomic model trained autoencoder: T. Ishikawa, Y. Takeo, K. Sakurai, K. Yoshinaga, N. Furuya, Y. Inubushi, K. Tono, Y. Joti, M. Yabashi, T. Kimura and K. Yoshimi, Opt. Express **32**, 18301 (2024).
4. †*H-wave – A Python package for the Hartree-Fock approximation and the random phase approximation: T. Aoyama, K. Yoshimi, K. Ido, Y. Motoyama, T. Kawamura, T. Misawa, T. Kato and A. Kobayashi, Computer Physics Communications **298**, 109087(1-10) (2024).
5. †*Orbital hybridization of donor and acceptor to enhance the conductivity of mixed-stack complexes: T. Fujino, R. Kameyama, K. Onozuka, K. Matsuo, S. Dekura, T. Miyamoto, Z. Guo, H. Okamoto, T. Nakamura, K. Yoshimi, S. Kitou, T.-H. Arima, H. Sato, K. Yamamoto, A. Takahashi, H. Sawa, Y. Nakamura and H. Mori, Nat Commun **15**, 3028 (2024).
6. †*Combined x-ray diffraction, electrical resistivity, and *ab initio* study of $(TMTTF)_2PF_6$ under pressure: Implications for the unified phase diagram: M. Itoi, K. Yoshimi, H. Ma, T. Misawa, T. Tsumuraya, D. Bhoi, T. Komatsu, H. Mori, Y. Uwatoko and H. Seo, Phys. Rev. Research **6**, 043308 (1-14) (2024).
7. †*Update of HΦ : Newly added functions and methods in versions 2 and 3: K. Ido, M. Kawamura, Y. Motoyama, K. Yoshimi, Y. Yamaji, S. Todo, N. Kawashima and T. Misawa, Comp. Phys. Commun. **298**, 109093(1-15) (2024).
8. *Pressure-induced topological changes in the Fermi surface of a two-dimensional molecular conductor: T. Kobayashi, K. Yoshimi, H. Ma, S. Sekine, H. Taniguchi, N. Matsunaga, A. Kawamoto and Y. Uwatoko, Phys. Rev. Materials **9**, L021801(1-8) (2025).

Okamoto group

The discovery of a new material has a potential to trigger the evolution of condensed matter physics. We aim at discovering new materials of crystalline solids that exhibit novel quantum phenomena and innovative electronic functions. In this year, we reported the results of our research on new superconductors Zr_6RuBi_2 and Zr_6FeBi_2 and new quasi-one-dimensional van der Waals crystal $Ta_2Ni_3Te_5$. The A_6MX_2 family with the hexagonal Zr_6CoAl_2-type structure is a hotspot for exploring new *d*-electron superconductors, in which ten new superconductors have been discovered in the past year. The highest T_c = 4.7 K is manifested in Sc_6FeTe_2, where the contribution of the Fe 3*d* orbitals is considerably large, indicating that A_6MX_2 can be a potential target for studying the correlation between superconductivity and various features of transition metals. In this year, we discovered the two new bulk superconductors Zr_6RuBi_2 and Zr_6FeBi_2 with T_c = 4.9 and 1.4 K, respectively. The former compound is a new material and its T_c is slightly higher than that of Sc_6FeTe_2, highest in the existing A_6MX_2 compounds. Based on the electrical resistivity, magnetization, and heat capacity data, the superconductivity in Zr_6RuBi_2 is found to be most likely a conventional BCS type, but the considerably higher T_c than that for Zr_6FeBi_2 differs from the trend in the other A_6MX_2 superconductors, suggesting the high potential of A_6MX_2 family to realize higher T_c and unusual properties. We succeeded in synthesizing the single crystals of chemically doped $Ta_2Ni_3Te_5$. Cr-doped $Ta_2Ni_3Te_5$ was found to show high thermoelectric performance, in which the telluride with the one-dimensional crystal structure plays an important role.

1. Superconductivity in Ternary Germanide ScPdGe and Silicide ScPdSi: Y. Shinoda, Y. Okamoto, Y. Yamakawa, H. Takatsu, H. Kageyama, D. Hirai and K. Takenaka, J. Phys. Soc. Jpn. **93**, 023701(1-4) (2024).
2. Superconductivity in Ternary Zirconium Telluride Zr_6MTe_2 with 3d Transition Metals: H. Matsumoto, Y. Yamakawa, R. Okuma, D. Nishio-Hamane and Y. Okamoto, J. Phys. Soc. Jpn. **93**, 023705(1-5) (2024).

3. †Anisotropic Optical Conductivity Accompanied by a Small Energy Gap in One-Dimensional Thermoelectric Telluride Ta_4SiTe_4: F. Matsunaga, Y. Okamoto, Y. Yokoyama, K. Takehana, Y. Imanaka, Y. Nakamura, H. Kishida, S. Kawano, K. Matsuhira and K. Takenaka, Phys. Rev. B **109**, L161105(1-6) (2024).

4. １次元ファンデルワールス結晶 Ta_4SiTe_4 における熱電効果: 岡本 佳比古, 山川 洋一, 竹中 康司, 固体物理 **59**, 95-105 (2024).

5. 無機化合物における柔粘性結晶状態: 片山 尚幸, 小島 慶太, 固体物理 **59**, 457-468 (2024).

6. Electric Field-Induced Volume Change in Pyro-Vanadate-Phosphates: Toward an Alternative Actuator Architecture: K. Takada, J. Shibutani, K. Yagi, F. Ikawa, Y. Yokoyama, D. Hirai, Y. Okamoto, N. Katayama, Y. Uemura, L. M. G. H. Chavas, T. Hatano, A. Fujita and K. Takenaka, Appl. Phys. Lett. **125**, 041903(1-6) (2024).

7. クロムテルル化物焼結体に現れる巨大な磁場誘起体積変化: 岡本佳比古, 竹中康司, FC Report **42**, 7-12 (2024).

8. Unbalanced Charge Distribution Stabilized by Orbital Ordering: Y. Okamoto, JPSJ News and Comments **21**, 13(1-2) (2024).

9. †Observation of Current-Induced Lattice Distortion in Spin–Orbit Coupled Iridium Oxide $Ca_5Ir_3O_{12}$: K. Kadohiro, H. Hanate, M. Hayashida, T. Hasegawa, H. Nakao, Y. Okamoto, K. Miyazaki, S. Tsutsui and K. Matsuhira, J. Phys. Soc. Jpn. **94**, 023601(1-4) (2025).

10. *Superconductivity in Hexagonal Zr_6CoAl_2-Type Zr_6RuBi_2 and Zr_6FeBi_2: K. Yuchi, D. Nishio-Hamane, K. Kojima, K. Moriyama, R. Okuma and Y. Okamoto, J. Phys. Soc. Jpn. **94**, 013701(1-5) (2025).

11. Anisotropic superconducting gap probed by Te^{125} NMR in noncentrosymmetric Sc_6MTe_2 (M = Fe, Co): K. Doi, H. Takei, Y. Shinoda, Y. Okamoto, D. Hirai, K. Takenaka, T. Matsushita, Y. Kobayashi and Y. Shimizu, Phys. Rev. B **111**, 214502(1-7) (2025).

12. Sc_6MTe_2：六方晶 Fe_2P 型構造をもつ新しい超伝導ファミリー: 岡本 佳比古, 山川 洋一, 固体物理 **60**, 215-223 (2025).

13. Composition evolution of crystal structure and negative thermal expansion in pyro-vanadate–phosphate $Cu_{1.8}Zn_{0.2}V_{2-x}P_xO_7$: M. Kawakita, F. Ikawa, K. Yagi, M. Kano, T. Kubo, Y. Yokoyama, N. Katayama, Y. Okamoto, D. Hirai and K. Takenaka, Appl. Phys. Lett. **126**, 091902(1-5) (2025).

14. さまざまな遷移金属元素を含む新しい超伝導体ファミリー: 岡本 佳比古, 湯池 宏介, 篠田 祐作, 竹中 康司, 日本物理学会誌 **80**, 240-245 (2025).

15. *Topological Semimetal KAlGe with Novel Electronic Instability: T. Ikenobe, T. Yamada, J.-I. Yamaura, T. Oguchi, R. Okuma, D. Hirai, H. Sagayama, Y. Okamoto and Z. Hiroi, Chem. Mater. **37**, 189-197 (2025).

16. Electronic Self-Organization in the β-Pyrochlore Oxide CsW_2O_6: Y. Okamoto, J. Phys. Soc. Jpn. **93**, 111006(1-16) (2024).

Yamaura group

This year, the structures of numerous materials were elucidated utilizing quantum beams and laboratory-based diffractometers for fundamental to advanced materials such as innovative ferroelectrics, high dielectrics, unique thermoelectric materials, boron crystals, and nanowire sensors. The collaborative research in the X-ray diffraction section of the Materials Design and Characterisation Laboratory (MDCL) advanced effectively, offering user support to numerous individuals both within and beyond the laboratory, as well as analytical guidance, innovative research proposals, and avenues for quantum beam applications. In addition, the radiation safty laboratory was operated to educate and control radiation workers at the facility, control nuclear fuel materials, and conduct periodic inspections of X-ray generators.

1. Symmetry change in $LaNiO_3$ films caused by epitaxial strain from $LaAlO_3$, $SrTiO_3$, and $DyScO_3$ pseudocubic (001) surfaces: F. Izumisawa, Y. Ishii, M. Kimura, T. Katase, T. Kamiya, J.-I. Yamaura and Y. Wakabayashi, J. Appl. Phys. **136**, 075303 (2024).

2. *J_{eff} = 1/2 Hyperoctagon Lattice in Cobalt Oxalate Metal-Organic Framework: H. Ishikawa, S. Imajo, H. Takeda, M. Kakegawa, M. Yamashita, J.-I. Yamaura and K. Kindo, Phys. Rev. Lett. **132**, 156702 (2024).

3. Phonon drag thermopower persisting over 200 K in $FeSb_2$ thin film on $SrTiO_3$ single crystal: C. Yamamoto, X. He, K. Hanzawa, T. Katase, M. Sasase, J.-I. Yamaura, H. Hiramatsu, H. Hosono and T. Kamiya, Appl. Phys. Lett. **124**, 193902 (2024).

4. †*Crystal structure and properties of perovskite-type rubidium niobate, a high-pressure phase of $RbNbO_3$: A. Yamamoto, K. Murase, T. Sato, K. Sugiyama, T. Kawamata, Y. Inaguma, J.-I. Yamaura, K. Shitara, R. Yokoi and H. Moriwake, Dalton Trans. **53**, 7044 (2024).

5. *Macroscopic sheets of hydrogen boride and their spectroscopic evaluation: K. Yamaguchi, M. Niibe, X. Zhang, T. Sumi, M. Horio, Y. Ando, J.-I. Yamaura, E. Nakamura, K. Tanaka, T. Kondo and I. Matsuda, Phys. Rev. Materials **8**, 074005 (2024).

6. Nonequilibrium Layered PbS Stabilized by Sn Doping: Bipolar Semiconductors with Low Thermal Conductivity: M. Hiramatsu, Z. Hu, S. Yoshikawa, Z. Yang, X. He, T. Katase, J.-I. Yamaura, H. Sagayama, T. Tadano, S. Ueda, H. Hiramatsu, H. Hosono and T. Kamiya, ACS Appl. Electron. Mater. **6**, 8339 (2024).

7. *Topological Semimetal KAlGe with Novel Electronic Instability: T. Ikenobe, T. Yamada, J.-I. Yamaura, T. Oguchi, R. Okuma, D. Hirai, H. Sagayama, Y. Okamoto and Z. Hiroi, Chem. Mater. **37**, 189-197 (2025).

8. *Evaluating chemical states in a single microcrystal of chromium boride with the micro-focused ion and quantum beams: Y. Guan, X. Zhang, M. Miyamoto, Y. Tsujikawa, K. Yubuta, M. Horio, H. Isshiki, J.-I. Yamaura, T. Abukawa, F. Komori and I. Matsuda, Solid State Sciences **161**, 107838 (2025).

9. †Dielectric properties depend on the crystal structure of perovskite-type $RbTaO_3$ synthesized at high pressure: K. Murase, J.-I. Yamaura, Y. Hamasaki, T. Kato, H. Sagayama and A. Yamamoto, Dalton Trans. **54**, 2252 (2025).

10. *Spontaneous Hall effect induced by collinear antiferromagnetic order at room temperature: R. Takagi, R. Hirakida, Y. Settai, R. Oiwa, H. Takagi, A. Kitaori, K. Yamauchi, H. Inoue, J.-I. Yamaura, D. Nishio-Hamane, S. Itoh, S. Aji, H. Saito, T. Nakajima, T. Nomoto and R. A. &. S. Seki, Nature Materials **24**, 63-68 (2025).

11. Nano-Patterned CuO Nanowire Nanogap Hydrogen Gas Sensor with Voids: M. Zhao, R. Nitta, S. Izawa, J. Yamaura and Y. Majima, Adv Funct Materials **35**, 2415971 (2025).

Kitagawa group

Kitagawa lab. started in FY2024. We are developing state-of-the-art high-pressure measurement techniques including quantum sensing, and exploring new phenomena under pressure. Our main targets in FY2024 included, nickelate high-temperature supeconductors, and instrumental development of ultrahigh-pressure devices for SQUID magnetometry and optically-detected magnetic resonance (ODMR).

We established bulkiness of superconductivity for high-temperature two-layer-type nickelate superconductors for the first time. The nickelate superconductor was first discovered as a resistivity drop under pressure as high as 14 GPa in 2023, but there has been controversy whether the superconductivity is real (bulk) or not. We successfully measured Meissner effect using 6-8 multi anvil apparatus and conventional micro-coil mutual inductance method.

To accelerate research for novel superconductors or magnetic materials, we are developing two types of opposed-anvil type pressure devices. One fits to magnetization measurement using a commercial SQUID magnetometer, which allows a highly sensitive magnetometry a with a resolution of volume susceptibility as small as 10^{-3} under very high pressures up to 20 GPa. The other is a large-scale high-pressure system intended to be used with wide field-of-view ODMR of diamond NV center or other solid-state qunatum sensors. We are now testing these technologies with pressure-induced superconductors including nickelates.

1. *Bulk high-temperature superconductivity in pressurized tetragonal $La_2PrNi_2O_7$: N. Wang, G. Wang, X. Shen, J. Hou, J. Luo, X. Ma, H. Yang, L. Shi, J. Dou, J. Feng, J. Yang, Y. Shi, Z. Ren, H. Ma, P. Yang, Z. Liu, Y. Liu, H. Zhang, X. Dong, Y. Wang, K. Jiang, J. Hu, S. Nagasaki, K. Kitagawa, S. Calder, J. Yan, J. Sun, B. Wang, R. Zhou, Y. Uwatoko and J. Cheng, Nature **634**, 579-584 (2024).

Materials Synthesis and Characterization group

1. *J_{eff} = 1/2 Hyperoctagon Lattice in Cobalt Oxalate Metal-Organic Framework: H. Ishikawa, S. Imajo, H. Takeda, M. Kakegawa, M. Yamashita, J.-I. Yamaura and K. Kindo, Phys. Rev. Lett. **132**, 156702 (2024).

2. †*Crystal structure and properties of perovskite-type rubidium niobate, a high-pressure phase of $RbNbO_3$: A. Yamamoto, K. Murase, T. Sato, K. Sugiyama, T. Kawamata, Y. Inaguma, J.-I. Yamaura, K. Shitara, R. Yokoi and H. Moriwake, Dalton Trans. **53**, 7044 (2024).

Neutron Science Laboratory

Yamamuro group

Our laboratory is studying chemical physics of complex condensed matters by using neutron scattering, X-ray diffraction, calorimetric, dielectric, and viscoelastic techniques. Our target materials are glasses, liquids, and various disordered solids. In 2024, we measured X-ray diffraction of hydrogen (H_2) and xenon (Xe) amorphous hydrates M-5.75H_2O (M: guest molecule) using a custom-made vapor-deposition cryostat and a high-energy X-ray diffractometer at BL04B2, SPring-8. We found that both amorphous hydrates had many distorted hydrogen-bonded H_2O cages containing guest molecules, and they became more well-defined by annealing below T_g (= 130 K). It was also clarified that amorphous Xe hydrate transformed to crystalline Xe hydrate by annealing around 165 K. We performed the neutron powder diffraction (NPD) and quasielastic neutron scattering (QENS) experiments on a new hydrogen cluster material Mg_6WH_{16}. The orientation of the MoH_8^{4+} ions remain disordered down to 8 K and the QENS spectra were well fitted by the Kohlrausch-Williams-Watts (KWW) functions with small non-exponential parameters ($\beta < 0.4$) corresponding to large distribution of relaxation time. The heat capacities of vapor-deposited amorphous H_2O and CS_2 were measured to obtain absolute density of states corresponding to boson peaks. We also measured the heat capacity of a metal-organic framework MOF-101 including acetonitrile (AN) molecules with/without Mg(TFSI) $_2$ in the pores to investigate the states of AN molecules from an entropic point of view.

1. Improvement of a Time-of-Flight Spectrometer AGNES at JRR-3 Using Supermirror Techniques: H. Akiba, Y. Ohmasa, M. Kofu, M. Zhang, S. Sato and O. Yamamuro, J. Phys. Soc. Jpn. **93**, 091010 (2024).

2. Ice-Like Dynamics of Water Clusters: K. Oka, H. Akiba, N. Tohnai, T. Shibue and O. Yamamuro, J. Phys. Chem. Lett. **15**, 267-271 (2024).

3. Non-Newtonian Dynamics in Water-in-Salt Electrolytes: T. Yamaguchi, A. Dukhin, Y. -J. Ryu, D. Zhang, O. Borodin, M. A. Gonza´lez, O. Yamamuro, D. L. Price and M. -L. Saboungi, J. Phys. Chem. Lett. **15**, 76-80 (2024).

4. *Higher conductivity in doped ethylenedioxythiophene (EDOT) dimers with chalcogen-substituted end groups: K. Onozuka, T. Fujino, T. Miyamoto, T. Yamakawa, H. Okamoto, H. Akiba, O. Yamamuro, E. Kayahara, S. Yamago, H. Oike and H. Mori, J. Mater. Chem. C **12**, 13956 (2024).

Masuda group

The goal of our research is to discover a new quantum phenomenon and to reveal the mechanism of it. In this fiscal year we studied the following topics; inelastic neutron scattering study on Skyrmion host compound GaV_4Se_8, chiral split magnon in altermagnetic MnTe, field control of quasiparticle decay in a quantum antiferromagnet, spin dynamics in equilateral triangular spin tube material $CsCrF_4$ and so on. We also developed a new inelastic neutron spectrometer HODACA.

1. A New Inelastic Neutron Spectrometer HODACA: H. Kikuchi, S. Asai, T. J. Sato, T. Nakajima, L. Harriger, I. Zaliznyak and T. Masuda, J. Phys. Soc. Jpn. **93**, 091004(1-11) (2024).

2. Inelastic Neutron Scattering Study on Skyrmion Host Compound GaV_4Se_8: Z. Liu, R. Ide, T.-H. Arima, S. Itoh, S. Asai and T. Masuda, J. Phys. Soc. Jpn. **93**, 124707(1-4) (2024).

3. †*Polarized and Unpolarized Neutron Scattering for Magnetic Materials at the Triple-axis Spectrometer PONTA in JRR-3: T. Nakajima, H. Saito, N. Kobayashi, T. Kawasaki, T. Nakamura, H. Kawano-Furukawa, S. Asai and T. Masuda, J. Phys. Soc. Jpn. **93**, 091002 (2024).

4. †*Elastic and inelastic neutron scattering experiments under high pressure in the frustrated antiferromagnet $CuFeO_2$: N. Terada, D. D. Khalyavin, P. Manuel, S. Asai, T. Masuda, H. Saito, T. Nakajima and T. Osakabe, Phys. Rev. B **110**, 024406 (2024).

5. Inelastic neutron scattering studies on the eight-spin zigzag-chain compound $KCu_4P_3O_{12}$: Confirmation of the validity of a data-driven technique based on machine learning: M. Hase, R. Tamura, K. Hukushima, S. Asai, T. Masuda, S. Itoh and A. Do¨nni, Phys. Rev. B **109**, 094434(1-8) (2024).

6. Neutron scattering study on dimerized 4f1 intermetallic compound Ce_5Si_3: D. Ueta, Y. Iwata, R. Kobayashi, K. Kuwahara, T. Masuda and S. Itoh, Phys. Rev. B **109**, 205127(1-8) (2024).

7. Chiral Split Magnon in Altermagnetic MnTe: Z. Liu, M. Ozeki, S. Asai, S. Itoh and T. Masuda, Phys. Rev. Lett. **133**, 156702(1-6) (2024).

8. Imaging and Control of Magnetic Domains in a Quasi-One-Dimensional Quantum Antiferromagnet $BaCu_2Si_2O_7$: M. Moromizato, T. Miyake, T. Masuda, T. Kimura and K. Kimura, Phys. Rev. Lett. **133**, 086701(1-6) (2024).

9. ∗Sample Environment of the HRC Spectrometer at J-PARC: D. Ueta, S. Itoh, T. Masuda, T. Yokoo, T. Nakajima, S. Asai, H. Saito, D. Kawana, R. Sugiura, T. Asami, S. Yamauchi, S. Torii, Y. Ihata and H. Tanino, JPS Conf. Proc. **41**, 011008(1-5) (2024).

10. Field control of quasiparticle decay in a quantum antiferromagnet: S. Hasegawa, H. Kikuchi, S. Asai, Z. Wei, B. Winn, G. Sala, S. Itoh and T. Masuda, Nat Commun **15**, 125(1-7) (2024).

11. Spin dynamics in linear magnetoelectric material $Mn_3Ta_2O_8$: H. Kikuchi, S. Hasegawa, S. Asai, T. Hong, K. Kimura, T. Kimura, S. Itoh and T. Masuda, J. Phys.: Condens. Matter **37**, 195804(1-6) (2025).

12. Dirac Magnon in Honeycomb Lattice Magnet $NiTiO_3$: H. Kikuchi, M. Ozeki, N. Kurita, S. Asai, T. J. Williams, T. Hong and T. Masuda, J. Phys. Soc. Jpn. **94**, 024703(1-4) (2025).

13. Neutron Spectroscopy Study on Crystalline Electric Field Excitations in NdB_4: H. Yamauchi, N. Metoki, R. Watanuki, T. Hong, J. A. Fernandez-Baca, M. Hagihala, T. Masuda, H. Yoshizawa and S. Itoh, J. Phys. Soc. Jpn. **94**, 054705(1-8) (2025).

14. Anomalous Electrical Transport in the Kagome Magnet $YbFe_6Ge_6$: W. Yao, S. Liu, H. Kikuchi, H. Ishikawa, O. S. Fjellvag, D. W. Tam, F. Ye, D. L. Abernathy, G. D. A. Wood, D. Adroja, C.-M. Wu, C.-L. Huang, B. Gao, Y. Xie, Y. Gao, K. Rao, E. Morosan, K. Kindo, T. Masuda, K. Hashimoto, T. Shibauchi and P. Dai, Phys. Rev. Lett. **134**, 186501(1-7) (2025).

15. Neutron scattering studies on $NdCrTiO_5$ and $RCrGeO_5$ (R = Nd, Ho, Er) possessing spin-3/2 antiferromagnetic alternating chains of $Cr^{3\Gamma}$ spins: M. Hase, S. Asai, M. Soda, D. Kawana, T. Masuda, S. Itoh, T. Yokoo, M. Kohno, V. Yu. Pomjakushin, A. Do¨nni and M. Rotter, Journal of Magnetism and Magnetic Materials **623**, 172970(1-11) (2025).

16. Spin Dynamics in Equilateral Triangular Spin Tube Material $CsCrF_4$: H. Kikuchi, S. Asai, H. Manaka, M. Hagihala, S. Itoh and T. Masuda, Neutron News **35**, 13-14 (2024).

Nakajima group

Nakajima group is studying magnetic materials with cross-correlated phenomena associated with the symmetry of the magnetic structures by means of neutron and X-ray scattering techniques. We are responsible for a polarized-neutron triple-axis neutron spectrometer PONTA in the research reactor JRR-3 in Tokai, and have been supporting the users of the ISSP-NSL joint-use program. One of the research highlights at PONTA in the fiscal year of 2024 is the discovery of a non-coplanar helimagnetic order in the van der Waals compound $DyTe_3$. Prof. Hirschberger's group in the university of Tokyo grew a single crystal of this compound, and performed neutron diffraction measurements at PONTA. They revealed that commensurate and incommensurate magnetic peaks emerge below the antiferromagnetic transition temperature of T_N =3.85 K, which was determined by magnetic susceptibility and heat capacity measurements. By utilizing the polarized neutron scattering technique, they successfully elucidated that the magnetic structure of this compound is an alternating transverse conical magnetic structure. The complex helimagnetic ordering on cleavable van der Waals layers would be potentially appricable for spintronics devices. Nakajima group is also working on developing new neutron scattering techniques in extreme conditions. In this fiscal year, we have published a paper reporting neutron time-of-flight diffraction measurements in long pulsed-magnetic fields in collaboration with Prof. Kohama's group in IMGSL of ISSP. By combining the high-intensity pulsed neutron beam in J-PARC and long pulsed magnetic field developed by Prof. Kohama, we successfully observed diffraction patterns corresponding to field induced magnetic phases in a triangular lattice antiferromagnet $CuFe_{1-x}Ga_xO_2$. We are planning to introduce spin-polarization analyzer for scattered neutrons, which enables us to determine the symmetry of the magnetic structure from a limited number of magnetic reflections, in the future.

1. †∗Polarized and Unpolarized Neutron Scattering for Magnetic Materials at the Triple-axis Spectrometer PONTA in JRR-3: T. Nakajima, H. Saito, N. Kobayashi, T. Kawasaki, T. Nakamura, H. Kawano-Furukawa, S. Asai and T. Masuda, J. Phys. Soc. Jpn. **93**, 091002 (2024).

2. †Polarized Neutron Diffraction Study on UPt_2Si_2: F. Kon, C. Tabata, H. Saito, T. Nakajima, H. Hidaka, T. Yanagisawa and H. Amitsuka, J. Phys. Soc. Jpn. **93**, 044701 (2024).

3. †∗Spin–Lattice-Coupled Helical Magnetic Order in Breathing Pyrochlore Magnets, $CuAlCr_4S_8$ and $CuGaCr_4S_8$: M. Gen, T. Nakajima, H. Saito, Y. Tokunaga and T.-H. Arima, J. Phys. Soc. Jpn. **93**, 104602 (2024).

4. †∗Elastic and inelastic neutron scattering experiments under high pressure in the frustrated antiferromagnet $CuFeO_2$: N. Terada, D. D. Khalyavin, P. Manuel, S. Asai, T. Masuda, H. Saito, T. Nakajima and T. Osakabe, Phys. Rev. B **110**, 024406 (2024).

5. Development of Polarization Analysis at TAIKAN under Magnetic Field at Low Temperature: T. Morikawa, K. Ohishi, K. Hiroi, Y. Kawamura, S.-I. Takata, J.-I. Suzuki and T. Nakajima, JPS Conf. Proc. **41**, 011012 (2024).

6. *Sample Environment of the HRC Spectrometer at J-PARC: D. Ueta, S. Itoh, T. Masuda, T. Yokoo, T. Nakajima, S. Asai, H. Saito, D. Kawana, R. Sugiura, T. Asami, S. Yamauchi, S. Torii, Y. Ihata and H. Tanino, JPS Conf. Proc. **41**, 011008(1-5) (2024).

7. †Non-coplanar helimagnetism in the layered van-der-Waals metal $DyTe_3$: S. Akatsuka, S. Esser, S. Okumura, R. Yambe, R. Yamada, M. M. Hirschmann, S. Aji, J. S. White, S. Gao, Y. Onuki, T.-H. Arima, T. Nakajima and M. Hirschberger, Nat Commun **15**, 4291 (2024).

8. *Multistep topological transitions among meron and skyrmion crystals in a centrosymmetric magnet: H. Yoshimochi, R. Takagi, J. Ju, N. D. Khanh, H. Saito, H. Sagayama, H. Nakao, S. Itoh, Y. Tokura, T. Arima, S. Hayami, T. Nakajima and S. Seki, Nature Physics **20**, 1001-1008 (2024).

9. Stroboscopic time-of-flight neutron diffraction in long pulsed magnetic fields: T. Nakajima, M. Watanabe, Y. Inamura, K. Matsui, T. Kanda, T. Nomoto, K. Ohishi, Y. Kawamura, H. Saito, H. Tamatsukuri, N. Terada and Y. Kohama, Phys. Rev. Research **6**, 023109 (2024).

10. Probing the Sense of Spin Twisting in Magnetic Skyrmion Lattice by Resonant X-ray Scattering: T. Nakajima, JPSJ News Comments **21**, 14 (2024).

11. Magnetoelastic coupling and large uniaxial pressure dependence of antiferromagnetic order in two-dimensional van der Waals $Fe_2P_2S_6$ and $Ni_2P_2S_6$ single crystals: K. K. Bestha, V. Kocsis, O. Janson, Y. Shemerliuk, S. Selter, S. Aswartham, T. Nakajima, H. Saito, B. Bu¨chner, L. T. Corredor and A. U. B. Wolter, Phys. Rev. B **111**, L020409 (2025).

12. †Electronic commensuration of a spin moire´ superlattice in a layered magnetic semimetal: T. Kurumaji, N. Paul, S. Fang, P. M. Neves, M. Kang, J. S. White, T. Nakajima, D. Graf, L. Ye, M. K. Chan, T. Suzuki, J. Denlinger, C. Jozwiak, A. Bostwick, E. Rotenberg, Y. Zhao, J. W. Lynn, E. Kaxiras, R. Comin, L. Fu and J. G. Checkelsky, Sci. Adv. **11**, eadu6686 (2025).

13. *Spontaneous Hall effect induced by collinear antiferromagnetic order at room temperature: R. Takagi, R. Hirakida, Y. Settai, R. Oiwa, H. Takagi, A. Kitaori, K. Yamauchi, H. Inoue, J.-I. Yamaura, D. Nishio-Hamane, S. Itoh, S. Aji, H. Saito, T. Nakajima, T. Nomoto and R. A. &. S. Seki, Nature Materials **24**, 63-68 (2025).

Mayumi group

Contrast variation small-angle neutron scattering (CV-SANS) is a powerful tool to evaluate the structure of multi-component systems by decomposing scattering intensities I(Q) measured with different scattering contrasts into partial scattering functions S(Q) of self- and cross-correlations between components. The measured I(Q) contains a measurement error, ΔI(Q), and ΔI(Q) results in an uncertainty of partial scattering functions, ΔS(Q). However, the error propagation from ΔI(Q) to ΔS(Q) has not been quantitatively clarified. We have established deterministic and statistical approaches to determine ΔS(Q) from ΔI(Q). We have applied the two methods to (i) computational data of a core-shell sphere and experimental CV-SANS data of (ii) clay/polyethylene glycol (PEG) aqueous solutions and (iii) polyrotaxane solutions, and have successfully estimated the errors of S(Q). The quantitative error estimation of S(Q) offers us a strategy to optimize the combination of scattering contrasts to minimize error propagation.

1. †Hierarchical Structure of Soft Materials Studied at Small-Angle Neutron Scattering Instrument, SANS-U: K. Mayumi, L. Geonzon, K. Hashimoto and T. Oda, J. Phys. Soc. Jpn. **93**, 091007 (2024).

2. †Effects of Heterogeneous Mixing of Imidazolium-Based Ionic Liquids with Alcohols on Complex Formation of Ni(II) Ion: T. Takamuku, A. Ogawa, S. Tsutsui, K. Sadakane, H. Iwase, K. Mayumi and K. Ozutsumi, J. Phys. Chem. B **128**, 8567 (2024).

3. Strain-Induced Crystallization in Tetra-Branched Poly(ethylene glycol) Hydrogels with a Common Network Structure: K. Hashimoto, T. Enoki, C. Liu, X. Li, T. Sakai and K. Mayumi, Macromolecules **57**, 1461 (2024).

4. †Tough and Durable Slide-Ring Ion Gels for Stretchable Electronics Leveraging Strain-Induced Crystallization of Poly(ethylene glycol): T. Enoki, K. Hashimoto, T. Oda, K. Ito and K. Mayumi, Macromolecules **57**, 11498 (2024).

5. †Bridge-rich and loop-less hydrogel networks through suppressed micellization of multiblock polyelectrolytes: J. Han, S. Najafi, Y. Byun, L. Geonzon, S.-H. Oh, J. Park, J. M. Koo, J. Kim, T. Chung, I. K. Han, S. Chae, D. W. Cho, J. Jang, U. Jeong, G. H. Fredrickson, S.-H. Choi, K. Mayumi, E. Lee, J.-E. Shea and Y. S. Kim, Nat Commun **15**, 6553 (2024).

6. †Ionic Conductive Organogels Based on Cellulose and Lignin-Derived Metabolic Intermediates: H. Jia, K. Jimbo, K. Mayumi, T. Oda, T. Sawada, T. Serizawa, T. Araki, N. Kamimura, E. Masai, E. Togawa, M. Nakamura and T. Michinobu, ACS Sustainable Chem. Eng. **12**, 501 (2024).

7. Understanding the rheological properties from linear to nonlinear regimes and spatiotemporal structure of mixed kappa and reduced molecular weight lambda carrageenan gels: L. C. Geonzon, T. Enoki, S. Humayun, R. Tuvikene, S. Matsukawa and K. Mayumi, Food Hydrocolloids **150**, 109752 (2024).

8. Mechanical properties of polymer networks with polyrotaxane crosslinkers with different molecular structures based on polyethylene glycol and α-cyclodextrin: S. Liu, K. Watanabe, E. Miwa, M. Hara, T. Seki, K. Mayumi, K. Ito and Y. Takeoka, Giant **17**, 100224 (2024).

9. Composites with aligned and plasma-surface-modified graphene nanoplatelets and high dielectric constants: K. Nagayama, T. Goto, K. Mayumi, R. Maeda, T. Ito, Y. Shimizu, K. Ito, Y. Hakuta and K. Terashima, Materials Letters: X **22**, 100233 (2024).

10. †Error evaluation of partial scattering functions obtained from contrast-variation small-angle neutron scattering: K. Mayumi, T. Oda, S. Miyajima, I. Obayashi and K. Tanaka, J Appl Crystallogr **58**, 4 (2025).

11. †Size-exclusion chromatography–small-angle neutron scattering system optimized for an instrument with medium neutron flux: K. Morishima, R. Inoue, T. Nakagawa, M. Shimizu, R. Sakamoto, T. Oda, K. Mayumi and M. Sugiyama, J Appl Crystallogr **58**, 595 (2025).

12. †Tough polymer gels reinforced by strain-induced crystallization: K. Mayumi, Polym J **57**, 449 (2025).

13. †Adsorption suppression and viscosity transition in semidilute PEO/silica nanoparticle mixtures under the protein limit: S. Kusakabe, X. Li, K. Mayumi, T. Katashima, I. Sakuma and Y. Akagi, Journal of Colloid and Interface Science **692**, 137377 (2025).

Kofu group

Our laboratory started in January 2025. We study the dynamics of atoms, molecules, and spins in various materials using neutron scattering techniques to discover novel phenomena and universality inherent in a wide range of materials. In this financial year, we performed inelastic/quasielastic scattering measurements of Ising spin glass $(Fe,Mn)TiO_3$, martyite, and amorphous metal hydride PdSiH using AMATERAS at J-PARC and AGNES at JRR-3. We also supported user experiments on liquids, hydrates, and polymer systems using AGNES and contributed in part to the joint-use operation of AMATERAS.

International MegaGauss Science Laboratory

Kindo group

We have found the process of fabricating the Cu-Ag wire for a stable 85 T shot. Every coil wound by the new wire can generate the magnetic field exceeding 85 T without failure in this year.

1. †High-temperature magnetic anomaly via suppression of antisite disorder through synthesis route modification in a Kitaev candidate Cu_2IrO_3: Y. Haraguchi, D. Nishio-Hamane, A. Matsuo, K. Kindo and H. A. Katori, J. Phys.: Condens. Matter **36**, 405801 (2024).

2. †Field-induced Insulator–Metal Transition in $EuTe_2$: T. Takeuchi, F. Honda, D. Aoki, Y. Haga, T. Kida, Y. Narumi, M. Hagiwara, K. Kindo, K. Karube, H. Harima and Y. Onuki, J. Phys. Soc. Jpn. **93**, 044708 (2024).

3. *Field-Induced Quantum Phase Transitions in the Pressure-Tuned Triangular-Lattice Antiferromagnet $CsCuCl_3$: K. Nihongi, T. Kida, D. Yamamoto, Y. Narumi, J. Zaccaro, Y. Kousaka, K. Inoue, Y. Uwatoko, K. Kindo and M. Hagiwara, J. Phys. Soc. Jpn. **93**, 084704(1-7) (2024).

4. †Invariable Simultaneous Emergence of Antiferromagnetic Order and Tetragonal Deformation in CoO Nanocrystals: Y. Ishiwata, G. Kawahara, K. Akase, T. Tominaga, H. Miyazaki, H. Ishii, A. Matsuo, K. Kindo, Y. Inagaki, K. Akashi, T. Kawae, T. Kida, S. Suehiro, M. Nantoh and K. Ishibashi, J. Phys. Soc. Jpn. **93**, 044603 (2024).

5. †Magnetic Properties of Single Crystalline Eu_2Ga_3Ir: R. Nakachi, Y. Onuki, Y. Homma, A. Nakamura, D. Aoki, M. Nakashima, T. Takeuchi, T. Kida, Y. Narumi, M. Hagiwara, K. Kindo, F. Honda, Y. Uwatoko, R. Higashinaka, Y. Aoki and T. D. Matsuda, J. Phys. Soc. Jpn. **93**, 115001 (2024).

6. †$CaCo_2TeO_6$: A topochemically prepared $3d^7$ honeycomb Kitaev magnet: Y. Haraguchi, Y. Yoshida, A. Matsuo, K. Kindo and H. A. Katori, Phys. Rev. B **110**, 184411 (2024).

7. †∗ Crystal field magnetostriction of spin ice under ultrahigh magnetic fields: N. Tang, M. Gen, M. Rotter, H. Man, K. Matsuhira, A. Matsuo, K. Kindo, A. Ikeda, Y. H. Matsuda, P. Gegenwart, S. Nakatsuji and Y. Kohama, Phys. Rev. B **110**, 214414 (1-10) (2024).

8. ∗Dimerization-enhanced exotic magnetization plateau and magnetoelectric phase diagrams in skew-chain $Co_2V_2O_7$: Z. H. Li, X. T. Han, C. Dong, H. W. Wang, Z. Z. He, R. Chen, W. X. Liu, C. L. Lu, Y. Kohama, M. Tokunaga, K. Kindo, Z. W. Ouyang, J. F. Wang and M. Yang, Phys. Rev. B **109**, 094432 (2024).

9. Evidence of random spin-singlet state in the three-dimensional quantum spin liquid candidate $Sr_3CuNb_2O_9$: S. M. Hossain, S. S. Rahaman, H. Gujrati, D. Bhoi, A. Matsuo, K. Kindo, M. Kumar and M. Majumder, Phys. Rev. B **110**, L020406 (2024).

10. †∗Geometric frustration and Dzyaloshinskii-Moriya interactions in a quantum star lattice hybrid copper sulfate: H. Ishikawa, Y. Ishii, T. Yajima, Y. H. Matsuda, K. Kindo, Y. Shimizu, I. Rousochatzakis, U. K. Ro¨ßler and O. Janson, Phys. Rev. B **109**, L180401 (2024).

11. ∗Magnetic anisotropy of CeCoSi under high magnetic field: T. Kanda, H. Ishikawa, S. Imajo, K. Kindo, H. Tanida and Y. Kohama, Phys. Rev. B **109**, 174402 (2024).

12. †Magnetic field induced insulator-to-metal Mott transition in λ-type organic conductors: S. Fukuoka, T. Oka, Y. Ihara, A. Kawamoto, S. Imajo and K. Kindo, Phys. Rev. B **109**, 195142 (2024).

13. †One-half magnetization plateau in the spin-1/2 fcc lattice antiferromagnet Sr_2CoTeO_6: H. Tanaka, A. Matsuo and K. Kindo, Phys. Rev. B **109**, 094414 (2024).

14. †Quantum spin state stabilized by coupling with classical spins: H. Yamaguchi, T. Okubo, A. Matsuo, T. Kawakami, Y. Iwasaki, T. Takahashi, Y. Hosokoshi and K. Kindo, Phys. Rev. B **109**, L100404 (2024).

15. ∗J_{eff} = 1/2 Hyperoctagon Lattice in Cobalt Oxalate Metal-Organic Framework: H. Ishikawa, S. Imajo, H. Takeda, M. Kakegawa, M. Yamashita, J.-I. Yamaura and K. Kindo, Phys. Rev. Lett. **132**, 156702 (2024).

16. ∗Quantum Liquid States of Spin Solitons in a Ferroelectric Spin-Peierls State: S. Imajo, A. Miyake, R. Kurihara, M. Tokunaga, K. Kindo, S. Horiuchi and F. Kagawa, Phys. Rev. Lett. **132**, 096601/1-6 (2024).

17. Suppression of a Structural Phase Transition by an Orientational Disorder of Counteranions in an Organic Conductor, β-β-(BEDT-TTF) $_2ClC_2H_4SO_3$: H. Akutsu, M. Uruichi, S. Imajo, K. Kindo, T. Masuta, H. Manabe, Y. Nakazawa and S. S. Turner, Inorg. Chem. **63**, 16872 (2024).

18. †Magnetic properties of the Co-doped MnNiGe system in high magnetic field: M. Ito, K. Onda, A. Matsuo and K. Kindo, Physica B: Condensed Matter **688**, 416151 (2024).

19. ∗High-Field Magnetism of the Spin-1/2 Two-Leg-Ladder Antiferromagnet Cu(DEP)Cl_2 under High Pressure: T. Morimoto, E. Morikawa, K. Nihongi, T. Kida, Y. Narumi, Z. Honda, S. Furukawa, Y. Uwatoko, K. Kindo and M. Hagiwara, J. Phys. Soc. Jpn. **94**, 024701 (2025).

20. †Continuously evolving antiferromagnetic order within the superconducting phase in Zn-doped $CeCoIn_5$: K. Inoh, R. Koizumi, T. Takahashi, H. Fujimoto, H. Ebisawa, A. Yashiro, M. Kohinata, A. Hosogai, A. Matsuo, K. Kindo, I. Kawasaki, D. Okuyama, H.-C. Wu, T. J. Sato, K. Tenya, K. Ohoyama, K. Iwasa and M. Yokoyama, Phys. Rev. B **111**, 104510 (2025).

21. ∗Properties of an organic model S=1 Haldane chain system: I. Jakovac, T. Cvitanic, D. Arcon, M. Herak, D. Cincic, N. B. Topic, Y. Hosokoshi, T. Ono, K. Iwashita, N. Hayashi, N. Amaya, A. Matsuo, K. Kindo, I. Loncaric, M. Horvatic, M. Takigawa and M. S. Grbic, Phys. Rev. B **111**, 064407 (2025).

22. †Piezoelectric Transition in a Nonpyroelectric Gyroidal Metal–Organic Framework: S. Kitou, H. Ishikawa, Y. Tokunaga, M. Ueno, H. Sawa, Y. Nakamura, Y. Kinoshita, T. Miyamoto, H. Okamoto, K. Kindo and T.-H. Arima, J. Am. Chem. Soc. **147**, 13642 (2025).

23. Frustrated Magnetism in a Gyroidal Metal–Organic Framework Magnet: S. Imajo, H. Ishikawa, K. Kindo, K. Nakashima, R. Suizu and K. Awaga, Chem. Mater. **37**, 297 (2025).

24. †Possible field-induced quantum state in a rhombic lattice antiferromagnet $KCoPO_4 \cdot H_2O$: M. Fujihala, M. Hagihala, A. Koda, J. G. Nakamura, A. Matsuo, K. Kindo and M. Ishikado, Phys. Rev. Materials **9**, 014406 (2025).

Tokunaga group

Magnetization measurements in pulsed magnetic fields up to 66 T in a honeycomb lattice antiferromagnet $Fe_2Mo_3O_8$ with strong Ising magnetic anisotropy revealed a six-step magnetization plateau. The results of electric polarization measurements also showed plateaus corresponding to the magnetization process. We successfully reproduce these plateaus in a model that includes the interaction between the second-nearest neighbor spins.

1. †Edge and Bulk States in Weyl-Orbit Quantum Hall Effect as Studied by Corbino Measurements: Y. Nakazawa, R. Kurihara, M. Miyazawa, S. Nishihaya, M. Kriener, M. Tokunaga, M. Kawasaki and M. Uchida, J. Phys. Soc. Jpn. **93**, 023706/1-5 (2024).

2. ∗Dimerization-enhanced exotic magnetization plateau and magnetoelectric phase diagrams in skew-chain $Co_2V_2O_7$: Z. H. Li, X. T. Han, C. Dong, H. W. Wang, Z. Z. He, R. Chen, W. X. Liu, C. L. Lu, Y. Kohama, M. Tokunaga, K. Kindo, Z. W. Ouyang, J. F. Wang and M. Yang, Phys. Rev. B **109**, 094432 (2024).

3. Field-induced electric polarization and elastic softening caused by parity-mixed *d-p* hybridized states with electric multipoles in $Ba_2CuGe_2O_7$: R. Kurihara, Y. Sato, A. Miyake, M. Akaki, K. Mitsumoto, M. Hagiwara, H. Kuwahara and M. Tokunaga, Phys. Rev. B **109**, 125129/1-26 (2024).

4. Multiple magnetoelectric plateaus in the polar magnet $Fe_2Mo_3O_8$: Q. Chen, A. Miyake, T. Kurumaji, K. Matsuura, F. Kagawa, S. Miyahara, Y. Tokura and M. Tokunaga, Phys. Rev. B **109**, 094419//1-7 (2024).

5. Pressure-induced quantum melting of chiral spin order and subsequent transition to a degenerate semiconductor state in FeGe: Y. Fujishiro, C. Terakura, A. Miyake, N. Kanazawa, K. Nakazawa, N. Ogawa, H. Kadobayashi, S. Kawaguchi, T. Kagayama, M. Tokunaga, Y. Kato, Y. Motome, K. Shimizu and Y. Tokura, Phys. Rev. B **110**, L220401/1-7 (2024).

6. Realization of nodal-ring semimetal in pressurized black phosphorus: K. Akiba, Y. Akahama, M. Tokunaga and T. C. Kobayashi, Phys. Rev. B **109**, L201103/1-6 (2024).

7. Microwave Hall measurements using a circularly polarized dielectric cavity: M. Roppongi, T. Arakawa, Y. Yoshino, K. Ishihara, Y. Kinoshita, M. Tokunaga, Y. Matsuda, K. Hashimoto and T. Shibauchi, Rev. Sci. Instrum. **95**, 124704/1-11 (2024).

8. †Emergent Spin-Gapped Magnetization Plateaus in a Spin-1/2 Perfect Kagome Antiferromagnet: S. Suetsugu, T. Asaba, Y. Kasahara, Y. Kohsaka, K. Totsuka, B. Li, Y. Zhao, Y. Li, M. Tokunaga and Y. Matsuda, Phys. Rev. Lett. **132**, 226701/1-6 (2024).

9. ∗Quantum Liquid States of Spin Solitons in a Ferroelectric Spin-Peierls State: S. Imajo, A. Miyake, R. Kurihara, M. Tokunaga, K. Kindo, S. Horiuchi and F. Kagawa, Phys. Rev. Lett. **132**, 096601/1-6 (2024).

10. †Synthesis and High-Field Magnetic Measurement of $Ba_2Sn_{2+x}Me_{1+x}Fe_{10-2x}O_{22}$: H. Harasawa, H. Mitamura, M. Tokunaga, K. Kakizaki and K. Kamishima, J. Magn. Soc. Jpn. **48**, 88/1-6 (2024).

11. Nernst Effect of High-Mobility Weyl Electrons in NdAlSi Enhanced by a Fermi Surface Nesting Instability: R. Yamada, T. Nomoto, A. Miyake, T. Terakawa, A. Kikkawa, R. Arita, M. Tokunaga, Y. Taguchi, Y. Tokura and M. Hirschberger, Phys. Rev. X **14**, 021012/1-12 (2024).

12. †Magnetic properties and magnetocaloric effect of $DyCo_9Si_4$: N. Tsujii, A. Miyake, M. Tokunaga, J. Valenta and H. Sakurai, Journal of Alloys and Compounds **980**, 173653/1-7 (2024).

13. Novel anisotropy of upper critical fields in $Fe_{1+y}Te_{0.6}Se_{0.4}$: Y. Pan, Y. Sun, N. Zhou, X. Yi, Q. Hou, J. Wang, Z. Zhu, H. Mitamura, M. Tokunaga and Z. Shi, Journal of Alloys and Compounds **976**, 173262/1-6 (2024).

14. †Higher order exchange driven noncoplanar magnetic state and large anomalous Hall effects in electron doped kagome magnet Mn_3Sn: C. Singh, S. Jamaluddin, S. Pradhan, A. K. Nandy, M. Tokunaga, M. Avdeev and A. K. Nayak, npj Quantum Mater. **9**, 43/1-10 (2024).

15. †High-field immiscibility of electrons belonging to adjacent twinned bismuth crystals: Y. Ye, A. Yamada, Y. Kinoshita, J. Wang, P. Nie, L. Xu, H. Zuo, M. Tokunaga, N. Harrison, R. D. McDonald, A. V. Suslov, A. Ardavan, M.-S. Nam, D. LeBoeuf, C. Proust, B. Fauque´, Y. Fuseya, Z. Zhu and K. Behnia, npj Quantum Mater. **9**, 12/1-9 (2024).

16. Effects of strain-tunable valleys on charge transport in bismuth: S. Hosoi, F. Tachibana, M. Sakaguchi, K. Ishida, M. Shimozawa, K. Izawa, Y. Fuseya, Y. Kinoshita and M. Tokunaga, Phys. Rev. Research **6**, 033096/1-12 (2024).

17. †Observation of nonvolatile magneto-thermal switching in superconductors: H. Arima, Md. Riad Kasem, H. Sepehri-Amin, F. Ando, K.-I. Uchida, Y. Kinoshita, M. Tokunaga and Y. Mizuguchi, Commun Mater **5**, 34/1-8 (2024).

18. †Peculiar magnetotransport properties in epitaxially stabilized orthorhombic Ru^{3+} perovskite $LaRuO_3$ and $NdRuO_3$: L. Zhang, T. C. Fujita, Y. Masutake, M. Kawamura, T.-H. Arima, H. Kumigashira, M. Tokunaga and M. Kawasaki, Commun Mater **5**, 35/1-8 (2024).

19. Insulating Behavior in the Quantum Limit State of $Bi_{1-x}Sb_x$ ($x \sim 0.04$) in the Vicinity of Semimetal–Semiconductor Transition: Y. Yamaguchi, T. Fujita, Y. Kinoshita, A. Yamada, A. Miyake, R. Hiraoka, T. D. Matsuda, R. Ninohira, R. Kurihara, H. Yaguchi, Y. Fuseya and M. Tokunaga, J. Phys. Soc. Jpn. **94**, 043701/1-5 (2025).

20. †Removal of excess iron by annealing processes and emergence of bulk superconductivity in sulfur-substituted FeTe: R. Kurihara, R. Kogure, T. Ota, Y. Kinoshita, S. Hakamada, M. Tokunaga and H. Yaguchi, Phys. Rev. Materials **9**, 034802/1-12 (2025).

21. †Metamagnetic transition behaviors and dissipation energy at low temperatures of (Ni–Co)50–Mn–Sn alloys under pulsed high magnetic fields: T. Miyakawa, A. Miyake, X. Xu, T. Omori, M. Tokunaga and R. Kainuma, Materials Letters **382**, 137888/1-3 (2025).

22. †Polarization Change via Spin Crossover and Valence Tautomerism Behavior in [FeGa] Complexes: Q. Shui, S. -Q. Wu, W. Zheng, X. Zhang, Z. Zhou, M. Kondo, M. Tokunaga, R. Shimada, A. Sakamoto, S. Kanegawa, S. -Q. Su and O. Sato, CCS Chem **7**, 1 (2025), accepted for publication.

Y. Matsuda group

We have studied the magnetic field-induced phase transitions in several intriguing magnetic materials, $LaCoO_3$, $Ho_2Ti_2O_7$, $Pr_2Zr_2O_7$, and a layered, spin- 1/2 organic-inorganic copper sulfate. Also, we have investigated the strong anisotropic magnetization process in a potential permanent magnet, $SmCo_4B$. In addition to the compounds mentioned above, several materials, including a ferroelectric material, transition metal intermetallic compounds, and organic solids, have been studied by several techniques such as the dielectric constant measurement, electric impedance measurement, magnetostriction measurement, and streak camera spectroscopy. The aim of the recent research of our group is to explore the unique non-perturbative magnetic field effect (NPME) in ultrahigh magnetic fields exceeding 100 T. One of the typical NPMEs is the field-induced crystal structural change, which should be interpreted as the modification of the chemical bond in a solid in some sense. The strong spin-lattice coupling is the key physical parameter and can lead to the discovery of novel crystals appear only in an ultrahigh magnetic field.

1. A Review on Magnetic Field Induced Spin Crossover in $LaCoO_3$ up to 600 T: A. Ikeda, Y. H. Matsuda, K. Sato and J. Nasu, J. Phys. Soc. Jpn. **93**, 121005 (13 pages) (2024).

2. †*Crystal field magnetostriction of spin ice under ultrahigh magnetic fields: N. Tang, M. Gen, M. Rotter, H. Man, K. Matsuhira, A. Matsuo, K. Kindo, A. Ikeda, Y. H. Matsuda, P. Gegenwart, S. Nakatsuji and Y. Kohama, Phys. Rev. B **110**, 214414 (1-10) (2024).

3. †*Geometric frustration and Dzyaloshinskii-Moriya interactions in a quantum star lattice hybrid copper sulfate: H. Ishikawa, Y. Ishii, T. Yajima, Y. H. Matsuda, K. Kindo, Y. Shimizu, I. Rousochatzakis, U. K. Ro¨ßler and O. Janson, Phys. Rev. B **109**, L180401 (2024).

4. Development of techniques for the dielectric constant measurement in matter in ultrahigh magnetic fields exceeding 100thinsp;T: P. Chiu, Y. Ishii and Y. H. Matsuda, J. Appl. Phys. **137**, 155903 1-7 (2025).

5. †*Polarization Switching from Valence Trapping in an Oxo-Bridged Trinuclear Iron Complex: W.-H. Xu, S.-Q. Wu, S.-Q. Su, Y.-B. Huang, W. Zheng, X. Zhang, T. Ji, K. Gao, X.-G. Zhou, S. Peng, Q. Chen, M. Tokunaga, Y. H. Matsuda, A. Okazawa and O. Sato, J. Am. Chem. Soc. **147**, 5051-5059 (2025).

6. Experimental and Numerical Studies of the Collapse of Dense Clouds Induced by Herbig–Haro Stellar Jets: M. Fontaine, C. Busschaert, Y. Benkadoum, I. A. Bertrix, M. Koenig, F. Lefe`vre, J.-R. Marque`s, D. Oportus, A. Ikeda, Y. H. Matsuda, &. Falize and B. Albertazzi, ApJ **981**, 172 (8pages) (2025).

7. The Potential of $SmC_{o4}B$-Based Compounds as a Permanent Magnet: P. Tozman, A. Aubert, K. Skokov, H. Sepehri-Amin, Y. Skourski, Y. Ishii, Y. H. Matsuda and O. Gutfleisch, in: *2024 IEEE International Magnetic Conference - Short papers (INTERMAG Short papers)* (IEEE, 2024), 2 pages.

Kohama group

We have investigated high-field properties on several compounds. In itinerant systems, such as CeCoSi and YbB_{12}, the field-induced anomalies have been investigated by calorimetry and magnetic transport experiments using non-destructive pulsed magnetic fields. Here we also collaborated with the Grenoble high-field laboratory and IMR. In magnetic materials, we have investigated the spin-lattice coupling in destructive pulsed fields. We have also developed the Jc measurement technique in pulsed fields for the application to the applied superconductivity.

1. †*Spin–Lattice-Coupled Helical Magnetic Order in Breathing Pyrochlore Magnets, $CuAlCr_4S_8$ and $CuGaCr_4S_8$: M. Gen, T. Nakajima, H. Saito, Y. Tokunaga and T.-H. Arima, J. Phys. Soc. Jpn. **93**, 104602 (2024).

2. Analytical model for a hydrogen atom in a magnetic field: Implications for the diamagnetic shift: D. K. Maude, P. Plochocka and Z. Yang, Phys. Rev. B **109**, 155201 (2024).

3. †*Crystal field magnetostriction of spin ice under ultrahigh magnetic fields: N. Tang, M. Gen, M. Rotter, H. Man, K. Matsuhira, A. Matsuo, K. Kindo, A. Ikeda, Y. H. Matsuda, P. Gegenwart, S. Nakatsuji and Y. Kohama, Phys. Rev. B **110**, 214414 (1-10) (2024).

4. *Dimerization-enhanced exotic magnetization plateau and magnetoelectric phase diagrams in skew-chain $Co_2V_2O_7$: Z. H. Li, X. T. Han, C. Dong, H. W. Wang, Z. Z. He, R. Chen, W. X. Liu, C. L. Lu, Y. Kohama, M. Tokunaga, K. Kindo, Z. W. Ouyang, J. F. Wang and M. Yang, Phys. Rev. B **109**, 094432 (2024).

5. *Magnetic anisotropy of CeCoSi under high magnetic field: T. Kanda, H. Ishikawa, S. Imajo, K. Kindo, H. Tanida and Y. Kohama, Phys. Rev. B **109**, 174402 (2024).

6. Characterization of In-Field Critical Currents in REBCO Tapes Over Wide Temperature Range by Pulsed Current Source With Supercapacitor: Y. Tsuchiya, K. Mizuno, Y. Kohama, A. Zampa, T. Okada and S. Awaji, IEEE Trans. Appl. Supercond. **34**, 1 (2024).

7. Evidence for large thermodynamic signatures of in-gap fermionic quasiparticle states in a Kondo insulator: Z. Yang, C. Marcenat, S. Kim, S. Imajo, M. Kimata, T. Nomura, A. Muer, D. K. Maude, F. Iga, T. Klein, D. Chowdhury and Y. Kohama, Nature Communications **15**, 7801 (2024).

8. Magnetic Field Effect on Spin-Polarized Excitons in Two-Dimensional Cesium Lead Bromide Perovskites: R. Huang, J. Hu, Z. Yang, Y. Kohama, X. Zhang, X. Zhu, H. Zuo, J. Zou, T. Peng, L. Li, G. Xu and Y. Han, ACS Photonics **11**, 3160 (2024).

9. Triangular Lattice Magnet $GdGa_2$ with Short-Period Spin Cycloids and Possible Skyrmion Phases: P. R. Baral, N. D. Khanh, M. Gen, H. Sagayama, H. Nakao, T.-H. Arima, Y. Onuki, Y. Tokura and M. Hirschberger, J. Phys. Soc. Jpn. **94**, 024705 (2025).

10. Incommensurate broken helix induced by nonstoichiometry in the axion insulator candidate $EuIn_2As_2$: M. Gen, Y. Fujishiro, K. Okigami, S. Hayami, M. T. Birch, K. Adachi, D. Hashizume, T. Kurumaji, H. Sagayama, H. Nakao, Y. Tokura and T.-H. Arima, Phys. Rev. B **111**, L081109 (2025).

11. Magnetization process of a quasi-two-dimensional quantum magnet: Two-step symmetry restoration and dimensional reduction: A. Reinold, L. Berger, M. Raczkowski, Z. Zhao, Y. Kohama, M. Gen, D. I. Gorbunov, Y. Skourski, S. Zherlitsyn, F. F. Assaad, T. Lorenz and Z. Wang, Phys. Rev. B **111**, L100405 (2025).

12. Critical Current Evaluation of REBCO Tapes across Entire Temperatures and Magnetic Fields up to 25 T Using a 5 kA Pulsed Current Supply: Y. Tsuchiya, K. Mizuno, Y. Kohama and S. Awaji, IEEE Trans. Appl. Supercond. **N/A**, 1 (2025).

13. Canted antiferromagnetism in a spin-orbit coupled Seffnbsp;=nbsp;3/2 triangular-lattice magnet DyAuGe: T. Kurumaji, M. Gen, S. Kitou, K. Ikeuchi, H. Sagayama, H. Nakao, T. R. Yokoo and T.-H. Arima, Nat Commun **16**, 2176 (2025).

14. Probing and manipulating the Mexican hat-shaped valence band of In_2Se_3: J. Felton, J. Harknett, J. Page, Z. Yang, N. Alghofaili, J. N. O'Shea, L. Eaves, Y. Kohama, M. T. Greenaway and A. Patane`, Nat Commun **16**, 922 (2025).

15. *Zero-field Hall effect emerging from a non-Fermi liquid in a collinear antiferromagnet $V_{1/3}NbS_2$: M. K. Ray, M. Fu, Y. Chen, T. Chen, T. Nomoto, S. Sakai, M. Kitatani, M. Hirayama, S. Imajo, T. Tomita, A. Sakai, D. Nishio-Hamane, G. T. McCandless, M.-T. Suzuki, Z. Xu, Y. Zhao, T. Fennell, Y. Kohama, J. Y. Chan, R. Arita, C. Broholm and S. Nakatsuji, Nat Commun **16**, 3532 (2025).

Miyata group

We have worked on magneto-optical experiments under pulsed magnetic fields to search for exotic magneto-optical phenomena in antiferromagnets (especially, van der Waals antiferromagnets). The magnetoelectric material $LiNi_PO_4$ has complex magnetic exchange interactions, leading to a sequence of magnetic phase transitions in high magnetic fields. Our pulsed field experiments revealed that $LiNiPO_4$ exhibits complex linear dichroism (LD) and directional dichroism (DD), arising from low magnetic symmetries induced by high magnetic fields. The vdW antiferromagnet NiI_2 is the first known candidate to show multiferroicity even at the atomic layer scale. It also shows magnetic excitons that are strongly coupled to its magnetic structure. Our experiments demonstrated that the magnetic exciton shows a shoulder-like structure between 20-30 T and undergoes a significant shift above 30 T due to magnetic phase transitions.

1. Magnon-phonon interactions in the spinel compound $MnSc_2Se_4$: J. Sourd, Y. Skourski, L. Prodan, V. Tsurkan, A. Miyata, J. Wosnitza and S. Zherlitsyn, Phys. Rev. B **110**, 094414 (2024).

Center of Computational Materials Science

Misawa group

We have developed numerical methods and software packages for strongly correlated electron systems. We have updated HΦ (software for exact diagonalization), many-variable variational Monte Carlo method (mVMC), and released H-wave (software for Hartree-Fock calculations and random phase approximations). Using these software packages, we have performed ab initio calculations for molecular solids, and a variational Monte Carlo study for the Kondo lattice model on a triangular lattice.

1. †Many-body Chern insulator in the Kondo lattice model on a triangular lattice: K. Ido and T. Misawa, Phys. Rev. B **109**, 245114(1-6) (2024).
2. †Monte Carlo study on low-temperature phase diagrams of the J_1-J_2 classical XY kagome antiferromagnet: F. Kakizawa, T. Misawa and H. Shinaoka, Phys. Rev. B **109**, 014439(1-15) (2024).
3. †*Compensated Ferrimagnets with Colossal Spin Splitting in Organic Compounds: T. Kawamura, K. Yoshimi, K. Hashimoto, A. Kobayashi and T. Misawa, Phys. Rev. Lett. **132**, 156502(1-6) (2024).
4. †*H-wave – A Python package for the Hartree-Fock approximation and the random phase approximation: T. Aoyama, K. Yoshimi, K. Ido, Y. Motoyama, T. Kawamura, T. Misawa, T. Kato and A. Kobayashi, Computer Physics Communications **298**, 109087(1-10) (2024).
5. †*Combined x-ray diffraction, electrical resistivity, and *ab initio* study of $(TMTTF)_2PF_6$ under pressure: Implications for the unified phase diagram: M. Itoi, K. Yoshimi, H. Ma, T. Misawa, T. Tsumuraya, D. Bhoi, T. Komatsu, H. Mori, Y. Uwatoko and H. Seo, Phys. Rev. Research **6**, 043308 (1-14) (2024).
6. †*Update of HΦ : Newly added functions and methods in versions 2 and 3: K. Ido, M. Kawamura, Y. Motoyama, K. Yoshimi, Y. Yamaji, S. Todo, N. Kawashima and T. Misawa, Comp. Phys. Commun. **298**, 109093(1-15) (2024).
7. †Spin Seebeck Effect as a Probe for Majorana Fermions in Kitaev Spin Liquids: Y. Kato, J. Nasu, T. Okubo, T. Misawa and Y. Motome, Phys. Rev. X **15**, 011050(1-18) (2025).

Inui group

We advanced an automatic-differentiation–driven inverse-design platform for quantum-material functionalities. The major achievements in 2024 are (1) optimizing disorder landscapes in mesoscopic conductors to precisely reproduce target magnetotransport responses, and (2) designing spin-exchange Hamiltonians that maximize many-body entanglement, naturally yielding quantum-spin-liquid ground states. These results showcase computation-guided inverse design as a versatile route to engineer electronic and magnetic properties from the nanoscale upward.

1. Inverse magnetoconductance design by automatic differentiation: Y. Hirasaki, K. Inui and E. Saitoh, Phys. Rev. B **110**, 214201 (2024).
2. Inverse Hamiltonian design of highly entangled quantum systems: K. Inui and Y. Motome, Phys. Rev. Research **6**, 033080 (2024).

Laser and Synchrotron Research Center

Kobayashi group

Laser Development and cyber physical system

1. *Spin-polarized saddle points in the topological surface states of elemental bismuth revealed by pump-probe spin- and angle-resolved photoemission spectroscopy: Y. Fukushima, K. Kawaguchi, K. Kuroda, M. Ochi, M. Hirayama, R. Mori, H. Tanaka, A. Harasawa, T. Iimori, Z. Zhao, S. Tani, K. Yaji, S. Shin, F. Komori, Y. Kobayashi and T. Kondo, Phys. Rev. B **110**, L041401 (2024).
2. *Anomalous Hall Transport by Optically Injected Isospin Degree of Freedom in Dirac Semimetal Thin Film: Y. Murotani, N. Kanda, T. Fujimoto, T. Matsuda, M. Goyal, J. Yoshinobu, Y. Kobayashi, T. Oka, S. Stemmer and R. Matsunaga, Nano Lett. **24**, 222 (2024).
3. Sub-10-fs pulse generation from 10 nJ Yb-fiber laser with cascaded nonlinear pulse compression: D. Kang, T. Otsu, S. Tani and Y. Kobayashi, Opt. Express **32**, 5214 (2024).

4. †*Comprehensive study of the luminescence properties of elemental metals: T. Suemoto, S. Ono, A. Asahara, T. Okuno, T. Suzuki, K. Okazaki, S. Tani and Y. Kobayash, Phys. Rev. B **1114**, 035150 (2025).

5. *Portable laser diode module of sub-10 ps gain-switched pulse source at 1030 nm wavelength: M. Kobayashi, H. Nakamae, C. Kim, T. Nakamura, T. Ito, S. Chen, Y. Kobayashi and H. Akiyama, Jpn. J. Appl. Phys. **64**, 038004 (2025).

6. Monolithic Er:YAG ceramic waveguide laser fabricated by femtosecond direct laser writing: T. Sumiya, S. Tani, A. Tsunoda, M. Nakazaki and Y. Kobayashi, Opt. Express **33**, 10047 (2025).

Harada group

In 2024, we utilized soft X-ray absorption (XAS) and resonant emission spectroscopy (RXES) to investigate advanced materials for energy storage and the behavior of water in confined environments. We elucidated the charge compensation mechanisms in layered oxyfluorides and oxyfluorosulfides for fluoride-ion batteries, revealing anion redox processes that enable high capacities of 200-340 mAh/g. The XES studies on water structure yielded insights into hydrogen bonding configurations in various systems, including polymer interfaces, nanochannels, and zwitterionic block copolymers. We correlated these molecular-level water structures to macroscopic properties such as biocompatibility and material functionality. The oxygen K-edge XES measurements on metal-organic frameworks revealed the electronic perturbations driving structural breathing transitions through carboxylate oxygen lone pair orbital reconfigurations. To enhance our analytical capabilities, we implemented a sophisticated rotation mechanism to the X-ray emission spectrometer that enables flexible scattering angle adjustments between 45-135^{o}. This advancement streamlines angle-resolved XES measurements and expands it's versatility to include diffraction experiments.

1. †Double-Layered Perovskite Oxyfluoride Cathodes with High Capacity Involving O–O Bond Formation for Fluoride-Ion Batteries: H. Miki, K. Yamamoto, H. Nakaki, T. Yoshinari, K. Nakanishi, S. Nakanishi, H. Iba, J. Miyawaki, Y. Harada, A. Kuwabara, Y. Wang, T. Watanabe, T. Matsunaga, K. Maeda, H. Kageyama and Y. Uchimoto, J. Am. Chem. Soc. **146**, 3844-3853 (2024).

2. †Pronounced Cold Crystallization and Hydrogen Bonding Distortion of Water Confined in Microphases of Double Zwitterionic Block Copolymer Aqueous Solutions: Y. Higaki, T. Masuda, S. Shiomoto, Y. Tanaka, H. Kiuchi, Y. Harada and M. Tanaka, Langmuir **40**, 19612-19618 (2024).

3. †Revealing the Unusual Mechanism of Mixed Cationic and Anionic Redox in Oxyfluorosulfide Cathode for All-Solid-State Fluoride-Ion Batteries: Z. Cao, K. Yamamoto, T. Matsunaga, T. Watanabe, M. Kumar, N. Thakur, R. Ohashi, S. Tachibana, H. Miki, K. Ide, H. Iba, H. Kiuchi, Y. Harada, Y. Orikasa and Y. Uchimoto, Chem. Mater. **36**, 1928-1940 (2024).

4. *Enhancement of high harmonic generation in liquid water by resonant excitation in the mid-infrared: T. Yang, T. Kurihara, Y. Hua, T. Mizuno, T. Kanai, S. Ashihara, Y. Harada and J. Itatani, Appl. Phys. Express **17**, 122006 1-5 (2024).

5. †Hydrogen-Bonded Structures of Water Molecules in Hydroxy-Functionalized Nanochannels of Columnar Liquid Crystalline Nanostructured Membranes Studied by Soft X-ray Emission Spectroscopy: K. Hamaguchi, T. Sakamoto, N. Kurahashi, Y. Harada and T. Kato, J. Phys. Chem. Lett. **15**, 454-460 (2024).

6. †Effects of hydration water on bioresponsiveness of polymer interfaces revealed by analysis of linear and cyclic polymer-grafted substrates: S.-N. Nishimura, N. Kurahashi, S. Shiomoto, Y. Harada and M. Tanaka, Soft Matter **20**, 9454-9463 (2024).

7. †Hydrogen-bonded structure of hydrated water in polyvinyl pyrrolidone aqueous solution investigated by X-ray absorption and emission spectroscopy: K. Ozaki, M. Nakada, M. Kunisu, J. Yahiro, K. Yamazoe, Y. Cui, J. Miyawaki and Y. Harada, Journal of Molecular Liquids **403**, 124822 1-6 (2024).

8. †Angle-resolved X-ray emission spectroscopy facility realized by an innovative spectrometer rotation mechanism at SPring-8 BL07LSU: J. Miyawaki, Y. Kosegawa and Y. Harada, J Synchrotron Rad **31**, 208-216 (2024).

9. †The role of carboxylate ligand orbitals in the breathing dynamics of a metal-organic framework by resonant X-ray emission spectroscopy: R. Ugalino, K. Yamazoe, J. Miyawaki, H. Kiuchi, N. Kurahashi, Y. Kosegawa and Y. Harada, J Synchrotron Rad **31**, 217-221 (2024).

10. Structural analysis of nano-water droplets: A molecular dynamics study: N. Shima, Y. Harada and O. Takahashi, Chemical Physics Letters **852**, 141521 1-5 (2024).

11. †Soft X-ray Emission Spectroscopy of Hydrogen Bonding in Water and Its Application to *Operando* Analysis: Y. HARADA, Vac. Surf. Sci. **67**, 224-228 (2024).

12. †* 中赤外における水薄膜中異常伝搬の第二高調波による観測: 栗原 貴之, 華洋 陽, 楊添 淇, 水野 智也, 原田 慈久, 板谷 治郎, 応用物理学会フォトニクスニュース **10-2**, 53 (2024).

13. †*Chemical-state imaging of a mammalian cell through multi-elemental soft x-ray spectro-ptychography: K. Sakurai, Y. Takeo, S. Takaramoto, N. Furuya, K. Yoshinaga, T. Shimamura, J. T. O'Neal, Y. Nakata, S. Egawa, K. Yoshimi, H. Ohashi, H. Mimura, Y. Harada, K. Inoue, M. Shimura and T. Kimura, Appl. Phys. Lett. **126**, 043702(1-7) (2025).

14. †Cathode Design Based on Nitrogen Redox and Linear Coordination of Cu Center for All-Solid-State Fluoride-Ion Batteries: D. Zhang, K. Yamamoto, Z. Cao, Y. Wang, Z. Zhong, H. Kiuchi, T. Watanabe, T. Matsunaga, K. Nakanishi, H. Miki, H. Iba, Y. Harada, K. Amezawa, K. Maeda, H. Kageyama and Y. Uchimoto, J. Am. Chem. Soc. **147**, 5649–5657 (2025).

15. †High Oxygen Storage Capacity of Ultrasmall Mn-Doped CeO_2 Nanoparticles via Enhanced Local Distortion and Mn(II) Lattice Substitution: C. Han, A. Yoko, A. Taufik, S. Ohara, M. Nishibori, K. Ninomiya, H. Kiuchi, Y. Harada and T. Adschiri, Chem. Mater. **37**, 1205-1214 (2025).

16. †Elucidation of the Co^{4+} state with strong charge-transfer effects in charged $LiCoO_2$ by resonant soft X-ray emission spectroscopy at the Co L_3 edge: D. Asakura, T. Sudayama, Y. Nanba, E. Hosono, H. Kiuchi, K. Yamazoe, J. Miyawaki, Y. Harada, A. Yamada, R.-P. Wang and F. M. F. D. Groot, Phys. Chem. Chem. Phys. **27**, 4092-4098 (2025).

17. †Electronic structures of blue copper centers of amicyanin and azurin in the solution state: Y. Izumi, R. Ugalino, J. Miyawaki, C. Shibazaki, M. Adachi, N. Kurahashi, H. Kiuchi, Y. Harada and K. Fujii, Dalton Trans. **54**, 1980-1985 (2025).

18. Iron-complex-based catalytic system for high-performance water oxidation in aqueous media: T. Matsuzaki, K. Kosugi, H. Iwami, T. Kambe, H. Kiuchi, Y. Harada, D. Asakura, T. Uematsu, S. Kuwabata, Y. Saga, M. Kondo and S. Masaoka, Nat Commun **16**, 2145 1-11 (2025).

19. †Facet-dependent photocatalytic performance and electronic structure of single-crystalline anatase TiO_2 particles revealed by X-ray photoelectron spectromicroscopy: W. Zhang, M. A. Samarai, H. Zhao, D. Liu, H. Kiuchi, R. Ugalino, S. Li, F. Yao, Q. Feng and Y. Harada, J. Mater. Chem. C **13**, 61-67 (2025).

20. ∗Macroscopic Structural Transition of Nickel Dithiolate Capsule with Uniaxial Magnetic Anisotropy in Water: T. Fujino, M. Hishida, M. Ito, T. Nakamura, M. Asada, N. Kurahashi, H. Kiuchi, Y. Harada, K. Harano, R. Makiura, K. J. Takeno, S. Yokomori, H. Oike and H. Mori, Adv. Science (2025), accepted for publication.

I. Matsuda group

The new synchrotron radiation facility, NanoTerasu, was launched at Sendai in Miyagi-prefecture and we started the user operation with our end-stations at the soft X-ray beamline BL08U. At the station of ambient-pressure X-ray spectroscopy, we have made experiments with users on gas/solid interfaces of various materials, such as model catalysts. We have also upgraded the instrument and succeeded in measuring soft X-ray photoelectron spectra at the real ambient pressure condition (1 bar). The achievement is for the first time in human history and it has opened the real operando experiments on the real functional materials. At the station of X-ray spectromicroscopy, two-dimensional scan of X-ray absorption spectroscopy can be performed with automatic controls. The system has continuously been developed as the autonomous robot system with process-informatics.

Our group has conducted synthesis of the boron materials by the film growth and the subsequent chemical exfoliations. On copper crystal surface, we have discovered one-dimensional (1-D) structure with quasi-periodicity. We have also succeeded in growing millimeter-sized crystals of 3-D metal boride and 2-D hydrogen boride. These novel materials are expected to provide various functionalities that will be useful in our society.

1. Phase stability and band degeneracy of quasi-one-dimensional boron chain polymorphs embedded in LiB crystals: T. Nakashima, I. Tateishi, Y. Tsujikawa, M. Horio, T. Kondo, I. Matsuda and Y. Ando, Phys. Rev. B **109**, 165104 (2024).

2. Evolution from ultrafast demagnetization to magnetization reversal at the Fe sites in $Gd_{23}Fe_{67}Co_{10}$ with laser fluence, observed by the element-selective magneto-optical Kerr effect using an X-ray free electron laser: S. E. Moussaoui, T. Sumi, T. Senoo, Y. Hirata, K. Yamamoto, H. Yoshikawa, M. Horio, Y. Kubota, S. Owada, H. Wadati, M. Yabashi, A. Tsukamoto and I. Matsuda, Jpn. J. Appl. Phys. **63**, 09SP25 (2024).

3. Pioneering preparation and analysis of a clean surface on a microcrystal, mined by a focused ion beam: Y. Guan, F. Komori, M. Horio, A. Fukuda, Y. Tsujikawa, K. Ozawa, M. Kamiko, D. Nishio-Hamane, T. Kawauchi, K. Fukutani, Y. Tokumoto, K. Edagawa, R. Tamura and I. Matsuda, Jpn. J. Appl. Phys. **63**, 030906 (2024).

4. †*Quasi-Periodic Growth of One-Dimensional Copper Boride on Cu(110): Y. Tsujikawa, X. Zhang, K. Yamaguchi, M. Haze, T. Nakashima, A. Varadwaj, Y. Sato, M. Horio, Y. Hasegawa, F. Komori, M. Oshikawa, M. Kotsugi, Y. Ando, T. Kondo and I. Matsuda, Nano Lett. **24**, 1160 (2024).

5. Fermi Edge of Semimetallic Borophane Sheets and its Reduction by a Porous Structure: X. Zhang, M. Miyamoto, M. Yuan, Y. Tsujikawa, K. Yamaguchi, M. Horio, K. Ozawa, K. Yubuta, T. Kondo and I. Matsuda, J. Phys. Chem. Lett. **15**, 9349-9355 (2024).

6. Interlayer Hydrogen Recombination from Hydrogen Boride Nanosheets Elucidated by Isotope Labeling: S.-I. Ito, K. I. M. Rojas, Y. Yasuda, N. Noguchi, K. Fukuda, M. Hikichi, Z. Kang, M. Yuan, R. Tsuji, O. Oki, S. Roy, Y. Hikita, I. Matsuda, M. Miyauchi, I. Hamada and T. Kondo, J. Phys. Chem. Lett. **15**, 10965-10976 (2024).

7. Adsorption of Atomic Hydrogen on Hydrogen Boride Sheets Studied by Photoelectron Spectroscopy: H. Yin, J. Tang, K. Yamaguchi, H. Sakurai, Y. Tsujikawa, M. Horio, T. Kondo and I. Matsuda, Materials **17**, 4806 (2024).

8. †*Dimensional crossover and chirality of boron adsorbates on copper (110) surfaces: Y. Tsujikawa, T. Nakashima, X. Zhang, K. Yamaguchi, M. Horio, M. Haze, Y. Hasegawa, F. Komori, T. Kondo, Y. Ando and I. Matsuda, Phys. Rev. Materials **8**, 084003 1-7 (2024).

9. *Macroscopic sheets of hydrogen boride and their spectroscopic evaluation: K. Yamaguchi, M. Niibe, X. Zhang, T. Sumi, M. Horio, Y. Ando, J.-I. Yamaura, E. Nakamura, K. Tanaka, T. Kondo and I. Matsuda, Phys. Rev. Materials **8**, 074005 (2024).

10. Millimeter-scale growth of $YCrB_4$ single crystals and observation of the metallic surface state: X. Zhang, Y. Tsujikawa, K. Yamaguchi, M. Miyamoto, M. Horio, K. Yubuta, H. Ando, M. Yuan, K. Ozawa, K. Sugiyama, T. Kondo and I. Matsuda, Phys. Rev. Materials **8**, 054001 (2024).

11. †Structure and Electronic State of Boron Atomic Chains on a Noble Metal (111) Surface: Y. Tsujikawa, X. Zhang, M. Horio, F. Komori, T. Nakashima, Y. Ando, T. Kondo and I. Matsuda, e-J. Surf. Sci. Nanotechnol. **22**, 1 (2024).

12. Non-equilibrium pathways to emergent polar supertextures: V. A. Stoica and I. Matsuda et al., Nat. Mater. **23**, 1394-1401 (2024).

13. *Fabrication of Microcrystals by Focused Ion Beam for Surface Analyses: F. KOMORI, Y. GUAN and I. MATSUDA, Vac. Surf. Sci. **67**, 340-346 (2024).

14. †**Operando* Observation of Hydrogenation of Carbon Dioxide by Near Ambient Pressure X-ray Photoelectron Spectroscopy: T. KOITAYA, S. YAMAMOTO, I. MATSUDA, J. YOSHINOBU and T. YOKOYAMA, Vac. Surf. Sci. **67**, 117-122 (2024).

15. Inhomogeneous reduction-annealing effects on the electron-doped cuprate superconductor $Pr_{1.3-x}La_{0.7}Ce_xCuO_4$ (x=0.08) revealed by microfocused angle-resolved photoemission spectroscopy: M. Miyamoto, M. Horio, K. Moriya, A. Takahashi, J. Osiecki, B. Thiagarajan, C. M. Polley, Y. Koike, T. Adachi, T. Mizokawa and I. Matsuda, Phys. Rev. B **111**, 125134 (2025).

16. *Evaluating chemical states in a single microcrystal of chromium boride with the micro-focused ion and quantum beams: Y. Guan, X. Zhang, M. Miyamoto, Y. Tsujikawa, K. Yubuta, M. Horio, H. Isshiki, J.-I. Yamaura, T. Abukawa, F. Komori and I. Matsuda, Solid State Sciences **161**, 107838 (2025).

17. Soft X-ray photoelectron spectroscopy under real ambient pressure conditions: T. Wada, M. Horio, Y. Liu, Y. Murano, H. Sakurai, T. Sumi, M. Miyamoto, S. Yamamoto and I. Matsuda, Appl. Phys. Express **18**, 036504 (2025).

18. *Surface structure of the 3x3-Si phase on Al(111), studied by the multiple usages of positron diffraction and core-level photoemission spectroscopy: Y. Sato, Y. Fukaya, A. Nakano, T. Hoshi, C.-C. Lee, K. Yoshimi, T. Ozaki, T. Nakashima, Y. Ando, H. Aoyama, T. Abukawa, Y. Tsujikawa, M. Horio, M. Niibe, F. Komori and I. Matsuda, Phys. Rev. Materials **9**, 014002 (2025).

19. Developing a Machine-Learning-based Robotic System for Mixing Solvents: J. Tang, T. Nakashima, M. Miyamoto, X. Zhang, M. Horio, Y. Ando and I. Matsuda, e-J. Surf. Sci. Nanotechnol. **23**, 59-64 (2025).

20. *Discovery of bicyclic borane molecule $B_{14}H_{26}$: X. Zhang, T. Fujino, Y. Ando, Y. Tsujikawa, T. Wang, T. Nakashima, H. Sakurai, K. Yamaguchi, M. Horio, H. Mori, J. Yoshinobu, T. Kondo and I. Matsuda, Commun Chem **8**, 14 (2025).

Itatani group

The enhancement of harmonic generation in thin water jets under intense mid-infrared excitation is found to be due to the creation of novel high temperature and high pressure state of water caused by resonant vibrational excitation and hydrogen bond perturbation. We have also experimentally clarified the superluminal propagation associated with strong resonant absorption in the 2.9-μm band. These experiments using a thin flat liquid jet demonstrate a new platform for attosecond experiments of condensed matter using intense laser fields. We have also started the development of a Cr:ZnSe solid-state laser amplifier to realize a high-intensity infrared source at 2 μm. We also started the development of a femtosecond VUV source with a repetition rate of 100 kHz at a photon energy of 11 eV for ultrafast angle-resolved photoemission spectroscopy.

1. †Subharmonic Lock-in Detection and Its Optimization for Femtosecond Noise Correlation Spectroscopy: M. A. Weiss, F. S. Herbst, S. Eggert, M. Nakajima, A. Leitenstorfer, S. T. B. Goennenwein and *T. Kurihara, Rev. Sci. Instrum. **95**, 083005 (2024).
2. *Time- and angle-resolved photoemission spectroscopy with wavelength-tunable pump and extreme ultraviolet probe enabled by twin synchronized amplifiers: T. Suzuki, Y. Zhong, K. Liu, T. Kanai, J. Itatani and K. Okazaki, Rev. Sci. Instrum. **95**, 073001 (2024).
3. †*Observation of Terahertz Spin Hall Conductivity Spectrum in GaAs with Optical Spin Injection: T. Fujimoto, T. Kurihara, Y. Murotani, T. Tamaya, N. Kanda, C. Kim, J. Yoshinobu, H. Akiyama, T. Kato and R. Matsunaga, Phys. Rev. Lett. **132**, 016301(1-7) (2024).
4. *Enhancement of high harmonic generation in liquid water by resonant excitation in the mid-infrared: T. Yang, T. Kurihara, Y. Hua, T. Mizuno, T. Kanai, S. Ashihara, Y. Harada and J. Itatani, Appl. Phys. Express **17**, 122006 1-5 (2024).
5. THz・中赤外光を用いた電子励起による磁気異方性の超高速制御: 栗原 貴之, まぐね **19-3**, - (2024).
6. Spin switching in $Sm_{0.7}Er_{0.3}FeO_3$ triggered by terahertz magnetic-field pulses: Z. Z. M. Kanega, K. Maruyama, T. Kurihara, M. Nakajima, T. Tachizaki, M. Sato, Y. Kanemitsu and H. Hirori, Nature Materials **24**, 219-225 (2024).
7. [コラム] アト秒科学: 板谷 治郎, 数理科学（特集 様々な視点で捉えなおすの概念） **732**, 38-39 (2024).
8. †* 中赤外における水薄膜中異常伝搬の第二高調波による観測: 栗原 貴之, 華洋 陽, 楊添 淇, 水野 智也, 原田 慈久, 板谷 治郎, 応用物理学会フォトニクスニュース **10-2**, 53 (2024).
9. †*Photo-induced Nonlinear Band Shift and Valence Transition in SmS,: Y. Chen, T. Nakamura, H. Watanabe, T. Suzuki, Q. Ren, K. Liu, Y. Zhong, T. Kanai, J. Itatani, K. Okazaki, H. S. Suzuki, S. Shin, K. Imura, N. K. Sato and S.-I. Kimura, J. Phys. Soc. Jpn. **94**, 013702-1-4 (2025).
10. *Light-induced inverse spin Hall effect and field-induced circular photogalvanic effect in GaAs revealed by two-dimensional terahertz Fourier analysis: T. Fujimoto, Y. Murotani, T. Tamaya, T. Kurihara, N. Kanda, C. Kim, J. Yoshinobu, H. Akiyama, T. Kato and R. Matsunaga, Phys. Rev. B **111**, L201201 (2025).
11. 2023 年ノーベル物理学賞：Pierre Agostini 氏, Ferenc Krausz 氏, Anne L'Huillier 氏 - 物質中の電子ダイナミクスを研究するためのアト秒パルス光の生成に関する実験的手法の業績（学界ニュース）: 板谷 治郎, 「日本物理学会誌」, 日本物理学会, (日本物理学会, 東京都文京区, 2024), 36.
12. 高繰り返しアト秒光源の開発とその応用（解説・「高次高調波とアト秒光科学の将来」特集）: 板谷治郎, 「月刊オプトロニクス」, 株式会社オプトロニクス社, (株式会社オプトロニクス社, 2024), 153-158.

Kondo group

We uncovered novel electronic phenomena in correlated and topological materials. Using ARPES, we demonstrated that Fermi surface nesting drives skyrmion formation in centrosymmetric Gd_2PdSi_3 and discovered anomalous Fermi pockets on the Hund's metal surface of Sr_2RuO_4 due to enhanced spin-orbit coupling. We also visualized symmetry-protected spin-polarized states in bismuth and identified gap features in Dirac semimetals. These studies deepen our understanding of nontrivial topological states, magnetic interactions, and quantum coherence, contributing broadly to the design of future spintronic and quantum materials.

1. *Spin-polarized saddle points in the topological surface states of elemental bismuth revealed by pump-probe spin- and angle-resolved photoemission spectroscopy: Y. Fukushima, K. Kawaguchi, K. Kuroda, M. Ochi, M. Hirayama, R. Mori, H. Tanaka, A. Harasawa, T. Iimori, Z. Zhao, S. Tani, K. Yaji, S. Shin, F. Komori, Y. Kobayashi and T. Kondo, Phys. Rev. B **110**, L041401 (2024).

2. ∗Broken Screw Rotational Symmetry in the Near-Surface Electronic Structure of *AB*-Stacked Crystals: H. Tanaka, S. Okazaki, M. Kobayashi, Y. Fukushima, Y. Arai, T. Iimori, M. Lippmaa, K. Yamagami, Y. Kotani, F. Komori, K. Kuroda, T. Sasagawa and T. Kondo, Phys. Rev. Lett. **132**, 136402 (1-6) (2024).

3. Anomalous Fermi pockets on the Hund's metal surface of $Sr_2Ru_2O_4$ induced by correlation-enhanced spin-orbit coupling.: T. Kondo, M. Ochi, S. Akebi, Y. Dong, H. Taniguchi, Y. Maeno and S. Shin, Physical Review B **109**, L241107 (2024).

4. ∗Photoemission angular distribution beyond the single wavevector description of photoelectron final states.: H. Tanaka, S. Okazaki, Y. Fukushima, K. Kawaguchi, A. Harasawa, T. Iimori, F. Komori, M. Arita, R. Mori, K. Kuroda, T. Sasagawa and T. Kondo, Physical Review B **109**, L241114 (2024).

5. Momentum-dependent scaling exponents of nodal self-energies measured in strange metal cuprates and modelled using semi-holography.: S. Smit, E. Mauri, L. Bawden, F. Heringa, F. Gerritsen, E. van Heumen, Y. K. Huang, T. Kondo, T. Takeuchi, N. E. Hussey, M. Allan, T. K. Kim, C. Cacho, A. Krikun, K. Schalm and H. T. C. Stoof & M. S. Golden, Nature Communications **15**, 4581 (2024).

6. Universal correlation between H-linear magnetoresistance and T-linear resistivity in high-temperature superconductors.: J. Ayres, M. Berben, C. Duffy, R. D. H. Hinlopen, Y. -T. Hsu, A. Cuoghi, M. Leroux, I. Gilmutdinov, M. Massoudzadegan, D. Vignolles, Y. Huang, T. Kondo, T. Takeuchi, S. Friedemann, A. Carrington, C. Proust and N. E. Hussey, Nature Communications **15**, 8406 (2024).

7. Topological and chiral matter—Physics and applications: M. G. Vergniory, T. Kondo, N. A. Kotov and A. A. Balandin, Applied Physics Letters **125**, 160401 (2024).

8. *Spontaneous Gap Opening and Potential Excitonic States in an Ideal Dirac Semimetal $Ta_2Pd_3Te_5$.: P. Zhang, Y. Dong, D. Yan, B. Jiang, T. Yang, J. Li, Z. Guo, Y. Huang, B. Hao, Q. Li, Y. Li, K. Kurokawa, R. Wang, Y. Nie, M. Hashimoto, D. Lu, W.-H. Jiao, J. Shen, T. Qian, Z. Wang, Y. Shi and T. Kondo, Physical Review X 14, 011047 **14**, 011047 (2024).

9. Fermi Surface Nesting Driving the RKKY Interaction in the Centrosymmetric Skyrmion Magnet Gd_2PdSi_3.: Y. Dong, Y. Arai, K. Kuroda, M. Ochi, N. Tanaka, Y. Wan, M. D. Watson, T. K. Kim, C. Cacho, M. Hashimoto, D. Lu, Y. Aoki, T. D. Matsuda and T. Kondo, Physical Review Letter **133**, 016401 (2024).

10. Robust Weak Topological Insulator in the Bismuth Halide $Bi_4Br_2I_2$.: R. Noguchi, M. Kobayashi, K. Kawaguchi, W. Yamamori, K. Aido, C. Lin, H. Tanaka, K. Kuroda, A. Harasawa, V. Kandyba, M. Cattelan, A. Barinov, M. Hashimoto, D. Lu, M. Ochi, T. Sasagawa and T. Kondo, Physical Review Letter **133**, 086602 (2024).

11. Moire´ superlattices of antimonene on a Bi(111) substrate with van Hove singularity and Rashba-type spin polarization.: T. Nakamura, Y. Chen, R. Nemoto, W. Qian, Y. Fukushima, K. Kawaguchi, R. Mori, T. Kondo, Y. Yamaji, S. Tsuda, K. Yaji and T. Uchihashi, Communications Materials **5**, 167 (2024).

12. ∗Emergence of high-mobility carriers in topological kagome bad metal Mn_3Sn by intense photoexcitation: T. Matsuda, T. Higo, K. Kuroda, T. Koretsune, N. Kanda, Y. Hirai, H. Peng, T. Matsuo, C. Bareille, A. Varykhalov, N. Yoshikawa, J. Yoshinobu, T. Kondo, R. Shimano, S. Nakatsuji and R. Matsunaga, Phys. Rev. Materials **9**, 014202 (2025).

Matsunaga group

We have studied light-matter interactions and light-induced nonequilibrium phenomena in solids by utilizing terahertz (THz) pulse. By using polarization-resolved THz spectroscopy and a semiconductor GaAs, we have reported the first observation of spin Hall conductivity spectrum of electrons. The frequency dependence of spin Hall conductivity exhibits an excellent quantitative agreement with theory, demonstrating a crossover in the dominant origin from impurity scattering in the dc regime to the intrinsic Berry-curvature mechanism in the terahertz regime. Our spectroscopic technique opens a new pathway to analyze anomalous transports. In addition, we successfully generated phase-stable counterrotating bicircular light pulses in the 14–39 THz frequency range. Use of the spatial light modulator enabled programmable control over the shape, orientation, rotational symmetry, and helicity of the bicircular light field trajectory. This advancement provides a novel pathway for the programmable manipulation of light fields.

1. †*Observation of Terahertz Spin Hall Conductivity Spectrum in GaAs with Optical Spin Injection: T. Fujimoto, T. Kurihara, Y. Murotani, T. Tamaya, N. Kanda, C. Kim, J. Yoshinobu, H. Akiyama, T. Kato and R. Matsunaga, Phys. Rev. Lett. **132**, 016301(1-7) (2024).

2. 3 次元ディラック半金属によるテラヘルツ高次高調波発生: 松永 隆佑, 神田 夏輝, 池田 達彦, 日本物理学会誌 **79**, 12 (2024).

3. *Ultra-broadband detection of coherent infrared pulses by sum-frequency generation spectroscopy in reflection geometry: R. Kameyama, S. Tanaka, Y. Murotani, T. Matsuda, N. Kanda, R. Matsunaga and J. Yoshinobu, Opt. Lett. **49**, 3978 (2024).

4. 光誘起異常ホール効果を解き明かすテラヘルツ偏光計測: 室谷悠太, 神田夏輝, 松永隆佑, 光アライアンス **35**, 44 (2024).

5. *Anomalous Hall Transport by Optically Injected Isospin Degree of Freedom in Dirac Semimetal Thin Film: Y. Murotani, N. Kanda, T. Fujimoto, T. Matsuda, M. Goyal, J. Yoshinobu, Y. Kobayashi, T. Oka, S. Stemmer and R. Matsunaga, Nano Lett. **24**, 222 (2024).

6. Time-domain characterization of electric field vector in multi-terahertz pulses using polarization-modulated electro-optic sampling: N. Kanda, M. Nakagawa, Y. Murotani and R. Matsunaga, Opt. Express **32**, 1576 (2024).

7. Programmable generation of counterrotating bicircular light pulses in the multi-terahertz frequency range: K. Ogawa, N. Kanda, Y. Murotani and R. Matsunaga, Nat Commun **15**, 6310 (2024).

8. *Light-induced inverse spin Hall effect and field-induced circular photogalvanic effect in GaAs revealed by two-dimensional terahertz Fourier analysis: T. Fujimoto, Y. Murotani, T. Tamaya, T. Kurihara, N. Kanda, C. Kim, J. Yoshinobu, H. Akiyama, T. Kato and R. Matsunaga, Phys. Rev. B **111**, L201201 (2025).

9. *Valley polarization dynamics of photoinjected carriers at the band edge in room-temperature silicon studied by terahertz polarimetry: A. M. Shirai, Y. Murotani, T. Fujimoto, N. Kanda, J. Yoshinobu and R. Matsunaga, Phys. Rev. B **111**, L121201 (2025).

10. *Robust asynchronous optical sampling terahertz spectroscopy using commercially available free-running lasers: M. Nakagawa, N. Kanda, H. Nakamae, H. Akiyama and R. Matsunaga, Opt. Express **33**, 23145 (2025).

11. *Emergence of high-mobility carriers in topological kagome bad metal Mn_3Sn by intense photoexcitation: T. Matsuda, T. Higo, K. Kuroda, T. Koretsune, N. Kanda, Y. Hirai, H. Peng, T. Matsuo, C. Bareille, A. Varykhalov, N. Yoshikawa, J. Yoshinobu, T. Kondo, R. Shimano, S. Nakatsuji and R. Matsunaga, Phys. Rev. Materials **9**, 014202 (2025).

Okazaki group

We have investigated superconducting gap structures of unconventional superconductors by a low-temperature and high-resolution laser ARPES apparatus, and transient electronic structures in photoexcited non-equilibrium states by a time-resolved ARPES apparatus using EUV and SX lasers. In the academic year 2024, we investigated the superconducting gap structure of the iron-based superconductor BaNaFeAs with a reentrant C_4 phase by high-resolution laser ARPES. In addition, we successfully observed a photoinduced modulation of the van Hove singularity in the kagome superconductor CsVSb by HHG laser time-resolved ARPES.

1. *Time- and angle-resolved photoemission spectroscopy with wavelength-tunable pump and extreme ultraviolet probe enabled by twin synchronized amplifiers: T. Suzuki, Y. Zhong, K. Liu, T. Kanai, J. Itatani and K. Okazaki, Rev. Sci. Instrum. **95**, 073001 (2024).

2. Ta_2NiSe_5 における高次高調波レーザー時間・角度分解光電子分光: 鈴木 剛, 岡崎 浩三, 溝川 貴司, 固体物理 **59**, 321 (2024).

3. Uniform Diffusion of Cooper Pairing Mediated by Hole Carriers in Topological Sb_2Te_3/Nb: J. A. Hlevyack, S. Najafzadeh, Y. Li, T. Nagashima, A. Mine, Y. Zhong, T. Suzuki, A. Fukushima, M. -K. Lin, S. Suresh Babu, J. Hwang, J. -E. Lee, S. -K. Mo, J. N. Eckstein, S. Shin, K. Okazaki and T. -C. Chiang, ACS Nano **18**, 31323-31331 (2024).

4. Depth-dependent study of time-reversal symmetry-breaking in the kagome superconductor AV_3Sb_5: J. N. Graham, C. Mielke III, D. Das, T. Morresi, V. Sazgari, A. Suter, T. Prokscha, H. Deng, R. Khasanov, S. D. Wilson, A. C. Salinas, M. M. Martins, Y. Zhong, K. Okazaki, Z. Wang, M. Z. Hasan, M. H. Fischer, T. Neupert, J. X. Yin, S. Sanna, H. Luetkens, Z. Salman, P. Bonfa` and Z. Guguchia, Nat. Commun. **15**, 8978 (2024).

5. Unveiling van Hove singularity modulation and fluctuated charge order in kagome superconductor CsV_3Sb_5 via time-resolved ARPES: Y. Zhong, T. Suzuki, H. Liu, K. Liu, Z. Nie, Y. Shi, S. Meng, B. Lv, H. Ding, T. Kanai, J. Itatani, S. Shin and K. Okazaki, Phys. Rev. Res. **6**, 043328 (2024).

6. †*Photo-induced Nonlinear Band Shift and Valence Transition in SmS,: Y. Chen, T. Nakamura, H. Watanabe, T. Suzuki, Q. Ren, K. Liu, Y. Zhong, T. Kanai, J. Itatani, K. Okazaki, H. S. Suzuki, S. Shin, K. Imura, N. K. Sato and S.-I. Kimura, J. Phys. Soc. Jpn. **94**, 013702-1-4 (2025).

7. †*Comprehensive study of the luminescence properties of elemental metals: T. Suemoto, S. Ono, A. Asahara, T. Okuno, T. Suzuki, K. Okazaki, S. Tani and Y. Kobayash, Phys. Rev. B **1114**, 035150 (2025).

8. A simple method to find temporal overlap between THz and x-ray pulses using x-ray-induced carrier dynamics in semiconductors: Y. Kubota, T. Suzuki, S. Owada, K. Tamasaku, H. Osawa, T. Togashi, K. Okazaki and M. Yabashi, Appl. Phys. Lett. **126**, 052101 (2025).

Kimura group

In fiscal year 2024, we worked on the development and application of soft X-ray microscopy systems using SPring-8 BL07LSU and SACLA BL1. We attempted to measure mammalian cells using soft X-ray ptychography with a total reflection Wolter mirror, and performed live cell imaging with a single femtosecond X-ray free-electron laser pulse and intracellular chemical state mapping combined with soft X-ray spectro-microscopy.

1. †*Sub-photon accuracy noise reduction of a single shot coherent diffraction pattern with an atomic model trained autoencoder: T. Ishikawa, Y. Takeo, K. Sakurai, K. Yoshinaga, N. Furuya, Y. Inubushi, K. Tono, Y. Joti, M. Yabashi, T. Kimura and K. Yoshimi, Opt. Express **32**, 18301 (2024).

2. Observation of mammalian living cells with femtosecond single pulse illumination generated by a soft X-ray free electron laser: S. Egawa, K. Sakurai, Y. Takeo, K. Yoshinaga, M. Takei, S. Owada, G. Yamaguchi, S. Yokomae, H. Mimura, Y. Yamagata, M. Yabashi, M. Shimura and T. Kimura, Optica **11**, 736 (2024).

3. Ultracompact mirror device for forming 20-nm achromatic soft-X-ray focus toward multimodal and multicolor nanoanalyses: T. Shimamura, Y. Takeo, F. Moriya, T. Kimura, M. Shimura, Y. Senba, H. Kishimoto, H. Ohashi, K. Shimba, Y. Jimbo and H. Mimura, Nat Commun **15**, 665 (2024).

4. †*Chemical-state imaging of a mammalian cell through multi-elemental soft x-ray spectro-ptychography: K. Sakurai, Y. Takeo, S. Takaramoto, N. Furuya, K. Yoshinaga, T. Shimamura, J. T. O'Neal, Y. Nakata, S. Egawa, K. Yoshimi, H. Ohashi, H. Mimura, Y. Harada, K. Inoue, M. Shimura and T. Kimura, Appl. Phys. Lett. **126**, 043702(1-7) (2025).

5. 超精密加工と X 線で覗くナノの世界: 木村 隆志, Journal of the Japan Society for Precision Engineering **91**, 356 (2025).

† Joint research with outside partners.
* Joint research between groups within ISSP.

Subjects of Joint Research

2024年度　共同利用課題一覧（前期）/ Joint Research List (First Term)

※実施課題一覧、所属は申請時のデータ

嘱託課題 / Comission Research Project

No.	課題番号	課題名	氏名	所属	分担者	Title	Name	Organization	Member of reseach project	担当所員
1	202310-CMBXX-0001	酸化亜鉛単結晶薄膜の極性評価	高橋 竜太	日本大学		Polarity of ZnO signle crystal films	Ryota Takahashi	Nihon University		Mikk Lippmaa
2	202403-CMBXX-0041	先端計測むけデータ解析フレームワークの汎用化	星 健夫	自然科学研究機構 核融合科学研究所		Generalization of data-analysis framework for advanced measurements	Takeo Hoshi	National Institute for Fusion Science		川島 直輝
3	202403-CMBXX-0042	動的平均場法プログラムDCoreへの動的感受率計算機能の追加	大槻 純也	岡山大学		Adding dynamical susceptibility calculation to dynamical mean-field software DCore	Junya Otsuki	Okayama University		川島 直輝
4	202311-CMBXX-0003	4G、T2-2における共同利用推進（B）	那波 和宏	東北大学		Research and Support of General-Use at 4G and T2-2（B）	Kazuhiro Nawa	Tohoku University		眞弓 皓一
5	202311-CMBXX-0004	6G、T1-2、T1-3における共同利用推進（A）	藤田 全基	東北大学		Research and Support of General-Use at 6G, T1-2 and T1-3（A）	Masaki Fujita	Tohoku University		眞弓 皓一
6	202311-CMBXX-0005	6G、T1-2、T1-3における共同利用推進（B）	南部 雄亮	東北大学		Research and Support of General-Use at 6G, T1-2 and T1-3（B）	Yusuke Nambu	Tohoku University		眞弓 皓一
7	202311-CMBXX-0006	6G、T1-2、T1-3における共同利用推進（C）	池田 陽一	東北大学金属材料研究所		Research and Support of General-Use at 6G, T1-2 and T1-3（C）	Yoichi Ikeda	Institute for materials research, Tohoku university		眞弓 皓一
8	202311-CMBXX-0007	6G、T1-2、T1-3における共同利用推進（D）	谷口 貴紀	東北大学		Research and Support of General-Use at 6G, T1-2 and T1-3（D）	Takanori Taniguchi	Tohoku University		眞弓 皓一
9	202311-CMBXX-0008	6G、T1-1における共同利用推進	岩佐 和晃	茨城大学		Research and Support of General-Use at 6G and T1-1	Kazuaki Iwasa	Ibaraki University		眞弓 皓一
10	202311-CMBXX-0009	T1-1における共同利用推進（A）	大山 研司	茨城大学		Research and Support of General-Use at T1-1（A）	Kenji Ohoyama	Ibaraki Univ.		眞弓 皓一
11	202311-CMBXX-0010	T1-1における共同利用推進（B）	桑原 慶太郎	茨城大学		Research and Support of General-Use at T1-1（B）	Keitaro Kuwahara	Ibaraki University		眞弓 皓一
12	202311-CMBXX-0015	C1-2における共同利用推進（A）	杉山 正明	京都大学		Research and Support of General-Use at C1-2（A）	Masaaki Sugiyama	Kyoto University		眞弓 皓一
13	202311-CMBXX-0016	C1-2、C2-3-1における共同利用推進	井上 倫太郎	京都大学		Research and Support of General-Use at C1-2 and C2-3-1	Rintaro Inoue	Kyoto University		眞弓 皓一
14	202311-CMBXX-0017	C1-2における共同利用推進（B）	守島 健	京都大学		Research and Support of General-Use at C1-2（B）	Ken Morishima	Kyoto University		眞弓 皓一
15	202311-CMBXX-0019	C3-1-2における共同利用推進（A）	日野 正裕	京都大学		Research and Support of General-Use at C3-1-2（A）	Masahiro Hino	Kyoto University		眞弓 皓一
16	202311-CMBXX-0022	C3-1-2における共同利用推進（D）	關 義親	東北大学		Research and Support of General-Use at C3-1-2（D）	Yoshichika Seki	Tohoku University		眞弓 皓一
17	202311-CMBXX-0023	4Gにおける共同利用推進	金城 克樹	東北大学		Research and Support of General-Use at 4G	Katsuki Kinjo	Tohoku University		眞弓 皓一
18	202311-CMBXX-0024	T2-2における共同利用推進（A）	高橋 美和子	筑波大学		Research and Support of General-Use at T2-2（A）	Miwako Takahashi	University of Tsukuba		眞弓 皓一

19	202311-CMBXX-0025	T2-2における共同利用推進（B）	小林 悟	岩手大学		Research and Support of General-Use at T2-2 (B)	Satoru Kobayashi	Iwate University		眞弓 皓一
20	202311-CMBXX-0026	高分解能スピン分解光電子分光による強相関物質の研究	横谷 尚睦	岡山大学		High resolution spin-resolved photoemission study on strongly correlated materials	Takayoshi Yokoya	Okayama University		近藤 猛
21	202311-CMBXX-0029	光電子分光法を用いた各種分子性結晶の電子状態の研究及び装置の低温化	木須 孝幸	大阪大学		Research on electron state of molecular crystals using photoemission spectroscopy	Kisu Takayuki	Osaka University		近藤 猛
22	202311-CMBXX-0031	レーザースピン角度分解光電子分光による表面電子状態の研究	矢治 光一郎	物質・材料研究機構		SARPES studies of atomic layer materials at surfaces	Koichiro Yaji	National Institute for Materials Science		近藤 猛
23	202311-CMBXX-0034	光スピントロニクスに向けたスピン軌道ダイナミクスの研究	黒田 健太	広島大学		Studying spin-orbit dynamics for opt-spintronics	Kenta Kuroda	Hiroshim University		近藤 猛
24	202311-CMBXX-0036	鉄系超伝導体のレーザー光電子分光	下志万 貴博	名古屋大学		Laser-ARPES on Fe superconductor	Takahiro Shimojima	Nagoya University		岡崎 浩三
25	202311-CMBXX-0038	固体中のマヨラナ粒子の研究	松田 祐司	京都大学		Study of Majorana Fermion in Solids by Laser Photoemission Spectroscopy	Matsuda Yuji	Kyoto University		岡崎 浩三

一般課題 / General Research Project

No.	課題番号	課題名	氏名	所属	分担者	Title	Name	Organization	Member of reseach project	担当所員
1	202311-GNBXX-0019	末端基に着目したオリゴマー型有機伝導体の開発	小野塚 洸太	長岡工業高等専門学校		Development of oligomeric organic conductors with focus on terminal group	Kota Onozuka	National Institute of Technology, Nagaoka College		森 初果
2	202312-GNBXX-0035	可溶な傾角反強磁性単一成分分子性導体における分子修飾・固溶化による物性変調	横森 創	茨城大学		Modulation of physical properties by molecular modification and solid-solution in soluble single-component molecular conductors with canted antiferromagnetism	So Yokomori	Ibaraki University		森 初果
3	202406-GNBXX-0109	フッ素により誘起される特異な歪みを利用する合成反応に関する研究	渕辺 耕平	筑波大学		Study on synthetic reactions based on the unique distortion induced by fluorine	Kohei Fuchibe	The University of Tsukuba		森 初果
4	202407-GNBXX-0112	Eu3Bi2S4F4における磁化異常	石垣 賢卯	東京理科大学	小内 貴祥	Anomalous magnetization of Eu3Bi2S4F4	Kento Ishigaki	Tokyo University of Science	Takayoshi Kouchi	森 初果
5	202310-GNBXX-0002	有機スピン液体候補物質の核磁気共鳴測定による研究	宮川 和也	東京大学		NMR Studies on organic spin liquid candidate materials	Kazuya Miyagawa	The University of Tokyo		高木 里奈
6	202311-GNBXX-0006	2次元有機金属薄膜が持つゲスト吸着原子・分子トラップ機能の解明	塚原 規志	群馬工業高等専門学校		The trap function for guest atoms and molecules in two-dimensionalorganometallic films	Noriyuki Tsukahara	National Institute of Technology, Gunma College		吉信 淳
7	202311-GNBXX-0024	STMによるCu(111)上に形成された自己組織化カゴメ格子の電子構造の観測	金井 要	東京理科大学	馬上 怜奈） 山崎 弘人 磯部 桃花	Observation of electronic structure of self-assembled Kagome lattice on Cu(111) by means of STM	Kaname Kanai	Tokyo University of Science	Rena Moue Hiroto Yamazaki Momoka Isobe	吉信 淳
8	202311-GNBXX-0025	透過 FTIR によるかんらん石単結晶表面の水素吸着および同位体効果の観察	橘 省吾	東京大学	稲田 栞里	Transmission FTIR spectroscopy of adsorbtion of hydrogen on olivine single crystals and the deuterium isotope effect	Shogo Tachibana	The University of Tokyo	Inada Shiori	吉信 淳
9	202312-GNBXX-0026	Si(111)√3×√3超構造基板上に成長したBi(110)超薄膜の電子状態	中辻 寛	東京科学大学	小森 文夫 吉田 陸馬 片野 達貴 加賀 大暉	Electronic structure of Bi(110) ultra-thin films grown on Si(111)√3×√3 superstructures	Kan Nakatsuji	Institute of Science Tokyo	Fumio Komori Yoshida Rikuma KATANO TATSUKI Taiki Kaga	吉信 淳

10	202312-GNBXX-0027	SiC基板上に成長したグラフェンへの金属原子インターカレーション	中辻 寛	東京科学大学	小森 文夫 片野 達貴 吉田 陸馬 加賀 大暉	Intercalation of metal atoms into graphene grown on a SiC substrate	Kan Nakatsuji	Institute of Science Tokyo	Fumio Komori KATANO TATSUKI Yoshida Rikuma Taiki Kaga	吉信 淳
11	202311-GNBXX-0010	希土類金属間化合物および金属超伝導体の結晶育成と低温基礎電子物性	海老原 孝雄	静岡大学	エスティアク アフメド 鵜飼 竜盛	Crystal Growth and Physical Properties at low temperatures in rare earth intermetallic compounds and metallic superconductors	Takao Ebihara	Shizuoka University	Esteaque Ahmed Ryusei Ukai	大谷 義近
12	202312-GNBXX-0029	カイラル結晶超伝導体における非相反伝導の研究	石原 滉大	東京大学	劉 蘇鵬 渡邊 優希	Study of nonreciprocal transport in a chiral lattice superconductor	Kota Ishihara	The University of Tokyo	SUPENG LIU Watanabe Yuki	大谷 義近
13	202311-GNBXX-0011	金属堆積膜の厚さ計測	梶田 信	東京大学		Thickness measurement of metallic deposition layer	Shin Kajita	The University of Tokyo		Mikk Lippmaa
14	202311-GNBXX-0008	365nm光照射によるケージド化合物の光開裂研究	樋山 みやび	群馬大学	工藤 颯	Photocleavage of caged compound with 365nm irradiation	Miyabi Hiyama	Gunma university	Hayate Kudo	秋山 英文
15	202311-GNBXX-0009	ホタル生物発光における緩衝液の影響解明	樋山 みやび	群馬大学	川崎 郁未	Effect of Buffer Solution on Firefly Bioluminescence	Miyabi Hiyama	Gunma university	Ikumi Kawasaki	秋山 英文
16	202311-GNBXX-0016	二波長励起フォトルミネッセンス測定によるGaAsN混晶における光学遷移過程に関する研究	矢口 裕之	埼玉大学	高宮 健吾	Two-wavelength photolunescence study of optical transitions in GaAsN alloys	Hiroyuki Yaguchi	Saitama University	Kengo Takamiya	秋山 英文
17	202312-GNBXX-0032	干渉型高速撮像のための光源開発	大間知 潤子	関西学院大学		Light source development for interferometric high-speed imaging	Junko Omachi	Kwansei Gakuin University		秋山 英文
18	202406-GNBXX-0110	高輝度ホタルルシフェラーゼの発光経時変化	樋山 みやび	群馬大学	川崎 郁未	Time-dependent emission change of high-luminance luciferase	Miyabi Hiyama	Gunma university	Ikumi Kawasaki	秋山 英文
19	202311-GNBXX-0001	点接合分光法を用いた超伝導体/強磁性体界面の電子状態観測	志賀 雅亘	九州大学	寺本 翼	Observation of electronic density of state at superconductor/ferromagnet interface using point-contact spectroscopy.	Masanobu Shiga	Kyushu University	TSUBASA TERAMOTO	三輪 真嗣
20	202311-GNBXX-0005	ピコ秒レーザー照射による窒化ガリウムと金属界面の相互原子拡散	富田 卓朗	徳島大学	福田 海人	Inter-diffusion of atoms between gallium nitride and metal contact by picosecond laser irradiation	Takuro Tomita	Tokushima University	Kaito Fukuda	小林 洋平
21	202311-GNBXX-0022	次世代レーザーとレーザー加工の基礎技術研究	吉富 大	産業技術総合研究所	高田 英行 奈良崎 愛子 小川 博嗣 寺澤 英知 澁谷 達則 佐藤 大輔 黒田 隆之助	Basic research on next generation laser systems and laser machining technology	Dai Yoshitomi	National Institute of Advanced Industrial Science and Technology	Takada Hideyuki Aiko Narazaki Hiroshi Ogawa Eichi Terasawa Tatsunori Shibuya Daisuke Satoh Ryunosuke Kuroda	小林 洋平
22	202311-GNBXX-0042	紫外光レーザー光源を用いた加工応用研究	藤本 靖	千葉工業大学		Research on laser processing application by ultraviolet laser light source	Yasushi Fujimoto	Chiba Institute of Technology		小林 洋平
23	202312-GNBXX-0030	炭素繊維複合高分子におけるレーザー照射による局所結晶化度	山口 誠	秋田大学		Control of Microscopic Crystallinity in Carbon-Fiber-Reinforced Plastic by Laser Irradiation	Yamaguchi Makoto	Akita University		小林 洋平
24	202312-GNBXX-0033	イメージングのための光源開発と回路設計	大間知 潤子	関西学院大学		Light source development and circuit design for imaging	Junko Omachi	Kwansei Gakuin University		小林 洋平
25	202311-GNBXX-0014	SmSの時間分解高強度中赤外ポンプ近赤外プローブ分光	渡邊 浩	大阪大学		Time-resolved high-power mid infra-red laser pump near infra-red laser probe spectroscopy	Hiroshi Watanabe	Osaka University		板谷 治郎

26	202311-GNBXX-0020	層状MAB相化合物MoAlBのスピン分解角度分解光電子分光	伊藤 孝寛	名古屋大学	増田 圭亮 河野 健人 倪 遠致	Spin- and angle-resolved photoemission spectroscopy of layered MAB phase compound MoAlB	Takahiro Ito	Nagoya University	Keisuke Masuda Kento Kawano YUANZHI NI	近藤 猛
27	202311-GNBXX-0028	高濃度ホウ素ドープアモルファスカーボンの電子状態	横谷 尚睦	岡山大学	村岡 祐治 東川 知樹 大岸 勇太 脇田 高徳	Electronic structure of heavily boron-doped amorphous carbon	Takayoshi Yokoya	Okayama University	Yuji Muraoka higashikawa tomoki Okishi Yuta Takanori Wakita	近藤 猛
28	202311-GNBXX-0040	強磁性体基板上のグラフェンのスピン分解光電子分光	矢治 光一郎	物質・材料研究機構	竹澤 伸吾（東京理科大学） 津田 俊輔 ファンディン タン	SARPES study of graphene on ferromagnetic substrates	Koichiro Yaji	National Institute for Materials Science	Shingo Takezawa (Tokyo University of Science) Shunsuke Tsuda THANG DINH PHAN	近藤 猛
29	202310-GNBXX-0003	HfO2系強誘電体FETのゲート部分の強誘電分極ドメインの観察	糸矢 祐喜	東京大学		Ferroelectric domain observation of HfO2-based ferroelectric FET	Yuki Itoya	The University of Tokyo		岡﨑 浩三
30	202312-GNBXX-0034	励起子絶縁体及び鉄系超伝導体における光誘起相転移の研究	久保田 雄也	理化学研究所		Investigation of the photo-induced phase transitions in excitonic insulators and iron-based superconductors	Yuya Kubota	RIKEN		岡﨑 浩三
31	202312-GNBXX-0036	高分解能レーザー励起光電子顕微鏡を用いた鉄系超伝導体の電子ネマティック状態の実空間観察IX	影山 遥一	東京大学	大西 朝登	Real-space observation of electronic nematicity in iron-based superconductors by using a high-resolution laser photoemission electron microscope IX	Yoichi Kageyama	The University of Tokyo	Asato Onishi	岡﨑 浩三
32	202311-GNBXX-0013	量子ホール系におけるトポロジカルDNPの研究	福田 昭	兵庫医科大学		Study of topological DNP in quantum Hall system	Akira Fukuda	Hyogo College of Medicine		量子物質ナノ構造ラボ運営委員会（橋坂昌幸）
33	202311-GNBXX-0015	遷移金属酸化物のホール係数測定	神戸 士郎	山形大学大学院理工学研究科	魏 毓良 吉永 幸弘 大竹 開智 今井 大雅 闫 承程 高橋 祐稀	Hall coefficient measurement of transition metal oxides	Shiro Kambe	Graduate School of Science and Engineering, Yamagata University	Wei Yuliang Yukihiro Yoshinaga Kaichi Otake Taiga Imai YAN CHENG CHENG Takahashi Yuki	量子物質ナノ構造ラボ運営委員会（橋坂昌幸）
34	202311-GNBXX-0021	アルゴンイオン照射した酸化チタンナノ構造における電気・磁気特性	原 正大	熊本大学	黒木 玲央	Electrical and magnetic properties of Ar ion irradiated titanium oxide nanostructures	Masahiro Hara	Kumamoto University	Kurogi Reo	量子物質ナノ構造ラボ運営委員会（橋坂昌幸）
35	202404-GNBXX-0045	有機半導体メゾスコピックデバイスの開発	竹谷 純一	東京大学	安部 深月	Development of mesoscopic devices utilizing organic semiconductors	Jun Takeya	The University of Tokyo	Mizuki Abe	量子物質ナノ構造ラボ運営委員会（橋坂昌幸）

物質合成・評価設備Gクラス / Materials Synthesis and Characterization G Class Research Project

No.	課題番号	課題名	氏名	所属	分担者	Title	Name	Organization	Member of reseach project	担当実験室
1	202311-MCBXG-0004	欠損スピネル化合物の構造と物性の解明	鬼頭 俊介	東京大学		Elucidation of the crystal structure and physical properties of lacunar spinel compounds	Shunsuke Kitou	The University of Tokyo		X線測定室

2	202311-MCBXG-0022	新規複合アニオン固体電解質の開発	矢島 健	名古屋大学	越田 耕平 佐藤 大介	Exploring novel mixed anion solid electrolytes	Takeshi Yajima	Nagoya University	Kouhei Koshita sato taisuke	X線測定室
3	202311-MCBXG-0033	Co基ホイスラー合金におけるマルテンサイト変態材料の探索	重田 出	鹿児島大学		Search for materials with the Martensitic transformation in Co-based Heusler alloys	Iduru Shigeta	Kagoshima University		X線測定室
4	202311-MCBXG-0050	強誘電性ニオブおよびタンタル酸化物の構造解析	山本 文子	芝浦工業大学		Structural analysis of ferroelectric niobates and tantalates	Ayako Yamamoto	Shibaura Institute of Technology		X線測定室
5	202312-MCBXG-0035	反転対称心のない磁性絶縁体の磁気超構造の外場駆動	有馬孝尚	東京大学	徳永 祐介 YAN ZHICHEN 鬼頭 俊介 遠山 悠大	Field-Effect on Nanometric Magnetic Objects in Noncentrosymmetric Magnetic Insulators	Taka-hisa Arima	The University of Tokyo	Yusuke Tokunaga ZHICHEN YAN Shunsuke Kitou Yudai Toyama	X線測定室
6	202311-MCBXG-0017	亜臨界水と固体塩基触媒の組み合わせによる新規有機合成プロセスの開発	秋月信	東京大学	王 一琦	Development of novel organic synthesis process with a combination of subcritical water and solid base catalyst	Makoto Akizuki	The University of Tokyo	Yiqi Wang	化学分析室、X線測定室
7	202311-MCBXG-0005	タングステン堆積層のキャラクタリゼーション	梶田 信	東京大学	程 実	Characterization of tungsten co-deposition layer	Shin Kajita	The University of Tokyo	SHI CHENG	光学測定室
8	202311-MCBXG-0006	カルシウムケイ酸塩への高圧下での希ガス取り込み機構の解明	飯塚 理子	早稲田大学		Incorporation of noble gases into calcium silicate under lower mantle condition	Riko Iizuka-Oku	Waseda University		高圧合成室
9	202311-MCBXG-0007	ハニカム格子を持つRu(Br1-xIx)3単結晶の高圧合成	今井 良宗	東北大学	南條 拓希 李 愛琳	High pressure synthesis of Ru(Br1-xIx)3 single crystals with a honeycomb lattice	Yoshinori Imai	Tohoku university	Hiroki Nanjo Erin Lee	高圧合成室
10	202311-MCBXG-0015	高温高圧下におけるFeSの水素化挙動の解明	鍵 裕之	東京大学	森 悠一郎 高野 将大	Hydrogenation behavior of FeS at high temperature and high pressure	Hiroyuki Kagi	The University of Tokyo	Mori Yuichiro Masahiro Takano	高圧合成室
11	202311-MCBXG-0016	Nd系充填スクッテルダイト化合物の高圧合成と異常物性	関根 ちひろ	室蘭工業大学	渡辺 陸人 尾崎 蒼空 野呂 翼 藤田 優音	High-pressure synthesis and anomalous properties of Nd-based filled skutterudite compounds	Chihiro Sekine	Muroran Institute of Technology	Rikuto Watanabe Sora Ozaki Tsubasa Noro Fujita Yuto	高圧合成室
12	202312-MCBXG-0041	3d遷移金属–メタロイド化合物高圧相の高圧下単結晶育成と物性評価	佐々木 拓也	名古屋大学	北原 拓海 田中 洸史朗	High-pressure crystal growth physical properties of 3d transition metal–metalloid compound high-pressure phase	Takuya Sasaki	Nagoya University	Kitahara Takumi Tanaka Koshiro	高圧合成室
13	202311-MCBXG-0009	セラミックスナノ粒子の連続製造技術開発	陶 究	産業技術総合研究所		Development of continuous process for ceramics nanoparticles production	Kiwamu Sue	AIST		電子顕微鏡室
14	202311-MCBXG-0012	窒化物磁性材料の構造解析	齋藤 哲治	千葉工業大学		Study of magnetic nitrides	Tetsuji Saito	Chiba Institute of Technology		電子顕微鏡室
15	202311-MCBXG-0013	月資源現地利用を目指したレーザーによるアルミナ還元	高崎 大吾	東京大学	渡邊 真隆 峯松 涼 Christen Lucas-Brian Han Minwoo 藤森 蒼天 大日 勇海 山上 尋大	Laser alumina reduction toward utilization of lunar resources	Daigo Takasaki	The University of Tokyo	watanabe masataka Ryo Minematsu Lucas-Brian Christen Han Minwoo Aoma Fujimori Isami Dainichi Hiroto Yamakami	電子顕微鏡室
16	202311-MCBXG-0019	高温高圧水を利用した金属酸化物微粒子の二段階合成	秋月信	東京大学	高橋 陸人	Dual-stage synthesis of metal oxide nanoparticles in hot compressed water	Makoto Akizuki	The University of Tokyo	Takahashi Rikuto	電子顕微鏡室

17	202311-MCBXG-0023	高濃度リチウム含有新規固体電解質の開発	矢島 健	名古屋大学	松浦 信介 佐藤 大介 島 颯一	Exploring novel solid electrolytes with high lithium concentration	Takeshi Yajima	Nagoya University	Matsuura Shinsuke sato taisuke Shima Souichi	電子顕微鏡室
18	202312-MCBXG-0042	補償磁性とトポロジカルな電子構造による機能性材料の探索	酒井明人	東京大学	梶原 悠人 黒沢 駿一郎 段 之宜 上杉 良太 肥後 友也 朝倉 海寛 対馬 湧太郎 松本 卓也 蘇 杭 董 柏寛 リュウ ファン	functional material based on the compensated magnetism and topological electronic structure	Akito Sakai	The University of Tokyo	yuto kajiwara Shunichiro Kurosawa Zhiyi Duan Ryota Uesugi Tomoya Higo Mihiro Asakura Yutaro Tsushima Takuya Matsumoto Hang Su TUNG Po-Kuan Lyu Fang	電子顕微鏡室
19	202312-MCBXG-0044	耐熱材料の微細組織および変形組織解析	御手洗 容子	東京大学	松永 紗英	Microstructure and deformation structure analysis of high-temperature materials	Yoko Mitarai	The University of Tokyo	Sae Matsunaga	電子顕微鏡室
20	202311-MCBXG-0011	超臨界水中でのバイオマスからの水素生成に寄与するNi/MgO-La2O3触媒の合成	布浦 鉄兵	東京大学	李 磊	Synthesis of Ni/MgO-La2O3 catalyst for H2 production from biomass in supercritical water	Teppei Nunoura	The University of Tokyo	Lei LI	電子顕微鏡室、X線測定室
21	202311-MCBXG-0001	リグニンの有用化合物への連続変換を可能にする固体触媒及び反応条件の検討	布浦 鉄兵	東京大学	堂脇 大志	Study on solid catalysts and reaction conditions for continuous lignin conversion into valuable chemicals	Teppei Nunoura	The University of Tokyo	Taishi Dowaki	電子顕微鏡室、化学分析室、X線測定室
22	202311-MCBXG-0020	不均一系触媒による超臨界水ガス化を利用した医薬品製造プロセスにおけるセファロスポリン系抗生物質の分解とその生成物の毒性評価	布浦 鉄兵	東京大学	朱 凌嬌	Degradation of cephalosporin antibiotics from the pharmaceutical production processes using supercritical water gasification with heterogeneous catalyst and its products toxicity evaluation	Teppei Nunoura	The University of Tokyo	ZHU LINGJIAO	電子顕微鏡室、化学分析室、X線測定室、光学測定室
23	202312-MCBXG-0036	合金ナノ粒子のキャラクタリゼーション	佐々木岳彦	東京大学	張 凱朝 胡 寧睿	Characterization of alloy nanoparticles	Takehiko Sasaki	The University of Tokyo	KAICHAO ZHANG Hu Ningrui	電子顕微鏡室、光学測定室、X線測定室
24	202312-MCBXG-0043	Fe3O4ナノ粒子によるマイクロプラスチックの吸着除去	胡 磊	東京大学		Adsorptive removal of microplastics by Fe3O4 nanoparticles	HU LEI	The University of Tokyo		電子顕微鏡室、光学測定室、X線測定室
25	202310-MCBXG-0047	(La0.1Nd0.9)1-x(Ca0.4Sr0.6)xFeO3-δ (0.1≦x≦0.9) の高温における磁性と熱電特性に関する研究	中津川 博	横浜国立大学		Magnetism and thermoelectric properties at high temperature in (La0.1Nd0.9)1-x(Ca0.4Sr0.6)xFeO3-δ(0.1≦x≦0.9)	Hiroshi Nakatsugawa	Yokohama National University		電磁気測定室
26	202311-MCBXG-0010	オフカット基板に成長させたFe(Se,Te)薄膜の電磁異方性	飯田 和昌	日本大学		Electromagnetic anisotropy of Fe(Se,Te) grown on vicinal substrates	Kazumasa Iida	Nihon University		電磁気測定室

27	202311-MCBXG-0014	遷移金属酸化物の磁化率測定	神戸士郎	山形大学	魏 毓良 吉永 幸弘 大竹 開智 今井 大雅 闫 承程 髙橋 祐稀	Magnetic susceptibility measurement of transition metal oxides	Shiro Kambe	Yamagata University	Wei Yuliang Yukihiro Yoshinaga Kaichi Otake Taiga Imai YAN CHENG CHENG Takahashi Yuki	電磁気測定室
28	202311-MCBXG-0021	速度論的反応が及ぼす微視的結晶構造変化の磁性評価による解明	原口 祐哉	東京農工大学	金 貴美愛	Changes in Local Crystal Structure Influenced by Kinetic Reactions through Magnetic Evaluation	Yuya Haraguchi	Tokyo University of Agriculture and Technology	Kimie KIM	電磁気測定室
29	202311-MCBXG-0025	非対称な化学結合を有するスピン軌道結合磁性体の磁気特性評価	原口 祐哉	東京農工大学	久米田 理桜	Evaluation of magnetic properties of spin-orbit coupled magnets with asymmetric chemical bonds	Yuya Haraguchi	Tokyo University of Agriculture and Technology	Rio Kumeda	電磁気測定室
30	202311-MCBXG-0029	酸化チタンナノシートから変換したナノ構造における磁化測定	原 正大	熊本大学	黒木 玲央	Magnetization measurement of nanostructures converted from titanium oxide nanosheets	Masahiro Hara	Kumamoto University	Kurogi Reo	電磁気測定室
31	202311-MCBXG-0032	高スピン分極ホイスラー合金の磁気特性のスピンゆらぎ理論による解析に関する研究	重田 出	鹿児島大学		Study on analysis of magnetic properties for highly spin-polarized Heusler alloys by the spin fluctuation theory	Iduru Shigeta	Kagoshima University		電磁気測定室
32	202311-MCBXG-0038	ホイスラー化合物でのフェリ磁性・反強磁性の研究	廣井 政彦	鹿児島大学		Study on ferrimagnetism and antiferromagnetism in Heusler compounds	Masahiko HIROI	Kagoshima University		電磁気測定室
33	202312-MCBXG-0039	高濃度ホウ素ドープアモルファス炭素膜の電気伝導特性	村岡 祐治	岡山大学	稲垣 翔哉 中村 匠汰	Electrical conductivity of heavily boron-doped amorphous carbon films	Yuji Muraoka	Okayama Univ.	Inagaki Shoya Shota Nakamura	電磁気測定室
34	202311-MCBXG-0046	スピン軌道結合金属A2Re2O7（A = Ca, Pb）の合成と相転移の研究	平井 大悟郎	名古屋大学		Synthesis and phase transition of spin-orbit coupled metal A2Re2O7（A = Ca, Pb）	Daigorou Hirai	Nagoya University		電磁気測定室、高圧合成室
35	202311-MCBXG-0026	フェロアキシャル転移を示す化合物の合成と評価	木村剛	東京大学	永井 隆之 梶田 遥一 林田 健志 松本 滉永 喻 培森	Synthesis and characterization of compounds showing a ferroaxial transition	Tsuyoshi Kimura	The University of Tokyo	Takayuki Nagai Yoichi Kajita Takeshi Hayashida Koei Matsumoto Yu peisen	物質合成室
36	202311-MCBXG-0027	常磁性希土類化合物における電気磁気効果	阿部 伸行	日本大学		Magnetoelectric effect in paramagnetic rare earth compounds	Nobuyuki Abe	Nihon University		物質合成室
37	202311-MCBXG-0048	バナジウム酸化物の熱体積機能	片山 尚幸	名古屋大学	江見 方敏 久保 泰星	Thermal volume function of vanadium oxides	Naoyuki Katayama	Nagoya University	Masatoshi Emi taisei kubo	物質合成室
38	202311-MCBXG-0002	希土類オルソフェライト単結晶試料の合成	渡邉 紳一	慶應義塾大学	安高 幸佑	Synthesis of Rare-Earth Orthoferrite Single Crystal Samples	Shinichi Watanabe	Keio University	Kohsuke Ataka	物質合成室、X線測定室
39	202311-MCBXG-0008	アシンメトリ量子物質の結晶育成とその基礎物性評価	松平 和之	九州工業大学		Crystal growth of Asymmetric Quantum Matters and evaluation of their basic physical properties	KAZUYUKI MATSUHIRA	Kyushu Institute of Technology		物質合成室、X線測定室
40	202311-MCBXG-0023	高濃度リチウム含有新規固体電解質の開発	矢島 健	名古屋大学	松浦 信介 佐藤 大介 島 颯一	Exploring novel solid electrolytes with high lithium concentration	Takeshi Yajima	Nagoya University	Matsuura Shinsuke sato taisuke Shima Souichi	物質合成室、X線測定室
41	202311-MCBXG-0024	高イオン伝導率を有する固体電解質のイオン伝導機構解明	矢島 健	名古屋大学	島 颯一 佐藤 大介	Conduction mechanism of a solid electrolyte with high ionic conductivity	Takeshi Yajima	Nagoya University	Shima Souichi sato taisuke	物質合成室、X線測定室、電子顕微鏡室

42	202312-MCBXG-0040	新奇ネマティック超伝導体候補物質の単結晶合成と物性評価	石原 滉大	東京大学	大西 朝登 影山 遥一 六本木 雅生 近藤 玲央名 永島 拓也 渡邊 優希	Single crystal synthesis and characterization of novel nematic superconductor candidates	Kota Ishihara	The University of Tokyo	Asato Onishi Yoichi Kageyama Masaki Roppongi Reona Kondo Takuya Nagashima Watanabe Yuki	物質合成室、X線測定室、電磁気測定室

物質合成・評価設備Uクラス / Materials Synthesis and Characterization U Class Research Project

No.	課題番号	課題名	氏名	所属	分担者	Title	Name	Organization	Member of reseach project	担当実験室
1	202406-MCBXU-0118	W型フェライトSrFe18O27における構造相転移の検証	和氣 剛	京都大学		Verification of structural transition in W-type ferrite SrFe18O27	Takeshi Waki	Kyoto University		X線測定室
2	202407-MCBXU-0119	時間反転対称性の破れた反強磁性体金属における創発物性の開拓II: デバイス評価	北折 暁	東京大学	関 真一郎 ヌイエン ドウイ　カーン 井上 裕貴	Exploration of emergent properties in antiferromagnetic metals with broken time-reversal symmetry I	Aki Kitaori	The University of Tokyo	Shinichiro Seki Nguyen Duy Khanh Hiroki Inoue	電磁気測定室

国際超強磁場科学施設 / International MegaGauss Science Laboratory

No.	課題番号	課題名	氏名	所属	分担者	Title	Name	Organization	Member of reseach project	担当所員
1	202311-HMBXX-0002	非従来型超伝導をもたらす量子臨界状態の輸送特性	横山 淳	茨城大学	小泉 遼介	Transport properties in quantum critical superconductors	Makoto Yokoyama	Ibaraki University	Ryosuke Koizumi	金道 浩一
2	202311-HMBXX-0003	重い電子系化合物が示す非従来型超伝導と量子臨界的挙動の相関	横山 淳	茨城大学	高橋 哲平	Relationship between unconventional superconductivity and quantum critical behavior in heavy-fermion compounds	Makoto Yokoyama	Ibaraki University	Teppei Takahashi	金道 浩一
3	202311-HMBXX-0015	MnNiGe-RuNiGe系化合物の磁気熱量効果	伊藤 昌和	鹿児島大学	間野 遥菜	Magnet-caloric effect of the MnNiGe-RuNiGe system	Masakazu Ito	Institute for Comprehensive Education, Kagoshima University	Haruna Mano	金道 浩一
4	202311-HMBXX-0021	Kitaev-Γ-Heisenberg磁性体における強磁場誘起相	原口 祐哉	東京農工大学	伊藤 正明	Ultra-high magnetic field induced phases in Kitaev-Γ-Heisenberg magnets	Yuya Haraguchi	Tokyo University of Agriculture and Technology	Masaaki Ito	金道 浩一
5	202311-HMBXX-0028	NiS2ナノ結晶の比熱測定	石渡 洋一	佐賀大学	平木 陵雅	Heat capacity measurements of NiS2 nanocrystals	Yoichi Ishiwata	Saga University	Ryoga Hiraki	金道 浩一
6	202312-HMBXX-0032	トポロジカル近藤絶縁体YbB12と高圧合成希土類ホウ化物RBn（R=Ce, Pr, Nd; n=12, 66）の強磁場磁化と輸送特性	伊賀 文俊	茨城大学		Magnetic and transport properties in high fields of topological Kondo insulator YbB12 and novel rare earth borides RBn（R=Ce, Pr, Nd; n=12, 66）produced by high pressure synthesis	Fumitoshi Iga	Ibaraki University		金道 浩一
7	202403-HMBXX-0047	ニッケル酸化物超伝導体の強磁場輸送現象の研究	長田 礎	東京大学	石田 浩祐（東北大学）	High-field transport studies on nickelate superconductors	Motoki Osada	The University of Tokyo	Kousuke Ishida (Tohoku University)	金道 浩一
8	202406-HMBXX-0103	小型磁気冷凍セルを用いたサブケルビン温度域での高速比熱測定	志村 恭通	広島大学	渡邉 寛大 冨田 光太郎	High-speed heat-capacity measurements in the sub-Kelvin temperature region by compact magnetic-refrigeration cell	Yasuyuki Shimura	Hiroshima University	Kanta Watanabe Kotaro Tomita	金道 浩一

9	202311-HMBXX-0020	一巻きコイル法を用いたホイスラー合金NiCoMnGaの強磁場磁化測定	木原 工	岡山大学	許 晶（東北大学） 池田 暁彦（電気通信大学）	High Field Magnetization Measurements for Heusler Alloy NiCoMnGa Using Single Turn Coil Method	Takumi Kihara	Research Institute for Interdisciplinary Science, Okayama University	Xiao Xu (Tohoku University) Akihiko Ikeda (University of Electro-Communications)	松田 康弘
10	202311-HMBXX-0025	強磁場による分子軌道結晶の破壊に関する研究	平井 大悟郎	名古屋大学	井口 寛太	Breaking of molecular orbital crystals by high magnetic fields	Daigorou Hirai	Nagoya University	Inokuchi Kanta	松田 康弘
11	202312-HMBXX-0038	トポロジカル近藤絶縁体YbB12と高圧合成希土類ホウ化物RBn（n=12, 66）の100T超強磁場領域の磁化過程	伊賀 文俊	茨城大学		Magnetic properties in over 100 T of high fields for topological Kondo insulator YbB12 and novel rare earth borides RBn（n=12, 66）produced by high pressure synthesis	Fumitoshi Iga	Ibaraki University		松田 康弘
12	202405-HMBXX-0058	Exploring Compounds Containing Quasi-1D Co(II)O6 Ising Chains under High Magnetic Fields	Jin Lun	Princeton University		Exploring Compounds Containing Quasi-1D Co(II)O6 Ising Chains under High Magnetic Fields	Lun Jin	Princeton University		松田 康弘
13	202311-HMBXX-0004	オクタシアノ系分子磁性体における光磁気ドメインのKerr効果顕微鏡観察	所裕子	筑波大学	長島 俊太郎	Observation of magnetic domain in photo-induced magnetization of octacyano-based molecular magnet using Kerr effect microscopy	Hiroko Tokoro	University of Tsukuba	Shuntaro Nagashima	徳永 将史
14	202311-HMBXX-0007	六方晶QS型鉄酸化物 Ba2Me1+xSn2+xFe10-2xO22 (Me=Fe2+, Li0.5Fe0.5) の強磁場磁気特性	神島 謙二	埼玉大学	吉島 丈史 落合 響	Magnetic properties of hexagonal QS-type iron oxides Ba2Me1+xSn2+xFe10-2xO22 (Me=Fe2+, Li0.5Fe0.5) under high magnetic fields	Kenji Kamishima	Saitama University	Takeshi Yoshijima Hibiki Ochiai	徳永 将史
15	202311-HMBXX-0016	らせん磁性体の強磁場下での物性	香取 浩子	東京農工大学	原口 祐哉	Physical properties of helical magnetic materials under high magnetic fields	Hiroko Katori	Tokyo University of Agriculture and Technology	Yuya Haraguchi	徳永 将史
16	202311-HMBXX-0022	高純度鉛における中間状態のダイナミクスの観察	井澤 公一	大阪大学	伏屋 雄紀（電気通信大学）	Observation of the dynamics of intermediate states in high-quality lead	Koichi Izawa	Osaka university	Yuki Fuseya (University of Electro-Communications)	徳永 将史
17	202311-HMBXX-0026	鉄カルコゲナイド超伝導体における磁気光学イメージングによる磁場分布の測定	矢口 宏	東京理科大学	栗原 綾佑 太田 知孝 袴田 怜志	Investigation of magnetic-field distributions in iron- chalcogenide superconductors using an MO imaging technique	Hiroshi Yaguchi	Tokyo University of Science	Ryosuke Kurihara Ota Tomotaka Satoshi Hakamada	徳永 将史
18	202311-HMBXX-0027	超音波計測による強相関電子系の磁場中量子状態と多極子効果	栗原 綾佑	東京理科大学	矢口 宏 太田 知孝 袴田 怜志	Ultrasonic study of high-field quantum states and multipole effects in strongly-correlated electron systems under pulsed-magnetic fields	Ryosuke Kurihara	Tokyo University of Science	Hiroshi Yaguchi Ota Tomotaka Satoshi Hakamada	徳永 将史
19	202311-HMBXX-0039	超伝導臨界磁場測定による鉄系超伝導体Fe(Te,S)の各種化学処理効果の検証	栗原 綾佑	東京理科大学	矢口 宏 太田 知孝 袴田 怜志	Chemical processing effects on iron-based superconductor Fe(Te,S) evaluated by upper critical field	Ryosuke Kurihara	Tokyo University of Science	Hiroshi Yaguchi Ota Tomotaka Satoshi Hakamada	徳永 将史
20	202312-HMBXX-0029	極性ディラック半金属の強磁場物性	酒井 英明	大阪大学	山下 淳志	Study of high-field transport for polar Dirac semimetals	Hideaki Sakai	Osaka University	Atsushi Yamashita	徳永 将史
21	202404-HMBXX-0049	Investigating emergent phenomena in SrRuO3/SrTiO3/SrRuO3 heterostructures with non-collinear spin texture	Das Sujit	Materials Research Centre, Indian Institute of Science, Bengaluru, India		Investigating emergent phenomena in SrRuO3/SrTiO3/SrRuO3 heterostructures with non-collinear spin texture	Sujit Das	Materials Research Centre, Indian Institute of Science, Bengaluru, India		徳永 将史

22	202404-HMBXX-0050	バックルドハニカム格子を持つ新規物質 Nd2Al3Ge4の磁気特性の解明	横井 滉平	学習院大学	山岸 敬太	Magnetic properties of buckled honeycomb lattice in Nd2Al3Ge4	Kohei Yokoi	Gakushuin University	Keita Yamagishi	徳永 将史
23	202404-HMBXX-0051	新奇超伝導体における磁場誘起現象の解明	三宅 厚志	東北大学	早坂 龍太	Study of Magnetic field-induced phenomena in novel superconductors	Atsushi Miyake	Tohoku University	Ryuta Hayasaka	徳永 将史
24	202311-HMBXX-0001	金属超伝導体および強相関電子系の結晶育成と強磁場物性研究	海老原 孝雄	静岡大学	エスティアク アフメド 鵜飼 竜盛	Crystal growth and physical Properties at high magnetic fields in metallic superconductors and strongly correlated electron system	Takao Ebihara	Shizuoka University	Esteaque Ahmed Ryusei Ukai	小濱 芳允
25	202405-HMBXX-0057	Quantum oscillation on CaAs3 and Eu doped CaAs3	Jun Sung-Kim	POSTECH		Quantum oscillation on CaAs3 and Eu doped CaAs3	Sung-Kim Jun	POSTECH		小濱 芳允

大阪大学大学院理学研究科附属先端強磁場科学研究センター / Center for Advanced High Magnetic Field Science, Graduate School of Science, Osaka University

No.	課題番号	課題名	氏名	所属	分担者	Title	Name	Organization	Member of reseach project	担当所員
1	202311-HMOXX-0005	強磁性ホイスラー合金Ni2MnX(X= Ga,Sn)系合金の磁気的機能性の研究	左近 拓男	龍谷大学		Research on magnetic functionalities of Ni2MnX(X= Ga, Sn) type Heusler alloys	Takuo Sakon	Ryukoku University		萩原 政幸
2	202311-HMOXX-0006	S = 1/2一次元Ising型反強磁性体CsCoCl3の横磁場中の磁気励起	木村 尚次郎	東北大学		High field ESR measurements of the S = 1/2 one-dimensional Ising-like antiferromagnet CsCoCl3 in transverse fields	Shojiro Kimura	Tohoku University		萩原 政幸
3	202311-HMOXX-0008	価数揺動系化合物SmSn3の強磁場磁化	竹内 徹也	大阪大学	大貫 惇睦（東京都立大学）	High-Field Magnetization in Valence Fluctuating Compound SmSn3	Tetsuya Takeuchi	Osaka University	Yoshichika Onuki (Tokyo Metropolitan University)	萩原 政幸
4	202311-HMOXX-0010	非磁性エレメントを添加した電気磁気反強磁性Cr2O3薄膜の界面磁化検出	白土 優	大阪大学		Detection of interfacial magnetic moment in magnetoelectric Cr2O3 thin film with various doping nonmagnetic elements	Yu Shiratsuchi	Osaka University		萩原 政幸
5	202311-HMOXX-0011	カプセル蛋白質（encapsulin from Pyrococcus furiosus）内に合成した磁性ナノ粒子の磁気的性質	白土 優	大阪大学		Magnetic properties of magnetic nanoparticles synthesized in encapsulin from Pyrococcus furiosus	Yu Shiratsuchi	Osaka University		萩原 政幸
6	202311-HMOXX-0012	量子カゴメ反強磁性体InCu3(OH)6Cl3の極低温強磁場磁化測定	吉田 紘行	北海道大学	加藤 萌結	High-field magnetization measurements of quantum kagome antiferromagnet InCu3(OH)6Cl3 at very low temperature	Hiroyuki Kura Yoshida	Hokkaido University	KATO MOYU	萩原 政幸
7	202311-HMOXX-0013	ブリージングカゴメ反強磁性体Li2Cr3SbO8単結晶の強磁場磁化測定	吉田 紘行	北海道大学	加藤 萌結	High-field magnetization measurements on single crystal of breathing kagome antiferromagnet Li2Cr3SbO8	Hiroyuki Kura Yoshida	Hokkaido University	KATO MOYU	萩原 政幸
8	202311-HMOXX-0014	ワイドボアパルスマグネットを用いた圧力下ESR装置の開発	櫻井 敬博	神戸大学		Development of high-pressure ESR system using wide bore pulse magnet	Takahiro Sakurai	Kobe University		萩原 政幸
9	202311-HMOXX-0017	秩序型ハニカムネットワークを持つBaPtSbの超伝導状態についての研究	工藤 一貴	大阪大学		Study on the superconducting state of BaPtSb with a PtSb ordered honeycomb network	Kazutaka Kudo	Osaka University		萩原 政幸
10	202311-HMOXX-0018	SeドープPtBi2の超伝導状態についての研究	工藤 一貴	大阪大学		Study on the superconducting state of Se-doped PtBi2	Kazutaka Kudo	Osaka University		萩原 政幸
11	202311-HMOXX-0019	秩序型ラーベス相化合物の超伝導物質開発	工藤 一貴	大阪大学		Development of novel superconductors with ordered Laves phase structures	Kazutaka Kudo	Osaka University		萩原 政幸

12	202312-HMOXX-0030	新規Ce系層状物質の磁気特性	酒井 英明	大阪大学		Study of magnetic properties for a Ce-based layered material	Hideaki Sakai	Osaka University		萩原 政幸
13	202312-HMOXX-0033	ハニカム格子反強磁性体混晶 M1M2(pymca)3ClO4, (M1, M2 = Fe, Co, Ni, Cu, Zn)の磁性	本多 善太郎	埼玉大学		Magnetic properties of mixed crystals of the honeycomb lattice antiferromagnet M1M2(pymca)3ClO4, (M1, M2 = Fe, Co, Ni, Cu, Zn)	Zentaro Honda	Saitama University		萩原 政幸
14	202312-HMOXX-0037	強いスピン-軌道相互作用を活かした酸化物スピントロニクス	上田 浩平	大阪大学		Oxide spintronics utilizing strong spin-orbit coupling	Kohei Ueda	Osaka University		萩原 政幸
15	202312-HMOXX-0042	正方晶希土類化合物 ErRu2Si2 における強磁場スキルミオン相の探索	田畑 吉計	京都大学		Search for the high-field skyrmion phase in the tetragonal rare-earth intermetallic compound ErRu2Si2	Yoshikazu Tabata	Kyoto University		萩原 政幸
16	202403-HMOXX-0048	新奇カゴメ格子反強磁性体の合成とその基礎物性	大久保 晋	神戸大学		Synthesis and magnetic properties of novel Kagome lattice Antiferromagnets	Susumu Okubo	Kobe University		萩原 政幸

強磁場コラボラトリー / The High Magnetic Field Collaboratory

No.	課題番号	課題名	氏名	所属	分担者	Title	Name	Organization	Member of reseach project	担当所員
1	202311-HMBXX-0040	量子系有機物質群が創り出す新規スピンモデルの強磁場物性	山口 博則	大阪公立大学		High-field magnetic properties of new spin models formed by quantum organic materials	Hironori Yamaguchi	Osaka Metropolitan University		金道 浩一
2	202312-HMCXX-0035	強磁場を用いたPd2MnGa基合金における磁場誘起相変態の実験的調査	宮川 寅矢	東北大学	許 畠 今富 大介	Investigation on magnetic field induced phase transformation behaviors in Pd2MnGa-based alloys under high magnetic fields	Tomoya Miyakawa	Tohoku University	Xiao Xu Daisuke Imatomi	徳永 将史
3	202312-HMCXX-0036	FeCr錯体におけるスピン転移の詳細な研究	許 畠	東北大学	今富 大介	Investigation on metamagnetic transition behaviors of Mn-Zn alloys using high magnetic fields	Xiao Xu	Tohoku University	Daisuke Imatomi	徳永 将史
4	202312-HMCXX-0044	実用超伝導線材の多次元高速分析	土屋 雄司	東北大学		Multidimensional rapid analysis of practical superconducting wires	Tsuchiya Yuji	Tohoku University		小濱 芳允
5	202312-HMCXX-0045	New magnetic phase diagram of ultra-pure UTe2	Marcenat Christophe	Interdisciplinary Research Institute of Grenoble (IRIG), Alternative Energies and Atomic Energy Commission (CEA)		New magnetic phase diagram of ultra-pure UTe2	Christophe Marcenat	Interdisciplinary Research Institute of Grenoble (IRIG), Alternative Energies and Atomic Energy Commission (CEA)		小濱 芳允

留学研究課題 / External Research Project Long / Short-term

No.	課題番号	課題名	氏名	所属	分担者	Title	Name	Organization	Member of reseach project	担当所員
1	202311-VSBXS-0001	反応追跡に向けたケージドルシフェリンの光開裂実験	今西 勇輔	群馬大学		Photocleavage of coumarin caged luciferin for reaction tracking	Yusuke Imanishi	Gunma University		秋山 英文
2	202312-VSBXS-0002	精密定量計測を用いたルミノール化学発光における触媒効果	倉田 洋佑	群馬大学		Quantitative measurements of the effects of catalysts on luminol chemiluminescence	KURATA YOSUKE	GUNMA UNIVERSITY		秋山 英文

2024年度　共同利用課題一覧（後期）/ Joint Research List (Latter Term)

※実施課題一覧、所属は申請時のデータ

嘱託課題 / Comission Research Project

No.	課題番号	課題名	氏名	所属	分担者	Title	Name	Organization	Member of reseach project	担当所員
1	202405-CMBXX-0045	4G、T2-2 における共同利用推進（A）	佐藤 卓	東京大学物性研究所		Research and Support of General-Use at 4G and T2-2（A）	Taku J Sato	ISSP The University of Tokyo		眞弓 皓一
2	202405-CMBXX-0046	4G、T2-2 における共同利用推進(B)	那波 和宏	東北大学		Research and Support of General-Use at 4G and T2-2 (B)	Kazuhiro Nawa	Tohoku University		眞弓 皓一
3	202405-CMBXX-0047	6G、T1-2、T1-3 における共同利用推進(A)	藤田 全基	東北大学		Research and Support of General-Use at 6G , T1-2 and T1-3(A)	Masaki Fujita	Tohoku University		眞弓 皓一
4	202405-CMBXX-0048	6G、T1-2、T1-3 における共同利用推進(B)	南部 雄亮	東北大学		Research and Support of General-Use at 6G , T1-2 and T1-3(B)	Yusuke Nambu	Tohoku University		眞弓 皓一
5	202405-CMBXX-0049	6G、T1-2、T1-3 における共同利用推進(C)	池田 陽一	東北大学金属材料研究所		Research and Support of General-Use at 6G , T1-2 and T1-3(C)	Yoichi Ikeda	Institute for materials research, Tohoku university		眞弓 皓一
6	202405-CMBXX-0050	6G、T1-2、T1-3 における共同利用推進(D)	谷口 貴紀	東北大学		Research and Support of General-Use at 6G , T1-2 and T1-3(D)	Takanori Taniguchi	Tohoku University		眞弓 皓一
7	202405-CMBXX-0051	T1-1 における共同利用推進（A）	岩佐 和晃	茨城大学		Research and Support of General-Use at T1-1（A）	Kazuaki Iwasa	Ibaraki University		眞弓 皓一
8	202405-CMBXX-0052	T1-1 における共同利用推進 (B)	大山 研司	茨城大学		Research and Support of General-Use at T1-1 (B)	Kenji Ohoyama	Ibaraki Univ.		眞弓 皓一
9	202405-CMBXX-0053	T1-1 における共同利用推進(C)	桑原 慶太郎	茨城大学		Research and Support of General-Use at T1-1 (C)	Keitaro Kuwahara	Ibaraki University		眞弓 皓一
10	202405-CMBXX-0054	T1-1 における共同利用推進 (D)	横山 淳	茨城大学		Research and Support of General-Use at T1-1 (D)	Makoto Yokoyama	Ibaraki University		眞弓 皓一
11	202405-CMBXX-0056	T1-1 における共同利用推進(F)	中野 岳仁	茨城大学		Research and Support of General-Use at T1-1 (F)	Takehito Nakano	Ibaraki University		眞弓 皓一
12	202405-CMBXX-0058	C1-2 における共同利用推進 (A)	杉山 正明	京都大学		Research and Support of General-Use at C1-2 (A)	Masaaki Sugiyama	Kyoto University		眞弓 皓一
13	202405-CMBXX-0059	C1-2、C2-3-1 における共同利用推進	井上 倫太郎	京都大学		Research and Support of General-Use at C1-2 and C2-3-1	Rintaro Inoue	Kyoto University		眞弓 皓一
14	202405-CMBXX-0060	C1-2 における共同利用推進(B)	守島 健	京都大学		Research and Support of General-Use at C1-2 (B)	Ken Morishima	Kyoto University		眞弓 皓一
15	202405-CMBXX-0061	C3-1-2 における共同利用推進 (A)	日野 正裕	京都大学		Research and Support of General-Use at C3-1-2 (A)	Masahiro Hino	Kyoto University		眞弓 皓一
16	202405-CMBXX-0062	C3-1-2 における共同利用推進(B)	北口 雅暁	名古屋大学		Research and Support of General-Use at C3-1-2(B)	Masaaki Kitaguchi	Nagoya University		眞弓 皓一
17	202405-CMBXX-0063	C3-1-2 における共同利用推進 (C)	田崎 誠司	京都大学		Research and Support of General-Use at C3-1-2 (C)	Seiji Tasaki	Kyoto University		眞弓 皓一
18	202405-CMBXX-0064	C3-1-2 における共同利用推進 (D)	關 義親	東北大学		Research and Support of General-Use at C3-1-2 (D)	Yoshichika Seki	Tohoku University		眞弓 皓一
19	202405-CMBXX-0065	4G における共同利用推進	金城 克樹	東北大学		Research and Support of General-Use at 4G	Katsuki Kinjo	Tohoku University		眞弓 皓一

20	202405-CMBXX-0066	T2-2 における共同利用推進 (A)	高橋 美和子	筑波大学		Research and Support of General-Use at T2-2 (A)	Miwako Takahashi	University of Tsukuba		眞弓 皓一
21	202405-CMBXX-0068	C3-1-2 における共同利用推進 (E)	樋口 嵩	京都大学		Research and Support of General-Use at C3-1-2 (E)	Higuchi Takashi	Kyoto University		眞弓 皓一
22	202405-CMBXX-0072	光スピントロニクスに向けたスピン軌道ダイナミクスの研究	黒田 健太	広島大学		Studying spin-orbit dynamics for opt-spintronics	Kenta Kuroda	Hiroshim University		近藤 猛
23	202405-CMBXX-0074	有機化合物の光電子分光	金井 要	東京理科大学		Photoemission study on organic compounds	Kaname Kanai	Tokyo University of Science		近藤 猛
24	202405-CMBXX-0079	光電子分光法を用いた各種分子性結晶の電子状態の研究及び装置の低温化	木須 孝幸	大阪大学		Research on electron state of molecular crystals using photoemission spectroscopy	Kisu Takayuki	Osaka University		近藤 猛
25	202405-CMBXX-0080	溶液セルの開発	竹内 雅耶	兵庫県立大学		Development of liquid cell	Masaya Takeuchi	UNIVERSITY OF HYOGO		岡崎 浩三
26	202405-CMBXX-0081	高次高調波レーザー時間分解光電子分光を用いた強相関物質の研究	石坂 香子	工学系研究科		HHG laser time-resolve ARPES Study on strongly correlated materials	kyoko Ishizaka	Graduate School of Engineering		岡崎 浩三
27	202405-CMBXX-0083	時間分解光電子分光を用いた強相関物質の研究	溝川 貴司	早稲田大学		Time-resolved photoemission study on strongly-correlated materials	Takashi Mizokawa	Waseda University		岡崎 浩三
28	202405-CMBXX-0085	鉄系超伝導体のレーザー顕微光電子分光	下志万 貴博	名古屋大学		Laser-nano-ARPES Fe superconductor	Takahiro Shimojima	Nagoya University		岡崎 浩三

一般課題 / General Research Project

No.	課題番号	課題名	氏名	所属	分担者	Title	Name	Organization	Member of reseach project	担当所員
1	202406-GNBXX-0073	可溶な傾角反強磁性単一成分分子性導体における分子修飾・固溶化による物性変調	横森 創	茨城大学		Modulation of physical properties by molecular modification and solid-solution in soluble single-component molecular conductors with canted antiferromagnetism	So Yokomori	Ibaraki University		森 初果
2	202412-GNBXX-0115	明確に規定されたシロキサンオリゴマーの合成とナノ多孔体への転換	林 泰毅	東京大学	伊與木 健太	Synthesis of well-defined siloxanes oligomers and conversion of them into nanoporous materials	Taiki Hayashi	The University of Tokyo	Kenta Iyoki	森 初果
3	202404-GNBXX-0047	カゴメ量子スピン液体候補物質 YCu3(OH)6.5Br2.5の基底状態	末次 祥大	京都大学		Ground state of kagome quantum spin liquid candidate YCu3(OH)6.5Br2.5	Shota Suetsugu	Kyoto University		山下 穣
4	202405-GNBXX-0092	フラストレート磁性体DyRu2Si2の極低温磁化率測定	田畑 吉計	京都大学	吉本 周玄	Low temperaturte susceptibity measurement of the frustrated magnet DyRu2Si2	Yoshikazu Tabata	Kyoto University	Subaru Yoshimoto	山下 穣
5	202406-GNBXX-0084	サブmK超低温走査型トンネル顕微鏡/分光装置の開発	花栗 哲郎	理化学研究所		Development of sub-mK ultra-low-temperature scanning tunneling microscopy/spectroscopy	Tetsuo Hanaguri	RIKEN		山下 穣
6	202405-GNBXX-0058	有機スピン液体候補物質の核磁気共鳴測定による研究	宮川 和也	東京大学		NMR Studies on organic spin liquid candidate materials	Kazuya Miyagawa	The University of Tokyo		高木 里奈
7	202405-GNBXX-0059	分子性導体[Mn(Pc)(CN)]2Oの低温NMR実験	鳥塚 潔	千葉工業大学		NMR experiments on a molecular conductor [Mn(Pc)(CN)]2O at low temperatures	Kiyoshi Torizuka	Chiba Institute of Technology		高木 里奈
8	202405-GNBXX-0097	金属有機構造体のナノ細孔に閉じ込められたイオン液体の相転移	糸井 充穂	東京都市大学	横田 麻莉佳（日本大学） 開 康一（福島県立医科大学）	Study on the phase transitions of ionic liquids confined in nanopores of Metal Organic Frameworks	Miho Itoi	Tokyo City University	MARIKA YOKOTA (Nihon University) Ko-ichi HIRAKI (Fukushima Medical University)	高木 里奈

9	202405-GNBXX-0104	多型化合物RIr2Si2(R=希土類)の磁気特性	内間 清晴	学校法人沖縄キリスト教学院・沖縄キリスト教短期大学	繁岡 透（山口大学）	Magnetic characteristics of polymorphic compounds RIr2Si2(R=Rare earth)	Kiyoharu Uchima	Okinawa Christian Institute Okinawa christian junior College	Toru Shigeoka (Yamaguchi University)	高木 里奈
10	202405-GNBXX-0105	ファラデー法による新しい磁化率測定法の確立	鳥塚 潔	千葉工業大学		A New approach of susceptibility measurement by Faraday method	Kiyoshi Torizuka	Chiba Institute of Technology		高木 里奈
11	202406-GNBXX-0089	不定比化合物TmCr0.5Ge2単結晶の磁化測定	藤原 哲也	山口大学		Magnetization measurements of non-stoichiometric TmCr0.5Ge2 single crystal	Tetsuya Fujiwara	Yamaguchi University		高木 里奈
12	202405-GNBXX-0068	2次元有機金属分子ネットワークが持つゲスト吸着原子・分子トラップ機能の解明	塚原 規志	群馬工業高等専門学校		The trap function for guest atoms and molecules in two-dimensional organometallic films	Noriyuki Tsukahara	National Institute of Technology, Gunma College		吉信 淳
13	202406-GNBXX-0081	Si(111)√3×√3超構造基板上に成長したBi(110)超薄膜の電子状態	中辻 寛	東京科学大学	小森 文夫 片野 達貴 吉田 陸馬 加賀 大暉	Electronic structure of Bi(110) ultra-thin films grown on Si(111)√3×√3 superstructures	Kan Nakatsuji	Institute of Science Tokyo	Fumio Komori KATANO TATSUKI Yoshida Rikuma Taiki Kaga	吉信 淳
14	202406-GNBXX-0082	SiC基板上に成長したグラフェンへの金属原子インターカレーション	中辻 寛	東京科学大学	小森 文夫 片野 達貴 吉田 陸馬 加賀 大暉	Intercalation of metal atoms into graphene grown on a SiC substrate	Kan Nakatsuji	Institute of Science Tokyo	Fumio Komori KATANO TATSUKI Yoshida Rikuma Taiki Kaga	吉信 淳
15	202410-GNBXX-0113	TPDとIRASを用いたNi(110)表面におけるCO2の吸着状態の分析	数間 恵弥子	東京大学	小粥 徹 LEE MINHUI	Analysis of the CO2 adsorption states on Ni(110) surface using TPD and IRAS	Emiko Kazuma	The University of Tokyo	Toru Okai LEE MINHUI	吉信 淳
16	202406-GNBXX-0100	カイラル結晶超伝導体における非相反伝導の研究	石原 滉大	東京大学	劉 蘇 渡邊 優希	Study of nonreciprocal transport in a chiral lattice superconductor	Kota Ishihara	The University of Tokyo	SUPENG LIU Watanabe Yuki	大谷 義近
17	202405-GNBXX-0070	金属表面上のプランベンの電子状態の精密測定	柚原 淳司	名古屋大学	前田 匠太 川合 康佑	Electronic structure of plumbene on metal surfaces	Junji Yuhara	Nagoya University	Shota Maeda Kawaai Kosuke	長谷川 幸雄
18	202406-GNBXX-0091	極低温・強磁場下におけるRashba系原子層合金(Pb, Bi)/Ge(111)の電子状態の解明	高山 あかり	早稲田大学	Konermann Lars	Electronic structure of Rashba-type single-layer (Pb, Bi) alloy on Ge(111) at ultra-low temperatures and high-magnetic fields	Akari Takayama	Waseda University	Lars Konermann	長谷川 幸雄
19	202405-GNBXX-0054	吸収・蛍光計測によるクマリンの光褪色	樋山 みやび	群馬大学	今西 勇輔	Photobleaching measurements of coumarin by absorption and fluorescence spectra	Miyabi Hiyama	Gunma University	Yusuke Imanishi	秋山 英文
20	202405-GNBXX-0055	発光量絶対値測定系における較正方法の改良	樋山 みやび	群馬大学	川崎 郁未	Improved calibration method for absolute bioluminescence measurement system	Miyabi Hiyama	Gunma university	Ikumi Kawasaki	秋山 英文
21	202405-GNBXX-0056	赤外レーザーによるケージドルシフェリン光開裂の試み	樋山 みやび	群馬大学	工藤 颯	Photocleaving of caged luciferin with infrared laser	Miyabi Hiyama	Gunma University	Hayate Kudo	秋山 英文
22	202405-GNBXX-0106	GaPN混晶の２段階光吸収に寄与する局在状態の窒素濃度依存性	矢口 裕之	埼玉大学	高宮 健吾	Nitrogen concentration dependence of localized states contributing to two-step optical absorption in GaPN alloys	Hiroyuki Yaguchi	Saitama University	Kengo Takamiya	秋山 英文
23	202406-GNBXX-0088	テラヘルツ波用レーザーカオス光のパルス発振	桑島 史欣	福井工業大学		Pulse Oscillation of laser chaos for THz Wave	FUMIYOSHI KUWASHIMA	Fukui University of Technology		秋山 英文
24	202406-GNBXX-0098	干渉型高速撮像のための電気変調光源開発	大間知 潤子	関西学院大学		Development of electrically modified light source for interferometric high-speed imaging	Junko Omachi	Kwansei Gakuin University		秋山 英文
25	202406-GNBXX-0101	GaN/Siヘテロ接合界面の原子配列とその電気的特性	小柴 俊	香川大学	澁田 彼方 谷本 涼太	Atomic arrangement of GaN/Si heterojunction interface and its electrical properties	Shyun Koshiba	Kagawa University	KANATA SHIBUTA Tanimoto Ryota	秋山 英文

26	202410-GNBXX-0114	宇宙ガンマ線観測のための多層膜フィルターの開発	奥村 暁	名古屋大学	齋藤 隆之（宇宙線研究所） 安藤 大地 山本 常夏（甲南大学） 溝手 雅也（甲南大学）	Developing multilayer coating for celestial gamma-ray observations	Akira Okumura	Nagoya University	Takayuki Saito (Institute for Cosmic Ray Research) Daichi Ando (Institute for Space-Earth Environmental Research) tokonatsu Yamamoto (konan university) Masaya Mizote (Konan University Graduate fellow)	秋山 英文
27	202405-GNBXX-0049	発光定量計測系検証のための青色発光タンパク質合成	樋山 みやび	群馬大学	倉田 洋佑	Synthesis of blue bioluminescence proteins for validation of quantitative measurement systems	Miyabi Hiyama	GUNMA UNIVERSITY	KURATA YOSUKE	井上 圭一
28	202405-GNBXX-0075	ロドプシンタンパクの時間分解赤外分光法による研究	石橋 孝章	筑波大学	柴田 桂成	Time-resolved IR study of rhodopsin proteins	Taka-aki Ishibashi	University of Tsukuba	Shibata Keisei	井上 圭一
29	202405-GNBXX-0074	機械学習による第一原理擬ポテンシャルおよび数値原子軌道の開発	川井 弘之	新潟大学		Development of first-principles pseudopotentials and numerical atomic orbitals based on machine learning	Hiroyuki Kawai	Niigata University		尾崎 泰助
30	202406-GNBXX-0095	有機分子インターカレーションした量子磁性体の物性評価	原口 祐哉	東京農工大学	伊藤 正明 千野根 広大	Evaluation of physical properties of organic-molecule-intercalated quantum magnets	Yuya Haraguchi	Tokyo University of Agriculture and Technology	Masaaki Ito Kota Chinone	岡本 佳比古
31	202501-GNBXX-0116	超伝導Sr2RuO4単結晶の反磁性磁化の研究	松木 久和	京都大学	前野 悦輝	Research on the diamagnetism in superconducting single-crystalline Sr2RuO4	Hisakazu Matsuki	Kyoto University	Yoshiteru Maeno	岡本 佳比古
32	202405-GNBXX-0071	TbCaAl3O7における中性子回折実験のための結晶評価	阿部 伸行	日本大学		Crystal characterization for neutron diffraction experiments in TbCaAl3O7	Nobuyuki Abe	Nihon University		益田 隆嗣
33	202405-GNBXX-0050	超高速発光分光による金属の研究	末元 徹	電気通信大学		Studies on metals using ultrafast luminescence spectroscopy	Suemoto Tohru	The University of Electro-Communications		小林 洋平
34	202405-GNBXX-0057	次世代レーザーとレーザー加工の基礎技術研究	吉富 大	産業技術総合研究所	高田 英行 奈良崎 愛子 小川 博嗣 寺澤 英知 澁谷 達則 佐藤 大輔 黒田 隆之助	Basic research on next generation laser systems and laser machining technology	Dai Yoshitomi	National Institute of Advanced Industrial Science and Technology	Takada Hideyuki Aiko Narazaki Hiroshi Ogawa Eichi Terasawa Tatsunori Shibuya Daisuke Satoh Ryunosuke Kuroda	小林 洋平
35	202405-GNBXX-0062	ピコ秒レーザー照射による窒化ガリウムと金属界面の相互原子拡散	富田 卓朗	徳島大学	福田 海人	Inter-diffusion of atoms between gallium nitride and metal contact by picosecond laser irradiation	Takuro Tomita	Tokushima University	Kaito Fukuda	小林 洋平
36	202406-GNBXX-0087	炭素繊維複合高分子におけるレーザー照射による局所結晶化度	山口 誠	秋田大学	大和 光	Control of Microscopic Crystallinity in Carbon-Fiber-Reinforced Plastic by Laser Irradiation	Yamaguchi Makoto	Akita University	hikaru yamato	小林 洋平
37	202406-GNBXX-0099	イメージングのための光源開発とそれを評価する回路設計	大間知 潤子	関西学院大学	原 啓太	Light source development for imaging and circuit design for its evaluation	Junko Omachi	Kwansei Gakuin University	Keita Hara	小林 洋平

38	202405-GNBXX-0066	鉄フタロシアニンを基盤としたLieb格子の電子構造の観測	金井 要	東京理科大学	磯部 桃花	Observation of electronic structure of Lieb lattice in Fe phthalocyanine framework	Kaname Kanai	Tokyo University of Science	Momoka Isobe	近藤 猛
39	202406-GNBXX-0086	MXenes単結晶V2CTzのスピン分解角度分解光電子分光	伊藤 孝寛	名古屋大学	河野 健人 倪 遠致 與田 康人	Spin- and angle-resolved photoemission spectroscopy of MXenes V2CTz single-crystal	Takahiro Ito	Nagoya University	Kento Kawano YUANZHI NI Yasuto Yoda	近藤 猛
40	202405-GNBXX-0069	高分解能レーザー励起光電子顕微鏡を用いた鉄系超伝導体の電子ネマティック状態の実空間観察IX	影山 遥一	東京大学		Real-space observation of electronic nematicity in iron-based superconductors by using a high-resolution laser photoemission electron microscope IX	Yoichi Kageyama	The University of Tokyo		岡崎 浩三
41	202405-GNBXX-0072	カロリメトリによる金属ナノ構造の赤外吸収率測定	末元 徹	電気通信大学	須田 順子	Measurement of infrared absorptivity on metal nanostructures by calorimetry	Suemoto Tohru	The University of Electro-Communications	Yoriko Suda	岡崎 浩三
42	202406-GNBXX-0079	角度分解光電子分光を用いた鉄系超伝導体における新奇ネマティシティの探求	大西 朝登	東京大学	影山 遥一	ARPES study of novel electronic nematicity in Iron-based superconductors	Asato Onishi	The University of Tokyo	Yoichi Kageyama	岡崎 浩三
43	202406-GNBXX-0080	レーザー励起光電子顕微鏡を用いたカゴメ超伝導体における新奇秩序相の実空間観測	大西 朝登	東京大学		Real-space observation of novel electronic states in Kagome superconductors using laser-based photoemission electron microscope	Asato Onishi	The University of Tokyo		岡崎 浩三
44	202406-GNBXX-0094	カルシウム-グラフェン層間化合物における電子格子相互作用の研究	一ノ倉 聖	東京科学大学	中村 達哉	Study of electron-phonon interaction in Ca-graphene intercalation compounds	Satoru Ichinokura	Institute of Science Tokyo	Tatsuya Nakamura	岡崎 浩三
45	202406-GNBXX-0107	新規オクタシアノ金属錯体の共結晶の第二次高調波発生の測定	中林 耕二	東京大学	小西 達也	Measurement of second harmonic generation in cocrystals of novel octacyanometallate complexes	Koji Nakabayashi	The University of Tokyo	Tatsuya Konishi	岡崎 浩三
46	202405-GNBXX-0063	量子ホール系におけるトポロジカルDNPの研究	福田 昭	兵庫医科大学		Study of topological DNP in quantum Hall system	Akira Fukuda	Hyogo College of Medicine		量子物質ナノ構造ラボ運営委員会（橋坂昌幸）
47	202405-GNBXX-0076	ホール係数測定による遷移金属酸化物のキャリア濃度決定	神戸 士郎	山形大学	魏 毓良 吉永 幸弘 大竹 開智 今井 大雅 闫 承程 高橋 祐稀 石川 怜旺	Determining Carrier Concentration of Transition Metal Oxides by Hall Coefficient Measurement	Shiro Kambe	Yamagata University	Wei Yuliang Yukihiro Yoshinaga Kaichi Otake Taiga Imai YAN CHENG CHENG Takahashi Yuki Reo Ishikawa	量子物質ナノ構造ラボ運営委員会（橋坂昌幸）
48	202405-GNBXX-0077	アルゴンイオン照射した酸化チタンナノ構造における電気・磁気特性	原 正大	熊本大学	黒木 玲央 吉田 裕紀	Electrical and magnetic properties of Ar ion irradiated titanium oxide nanostructures	Masahiro Hara	Kumamoto University	Kurogi Reo Yuki Yoshida	量子物質ナノ構造ラボ運営委員会（橋坂昌幸）
49	202405-GNBXX-0078	宙吊りグラフェンのバリスティック伝導	原 正大	熊本大学	柿添 勇成	Ballistic transport in suspended graphene	Masahiro Hara	Kumamoto University	Yusei Kakizoe	量子物質ナノ構造ラボ運営委員会（橋坂昌幸）
50	202405-GNBXX-0108	有機半導体メゾスコピックデバイスの開発	竹谷 純一	東京大学	安部 深月	Development of mesoscopic devices utilizing organic semiconductors	Jun Takeya	Advanced Materials Science, Graduate School of Frontier Sciences	Mizuki Abe	量子物質ナノ構造ラボ運営委員会（橋坂昌幸）

物質合成・評価設備Gクラス / Materials Synthesis and Characterization G Class Research Project

No.	課題番号	課題名	氏名	所属	分担者	Title	Name	Organization	Member of reseach project	担当実験室
1	202406-MCBXG-0090	合金ナノ粒子のキャラクタリゼーション	佐々木 岳彦	東京大学	張 凱朝	Characterization of Alloy Nanoparticles	Takehiko Sasaki	The University of Tokyo	KAICHAO ZHANG	X線測定室、光学測定室、電子顕微鏡室
2	202406-MCBXG-0108	新奇ネマティック超伝導体候補物質の単結晶合成と物性評価	石原 滉大	東京大学	大西 朝登 影山 遥一 六本木 雅生 近藤 玲央名 永島 拓也 渡邊 優希 吉野 勇人 徐 子帆	Single crystal synthesis and characterization of novel nematic superconductor candidates	Kota Ishihara	The University of Tokyo	Asato Onishi Yoichi Kageyama Masaki Roppongi Reona Kondo Takuya Nagashima Watanabe Yuki Yuto Yoshino XU ZIFAN	X線測定室、電磁気測定室
3	202404-MCBXG-0094	LuInCo4の磁気構造変化に伴う磁歪	和氣 剛	京都大学		Magnetostriction associated with magnetic structure change in LuInCo4	Takeshi Waki	Kyoto University		X線測定室
4	202405-MCBXG-0056	層状水和物結晶の育成と結晶構造解析	野村 肇宏	静岡大学		Crystal growth and characterization of layered hydrates	Toshihiro Nomura	Shizuoka Univeristy		X線測定室
5	202405-MCBXG-0086	新規複合アニオン固体電解質の開発	矢島 健	名古屋大学	越田 耕平 佐藤 大介	Exploring novel mixed anion solid electrolytes	Takeshi Yajima	Nagoya University	Kouhei Koshita sato taisuke	X線測定室
6	202405-MCBXG-0088	高イオン伝導率を有する固体電解質のイオン伝導機構解明	矢島 健	名古屋大学	島 颯一 佐藤 大介	Conduction mechanism of a solid electrolyte with high ionic conductivity	Takeshi Yajima	Nagoya University	Shima Souichi sato taisuke	X線測定室
7	202405-MCBXG-0095	MgCo2の磁気構造変化に伴う磁歪の可能性	和氣 剛	京都大学		Possible magnetostriction associated with magnetic structure change in MgCo2	Takeshi Waki	Kyoto University		X線測定室
8	202406-MCBXG-0106	Co基ホイスラー合金におけるマルテンサイト変態材料の探索	重田 出	鹿児島大学		Search for materials with the Martensitic transformation in Co-based Heusler alloys	Iduru Shigeta	Kagoshima University		X線測定室
9	202406-MCBXG-0112	強誘電性ニオブおよびタンタル酸化物の結晶構造解析	山本 文子	芝浦工業大学		Crystal structure analysis of ferroelectric niobates and tantalates	Ayako Yamamoto	Shibaura Institute of Technology		X線測定室
10	202406-MCBXG-0113	磁性体における新規素励起の探索	水上 雄太	東北大学	大野 綾太郎	Search for novel elementary excitations in magnetic materials	Yuta Mizukami	Tohoku University	ryotaro ohno	X線測定室
11	202405-MCBXG-0083	高温高圧水を利用した金属酸化物微粒子の二段階合成	秋月 信	東京大学	高橋 陸人	Dual-stage synthesis of metal oxide nanoparticles in hot compressed water	Makoto Akizuki	The University of Tokyo	Takahashi Rikuto	X線測定室、化学分析室、電子顕微鏡室
12	202405-MCBXG-0059	欠損スピネル化合物の構造と物性の解明	鬼頭 俊介	東京大学	西田 祥太 YAN ZHICHEN 遠山 悠大 石内 優徳 山田 詩音 宝 迪	Elucidation of the crystal structure and physical properties of lacunar spinel compounds	Shunsuke Kitou	The University of Tokyo	Shota Nishida ZHICHEN YAN Yudai Toyama Yutoku Ishiuchi Shion Yamada bao di	X線測定室、電磁気測定室

13	202406-MCBXG-0103	反転対称心のない磁性絶縁体の磁気超構造の外場駆動	有馬 孝尚	東京大学	SU DAN) 徳永 祐介 西田 祥太 YAN ZHICHEN 鬼頭 俊介 遠山 悠大 石内 優徳 山田 詩音 宝 迪	Field-Effect on Nanometric Magnetic Objects in Noncentrosymmetric Magnetic Insulators	Taka-hisa Arima	The University of Tokyo	DAN SU Yusuke Tokunaga Shota Nishida ZHICHEN YAN Shunsuke Kitou Yudai Toyama Yutoku Ishiuchi Shion Yamada bao di	X線測定室、電磁気測定室
14	202405-MCBXG-0071	超臨界水中でのバイオマスからの水素生成に寄与する Ni/MgO-La2O3触媒の合成	布浦 鉄兵	東京大学	李 磊	Synthesis of Ni/MgO-La2O3 catalyst for H2 production from biomass in supercritical water	Teppei Nunoura	The University of Tokyo	Lei LI	X線測定室、電子顕微鏡室
15	202405-MCBXG-0068	リグニンの有用化合物への連続変換を可能にする固体触媒及び反応条件の検討	布浦 鉄兵	東京大学	堂脇 大志	Study on solid catalysts and reaction conditions for continuous lignin conversion into valuable chemicals	Teppei Nunoura	The University of Tokyo	Taishi Dowaki	X線測定室、化学分析室
16	202405-MCBXG-0067	不均一系触媒による超臨界水ガス化を利用したフルオロキノロン系抗生物質の分解とその生成物の毒性評価	布浦 鉄兵	東京大学	朱 凌嬌	Degradation of fluoroquinolone antibiotics using supercritical water gasification with heterogeneous catalyst and its products toxicity evaluation	Teppei Nunoura	The University of Tokyo	ZHU LINGJIAO	X線測定室、化学分析室、光学測定室、電子顕微鏡室
17	202405-MCBXG-0079	Nd 系充填スクッテルダイト化合物の高圧合成と異常物性	関根 ちひろ	室蘭工業大学	渡辺 陸人 尾崎 蒼空 野呂 翼 藤田 優音	High-pressure synthesis and anomalous properties of Nd-based filled skutterudite compounds	Chihiro Sekine	Muroran Institute of Technology	Rikuto Watanabe Sora Ozaki Tsubasa Noro Fujita Yuto	高圧合成室
18	202406-MCBXG-0091	高温高圧実験による地球深部における鉄炭酸塩と水との反応の解明	飯塚 理子	早稲田大学		High pressure and high temperature experimental studies on reaction between iron carbonates and water in deep earth	Riko Iizuka-Oku	Waseda University		高圧合成室
19	202406-MCBXG-0110	新規3d遷移金属ケイ化物の高圧合成と物性評価	佐々木 拓也	名古屋大学	北原 拓海 田中 洸史朗	High-pressure synthesis and physical properties of novel 3d transition-metal silicides	Takuya Sasaki	Nagoya University	Kitahara Takumi Tanaka Koshiro	高圧合成室
20	202405-MCBXG-0057	層状ニッケル酸化物における圧力誘起超伝導の探索	河底 秀幸	東京都立大学	彭 芋鑫	Exploration of pressure-induced superconductivity in layered nickelates	Hideyuki Kawasoko	Tokyo Metropolitan University	peng yuxin	高圧測定室
21	202405-MCBXG-0075	反強磁性体TbGa6の圧力効果	大貫 惇睦	東京都立大学	本多 史憲（九州大学） 三宅 雅尭	Effect of pressure on an antiferromagnet TbGa6	Yoshichika Onuki	Tokyo Metropolitan University	Fuminori Honda (Kyushu University) Masataka Miyake	高圧測定室
22	202405-MCBXG-0114	希土類三元化合物の高圧物性測定	繁岡 透	山口大学	内間 清晴（学校法人沖縄キリスト教学院・沖縄キリスト教短期大学）	High pressure measurements of physical property on the rare earth ternary compounds	Toru Shigeoka	Yamaguchi University	Kiyoharu Uchima (Okinawa Christian Institute Okinawa christian junior College)	高圧測定室

23	202406-MCBXG-0098	Eu2+状態を持つEu化合物の高圧下における電子状態の研究	本多 史憲	九州大学アイソトープ統合安全管理センター	大貫 惇睦（東京都立大学） 松田 達磨（東京都立大学） 三宅 雅尭（東京都立大学）	Electronic properties of Eu compounds with Eu2+ state under high pressures	Fuminori Honda	Central Institute of Radioisotope Science and Safety Management, Kyushu University	Yoshichika Onuki (Tokyo Metropolitan University) Tatsuma D. Matsuda (Tokyo Metropolitan Unversity) Masataka Miyake (The Tokyo Metropolitan University)	高圧測定室
24	202406-MCBXG-0111	非対称ドナー分子からなる空間反転対称性を持たない有機導体の超高圧下物性研究	谷口 弘三	埼玉大学	小林 拓矢（埼玉大学） 山田 英寿（埼玉大学） 八谷 司（埼玉大学） 関根 俊介（埼玉大学）	Research on the physical properties of noncentrosymmetric organic conductors composed of asymmetric donor molecules under ultrahigh pressures	Hiromi Taniguchi	Saitama University	Takuya Kobayashi (Saitama University) Yamada Hidetoshi (Saitama University) Tsukasa Hachiya (Saitama University) Shunsuke Sekine (Saitama University)	高圧測定室
25	202404-MCBXG-0053	月資源現地利用を目指したレーザーによるアルミナ還元	高崎 大吾	東京大学	渡邊 真隆 峯松 涼 Christen Lucas-Brian Han Minwoo 藤森 蒼天 大日 勇海 山上 尋大	Laser alumina reduction toward utilization of lunar resources	Daigo Takasaki	The University of Tokyo	watanabe masataka Ryo Minematsu Lucas-Brian Christen Han Minwoo Aoma Fujimori Isami Dainichi Hiroto Yamakami	電子顕微鏡室
26	202405-MCBXG-0062	窒化物磁性材料の構造解析	齋藤 哲治	千葉工業大学		Study of magnetic nitrides	Tetsuji Saito	Chiba Institute of Technology		電子顕微鏡室
27	202405-MCBXG-0063	補償磁性とトポロジカルな電子構造による機能性材料の探索	酒井 明人	東京大学	上杉 良太 肥後 友也 朝倉 海寛 梶原 悠人 黒沢 駿一郎 段 之宜 対馬 湧太郎 松本 卓也 蘇 杭 董 柏寛	functional material based on the compensated magnetism and topological electronic structure	Akito Sakai	The University of Tokyo	Ryota Uesugi Tomoya Higo Mihiro Asakura yuto kajiwara Shunichiro Kurosawa Zhiyi Duan Yutaro Tsushima Takuya Matsumoto Hang Su TUNG Po-Kuan	電子顕微鏡室
28	202405-MCBXG-0064	セラミックスナノ粒子の連続製造技術開発	陶 究	産業技術総合研究所		Development of continuous process for ceramics nanoparticles production	Kiwamu Sue	AIST		電子顕微鏡室
29	202405-MCBXG-0104	電荷移動スピン転移を起こすコア・シェル型プルシアンブルー類似体のTEM観測	糸井 充穂	東京都市大学		Direct observation of Charge Transfer Coupled Spin Transition for Core-Shell Prussian blue analogues by TEM measurement	Miho Itoi	Tokyo City University		電子顕微鏡室

30	202406-MCBXG-0096	高度に制御された凝縮相と高圧非平衡プラズマの相互作用による金属酸化物及びカーボン微粒子の合成の研究	宗岡 均	東京大学	小池 健 高畑 麟太郎	Syntheses of metal oxides and carbonaceous particles by interaction between highly controlled condensed phases and high-pressure non-equilibrium plasmas	Hitoshi Muneoka	The University of Tokyo	Takeru Koike Rintaro Takahata	電子顕微鏡室
31	202404-MCBXG-0052	非磁性有機無機ハイブリッド層状物質におけるスピン偏極輸送現象の電気化学的制御	黄 柏融	東京科学大学		Electrochemical manipulation of spin-polarized charge transport in nonmagnetic organic-inorganic hybrid layered materials	Po-Jung Huang	Institute of Science Tokyo		電磁気測定室
32	202405-MCBXG-0055	Sm1-xCaxFeO3-δ (0.1≦x≦0.9) の高温における磁性と熱電特性に関する研究	中津川 博	横浜国立大学		Magnetism and thermoelectric properties at high temperature in Sm1-xCaxFeO3-δ (0.1≦x≦0.9)	Hiroshi Nakatsugawa	Yokohama National University		電磁気測定室
33	202405-MCBXG-0065	ホイスラー化合物Fe3-xMnxSiの磁気転移の研究	廣井 政彦	鹿児島大学		Study on magnetic transitions in Heusler compound Fe3-xMnxSi	Masahiko HIROI	Kagoshima University		電磁気測定室
34	202405-MCBXG-0069	オフカット基板に成長させたFe(Se,Te)薄膜の電磁異方性	飯田 和昌	日本大学		Electromagnetic anisotropy of Fe(Se,Te) grown on vicinal substrates	Kazumasa Iida	Nihon University		電磁気測定室
35	202405-MCBXG-0081	電気伝導測定によるホウ素ドープアモルファス炭素膜の金属化の検証	村岡 祐治	岡山大学	中村 匠汰	Verification of metallization for the boron-doped amorphous carbon films by resistivity measurements	Yuji Muraoka	Okayama Univ.	Shota Nakamura	電磁気測定室
36	202405-MCBXG-0082	遷移金属酸化物にお ける磁化率の温度依存性	神戸 士郎	山形大学	魏 毓良 吉永 幸弘 大竹 開智 今井 大雅 闫 承程 髙橋 祐稀 石川 怡旺	Temperature dependence of magnetic susceptibility in transition metal oxides	Shiro Kambe	Graduate School of Science and Engineering, Yamagata University	Wei Yuliang Yukihiro Yoshinaga Kaichi Otake Taiga Imai YAN CHENG CHENG Takahashi Yuki Reo Ishikawa	電磁気測定室
37	202405-MCBXG-0089	酸化チタンナノシートから変換したナノ構造における磁化測定	原 正大	熊本大学	黒木 玲央 吉田 裕紀	Magnetization measurement of nanostructures converted from titanium oxide nanosheets	Masahiro Hara	Kumamoto University	Kurogi Reo Yuki Yoshida	電磁気測定室
38	202406-MCBXG-0100	有機無機ハイブリッド量子物質の物性評価	原口 祐哉	東京農工大学	千野根 広大 久米田 理桜	Evaluation of Physical Properties of Organic-Inorganic Hybrid Quantum Materials	Yuya Haraguchi	Tokyo University of Agriculture and Technology	Kota Chinone Rio Kumeda	電磁気測定室
39	202406-MCBXG-0101	粘土鉱物構造を有する２次元磁性体におけるスピン状態の解明	原口 祐哉	東京農工大学	伊藤 正明 北村 昌大	Spin states in two-dimensional magnetic materials with clay mineral structures	Yuya Haraguchi	Tokyo University of Agriculture and Technology	Masaaki Ito masahiro kitamura	電磁気測定室
40	202406-MCBXG-0105	高スピン分極ホイスラー合金の磁気特性のスピンゆらぎ理論による解析に関する研究	重田 出	鹿児島大学		Study on analysis of magnetic properties for highly spin-polarized Heusler alloys by the spin fluctuation theory	Iduru Shigeta	Kagoshima University		電磁気測定室
41	202406-MCBXG-0116	鉄系超伝導体に対する各種化学処理効果の検証	栗原 綾佑	東京理科大学	矢口 宏 太田 知孝 袴田 怜志	Chemical processing effects on iron-based superconductors	Ryosuke Kurihara	Tokyo University of Science	Hiroshi Yaguchi Ota Tomotaka Satoshi Hakamada	電磁気測定室
42	202405-MCBXG-0077	Ni2In型強磁性体の自発磁化の圧力依存性	安達 義也	山形大学	荻野 隆太	Pressure dependence of the spontaneous magnetization for Ni2In-type ferromagnets	Yoshiya Adachi	Yamagata University	Ryuta Ogino	電磁気測定室、高圧測定室

43	202406-MCBXG-0115	トポロジカル近藤絶縁体SmSの高圧下磁化測定	水戸 毅	兵庫県立大学	西川 智稀 吉田 章吾（東京理科大学）	High-pressure susceptibility measurements of topological Kondo insulator SmS	Takeshi Mito	University of Hyogo	Tomoki Nishikawa (University of Hyogo) Shogo Yoshida (Tokyo University of Science)	電磁気測定室、高圧測定室
44	202405-MCBXG-0060	希土類オルソフェライト単結晶試料の合成	渡邉 紳一	慶應義塾大学	安高 幸佑	Synthesis of Rare-Earth Orthoferrite Single Crystal Samples	Shinichi Watanabe	Keio University	Kohsuke Ataka	物質合成室、X線測定室
45	202405-MCBXG-0061	アシンメトリ量子物質の純良単結晶育成と物性評価	松平 和之	九州工業大学	運天 楓	High-quality single crystal growth of Asymmetric Quantum Matters and evaluation of their physical properties	KAZUYUKI MATSUHIRA	Kyushu Institute of Technology	Unten Kaede	物質合成室、X線測定室
46	202405-MCBXG-0070	常磁性希土類化合物における電気磁気効果	阿部 伸行	日本大学		Magnetoelectric effect in paramagnetic rare earth compounds	Nobuyuki Abe	Nihon University		物質合成室、X線測定室
47	202405-MCBXG-0087	高濃度リチウム含有新規固体電解質の開発	矢島 健	名古屋大学	松浦 信介 佐藤 大介	Exploring novel solid electrolytes with high lithium concentration	Takeshi Yajima	Nagoya University	Matsuura Shinsuke sato taisuke	物質合成室、X線測定室
48	202406-MCBXG-0102	スピン軌道結合金属A2Re2O7 （A = Ca, Pb）の合成と相転移の研究	平井 大悟郎	名古屋大学	草ノ瀬 優香	Synthesis and phase transition of spin-orbit coupled metal A2Re2O7（A = Ca, Pb）	Daigorou Hirai	Nagoya University	kusanose yuka	物質合成室、電磁気測定室
49	202406-MCBXG-0107	4f 2電子系立方晶PrMgNi4-xCuxの作製とPrMg1-xCdxNi4の比熱測定	草ノ瀬 優香	名古屋大学		Sample preparation for a cubic 4f 2 system PrMgNi4-xCux and specific heat measurement of PrMg1-xCdxNi4	kusanose yuka	Nagoya University		物質合成室、電磁気測定室

物質合成・評価設備Uクラス / Materials Synthesis and Characterization U Class Research Project

No.	課題番号	課題名	氏名	所属	分担者	Title	Name	Organization	Member of reseach project	担当実験室
1	202410-MCBXU-0123	高転移温度オルタマグネット金属の探索	北折 暁	東京大学	関 真一郎 ヌイエン ドウイ　カーン 井上 裕貴 荒木 那巨 野田 源文 山内 健聖 石岡 陸	Exploration of high-temperature metallic altermagnets	Aki Kitaori	The University of Tokyo	Shinichiro Seki Nguyen Duy Khanh Hiroki Inoue Araki Tomonao Noda Motofumi Kensei Yamauchi Riku Ishioka	X線測定室
2	202410-MCBXU-0125	反転中心対称性の破れた有機無機ハイブリッド層状物質におけるゼロバイアス光電流とシフト電流の評価	黄 柏融	東京科学大学	成瀬 泉心 紀 麟飛 松澤 亮矢）	Evaluation of zero-bias photocurrent and shift current in noncentrosymmetric organic-inorganic hybrid layered materials	Po-Jung Huang	Institute of Science Tokyo	Ichi Naruse Linfei Ji Ryoya Matsuzawa	X線測定室
3	202410-MCBXU-0122	三次元的フェルミ面を持つと期待される分子結晶の固体分光	内藤 俊雄	愛媛大学	池田 美沙子	Optical study on molecular crystals possibly with three-dimensional Fermi surfaces	Toshio Naito	Ehime University	Misako Ikeda	光学測定室
4	202409-MCBXU-0120	インジウム酸水酸化物の高速プロトン伝導性の解明	山﨑 智之	東北大学多元物質科学研究所		Unraveling fast protonic conduction in indium oxyhydroxide	Tomoyuki Yamasaki	Institute of Multidisciplinary Research for Advanced Materials Tohoku University		高圧合成室
5	202409-MCBXU-0121	層状ディラック磁性体の磁気秩序における応力効果の解明	酒井 英明	大阪大学	田中 健護	Impact of uniaxial pressure on a layered Dirac magnet	Hideaki Sakai	Osaka University	tanaka kengo	電磁気測定室

国際超強磁場科学施設 / International MegaGauss Science Laboratory

No.	課題番号	課題名	氏名	所属	分担者	Title	Name	Organization	Member of reseach project	担当所員
1	202405-HMBXX-0054	低次元量子磁性体の磁化過程	菊池 彦光	福井大学		Magnetization of low dimensional quantum magnets	Hikomitsu Kikuchi	University of Fukui		金道 浩一
2	202405-HMBXX-0055	非従来型超伝導をもたらす量子臨界状態の輸送特性	横山 淳	茨城大学	小泉 遼介 高橋 哲平 富士本 駿	Transport properties in quantum critical superconductors	Makoto Yokoyama	Ibaraki University	Ryosuke Koizumi Teppei Takahashi Fujimoto Hayao	金道 浩一
3	202405-HMBXX-0070	ハニカム化合物RuBr3単結晶の磁気トルク測定	今井 良宗	東北大学	南條 拓 李 愛琳	Magnetic torque measurement of honeycomb compound RuBr3 single crystal	Yoshinori Imai	Tohoku university	Hiroki Nanjo Erin Lee	金道 浩一
4	202406-HMBXX-0078	MnNiSi-RuNiSi系化合物の磁気熱量効果	伊藤 昌和	鹿児島大学	間野 遥菜 中里 尚貴	Magnet-caloric effect of the MnNiSi-RuNiSi system	Masakazu Ito	Kagoshima University	Haruna Mano Nakazato Naoki	金道 浩一
5	202406-HMBXX-0089	有機伝導体表面における二次元超伝導層の強磁場渦糸状態	杉浦 栞理	東北大学		High magnetic field vortex phases in 2D superconducting layer on the organic conductors	Shiori Sugiura	Tohoku University		金道 浩一
6	202410-HMBXX-0108	V2O3ナノ結晶の抵抗率測定	石渡 洋一	佐賀大学		Resistivity measurements of V2O3 nanocrystals	Yoichi Ishiwata	Saga University		金道 浩一
7	202311-HMBXX-0020	一巻きコイル法を用いたホイスラー合金NiCoMnGaの強磁場磁化測定	木原 工	東北大学	許 畠 池田 暁彦（電気通信大学）	High Field Magnetization Measurements for Heusler Alloy NiCoMnGa Using Single Turn Coil Method	Takumi Kihara	Research Institute for Interdisciplinary Science, Okayama University	Xiao Xu Akihiko Ikeda (University of Electro-Communications)	松田 康弘
8	202405-HMBXX-0062	開殻分子の光学特性に対する強磁場効果に関する研究	草本 哲郎	大阪大学		Studies on the optical properties of open-shell molecules under strong magnetic fields	Tetsuro Kusamoto	Osaka University		松田 康弘
9	202405-HMBXX-0063	フラストレート格子系の多量体形成と原子変位に対する強磁場効果	花咲 徳亮	大阪大学		High magnetic field effect on multimer formation and atomic displacement in frustrated lattice systems	Noriaki Hanasaki	Osaka University		松田 康弘
10	202406-HMBXX-0094	強磁場による分子軌道結晶の破壊に関する研究	平井 大悟郎	名古屋大学	井口 寛太	Breaking of molecular orbital crystals by high magnetic fields	Daigorou Hirai	Nagoya University	Inokuchi Kanta	松田 康弘
11	202406-HMBXX-0097	強磁場印加による魔法角ツイストグラフェンの創成	瀬尾 優太	生産技術研究所		Generating magic angle twisted bilayer graphene by applying high magnetic fields	Yuta Seo	Institute of Industrial Science		松田 康弘
12	202312-HMCXX-0036	FeCr錯体におけるスピン転移の詳細な研究	呉 樹旗	九州大学	蘇 勝群	Detailed investigations of spin transition in [FeCr] complexes	Shu-Qi Wu	Kyushu University	SHENGQUN SU	徳永 将史
13	202405-HMBXX-0052	高移動度熱電半金属における量子振動観測	中埜 彰俊	名古屋大学	長江 広晴 服部 奈菜子	Observation of quantum oscillation in a high mobility thermoelectric semimetal	Akitoshi Nakano	Nagoya university	Hiroharu NAGAE Nanako Hattori	徳永 将史
14	202405-HMBXX-0061	新規希土類化合物Re2Al3Ge4(Re:希土類元素)の磁気特性の解明	横井 滉平	学習院大学	山岸 敬太	Magnetic properties of new Lanthanoid compounds Re2Al3Ge4	Kohei Yokoi	Gakushuin University	Keita Yamagishi	徳永 将史
15	202405-HMBXX-0065	UTe2とその類似結晶構造を持つウラン化合物の強磁場物性	三宅 厚志	東北大学	青木 大	High-field physical properties of UTe2 and its related uranium compounds	Atsushi Miyake	Tohoku University	Dai Aoki	徳永 将史
16	202405-HMBXX-0066	強磁性/常磁性半導体ヘテロ接合における量子輸送現象	レデウック アイン	東京大学	白谷 治憲 伍 柏霖 原 拓嵩	Quantum transport phenomena in ferromagnetic/nonmagnetic semiconductor heterostructures	Le Duc Anh	The University of Tokyo	Harunori Shiratani WU BOLIN Hara Hirotaka	徳永 将史
17	202405-HMBXX-0067	鉄カルコゲナイド超伝導体における磁気光学イメージングによる磁場分布の測定	矢口 宏	東京理科大学	栗原 綾佑 太田 知孝 袴田 怜志	Investigation of magnetic-field distributions in iron-chalcogenide superconductors using an MO imaging technique	Hiroshi Yaguchi	Tokyo University of Science	Ryosuke Kurihara Ota Tomotaka Satoshi Hakamada	徳永 将史

18	202405-HMBXX-0068	RSb2(R: 希土類元素)磁場誘起磁化容易軸交換現象の解明	三宅 厚志	東北大学	青木 大 早坂 龍太	Study of magnetic field-induced magnetization-easy axis switching phenomena in RSb2 (R = rare earths)	Atsushi Miyake	Tohoku University	Dai Aoki Ryuta Hayasaka	徳永 将史
19	202406-HMBXX-0075	層状ディラック電子系物質の応力下での強磁場測定	酒井 英明	大阪大学	山下 淳志 田中 健護	Study of high-field transport for layered Dirac materials under strain	Hideaki Sakai	Osaka University	Atsushi Yamashita tanaka kengo	徳永 将史
20	202406-HMBXX-0086	らせん磁性体の強磁場下での物性	香取 浩子	東京農工大学	原口 祐哉	Physical properties of helical magnetic materials under high magnetic fields	Hiroko Katori	Tokyo University of Agriculture and Technology	Yuya Haraguchi	徳永 将史
21	202406-HMBXX-0101	超音波計測による強相関電子系の磁場中量子状態と多極子効果	栗原 綾佑	東京理科大学	矢口 宏 袴田 怜志	Ultrasonic study of high-field quantum states and multipole effects in strongly-correlated electron systems under pulsed-magnetic fields	Ryosuke Kurihara	Tokyo University of Science	Hiroshi Yaguchi Satoshi Hakamada	徳永 将史
22	202406-HMBXX-0102	超伝導臨界磁場測定による鉄系超伝導体Fe(Te,S)の各種化学処理効果の検証	栗原 綾佑	東京理科大学	矢口 宏 太田 知孝 袴田 怜志	Chemical processing effects on iron-based superconductor Fe(Te,S) evaluated by upper critical field	Ryosuke Kurihara	Tokyo University of Science	Hiroshi Yaguchi Ota Tomotaka Satoshi Hakamada	徳永 将史
23	202409-HMBXX-0104	Exchange bias in ferromagnetic and spin glass systemFe0.33TaSe2.	Nayak Jayita	Indian Institute of Technology, Kanpur, India		Exchange bias in ferromagnetic and spin glass systemFe0.33TaSe2.	Jayita Nayak	Indian Institute of Technology, Kanpur, India		徳永 将史
24	202409-HMBXX-0110	オクタシアノ系分子磁性体における光磁気ドメインのKerr効果顕微鏡観察	所 裕子	筑波大学	長島 俊太郎	Observation of magnetic domain in photo-induced magnetization of octacyano-based molecular magnet using Kerr effect microscopy	Hiroko Tokoro	University of Tsukuba	Shuntaro Nagashima	徳永 将史
25	202412-HMBXX-0111	六方晶QS型鉄酸化物 Ba2Sn2+xFe10.67-1.33xO22の強磁場磁気特性	神島 謙二	埼玉大学	落合 響	Magnetic properties of hexagonal QS-type iron oxides Ba2Sn2+xFe10.67-1.33xO22 under high magnetic fields	Kenji Kamishima	Saitama University	Hibiki Ochiai	徳永 将史
26	202405-HMBXX-0059	ロングパルス磁場を利用したNMR測定装置開発	井原 慶彦	北海道大学	神田 朋希	Development of NMR system for long pulsed magnet	Yoshihiko Ihara	Hokkaido University	Tomoki Kanda	小濱 芳允
27	202405-HMBXX-0069	Specific heat and magnetization measurements on CeIrIn5	Sheikin Ilya	LNCMI Grenoble	Sarrade Jeremy	Specific heat and magnetization measurements on CeIrIn5	Ilya Sheikin	LNCMI Grenoble	Jeremy Sarrade	小濱 芳允
28	202406-HMBXX-0096	三角格子反強磁性体YbCuGeの強磁場磁化測定	荒木 幸治	防衛大学校		High field magnetization measurements of a triangular lattice antiferromagnet YbCuGe	Koji Araki	National Defense Academy		宮田 敦彦

大阪大学大学院理学研究科附属先端強磁場科学研究センター / Center for Advanced High Magnetic Field Science, Graduate School of Science, Osaka University

No.	課題番号	課題名	氏名	所属	分担者	Title	Name	Organization	Member of reseach project	担当所員
1	202405-HMOXX-0060	ナノ構造界面を利用した異常ネルンスト係数増大	中村 芳明	大阪大学	石部 貴史 北浦 怜旺奈 小松原 祐樹	Enhancement of anomalous Nernst coefficient using the nanoscale interfaces	Yoshiaki Nakamura	The University of Osaka	Takafumi Ishibe reona kitaura Komatsubara Yuki	萩原 政幸
2	202405-HMOXX-0099	磁気フラストレーション化合物GdAl3の強磁場磁化	竹内 徹也	大阪大学	大貫 惇睦（東京都立大学）	High-Field Magnetization in Magnetic Frustration Compound GdAl3	Tetsuya Takeuchi	Osaka University	Yoshichika Onuki	萩原 政幸
3	202406-HMOXX-0072	秩序型ハニカムネットワークを持つBaPtSbの超伝導状態についての研究	工藤 一貴	大阪大学		Study on the superconducting state of BaPtSb with a PtSb ordered honeycomb network	Kazutaka Kudo	Osaka University		萩原 政幸
4	202406-HMOXX-0073	SeドープPtBi2の超伝導状態についての研究	工藤 一貴	大阪大学		Study on the superconducting state of Se-doped PtBi2	Kazutaka Kudo	Osaka University		萩原 政幸
5	202406-HMOXX-0074	秩序型ラーベス相化合物の超伝導物質開発	工藤 一貴	大阪大学		Development of novel superconductors with ordered Laves phase structures	Kazutaka Kudo	Osaka University		萩原 政幸

6	202406-HMOXX-0076	ビスマス二次元層を有する新規層状磁性体の磁気特性	酒井 英明	大阪大学		Study of magnetic properties for layered magnets with a 2D Bi layer	Hideaki Sakai	Osaka University		萩原 政幸
7	202406-HMOXX-0077	マイクロ波加熱合成した無機磁性材料の強磁場物性	浅野 貴行	福井大学	I Putu Abdi Karya Muhammad Al Jalali 仲川 晃平 岩本 拓馬	Magnetic properties under high magnetic fields of inorganic magnetic materials synthesized by microwave heating	Takayuki Asano	University of Fukui	I Putu Abdi Karya Muhammad Al Jalali Kohei Nakagawa Takuma Iwamoto	萩原 政幸
8	202406-HMOXX-0079	非磁性エレメントを添加した電気磁気反強磁性Cr2O3薄膜の界面磁化検出	白土 優	大阪大学		Detection of interfacial magnetic moment in magnetoelectric Cr2O3 thin film with various doping nonmagnetic elements	Yu Shiratsuchi	Osaka University		萩原 政幸
9	202406-HMOXX-0080	カプセル蛋白質（encapsulin from Pyrococcus furiosus）内に合成した磁性ナノ粒子の磁気的性質	白土 優	大阪大学		Magnetic properties of magnetic nanoparticles synthesized in encapsulin from Pyrococcus furiosus	Yu Shiratsuchi	Osaka University		萩原 政幸
10	202406-HMOXX-0081	非従来型フェロイック秩序を内包する磁性体の電気磁気特性評価	木村 健太	大阪公立大学		Magnetic and electrical characterization of magnetic materials with unconventional ferroic order	Kenta Kimura	Osaka Metropolitan University		萩原 政幸
11	202406-HMOXX-0082	強いスピン-軌道相互作用を活かした酸化物スピントロニクス	上田 浩平	大阪大学	松野 丈夫 塩貝 純一	Oxide spintronics utilizing strong spin-orbit coupling	Kohei Ueda	Osaka University	Jobu Matsuno Junichi Shiogai	萩原 政幸
12	202406-HMOXX-0083	パルス強磁場を用いた高圧下THz ESR装置の開発	櫻井 敬博	神戸大学		Development of high pressure THz ESR system using pulsed high magnetic field	Takahiro Sakurai	Kobe University		萩原 政幸
13	202406-HMOXX-0084	層状磁性半導体CeTe2-xSbxの異方性巨大磁気抵抗効果の研究	村川 寛	大阪大学		Research for the giant anisotropic magnetoresistance in the magnetic semiconductor CeTe2-xSbx	Hiroshi Murakawa	Osaka University		萩原 政幸
14	202406-HMOXX-0085	多孔質シリカガラス中に形成された遷移金属化合物の磁性	本多 善太郎	埼玉大学		Magnetic properties of transition metal compounds formed in the pores of porous silica glass	Zentaro Honda	Saitama University		萩原 政幸
15	202406-HMOXX-0087	多量体形成や原子変位を起こすフラストレート格子系物質の磁気特性	花咲 徳亮	大阪大学		Magnetic properties in frustrated lattice systems having multimer formation and atomic displacement	Noriaki Hanasaki	Osaka University		萩原 政幸
16	202406-HMOXX-0090	S = 1/2 一次元 Ising 型反強磁性体 CsCoCl3 の横磁場中の磁気励起	木村 尚次郎	東北大学		High field ESR measurements of the S = 1/2 one-dimensional Ising-like antiferromagnet CsCoCl3 in transverse fields	Shojiro Kimura	Tohoku University		萩原 政幸
17	202406-HMOXX-0091	鉄カルコゲナイド超伝導体微細構造のパルス強磁場下輸送特性	掛谷 一弘	京都大学	北野 晴久（青山学院大学）	Transport measurements on micro-structured iron chalcogenide superconductors under pulsed high magnetic fields	Itsuhiro Kakeya	Kyoto University	Haruhisa Kitano (Aoyama Gakuin University)	萩原 政幸
18	202406-HMOXX-0092	高異方性磁界を有する磁石の磁気特性評価	平山 悠介	産業技術総合研究所		Evaluation of magnetic properties for magnets with high anisotropy	Yusuke Hirayama	National Institute of Advanced Industrial Science and Technology		萩原 政幸
19	202406-HMOXX-0100	Cu-Coフェライトの磁歪特性	藤枝 俊	島根大学	小杉 静花（大阪大学）	Magnetostrictive properties of Cu-Co ferrites	Fujieda Shun	Shimane University	Kosugi Shizuka (Osaka University)	萩原 政幸

20	202409-HMOXX-0107	磁化率の違いを用いた物質の分離手法の開発	秋山 庸子	大阪大学		Development of a method for separating materials using differences in magnetic susceptibility	Yoko Akiyama	Osaka University		萩原 政幸

強磁場コラボラトリー / The High Magnetic Field Collaboratory

No.	課題番号	課題名	氏名	所属	分担者	Title	Name	Organization	Member of reseach project	担当所員
1	202311-HMBXX-0040	量子系有機物質群が創り出す新規スピンモデルの強磁場物性	山口 博則	大阪公立大学		High-field magnetic properties of new spin models formed by quantum organic materials	Hironori Yamaguchi	Osaka Metropolitan University		金道 浩一
2	202312-HMCXX-0035	強磁場を用いたPd2MnGa基合金における磁場誘起相変態の実験的調査	宮川 寅矢	東北大学	許 畠 今富 大介	Investigation on magnetic field induced phase transformation behaviors in Pd2MnGa-based alloys under high magnetic fields	Tomoya Miyakawa	Tohoku University	Xiao Xu Daisuke Imatomi	徳永 将史
3	202312-HMCXX-0036	FeCr錯体におけるスピン転移の詳細な研究	許 畠	東北大学	今富 大介	Investigation on metamagnetic transition behaviors of Mn-Zn alloys using high magnetic fields	Xiao Xu	Tohoku University	Daisuke Imatomi	徳永 将史
4	202312-HMCXX-0044	実用超伝導線材の多次元高速分析	土屋 雄司	東北大学		Multidimensional rapid analysis of practical superconducting wires	Tsuchiya Yuji	Tohoku University		小濱 芳允
5	202312-HMCXX-0045	New magnetic phase diagram of ultra-pure UTe2	Marcenat Christophe	Interdisciplinary Research Institute of Grenoble (IRIG), Alternative Energies and Atomic Energy Commission (CEA)		New magnetic phase diagram of ultra-pure UTe2	Christophe Marcenat	Interdisciplinary Research Institute of Grenoble (IRIG), Alternative Energies and Atomic Energy Commission (CEA)		小濱 芳允
6	202311-HMCXX-0041	ソーマチン結晶の磁場効果に関する研究	牧 祥	岡山理科大学		Research on the magnetic field effects in using thaumatin crystals	Syou Maki	Okayama University of Science		萩原 政幸
7	202312-HMCXX-0043	絶縁層に金属絶縁体転移物質を用いた超伝導コイル保護の手法の開発	櫻井 響介	東北大学	土屋 雄司	Development of a method for protecting superconducting magnets using a metal-insulator transition material in the insulation layer	Kyosuke Sakurai	Tohoku university	Tsuchiya Yuji	萩原 政幸

留学研究課題 / External Research Project Long / Short -term）

No.	課題番号	課題名	氏名	所属	分担者	Title	Name	Organization	Member of reseach project	担当所員
1	なし									

No.	課題名	氏名	所属	分担者（共同研究者）	Title	Name	Organization	Member of research project	装置	ビームポート
1	4G-GPTAS（汎用3軸中性子分光器）　IRT課題	那波　和宏	東北大学	Zheng Dongge、 稲垣 麦、 谷口 竣哉、 宮本 明佳、 伊賀 文俊、 You Hyelyn、 曾 焌維、 作田 楓斗、 横山 淳、 吉本 周玄、 田畑 吉計、 加倉井 和久、 Wu Hung-Cheng、 佐藤 卓、 金城 克樹	IRT Project of GPTAS	Kazuhiro Nawa	Tohoku University	Dongge Zheng, Mugi Inagaki, Shunya Yaguchi, Haruka Miyamoto, Fumitoshi Iga, Hyelyn You, Chun Wai Tsang, Futo Sakuda, Makoto Yokoyama, Subaru Yoshimoto, Yoshikazu Tabata, Kazuhisa Kakurai, Hung-Cheng Wu, Taku Sato, Katsuki Kinjo	GPTAS	4G
2	磁気スキルミオン格子の高電流印加に伴う低エネルギー励起の変化の観測	奥山　大輔	高エネルギー加速器研究機構		Observation of the variation of the low energy excitation of the magnetic skyrmion lattice under an electric current flow	Daisuke Okuyama	High energy accelerator research organization		GPTAS	4G
3	反強磁性量子臨界的挙動がもたらす異常超伝導物性	横山　淳	茨城大学	海老澤 秀明、 沢田 芙祐子、 富士本 駿、 小泉 遼介、 高橋 哲平	Anomalous superconducting properties coupled with antiferromagentic quantum criticality	Makoto Yokoyama	Ibaraki University	Hideki Ebisawa, Fuyuko Sawada, Hayao Fujimoto, Ryosuke Koizumi, Teppei Takahashi	GPTAS	4G
4	YFe2O4の分極ースピン相関と巨大磁歪	池田　直	岡山大学	加倉井 和久、 于 洪武、 朴 規相、 松田 里佳子、 矢野 優太、 藤原 孝将、 藤原 孝将	Spin correlation and magnetic striction in YFe2O4	Naoshi Ikeda	Okayama University	Kazuhisa Kakurai, Hongwu Yu, Gyusang Park, Rikako Matsuda, Yuta Yano, Kosuke Fujiwara, Kosuke Fujiwara	GPTAS	4G
5	Ga-Pd-Tb 2/1近似結晶の結晶場励起	那波　和宏	東北大学	You Hyelyn、 作田 楓斗、 佐藤 卓、 金城 克樹	Crystal field excitations of Ga-Pd-Tb 2/1 approximant crystals	Kazuhiro Nawa	Tohoku University	Hyelyn You, Futo Sakuda, Taku Sato, Katsuki Kinjo	GPTAS	4G
6	カゴメ格子反強磁性体におけるトポロジカルマグノンバンド	那波　和宏	東北大学	曾 焌維、 作田 楓斗、 佐藤 卓、 金城 克樹	Topological magnon bands in the kagome antiferromagnet	Kazuhiro Nawa	Tohoku University	Chun Wai Tsang, Futo Sakuda, Taku Sato, Katsuki Kinjo	GPTAS	4G
7	重い電子系超伝導体における超伝導と同時に発現する磁性の解明	金城　克樹	東北大学	佐藤 卓、 那波 和宏	Investigation of magnetism appearing simultaneously with superconductivity in heavy-fermion superconductors	Katsuki Kinjo	Tohoku University	Taku Sato, Kazuhiro Nawa	GPTAS	4G
8	Determination of the long-period incommensurate spin structure in the magnetic iron molybdate Fe2(MnO4)3 at low temperature	Chou　Hsiung	National Sun Yat-sen University		Determination of the long-period incommensurate spin structure in the magnetic iron molybdate Fe2(MnO4)3 at low temperature	Hsiung Chou	National Sun Yat-sen University		GPTAS	4G
9	Strength of electron-phonon scattering induced by Bi-doping in thermoelectric (Ge0.92-ySb0.08Biy)Te (y=0.04 and 0.06) single crystals	Li　Wen-Hsien	National Central University	Wu Hung-Cheng、 Yung Tung-Yuan、 Chen Tai-Cheng、 Tseng Yu-Shan、 Tseng Huei-Yin	Strength of electron-phonon scattering induced by Bi-doping in thermoelectric (Ge0.92-ySb0.08Biy)Te (y=0.04 and 0.06) single crystals	Wen-Hsien Li	Soochow University	Hung-Cheng Wu, Tung-Yuan Yung, Tai-Cheng Chen, Yu-Shan Tseng, Huei-Yin Tseng	GPTAS	4G
10	Investigation of topological phonon dispersion in β-Ga2O3 single crystals	Ok　Jong Mok	Pusan National University	Oh In-Hwan、 Park Sungkyun、 Ji Gwangcheol、 Kim Huiwon、 Choe Byeongcheol、 Park Seonguk、 Mun Yeongdeuk、 Im Suji、 Park Jitae	Investigation of topological phonon dispersion in β-Ga2O3 single crystals	Jong Mok Ok	Pusan National University	In-Hwan Oh, Sungkyun Park, Gwangcheol Ji, Huiwon Kim, Byeongcheol Choe, Seonguk Park, Yeongdeuk Mun, Suji Im, Jitae Park	GPTAS	4G
11	Mapping high energy spin waves in the layered inorganic-organic hybrid perovskite (C6H5CH2CH2NH3)2MnCl4	Beddrich Lukas	Technical University of Munich	Kim Ki-Yeon、 Park Jitae、 Oh In-Hwan、 李 哲虎	Mapping high energy spin waves in the layered inorganic-organic hybrid perovskite (C6H5CH2CH2NH3)2MnCl4	Lukas Beddrich	Forschungszentrum Jülich	Ki-Yeon Kim, Jitae Park, In-Hwan Oh, Chul-Ho Lee	GPTAS	4G

12	Elucidating the diffusive behavior and phonon instability in tin selenide	Wei Pai-Chun	Department of Materials Science and Engineering	Wu Bao-You、 Li Yu-Ju、 Hu Jia-Kai	Elucidating the diffusive behavior and phonon instability in tin selenide	Pai-Chun Wei	Department of Materials Science and Engineering	Bao-You Wu, Yu-Ju Lee, Jia-Kai Hu	GPTAS	4G
13	Revealing the phonon scattering mechanism behind the exceptionally low thermal conductivity in halide double perovskites	Wei Pai-Chun	Department of Materials Science and Engineering	Hsiao Wan-Chun、 Wu Cheng-Chieh、 Wu Bao-You、 Li Yu-Ju、 Hu Jia-Kai	Revealing the phonon scattering mechanism behind the exceptionally low thermal conductivity in halide double perovskites	Pai-Chun Wei	Department of Materials Science and Engineering	Wan-Chun Hsiao, Cheng-Chieh Wu, Bao-You Wu, Yu-Ju Lee, Jia-Kai Hu	GPTAS	4G
14	フラストレート磁性体DyRu2Si2の部分秩序相における低次元的磁気相関の観測	田畑 吉計	京都大学	吉本 周玄	Observation of the low-dimensional spin correlations in the partially-ordered phases of the frustrated magnet DyRu2Si2	Yoshikazu Tabata	Kyoto University	Subaru Yoshimoto	GPTAS	4G
15	Crカゴメ格子における磁性の研究	金城 克樹	東北大学	曾 焌維、 佐藤 卓、 那波 和宏	Investigation of magnetism on Cr-based kagome magnet	Katsuki Kinjo	Tohoku University	Chun Wai Tsang, Taku Sato, Kazuhiro Nawa	GPTAS	4G
16	Pt-Mn 合金における磁気散漫散乱	高橋 美和子	筑波大学		Magnetic diffuse scattering in the fcc magnet Pt-Mn	Miwako Takahashi	Tsukuba University		GPTAS	4G
17	5G PONTAを用いた中性子散乱研究	中島 多朗	東京大学	鈴木 大斗、 山田 詩音、 ヒルシュベルガー マックス、 山田 林介、 榊原 みら乃、 中村 翔太、 福島 優斗、 齋藤 開、 山岡 良太、 浦井 瑞紀、 高木 里奈、 酒井 英明	IRT Project of PONTA	Taro Nakajima	The University of Tokyo	Hiroto Suzuki, Shion Yamada, Max Hirschberger, Rinsuke Yamada, Mirano Sakakibara, Shota Nakamura, Yuto Fukushima, Hiraku Saito, Ryota Yamaoka, Mizuki Urai, Rina Takagi, Hideaki Sakai	PONTA	5G
18	Investigation of magnetic structure of breathing Kagome magnet Nd3Ru4Al12	ヒルシュベルガー マックス	東京大学	山田 林介、 Ranjan Baral Priya、 石原 由貴	Investigation of magnetic structure of breathing Kagome magnet Nd3Ru4Al12	Max Hirschberger	The University of Tokyo	Rinsuke Yamada, Priya Ranjan Baral, Yuki Ishihara	PONTA	5G
19	一軸応力による正方格子遍歴磁性体 EuAl4 の磁気スキルミオン相の制御	巌 正輝	東京大学		Uniaxial stress control of magnetic skyrmion phases in a square-lattice itinerant magnet EuAl4	Masaki Gen	The University of Tokyo		PONTA	5G
20	ブリージングパイロクロア磁性体CuInCr4S8のゼロ磁場基底状態の研究	巌 正輝	東京大学		Investigation on the ground state of the breathing pyrochlore magnet CuInCr4S8	Masaki Gen	The University of Tokyo		PONTA	5G
21	巨大磁気熱量効果を示すHoB2の磁気相転移の起源	寺田 典樹	物質材料研究機構	Larsen Simon	Origin of phase transitions in HoB2 with a giant magnetocaloric effect	Noriki Terada	National Institute for Materials Science	Simon Larsen	PONTA	5G
22	La3Co4Sn13のカイラル構造相転移におけるフォノンソフトニング	岩佐 和晃	茨城大学	高橋 和樹、 小佐野 七菜子、 宮田 一駿、 熊田 隆伸、 鈴木 陽太郎、 鈴村 貫太、 黒澤 航海、 浦本 結稜	Phonon softening at the chiral structure phase transformation of La3Co4Sn13	Kazuaki Iwasa	Ibaraki University	Kazuki Takahashi, Nanako Osano, Kazuma Miyata, Takanobu Kumada, Yotaro Suzuki, Kanta Suzumura, Wataru Kurosawa, Yui Uramoto	PONTA	5G
23	Tb3Co4Sn13の超格子構造相での結晶場分裂準位	岩佐 和晃	茨城大学	高橋 和樹、 小佐野 七菜子、 宮田 一駿、 熊田 隆伸、 鈴木 陽太郎、 鈴村 貫太、 黒澤 航海、 浦本 結稜	Crystalline Electric Field Splitting Levels in the superlattice structure phase of Tb3Co4Sn13	Kazuaki Iwasa	Ibaraki University	Kazuki Takahashi, Nanako Osano, Kazuma Miyata, Takanobu Kumada, Yotaro Suzuki, Kanta Suzumura, Wataru Kurosawa, Yui Uramoto	PONTA	5G
24	偏極回折法によるGaMo4S8の磁気構造決定	有馬 孝尚	東京大学	徳永 祐介、 遠山 悠大	Magnetic Structure Analysis of GaMo4S8 by Polarized Neutron Diffraction	Taka-hisa Arima	The University of Tokyo	Yusuke Tokunaga, Yudai Toyama	PONTA	5G
25	偏極中性子を用いたキラルフォノンとマグノンの結合の研究	有馬 孝尚	東京大学	徳永 祐介、 遠山 悠大	Polarized Neutron Study on Coupling between Chiral Phonon and Magnon	Taka-hisa Arima	The University of Tokyo	Yusuke Tokunaga, Yudai Toyama	PONTA	5G
26	中性子回折による反強磁性体RPt3Al5 (R: 希土類)の磁気構造の研究	本多 史憲	九州大学		Magnetic structure study of antiferromagnet RPt3Al5 using neutron diffraction	Fuminori Honda	Kyushu University		PONTA	5G
27	パイロクロア型Eu2Mo2O7 におけるトポロジカルホール効果と磁気構造探索	福田 光	東京大学		Topological Hall effect and magnetic structure exploration in Pyrochlore-type Eu2Mo2O7	Hikaru Fukuda	RIKEN		PONTA	5G

28	新規Ce系層状物質の磁気構造の解明	酒井　英明	大阪大学	山下 淳志	Study of the magnetic structure for a novel Ce-based layered material	Hideaki Sakai	Osaka University	Atsushi Yamashita	PONTA	5G
29	巨大な仮想磁場を生じる反強磁性体の磁気構造解析	関　真一郎	東京大学	山内 健聖、 小椋 悠樹、 北折 暁	Magnetic structure analysis of antiferromagnets hosting giant emergent magnetic field	Shinichiro Seki	The University of Tokyo	Kensei Yamauchi, Yuki Ogura, Aki Kitaori	PONTA	5G
30	TbCaAl3O7の電気磁気効果の起源についての研究	阿部　伸行	日本大学		Study on the origin of the magnetoelectric effect of TbCaAl3O7	Nobuyuki Abe	Nihon University		PONTA	5G
31	多段階の磁気相転移を示すEu系金属間化合物の磁気構造解析	高木　里奈	東京大学	顧 思怡、 浦井 瑞紀	Magnetic structure analysis of Eu-based intermetallic compounds with multi-step magnetic transition	Rina Takagi	The University of Tokyo	Siyi Gu, Mizuki Urai	PONTA	5G
32	6G-TOPAN IRT課題	池田　陽一	東北大学	苗代橋 吟京、 WANG TONG、 森口 晃大、 木村 耕治、 筒井 智嗣、 Podlensnyak Andrey Aleksandrovich、 Prokhnenko Oleksandr、 足立 匡、 小宮山 陽太、 清水 悠晴、 岡部 博孝、 高田 秀佐、 藤田 全基、 谷口 貴紀、 小林 悟	IRT Project of TOPAN	Yoichi Ikeda	Tohoku University	Otochika Nawashirobashi, Tong Wang, Kota Moriguchi, Koji Kimra, Satoshi Tsutsui, Andrey Aleksandrovich Podlesnyak, Oleksandr Prokhnenko, Tadashi Adachi, Yota Komiyama, Yusei Shimizu, Hirotaka Okabe, Shusuke Takada, Masaki Fujita, Takanori Taniguchi, Satoru Kobayashi	TOPAN	6G
33	塑性歪みを加えたPt3Fe反強磁性体における強磁性ドメインの磁気相関	小林　悟	岩手大学	北條 大輝	Magnetic correlations of ferromagnetic domains in plastically strained Pt3Fe antiferromagnet	Satoru Kobayashi	Iwate University	Hiroki Hojo	TOPAN	6G
34	二等辺三角格子反強磁性体Mn(Nb1-xTax)2O6の磁気秩序	小林　悟	岩手大学	藤田 真至、 北條 大輝	Magnetic ordering of isosceles-triangular-lattice antiferromagnet Mn(Nb1-xTax)2O6	Satoru Kobayashi	Iwate University	Shinji Fujita, Hiroki Hojo	TOPAN	6G
35	フォノン分散測定による鉄マンガン基恒弾性合金中の準安定相の探索	池田　陽一	東北大学		Search for metastable phases in iron-manganese-based Elinvar alloys through phonon dispersion measurements	Yoichi Ikeda	Tohoku University		TOPAN	6G
36	マクロな物性を同時に測定できる中性子散乱装置の整備Ⅰ ー交流磁化率測定システムー	池田　陽一	東北大学		Construction of a multi-probe neutron scattering instrument I - ac susceptibility measurement system -	Yoichi Ikeda	Tohoku University		TOPAN	6G
37	量子物質の準粒子構造の研究	益田　隆嗣	東京大学	胡 峻溪、 Ma Jie、 Zhong Ruidan、 Xiao Yusen、 Shu Mingfang、 浅井 晋一郎、 菊地 帆高、 小関 真、 Wei Zijun、 Liu Zheyuan	IRT Project of HER	Takatsugu Masuda	The University of Tokyo	Junxi Hu, Jie Ma, Ruidan Zhong, Yusen Xiao, Mingfang Shu, Shinichiro Asai, Hodaka Kikuchi, Makoto Ozeki, Zijun Wei, Zheyuan Liu	HER/HODACA	C1-1
38	Ce(Co,Rh)In5の磁性と超伝導発現機構の関係	古川　はづき	お茶の水女子大学	鈴木 萌香	Magnetism and Superconductivity in Ce(Co,Rh)In5	Hazuki Furukawa	Ochanomizu University	Moeka Suzuki	HER/HODACA	C1-1
39	La3Co4Sn13のカイラル構造相転移におけるフォノンソフトニング	岩佐　和晃	茨城大学	高橋 和樹、 小佐野 七菜子、 宮田 一駿、 熊田 隆伸、 鈴木 陽太郎、 鈴村 貫太、 黒澤 航海、 浦本 結稜	Phonon softening at the chiral structure phase transformation of La3Co4Sn13	Kazuaki Iwasa	Ibaraki University	Kazuki Takahashi, Nanako Osano, Kazuma Miyata, Takanobu Kumada, Yotaro Suzuki, Kanta Suzumura, Wataru Kurosawa, Yui Uramoto	HER/HODACA	C1-1
40	Pr3Co4Sn13のカイラル構造相での結晶場分裂準位	岩佐　和晃	茨城大学	高橋 和樹、 小佐野 七菜子、 宮田 一駿、 熊田 隆伸、 鈴木 陽太郎、 鈴村 貫太、 黒澤 航海、 浦本 結稜	Crystalline Electric Field Splitting Levels in the chiral structure phase of Pr3Co4Sn13	Kazuaki Iwasa	Ibaraki University	Kazuki Takahashi, Nanako Osano, Kazuma Miyata, Takanobu Kumada, Yotaro Suzuki, Kanta Suzumura, Wataru Kurosawa, Yui Uramoto	HER/HODACA	C1-1
41	フラストレート磁性体YBaCo4O7におけるZ2ボルテックス秩序の不純物置換効果	左右田　稔	お茶の水女子大学	猪越 絢、 小野 友莉、 茂木 麻琴	doping-effect of Z2-vortex ordering in frustrated magnet YBaCo4O7	Minoru Soda	Ochanomizu University	Aya Inokoshi, Yuri Ono, Makoto Mogi	HER/HODACA	C1-1
42	2等辺三角格子イジング磁性体CoNb2O6のワニエ状態における磁気揺動(継続)	満田　節生	東京理科大学	玉造 博夢	Magnetic fluctuation at the Wannier point in isosceles triangular lattice Ising magnet CoNb2O6	Setsuo Mitsuda	Tokyo University of Science	Hiromu Tamatsukuri	HER/HODACA	C1-1

43	TbCaAl3O7の結晶場励起についての研究	阿部　伸行	日本大学		Study of crystal field excitations in TbCaAl3O7	Nobuyuki Abe	Nihon University		HER/HODACA	C1-1
44	Neutron scattering study on QSL candidate NdMgAl11O19	Gao　Bin	Rice University	Chung Jae-Ho、 辛 勷禹	Neutron scattering study on QSL candidate NdMgAl11O19	Bin Gao	Rice University	Jae-Ho Chung, Kwangwoo Shin	HER/HODACA	C1-1
45	Neutron scattering study on monoclinic Na2Co2TeO6 single crystal	Chung　Jae-Ho	Korea University	Gao Bin、 辛 勷禹	Neutron scattering study on monoclinic Na2Co2TeO6 single crystal	Jae-Ho Chung	Korea University	Bin Gao, Kwangwoo Shin	HER/HODACA	C1-1
46	Neutron spectroscopy study of the dipolar-octupolar pyrochlore Nd2Sn2O7	Aczel　Adam	Oak Ridge National Laboratory	Lumsden Mark、 Hong Tao	Neutron spectroscopy study of the dipolar-octupolar pyrochlore Nd2Sn2O7	Adam Aczel	Oak Ridge National Laboratory	Mark Lumsden, Tao Hong	HER/HODACA	C1-1
47	Phonon dispersion of the Cs3Bi2Br9 perovskite with ultralow lattice thermal conductivity	Ren　Qingyong	China Spallation Neutron Source	Zhang Cuiping、 Li Lisi	Phonon dispersion of the Cs3Bi2Br9 perovskite with ultralow lattice thermal conductivity	Qingyong Ren	China Spallation Neutron Source	Cuiping Zhang, Lisi Li	HER/HODACA	C1-1
48	Unveiling the unique lattice dynamics leading to the ultralow thermal conductivity of halide double perovskites Cs2AgBiBr6	Wei　Pai-Chun	Department of Materials Science and Engineering	Yang Chun-Chuen、 Li Yu-Ju、 Wu Bao-You	Unveiling the unique lattice dynamics leading to the ultralow thermal conductivity of halide double perovskites Cs2AgBiBr6	Pai-Chun Wei	Department of Materials Science and Engineering	Chun-Chuen Yang, Yu-Ju Lee, Bao-You Wu	HER/HODACA	C1-1
49	SANS-U（二次元位置測定小角散乱装置）IRT課題	眞弓　皓一	東京大学	鈴木 道生、 浪川 勇人、 佐々木 初穂、 孟 作霖、 岡田 結夏、 高橋 健、 斎藤 雄星、 松本 悠汰、 亀田 太朗、 矢田 詩歩、 Li Xiang、 cheuk wing jamie chan、 山田 悟史、 坂本 璃月、 鈴木 晴陽、 亀谷 優樹、 温井 遥介、 中間 貴寛、 杉山 正明、 芝口 友隆、 岩瀬 裕希、 辻 優依、 佐藤 節夫、 相澤 秀樹、 日高 正基、 大久保 直樹、 貞包 浩一朗、 三田 一樹、 日下部 紗伎、 Geonzon Lester 、 渡我部 りさ、 Hou Lixin、 KOU HAO、 小田 達郎、 清水 将裕、 守島 健、 井上 倫太郎	IRT Project of SANS-U	Koichi Mayumi	The University of Tokyo	Michio Suzuki, Yuto Namikawa, Hatsuho Sasaki, Zuolin Meng, Yuna Okada, Ken Takahashi, Yusei Saito, Yuta Matsumoto, Taro Kameda, Shiho Yada, Xiang Li, Chan Cheuk Wing Jamie, Norifumi Yamada, Ritsuki Sakamoto, Haruaki Suzuki, Yuki Kametani, Yosuke Nukui, Takahiro Nakama, Masaaki Sugiyama, Tomotaka Oroguchi, Hiroki Iwase, Yui Tsuji, Setsuo Sato, Hideki Aizawa, masaki hidaka, Naoki Okubo, Koichiro Sadakane, Kazuki Mita, Saki Kusakabe, Lester Geonzon, Lisa Watakabe, Lixin Hou, Hao Kou, Tatsuro Oda, Masahiro Shimizu, Ken Morishima, Rintaro Inoue	SANS-U	C1-2
50	Investigating the structural relaxation of shake-gels using rheology and contrast variation small angle neutron scattering	Geonzon Lester	東京大学	孟 作霖	Investigating the structural relaxation of shake-gels using rheology and contrast variation small angle neutron scattering	Lester Geonzon	The University of Tokyo	Zuolin MENG, Takanobu Kumada, Huiyun XUE, Norifumi Yamada, Yasutoshi Kuriyama, Daichi Kawana, Lester Geonzon, HAO KOU, Koichi Mayumi	SANS-U	C1-2
51	Elaborating the origin of tough carrageenan gels based on the spatial characteristics of the aggregates by small angle neutron scattering	Geonzon Lester	東京大学		Elaborating the origin of tough carrageenan gels based on the spatial characteristics of the aggregates by small angle neutron scattering	Lester Geonzon	The University of Tokyo		SANS-U	C1-2
52	リサイクルのためのポリオレフィン／異種材料の界面構造の新しいコントラストによる可視化と制御	三田　一樹	総合科学研究機構	三戸 瑞稀、 難波 恵汰	New Contrast Visualization and Control of Polyolefin/Different Material Interfacial Structures for Recycling	Kazuki Mita	Comprehensive Research Organization for Science and Society	Mizuki Sando, Keita Namba	SANS-U	C1-2
53	小角中性子散乱によるスモールヒートショックプロテインとinsulin B chain の複合体解析	井上　倫太郎	京都大学	茶谷 絵理、 坂本 璃月、 杉山 正明、 清水 将裕、 守島 健	Structural anlysis of complex of small heat shock protein and insulin B chain studied by small-angle neutron scattering	Rintaro Inoue	Kyoto University	Eri Chatani, Ritsuki Sakamoto, Masaaki Sugiyama, Masahiro Shimizu, Ken Morishima	SANS-U	C1-2
54	強磁性超伝導体における自発的磁束格子構造の研究	古川　はづき	お茶の水女子大学	Foley Edward	Spontaneous vortex phase in ferromagnetic superconductors	Hazuki Furukawa	Ochanomizu University	Edward Foley	SANS-U	C1-2

55	分岐鎖含有糖型界面活性剤の泡沫の構造解析	吉村　倫一	奈良女子大学	矢田 詩歩、 岩瀬 裕希、 金子 理香、 高見 風夏	Structural Analysis of Foams by Sugar-Based Surfactant with Branched-Chains	Tomokazu Yoshimura	Nara Women's University	Shiho Yada, Hiroki Iwase, Rika Kaneko, Fuka Takami	SANS-U	C1-2
56	小角中性子散乱法による単分散二次元シート状PMMAの希薄溶液中の分子形態評価	土肥　侑也	山形大学		Evaluation of molecular conformations of two-dimensional sheet-shaped PMMA with narrow molecular weight distributions in dilute solutions by small-angle neutron scattering methods	Yuya Doi	Yamagata University		SANS-U	C1-2
57	コントラスト変調中性子小角散乱による時計タンパク質複合体の溶液構造解明	守島　健	京都大学	浪川 勇人、 坂本 璃月、 杉山 正明、 清水 将裕、 井上 倫太郎	Structural analysis of clock protein complex in solution using contrast variation small-angle neutron scattering	Ken Morishima	Kyoto University	Yuto Namikawa, Ritsuki Sakamoto, Masaaki Sugiyama, Masahiro Shimizu, Rintaro Inoue	SANS-U	C1-2
58	異方的形状Fe3O4ナノ粒子の磁場誘起配列	小林　悟	岩手大学	三上 翔也、 茅野 昂之介	Field-induced assembly of anisotropic-shaped Fe3O4 nanoparticles	Satoru Kobayashi	Iwate University	Shoya Mikami, Konosuke Chino	SANS-U	C1-2
59	超好熱性古細菌由来マルチドメインタンパク質の高温における動的構造解析	小田　隆	日本原子力研究開発機構	井上 倫太郎、 坂本 璃月、 守島 健	Dynamic structural analysis of a multidomain protein from hyperthermophilic archaeon at a high temperature.	Takashi Oda	Japan Atomic Energy Agency	Rintaro Inoue, Ritsuki Sakamoto, Ken Morishima	SANS-U	C1-2
60	金ナノ粒子と環状PEGが形成する物理吸着複合体の構造解析	山本　拓矢	北海道大学	渡邉 智久、 丸山 侑祈	Structural analysis of physisorbed complexes of gold nanoparticles and cyclic PEG	Takuya Yamamoto	Hokkaido University	Tomohisa Watanabe, Yuki Maruyama	SANS-U	C1-2
61	小角中性子散乱測定を用いた結晶性ポリオレフィンの流動結晶化に与える分子量の影響の評価	木田　拓充	滋賀県立大学		Influences of Molecular Weight on Flow-Induced Crystallization of Semi-Crystalline Polyolefins Evaluated using Small-Angle Neutron Scattering Measurement	Takumitsu Kida	The University of Shiga Prefecture		SANS-U	C1-2
62	小角中性子散乱測定によるピリジン四級化結合架橋樹脂中での水の局在化解明	林　幹大	名古屋工業大学		SANS investigation of the water localization in the cross-linked materials with quaternized pyridines	Mikihiro Hayashi	Nagoya Institute of Technology		SANS-U	C1-2
63	中性子散乱法によるアミロイド中間体の構造解析	森本　大智	京都大学		Structural analysis of amyloid intermediate by en.wikipedia.org からのSANS small angle small-angle neutron scattering	Daichi Morimoto	Kyoto University		SANS-U	C1-2
64	コントラスト変調中性子小角散乱による結核菌染色体構造の研究	清水　将裕	京都大学	坂本 璃月、 杉山 正明、 守島 健、 井上 倫太郎	Contrast-variation small-angle neutron scattering of bacterial DNA condensation	Masahiro Shimizu	Kyoto University	Ritsuki Sakamoto, Masaaki SUGIYAMA, Ken Morishima, Rintaro Inoue	SANS-U	C1-2
65	MOF鋳型法により合成した束状高分子の構造解析	温井　遥介	東京大学	亀谷 優樹	Structural analysis of bundled polymers synthesized by MOF-templated method	Yosuke Nukui	The University of Tokyo	Yuki Kametani	SANS-U	C1-2
66	中性子散乱法によるアニオン界面活性剤－高分子混合系の泡沫の構造解析	矢田　詩歩	東京理科大学	岩瀬 裕希、 岡田 結夏、 松本 悠汰、 高橋 健、 斎藤 雄星、 亀田 太朗	Structural Analysis of foam of anionic surfactant / polymer mixture by neutron scattering	Shiho Yada	Tokyo University of Science	Hiroki Iwase, Yuna Okada, Yuta Matsumoto, Ken Takahashi, yusei saito, Taro Kameda	SANS-U	C1-2
67	コントラストマッチング中性子散乱法による人工高分子膜タンパク質の構造解析	西村　智貴	信州大学	宮本 寛子、 稲田 智理	Structural Analysis of Artificial Macromolecular Membrane Proteins by Contrast-Matching Neutron Scattering	Tomoki Nishimura	Shinshu University	Noriko Miyamoto, Chieri Inada	SANS-U	C1-2
68	中性子散乱法によるsPS/PPEおよびaPS/PPEブレンドの相溶性に関する研究	西辻　祥太郎	山形大学	藤井 望、 武部 智明、 宮川 大輝	The study on solubility of sPS/PPE and aPS/PPE blends by Neutron scattering	Shotaro Nishitsuji	Yamagata University	Nozomu Fujii, Tomoaki Takebe, Hiroki Miyakawa	SANS-U	C1-2
69	高圧条件下における混合溶液系の新奇な臨界挙動と隠れた長距離相互作用の解明	貞包　浩一朗	同志社大学	三浦 聡汰、 日高 正基、 大久保 直樹	Novel critical behavior in a mixture of water/organic solvent under high-pressure condition	Koichiro Sadakane	Doshisha University	Sota Miura, Masaki Hidaka, Naoki Okubo	SANS-U	C1-2

70	コントラストマッチング法を用いたクモ糸の靭性と高次構造の相関に関する研究	辻　優依	京都大学		Correlation between higher order structure and toughness of spider silks with contrast matching small-angle neutron scattering	Yui Tsuji	Kyoto University		SANS-U	C1-2
71	中性子散乱法による重合誘起相分離の計測	鈴木　祥仁	大阪公立大学	佐々木 瑛介	Analysis of polymerization induced phase separation by small angle neutron scattering	Yasuhito Suzuki	Osaka Metropolitan University	Eisuke Sasaki	SANS-U	C1-2
72	SANS法による三元系深共晶溶媒の混合状態に関する研究	高椋　利幸	佐賀大学	佐々木 魁斗、 勝山 美空	A Study on Mixing States of Ternary Deep Eutectic Solvents by SANS	Toshiyuki Takamuku	Saga University	Kaito Sasaki, Miku Katsuyama	SANS-U	C1-2
73	カテナン型高分子の希薄溶液中における拡がりの評価	高野　敦志	名古屋大学	伊藤 正浩、 井田 彪吾	Evaluation of Chain Dimension of Catenated polymer in Dilute Solution	Atsushi Takano	Nagoya University	Masahiro Ito, Hyougo Ida	SANS-U	C1-2
74	Unravelling the mystery of clustering in polyelectrolyte solutions	Gonzalez Lopez Carlos	Pennsylvania State University	渡邉 貴一	Unravelling the mystery of clustering in polyelectrolyte solutions	Carlos Gonzalez Lopez	Pennsylvania State University	Takiachi Watanabe	SANS-U	C1-2
75	Incorporation of hydrophilic molecules into membranes based on semicrystalline syndiotactic polystyrene by contrast variation-SANS.	Radulescu Aurel	Forschungszentrum Jülich GmbH	岩瀬 裕希、 Joseph Boniface Brijitta、 有馬 寛、 金子 文俊	Incorporation of hydrophilic molecules into membranes based on semicrystalline syndiotactic polystyrene by contrast variation-SANS.	Aurel Radulescu	Forschungszentrum Jülich GmbH	Hiroki Iwase, Brijitta Joseph Boniface, Hiroshi Arima, Fumitoshi Kaneko	SANS-U	C1-2
76	High Shear, Capillary Rheology of PEG-stabilized Nanoparticles with Different Repulsions	Rehmann Kelsi, M.S.	Center for Neutron Research	Krzywon Jeffery、 Nagao Michihiro	High Shear, Capillary Rheology of PEG-stabilized Nanoparticles with Different Repulsions	Kelsi, M.S. Rehmann	Center for Neutron Research	Jeffery Krzywon, Michihiro Nagao	SANS-U	C1-2
77	Small Angle Neutron Scattering Studies on the Flocculation Behaviour of Polystyrene Particles Suspension	Joseph Boniface Brijitta	Jülich Centre for Neutron Science	岩瀬 裕希、 Radulescu Aurel	Small Angle Neutron Scattering Studies on the Flocculation Behaviour of Polystyrene Particles Suspension	Brijitta Joseph Boniface	Jülich Centre for Neutron Science	Hiroki Iwase, Aurel Radulescu	SANS-U	C1-2
78	ポリオキブチレン－ポリオキシエチレン系新規非イオン界面活性剤が 形成するミセルの構造解析	吉村　倫一	奈良女子大学	矢田 詩歩、 金子 理香、 高見 風夏	Structural Analysis of Micelles Formed by Homogeneous Polyoxybutylene–Polyoxyethylene-type Novel Nonionic Surfactants	Tomokazu Yoshimura	Nara Women's University	Shiho Yada, Rika Kaneko, Fuka Takami	SANS-U	C1-2
79	小角中性子散乱による多環状／線状ポリスチレン混合系の構造解析	海老井　大和	北海道大学	磯野 拓也	Structual analysis of multicyclic/linear polystyrene blends by small-angle neutron scattering	Yamato Ebii	Hokkaido University	Takuya Isono	SANS-U	C1-2
80	う蝕予防効果向上を目指した有機-無機複合体の構造解析	眞弓　皓一	東京大学	小野 真一、 高林 輝、 森垣 篤典、 正岡 幸子	Structural analysis of organic/inorganic composite dispersions	Koichi Mayumi	The University of Tokyo	Masakazu Ono, Hikaru Takabayashi, Atsunori Morigaki, Sachiko Masaoka	SANS-U	C1-2
81	2次元超格子構造を持つ超伝導体における磁束格子の研究	金城　克樹	東北大学		Investigation of vortex structure of two dimensional superlattice superconductor	Katsuki Kinjo	Tohoku University		SANS-U	C1-2
82	中性子・X線散乱法を利用した牛乳内のカゼインミセル構造の研究 ；殺菌温度によるミセル構造変化の解明	高木　秀彰	高エネルギー加速器研究機構		A study on a casein micelle structure using SAXS and SANS; revealing the origin of changes of micelle structure by heat treatment	Hideaki Takagi	High energy accelerator research organization		SANS-U	C1-2
83	iNSE（中性子スピンエコー分光器）	小田　達郎	東京大学	孟 作霖、 熊田 隆伸、 Xue Huiyun、 山田 悟史、 栗山 靖敏、 川名 大地、 Geonzon Lester 、 Kou Hao、 眞弓 皓一	IRT Project of iNSE	Tatsuro Oda	The University of Tokyo	Zuolin Meng, Takanobu Kumada, Huiyun Xue, Norifumi Yamada, Yasutoshi Kuriyama, Daichi Kawana, Lester Geonzon, Hao Kou, Koichi Mayumi	iNSE	C2-3-1
84	Elaborating the origin of tough carrageenan gels based on the dynamic of the aggregates using neutron spin echo	Geonzon Lester	東京大学		Elaborating the origin of tough carrageenan gels based on the dynamic of the aggregates using neutron spin echo	Lester Geonzon	The University of Tokyo		iNSE	C2-3-1
85	中性子スピンエコー法によるタンパク質内部運動観測	井上　倫太郎	京都大学	清水 将裕、 守島 健	Observation of protein internal dynamics by neutron spin echo	Rintaro Inoue	Kyoto University	Masahiro Shimizu, Ken Morishima	iNSE	C2-3-1

86	イオン液体高分子ゲルにおける高分子ダイナミクス研究	小田　達郎	東京大学		Polymer dynamics study in ionic liquid polymer gels	Tatsuro Oda	The University of Tokyo		iNSE	C2-3-1
87	高分子ナノコンポジット系の高分子吸着層のダイナミクス研究	小田　達郎	東京大学		Dynamics study of polymer adsorption layers in polymer nanocomposite systems	Tatsuro Oda	The University of Tokyo		iNSE	C2-3-1
88	塩が誘起する有機溶媒水溶液の２次元流体的な臨界挙動	貞包　浩一朗	同志社大学	日高 正基、 大久保 直樹	2D-Ising like critical behavior in mixtures of water/organic solvent/antagonistic salt	Koichiro Sadakane	Doshisha University	Masaki Hidaka, Naoki Okubo	iNSE	C2-3-1
89	AGNES(高分解能パルス冷中性子分光器)IRT課題	山室　修	理化学研究所	泉 謙一、 山村 浩樹、 古府 麻衣子、 Wu Xuejun、 小林 美加、 佐藤 駿、 秋葉 宙、 ZHANG Menghan、 遠藤 大成、 大政 義典、 伊藤 華苗	IRT Project of AGNES	Osamu Yamamuro	RIKEN	Kenichi Izumi, Hiroki Yamamura, Maiko Kofu, Xuejun Wu, Mika Kobayashi, Shun Sato, Hiroshi Akiba, Menghan Zhang, Taisei Endo, Yoshinori Ohmasa, Kanae Ito	AGNES	C3-1-1
90	深共晶溶媒と水の混合系における水のダイナミクス測定	吉田　亨次	福岡大学	茂渡 大空、 永井 哲郎	Water dynamics in deep eutectic solvent - water mixutre	Koji Yoshida	Fukuoka University	Sora Shigeto, Tetsuro Nagai	AGNES	C3-1-1
91	中性子準弾性散乱法による高水素配位錯イオン物質Mg6WH16の動的挙動解析	大政　義典	東京大学		Quasi-elastic neutron scattering study of hydride complex Mg6WAH16 with high hydrogen coordination	Yoshinori Ohmasa	Shimane University		AGNES	C3-1-1
92	Dynamics of water molecules in aqueous LiCl, MgCl2, and CaCl2 solutions confined in mesoporous silica	山口　敏男	福岡大学	永全 周、 Jing Zhuanfang	Dynamics of water molecules in aqueous LiCl, MgCl2, and CaCl2 solutions confined in mesoporous silica	Toshio Yamaguchi	Fukuoka University	Zhou Yongquan, Zhuanfang Jing	AGNES	C3-1-1
93	中性子非弾性散乱法による出土琥珀の研究	山口　繁生	元興寺文化財研究所		Study of Excavated Amber by Inelastic Neutron Scattering.	Shigeo Yamaguchi	Gangoji institute for research of cultural property		AGNES	C3-1-1
94	疎水性溶媒中で生成する水クラスターの詳細なダイナミクスの解明	岡　弘樹	東北大学		Elucidation of the detail dynamics of water clusters generated in hydrophobic solvents	Kouki Oka	Tohoku University		AGNES	C3-1-1
95	中性子準弾性散乱法によるカルシウム塩溶液の凍結濃縮ガラス転移挙動の解明	望月　匠峰	広島大学	山田 武、 加賀谷 勇生、 川井 清司	Elucidation of freeze-concentrated glass transition behavior of calcium salt solutions using quasi-elastic neutron scattering	Takumi Mochizuki	Hiroshima University	Takeshi Yamada, Yuki Kagaya, Kiyoshi Kawai	AGNES	C3-1-1
96	エポキシ樹脂の架橋ネットワーク中における溶媒分子のダイナミクス	眞弓　皓一	東京大学	花房 明宏	Solvent dynamics in cross-linked network of epoxy resins	Koichi Mayumi	The University of Tokyo	Akihiro Hanafusa	AGNES	C3-1-1
97	アモルファス金属Pd0.85Si0.15中の水素原子の拡散運動	秋葉　宙	東京大学		Diffusion dynamics of hydrogen in amorphous metal Pd0.85Si0.15	Hiroshi Akiba	The University of Tokyo		AGNES	C3-1-1
98	中性子散乱法によるレジン含有ゴムのダイナミクスと破壊耐性の研究２	菊地　龍弥	高エネルギー加速器研究機構		Study of dynamics and fracture resistance of resin-containing rubber by neutron scattering	Tatsuya Kikuchi	Sumitomo Rubber Industries, Ltd.		AGNES	C3-1-1
99	ポリマーの主鎖周りの回転障壁が速いダイナミクスに与える影響	鈴木　祥仁	大阪公立大学	稲垣 創太	Effect of rotational barrier along the main chain of the polymer on the fast process	Yasuhito Suzuki	Osaka Metropolitan University	Sota Inagaki	AGNES	C3-1-1
100	Dynamics of polymer network and water molecules within glassy hydrogels and their relationship	Hou　Lixin	the University of Tokyo	Kou Hao	Dynamics of polymer network and water molecules within glassy hydrogels and their relationship	Lixin Hou	The University of Tokyo	Hao Kou	AGNES	C3-1-1
101	Orientational fluctuations in aprotic organic liquids	de Souza Nicolas Raphael Louis	Australian Nuclear Science and Technology Organisation		Orientational fluctuations in aprotic organic liquids	Nicolas Raphael Louis de Souza	Australian Nuclear Science and Technology Organisation		AGNES	C3-1-1

102	A quasi-elastic neutron scattering study on the dynamics of water-1,4-dioxane mixture confined in MCM-41	山口　敏男	福岡大学		A quasi-elastic neutron scattering study on the dynamics of water-1,4-dioxane mixture confined in MCM-41	Toshio Yamaguchi	Fukuoka University		AGNES	C3-1-1
103	MINE（京大複合研：多層膜中性子干渉計・反射率計）IRT課題	日野　正裕	京都大学	藤谷 龍澄、 田崎 誠司、 北口 雅暁、 樋口 嵩、 小田 達郎	IRT Project of MINE	Masahiro Hino	Kyoto University	Ryuto Fujitani, Seiji Tasaki, Masaaki Kitaguchi, Takashi Higuchi, Tatsuro Oda	MINE	C3-1-2-2
104	BGaN中性子半導体イメージングセンサーに向けた中性子検出特性評価	中野　貴之	静岡大学	櫻井 辰大、 竹中 壮太郎	Neutron detection characteristics for BGaN neutron semiconductor imaging sensor	Takayuki Nakano	Shizuoka University	Tatsuhiro Sakurai, Sotaro Takenaka	MINE	C3-1-2-2
105	中性子基礎物理実験のためのデバイス開発	北口　雅暁	名古屋大学	南部 太郎	Development of neutron devices for fundamental physics	Masaaki Kitaguchi	Nagoya University	Taro Nambu	MINE	C3-1-2-2
106	太陽電池を応用した中性子検出素子の検出特性解明	奥野　泰希	理化学研究所		Clarification of Detection Characteristics of Neutron Detection Devices Applying Solar Cells	Yasuki Okuno	RIKEN		MINE	C3-1-2-2
107	ホスト-ゲスト錯体を用いた分子接着高分子材料の界面構造解析	山岡　賢司	大阪大学		Interfacial Structure Analysis of Molecular Adhesive Polymeric Materials using Host-Guest Inclusion complex	Kenji Yamaoka	Osaka University		MINE	C3-1-2-2
108	超冷中性子スピン解析器の開発	川崎　真介	高エネルギー加速器研究機構	樋口 嵩、 佐藤 仁哉	Development of a Spin Analyzer for Ultra-Cold Neutrons	Shinsuke Kawasaki	High energy accelerator research organization	Takashi Higuchi, Jinya Sato	MINE	C3-1-2-2
109	多層膜中性子ミラーの高度化と集光デバイス開発	日野　正裕	京都大学	樋口 嵩、 藤谷 龍澄	Development of advanced multilayer neutron mirrors and focusing device	Masahiro Hino	Kyoto University	Takashi Higuchi, Ryuto Fujitani	MINE	C3-1-2-2
110	Cold-neutron reflectometry for characterizing surface coating for ultracold-neutron transport and storage	樋口　嵩	京都大学	佐藤 仁哉	Cold-neutron reflectometry for characterizing surface coating for ultracold-neutron transport and storage	Takashi Higuchi	Kyoto University	Jinya Sato	MINE	C3-1-2-2
111	中性子スピン干渉による超冷中性子偏極膜の性能評価	樋口　嵩	京都大学		Neutron spin interferometry for performance evaluation of ultracold neutron spin polarizers	Takashi Higuchi	Kyoto University		MINE	C3-1-2-2
112	中性子共鳴スピンフリッパーによるスピン反転成分の位相測定	田崎　誠司	京都大学	田北 雄大、 杁山 瑞貴	Measurement of the phase of neutron spin wave flipped by neutron resonance spin flipper	Seiji Tasaki	Kyoto University	Yudai Takita, Mizuki Iriyama	MINE	C3-1-2-2
113	中性子スピン干渉計を用いた歪んだ振動磁場の測定	藤谷　龍澄	京都大学	樋口 嵩	Measurement of distorted oscillating magnetic fields using neutron spin interferometer	Ryuto Fujitani	Kyoto University	Takashi Higuchi	MINE	C3-1-2-2
114	反射型中性子タルボ・ロー干渉計による表面・界面構造評価手法の開発II	關　義親	東北大学		Development of reflective Talbot-Lau interferometer for surface/interface structure analysis II	Yoshichika Seki	Tohoku University		MINE	C3-1-2-2

115	T1-1　HQR　IRT課題	大山　研司	茨城大学	浅野 貴行、 高橋 和樹、 小佐野 七菜子、 宮田 一駿、 山岡 良太、 小林 星華、 相澤 憲太、 Park Sung Jin、 物江 海音、 河本 亘輝、 海老澤 秀明、 沢田 芙祐子、 富士本 駿、 小泉 遼介、 大塚 智瑛、 横山 淳、 高橋 哲平、 飛永 洋輝、 齋藤 皓太、 伊倉 勇希、 桑原 慶太郎、 古川 陽基、 柳沼 彰良、 上原 寛太、 藤森 安、 鈴木 龍治、 伊川 大樹、 熊田 隆伸、 川上 修汰、 滝田 正勝、 阿部 幸樹、 會澤 幸希、 鈴木 陽太郎、 中野 岳仁、 鈴村 貫太、 黒澤 航海、 岩佐 和晃、 浦本 結稜	IRT Project of HQR	Kenji Ohoyama	Ibaraki University	Takayuki Asano, Kazuki Takahashi, Nanako Osano, Kazuma Miyata, Ryota Yamaoka, Kirari Kobayashi, Kenta Aizawa, Sung Jin Park, Kaito Monoe, Kouki Kawamoto, Hideki Ebisawa, Fuyuko Sawada, Hayao Fujimoto, Ryosuke Koizumi, Tomoaki Otsuka, Makoto Yokoyama, Teppei Takahashi, Hiroki Tobinaga, Kohta Saito, Yuki Igura, Keitaro Kuwahara, Haruki Furukawa, Akira Yaginuma, Kanta Uehara, Ann Fujimori, Ryuji Suzuki, Taiki Igawa, Takanobu Kumada, Shuta Kawakami, Masakatsu Takita, Kouki Abe, Koki Aizawa, Yotaro Suzuki, Takehito Nakano, Kanta Suzumura, Wataru Kurosawa, Kazuaki Iwasa, Yui Uramoto	HQR	T1-1
116	中性子散乱法によるYbCu4Niの結晶場準位の研究	谷口　貴紀	東北大学		Neutron Scattering Study of Crystal Field Levels in YbCu4Ni	Takanori Taniguchi	Tohoku University		HQR	T1-1
117	AKANE（東北大金研：三軸型中性子分光器）IRT課題	谷口　貴紀	東北大学	Saha Suvayan、 井出 郁央、 橋本 尚法、 Podlensnyak Andrey Aleksandrovich、 Prokhnenko Oleksandr、 山本 孟、 奥 隆之、 高田 秀佐、 岡部 博孝、 藤田 全基、 池田 陽一	IRT Project of AKANE	Takanori Taniguchi	Tohoku University	Suvayan Saha, Ikuo Ide, Shota Hashimoto, Andrey Aleksandrovich Podlesnyak, Oleksandr Prokhnenko, Hajime Yamamoto, Takayuki Oku, Shusuke Takada, Hirotaka Okabe, Masaki Fujita, Yoichi Ikeda	AKANE	T1-2
118	マンガンが磁性をもつ新物質TbMn2Al10の磁気構造と結晶場の観測	中村　翔太	名古屋工業大学	榊原 みら乃	Observation of the magnetic structure and crystal field of TbMn2Al10, a new material with manganese magnetism	Shota Nakamura	Nagoya Institute of Technology	Mirano Sakakibara	AKANE	T1-2
119	キラル磁性体L酒石酸銅の特異な磁気挙動の研究	山口　明	兵庫県立大学	大江 真誠	Study of anomalous magnetic behavior of a chiral magnet, copper L-tartrate, at low temperatures	Akira Yamaguchi	University of Hyogo	Masato Oe	AKANE	T1-2
120	立方晶RRuSn3(R=Pr,Nd)における結晶場準位の同定	山根　悠	兵庫県立大学	森 賢太郎	Crystalline electric field schemes in cubic RRuSn3 (R=Pr, Nd)	Yu Yamane	University of Hyogo	Kentaro Mori	AKANE	T1-2
121	軸性アニーリングによるCeRhSn単結晶の非対称化の検出	志村　恭通	広島大学	來寶 大地、 渡邉 寛大	Detection of the anti-symmetry in the single-crystals of CeRhSn by uniaxial annealing	Yasuyuki Shimura	Hiroshima University	Daichi Kurumi, Kanta Watanabe	AKANE	T1-2
122	PrRu2Sn2Zn18における結晶場状態と多極子秩序	脇舎　和平	岩手大学	田村 柊斗	Crystalline electric field state and multipolar ordering in PrRu2Sn2Zn18	Kazuhei Wakiya	Iwate University	Shuto Tamura	AKANE	T1-2
123	二次元三角格子磁気ネットワークを有する銅水酸化物の低温磁気構造解析	藤田　渉	東京海洋大学		Crystal and Magnetic Structures of Copper Hydroxides Materials with Two-dimensional Triangular Lattice Magnetic Networks	Wataru Fujita	Tokyo University of Marine Science and Technology		AKANE	T1-2
124	電子ドープ型銅酸化物のT構造におけるNi置換効果	谷口　貴紀	東北大学	鄭 家傑、 藤田 全基	Effect of Ni substitution in the T'-type structure of electron-doped curates	Takanori Taniguchi	Tohoku University	Jiajie Zheng, Masaki Fujita	AKANE	T1-2
125	一軸圧下における密度波と超伝導の研究	谷口　貴紀	東北大学	藤田 全基	Density Waves and Superconductivity under Uniaxial Pressure	Takanori Taniguchi	Tohoku University	Masaki Fujita	AKANE	T1-2

126	T1-3 HERMES IRT	南部　雄亮	東北大学	Wu Wenzheng、 菊地 裕斗、 Lalan Vidhya、 Mahato Suraj、 Zhu Tong、 Larsen Simon、 寺田 典樹、 森口 椋太、 林 悠偉、 津森 竜也、 中村 理香、 黒岡 和巳、 Gabov Artem、 鶴田 侑也、 山田 周吾、 加藤 大地、 物江 太一、 荻野 拓、 松尾 祥史、 荒木 靖啓、 梅本 好日古、 川又 雅広、 高田 秀佐、 岡部 博孝、 藤田 全基、 谷口 貴紀、 池田 陽一、 Zhao Hongfei	IRT Project of HERMES	Yusuke Nambu	Tohoku University	Wenzheng Wu, Hiroto Kikuchi, Vidhya Lalan, Suraj Mahato, Tong Zhu, Simon Larsen, Noriki Terada, Ryota Moriguchi, Yui Hayashi, Tatsuya Tsumori, Rika Nakamura, kazumi kurooka, Artem Gabov, Yuya Tsuruta, Shugo Yamada, Daichi Kato, Taichi Monoe, Hiraku Ogino, Yoji Matsuo, Nobuhiro Araki, Yoshihiko Umemoto, Masahiro Kawamata, Shusuke Takada, Hirotaka Okabe, Masaki Fujita, Takanori Taniguchi, Yoichi Ikeda, Hongfei Zhao	HERMES	T1-3
127	Magnetic structure of the antiferromagnetic Au68Ga18Dy14 1/1 approximant crystal	Labib　FARID	東京理科大学	佐藤 卓、 金城 克樹、 那波 和宏	Magnetic structure of the antiferromagnetic Au68Ga18Dy14 1/1 approximant crystal	Farid Labib	Tokyo University of Science	Taku Sato, Katsuki Kinjo, Kazuhiro Nawa	HERMES	T1-3
128	Exploration of Phase Transition Behaviours and Magnetic Structures in Some Polar Sulphides Containing Diatomic Anions	Zhu　Tong	Kyoto University	Wu Wenzheng、 Vaishnav Yuvraj、 Banoo Maqsuma、 Lalan Vidhya、 中井 瑚太朗、 Yuan Yao、 Mahato Suraj	Exploration of Phase Transition Behaviours and Magnetic Structures in Some Polar Sulphides Containing Diatomic Anions	Tong Zhu	Kyoto University	Wenzheng Wu, Yuvraj Vaishnav, Maqsuma Banoo, Vidhya Lalan, Kotaro Nakai, Yao Yuan, Suraj Mahato	HERMES	T1-3
129	新規窒素リッチ窒化物の中性子構造解析	三浦　章	北海道大学	出村 萌々香、 久末 竜駆、 李 哲虎	Neutron diffraction analysis of new nitrogen-rich nitrides	Akira Miura	Hokkaido University	Momoka Demura, Ryuku Hisasue, Chul-Ho Lee	HERMES	T1-3
130	π電子反強磁性体RbO2の結晶構造相転移と磁気構造	中野　岳仁	茨城大学	真鍋 幸生、 神戸 高志、 古川 陽基、 柳沼 彰良、 上原 寛太	Magnetic and crystal structural studies on π-orbital antiferromagnet RbO2	Takehito Nakano	Ibaraki University	Kosei Manabe, Takashi Kambe, Haruki Furukawa, Akira Yaginuma, Kanta Uehara	HERMES	T1-3
131	巨大磁気熱量効果を示すEr(Ho)Co2系材料における磁気構造と結晶構造の関係の探査	寺田　典樹	物質材料研究機構	Larsen Simon	Relationship between magnetic and crystal structures in giant magnetocaloric Er(Ho)Co2-based materials	Noriki Terada	National Institute for Materials Science	Simon Larsen	HERMES	T1-3
132	Crystal and magnetic structures of Mg0.4Ni0.6Fe2O4/SrFe12O19 bi-composites	小林　悟	岩手大学	Bekhbaatar Enkhmend	Crystal and magnetic structures of Mg0.4Ni0.6Fe2O4/SrFe12O19 bi-composites	Satoru Kobayashi	Iwate University	Enkhmend Bekhbaatar	HERMES	T1-3
133	Tb3Co4Sn13の超格子構造相での反強磁気秩序	岩佐　和晃	茨城大学	高橋 和樹、 小佐野 七菜子、 宮田 一駿、 熊田 隆伸、 鈴木 陽太郎、 鈴村 貫太、 黒澤 航海、 浦本 結稜	Antiferromagnetic ordering in the superlattice structure phase of Tb3Co4Sn13	Kazuaki Iwasa	Ibaraki University	Kazuki Takahashi, Nanako Osano, Kazuma Miyata, Takanobu Kumada, Yotaro Suzuki, Kanta Suzumura, Wataru Kurosawa, Yui Uramoto	HERMES	T1-3
134	SrMn2Ni6Te3O18の粉末中性子回折	木村　健太	大阪公立大学	中村 凌也	Powder neutron diffraction of SrMn2Ni6Te3O18	Kenta Kimura	Osaka Metropolitan University	Ryoya Nakamura	HERMES	T1-3
135	イルメナイト型MnGeO3の粉末中性子回折	木村　健太	大阪公立大学	青木 一歩	Powder neutron diffraction of ilmenite-type MnGeO3	Kenta Kimura	Osaka Metropolitan University	Ippo Aoki	HERMES	T1-3
136	高強度・高靭性ミディアムエントロピー合金Cr-Co-Niの変位相関関数の評価と合金中のボンド短距離秩序の探索	池田　陽一	東北大学		Evaluation of displacement correlation function and search for bond short-range ordering in a medium-entropy alloys	Yoichi Ikeda	Tohoku University		HERMES	T1-3
137	Co系立方晶Laves相の磁気構造解析	田畑　吉計	京都大学	塩谷 太基、 吉本 周玄	Magnetic structure analyses of the Co-based cubic Laves phases	Yoshikazu Tabata	Kyoto University	Taiki Shiotani, Subaru Yoshimoto	HERMES	T1-3
138	酸ハロゲン化物イオン伝導体の結晶構造解析	藤井　孝太郎	東京工業大学	八島 正知、 姚 博文、 李 嘉晨、 梅田 健成、 宇田川 英寿、 杜 政澎、 馬場 光希、 作田 祐一、 兼則 祐輔、 齊藤 馨、 前田 凌、 青木 望	Crystal Structure Analysis of Oxyhalide Ionic Conductors	Kotaro Fujii	Hosei University	Masatomo Yashima, Bowen Yao, Jiachen Li, Kensei Umeda, Hidetoshi Udagawa, Zhengpeng Du, Mitsuki Baba, Yuichi Sakuda, Yusuke Kanenori, Kei Saito, Ryo Maeda, Nozomi Aoki	HERMES	T1-3

139	A3T4Sn13の電荷密度波の秩序変数	谷口　貴紀	東北大学		Charge density wave of A3T4Sn13	Takanori Taniguchi	Tohoku University		HERMES	T1-3
140	マルテンサイト変態を生じる新奇ホイスラー合金の磁気構造	重田　出	鹿児島大学		Magnetic structure of novel Heusler alloys inducing martensitic transformation	Iduru Shigeta	Kagoshima University		HERMES	T1-3
141	ホイスラー合金Ru2-xCrxSiの磁気構造	重田　出	鹿児島大学	渕崎 員弘	Magnetic structure of Heusler alloy Ru2-xCrxSi	Iduru Shigeta	Kagoshima University	Kazuhiro Fuchizaki	HERMES	T1-3
142	プロトン伝導性新材料の結晶構造解析	齊藤　馨	東京工業大学	姚 博文、 李 嘉晨、 梅田 健成、 宇田川 英寿、 杜 政澎、 馬場 光希、 作田 祐一、 兼則 祐輔、 藤井 孝太郎、 前田 凌、 青木 望	Crystal Structure Analysis of Proton Conducting Novel Materials	Kei Saito	Institute of Science Tokyo	Bowen Yao, Jiachen Li, Kensei Umeda, Hidetoshi Udagawa, Zhengpeng Du, Mitsuki Baba, Yuichi Sakuda, Yusuke Kanenori, Kotaro Fujii, Ryo Maeda, Nozomi Aoki	HERMES	T1-3
143	FONDER(中性子4軸回折装置)IRT課題	高橋　美和子	筑波大学	野田 幸男、 坂倉 輝俊、 藤田 真至、 北條 大輝、 佐藤 卓、 小林 悟、 那波 和宏	IRT Project of FONDER	Miwako Takahashi	Tsukuba University	Yukio Noda, Terutoshi Sakakura, Shinji Fujita, Hiroki Hojo, Taku Sato, Satoru Kobayashi, Kazuhiro Nawa	FONDER	T2-2
144	Neutron diffraction study on CsMnI3	Wei　Zijun	The University of Tokyo		Neutron diffraction study on CsMnI3	Zijun Wei	The University of Tokyo		FONDER	T2-2
145	一軸応力下におけるPt3Fe反強磁性体の磁気構造解析	小林　悟	岩手大学	北條 大輝	Magnetic structural analysis of Pt3Fe antiferromagnet under uniaxial pressure	Satoru Kobayashi	Iwate University	Hiroki Hojo	FONDER	T2-2
146	二等辺三角格子反強磁性体Mn(Nb1-xTax)2O6の磁気構造解析	小林　悟	岩手大学	藤田 真至、 北條 大輝	Magnetic structural analysis of isosceles-triangular-lattice antiferromagnet Mn(Nb1-xTax)2O6	Satoru Kobayashi	Iwate University	Shinji Fujita, Hiroki Hojo	FONDER	T2-2
147	マルチフェロイックLuMn2O5 の磁気秩序	小林　悟	岩手大学	野田 幸男、 藤田 真至、 北條 大輝	Magnetic ordering of multiferroic LuMn2O5	Satoru Kobayashi	Iwate University	Yukio Noda, Shinji Fujita, Hiroki Hojo	FONDER	T2-2
148	磁性イオンを持つ三角格子リラクサー誘電体における散漫散乱	左右田　稔	お茶の水女子大学	猪越 絢、 小林 星華	diffuse scattering in relaxor magnet having triangular lattice	Minoru Soda	Ochanomizu University	Aya Inokoshi, Kirari Kobayashi	FONDER	T2-2
149	中性子線回折を用いたリン酸1,2,3-トリアゾリウム単結晶の構造解析	森　初果	東京大学	西岡 海人、 出倉 駿	Structural analysis of 1,2,3-triazolium dihydrogen phosphate single crystal by neutron diffraction	Hatsumi Mori	The University of Tokyo	Kaito Nishioka, Shun Dekura	FONDER	T2-2
150	Mn3IrSiの磁気構造解析	社本　真一	放射線利用振興協会	Chang Lieh-Jeng	Magnetic structure analysis of Mn3IrSi	Shinichi Shamoto	RADA	Lieh-Jeng Chang	FONDER	T2-2
151	フラストレート磁性体BaFe12Se7O6の中間および低温相の磁気構造解析	辻本　吉廣	物質材料研究機構	野田 幸男	Magnetic structure analysis of the intermediate and ground magnetic states of a spin frustrated antiferromagnet BaFe12Se7O6	Yoshihiro Tsujimoto	National Institute for Materials Science	Yukio Noda	FONDER	T2-2
152	スピン1/2フラストレート正方格子磁性体 2VOSO4_H2SO4_nH2Oの室温結晶構造	那波　和宏	東北大学	佐藤 卓、 金城 克樹	Room temperature crystal structure of the spin-1/2 frustruated square lattice magnet 2VOSO4 H2SO4 nH2O	Kazuhiro Nawa	Tohoku University	Taku Sato, Katsuki Kinjo, Kazuhiro Nawa	FONDER	T2-2
153	インバー合金における格子歪波の観測	高橋　美和子	筑波大学		Lattice deformation and the Invar effect in Inver alloy	Miwako Takahashi	Tsukuba University		FONDER	T2-2
154	Topological Magnetism and Singular Magnetoresistance of a Weyl semimetal	Gaudet Jonathan	NIST Center for Neutron Research		Topological Magnetism and Singular Magnetoresistance of a Weyl semimetal	Jonathan Gaudet	NIST Center for Neutron Research		FONDER	T2-2
155	有機無機一次元ペロブスカイト型化合物半導体の構造と相転移	高橋　美和子	筑波大学		Structure and Phase Transitions in One-dimensional Organometal Perovskite	Miwako Takahashi	Tsukuba University		FONDER	T2-2
156	アクセサリーIRT課題	上床　美也	総合科学研究機構	宗像 孝司、 林田 翔平	IRT Project of Accessory	Yoshiya Uwatoko	Comprehensive Research Organization for Science and Society	Koji Munakata, Shohei Hayashida	Accessory	

※実施課題一覧、所属は申請時のデータ

No.	課題番号	課題名	氏名	所属	分担者（共同研究者）	Title	Name	Organization	Member of reseach project	担当所員
1	202311-GNBXX-0020	層状MAB相化合物MoAlBのスピン分解角度分解光電子分光	伊藤 孝寛	名古屋大学	Ni Yuanzhi 河野 健人	Spin- and angle- resolved photoemission spectroscopy of layered MAB phase compound MoAlB	Takahiro Ito	Nagoya University	Ni Yuanzhi Kento Kono	近藤　猛
2	202311-GNBXX-0040	強磁性体基板上のグラフェンのスピン分解光電子分光	矢治 光一郎	物質・材料研究機構	ファンディン タン	SARPES study of graphene on ferromagnetic substrates	Koichiro Yaji	National Institute for Materials Science	Phan Dinh Than	近藤　猛
3	202311-CMBXX-0031	レーザースピン角度分解光電子分光による表面電子状態の研究	矢治 光一郎	物質・材料研究機構	ファンディン タン	SARPES studies of atomic layer materials at surfaces	Koichiro Yaji	National Institute for Materials Science	Phan Dinh Than	近藤　猛
4	202405-GNBXX-0066	鉄フタロシアニンを基盤としたLeib格子の電子構造の観測	金井 要	東京理科大学	山崎泰輝 磯部桃花 岸川莉子	Observation of electronic structure of Leib lattice in Fe phthalocyanine framework	Kaname Kanai	Tokyo University of Science	Taiki Yamazaki Momoka Isobe Riko Kishikawa	近藤　猛
5	202405-CMBXX-0074	有機化合物の光電子分光	金井 要	東京理科大学	山崎泰輝 磯部桃花 岸川莉子	Photoemission study on organic compounds	Kaname Kanai	Tokyo University of Science	Taiki Yamazaki Momoka Isobe Riko Kishikawa	近藤　猛
6	202406-GNBXX-0086	MXenes単結晶V_2CT_zのスピン分解角度分解光電子分光	伊藤 孝寛	名古屋大学	Ni Yuanzhi	Spin- and angle-resolved photoemission spectroscopy of Mxenes V_2CT_z single-crystal	Takahiro Ito	Nagoya University	Ni Yuanzhi	近藤　猛
7	所内	Investigation of spin propaty in quantum materials	Hugo Dil	PSI(Paul Scherre Institut)	Huh Soonsang 川口 海周 近藤　猛	Investigation of spin propaty in quantum materials	Hugo Dil	PSI(Paul Scherre Institut)	Huh Soonsang Kaishu Kawaguchi Takeshi Kondo	近藤　猛

※実施課題一覧、所属は申請時のデータ

1. 第一原理計算 / First-Principles Calculation of Materials Properties

No.	課題番号	課題名	氏名	所属	Title	Name	Organization
1	2024-Eb-0010	密度汎関数理論と機械学習法による表面・界面反応過程の理論的研究	森川　良忠	大阪大学 大学院工学研究科 物理学系専攻	Theoretical study on chemical reaction processes at surfaces and interfaces using density functional theory and machine learning methods	Yoshitada Morikawa	Department of Precision Engineering, Graduate School of Engineering, Osaka University
2	2024-Ea-0015	第一原理計算に立脚したワイドギャップ半導体における構造と新機能の発現	松下　雄一郎	東京大学理学系研究科物理学専攻	Emergence of new functions by controlling atomic structures in wide-gap semiconductors based on first-principles calculations	Yu-Ichiro Matsushita	Department of physics, The university of Tokyo
3	2024-Ea-0014	密度汎関数理論と機械学習法による表面・界面反応過程の理論的研究	森川　良忠	大阪大学 大学院工学研究科 物理学系専攻	Theoretical study on chemical reaction processes at surfaces and interfaces using density functional theory and machine learning methods	Yoshitada Morikawa	Department of Precision Engineering, Graduate School of Engineering, Osaka University
4	2024-D-0003	ドーピングによるLiNbO3改良と固体電池性能向上の研究	ゾウ　ジーゼン	東京工業大学科学技術創成研究院化学生命科学研究所	Research on Improving Solid-State Battery Performance through Doped LiNbO3 Modification	Zizhen Zhou	Tokyo Institute of Technology Institute of Innovative Research Laboratory for Chemistry and Life Science
5	2024-Ea-0006	量子論大規模計算による半導体薄膜成長とデバイス界面形成の微視的機構解明	押山　淳	名古屋大学未来材料・システム研究所	Clarification of Microscopic Mechanisms of Semiconductor Epitaxial Growth and Device-Interface Formation by Large-Scale Quantum-Theory-Based Computations	Atsushi Oshiyama	Institute of Materials and Systems for Sustainability
6	2024-Ea-0013	不規則系におけるフォノン輸送特性解析	塩見　淳一郎	東京大学工学系研究科	Analysis of phonon transport properties in disordered systems	Junichiro Shiomi	School of Engineering, The University of Tokyo
7	2024-Eb-0009	第一原理計算によるSiC-MOSデバイスにおけるキラー欠陥の同定	松下　雄一郎	東京大学理学系研究科物理学専攻	Identification of Killer Defects in SiC-MOS Devices by First-Principles Calculations	Yu-Ichiro Matsushita	Department of physics, The university of Tokyo
8	2024-Ea-0008	金属および酸化物の物質機能性の研究	杉野　修	東京大学物性研究所	Computational study of the material property of metals and oxides	Osamu Sugino	Institute for Solid State Physics, University of Tokyo
9	2024-Cb-0048	第一原理手法によるスピン変換物性の計算プログラム開発と応用	石井　史之	金沢大学ナノマテリアル研究所	Development and application of computational programs for spin conversion physical properties using first-principles methods	Fumiyuki Ishii	Kanazawa University
10	2024-Ea-0002	第一原理計算を用いた非調和フォノン特性データベースの構築	大西　正人	統計数理研究所	Development of database of anharmonic phonon properties using first-principles calculation	Masato Ohnishi	The Institute of Statistical Mathematics
11	2024-Cb-0031	計算科学手法によるデバイス界面でのキャリア輸送解析	小野　倫也	神戸大学大学院工学研究科電気電子工学専攻	Computational investigation of carrier-transport property at device interface	Tomoya Ono	Department of Electrical and Electronic Engineering, Graduate School of Engineering, Kobe University
12	2024-Ca-0057	第一原理計算に基づく方法を用いた複雑構造における局所物性に関 する解析	渡邉　聡	東京大学大学院工学系研究科マテリアル工学専攻	Analyses on local properties at complex structures via ab-initio-based methods	Satoshi Watanabe	Department of Materials Engineering, School of Engineering, The University of Tokyo
13	2024-Cb-0022	複雑構造における物性と原子構造の相関に関する第一原理計算に基づく方法による解析	渡邉　聡	東京大学大学院工学系研究科マテリアル工学専攻	Analyses on correlation between material properties and atomic structures in complex structures via ab-initio-based methods	Satoshi Watanabe	Department of Materials Engineering, School of Engineering, The University of Tokyo
14	2024-Ca-0103	計算科学手法によるデバイス界面でのキャリア輸送解析	小野　倫也	神戸大学大学院工学研究科電気電子工学専攻	Computational investigation of carrier-transport property at device interface	Tomoya Ono	Department of Electrical and Electronic Engineering, Graduate School of Engineering, Kobe University
15	2024-D-0004	Naイオン電池の有望な正極材料の研究。	ルオン　フードック	東京工業大学	Investigation of promising cathode material for Na-ion battery.	Huuduc Luong	Tokyo Institute of Technology
16	2024-Ca-0095	極限環境下における構造不規則系の構造と電子状態の第一原理計算	下條　冬樹	熊本大学大学院先端科学研究部	First-Principles Molecular-Dynamics Study of Structural and Electronic Properties of Disordered Materials under Extreme Conditions	Fuyuki Shimojo	Department of Physics, Kumamoto University
17	2024-D-0014	多層複合アニオンニッケル酸化物系による常圧超伝導物質の理論的探索	榊原　寛史	鳥取大学大学院工学研究科	Theoretical exploration of ambient pressure superconducting materials based on multilayer mixed anion nickel oxide systems	Hirofumi Sakakibara	Graduate School of Engineering, Tottori University
18	2024-Cb-0044	第一原理計算と機械学習による欠陥構造・イオン移動に関する解析	清水　康司	産業技術総合研究所	Analysis of defect structures and ion migration using first-principles calculations and machine learning	Koji Shimizu	National Institute of Advanced Industrial Science and Technology
19	2024-Ca-0015	全電子混合基底法プログラムの改良と応用	大野　かおる	横浜国立大学大学院工学研究院	Improvement and application of all-electron mixed basis program	Kaoru Ohno	Graduate School of Engineering, Yokohama National University
20	2024-Ca-0079	薄膜系における熱電効果の第一原理計算手法開発とファンデルワールス系への応用	石井　史之	金沢大学ナノマテリアル研究所	Development of a first-principles computational method for thermoelectric effects in thin film systems and application to van der Waals systems	Fumiyuki Ishii	Kanazawa University
21	2024-Ca-0117	不均一固体系における高速イオン伝導のメカニズム解明	笠松　秀輔	山形大学学術研究院	Understanding Fast Ion Conduction in Inhomogeneous Materials	Shusuke Kasamatsu	Academic Assembly, Yamagata University
22	2024-Ca-0120	HPCを基盤とした実験解析･シミュレーション･データ駆動科学の融合	星　健夫	核融合科学研究所研究部プラズマ量子プロセスユニット	HPC-based fusion of simulation, experiment analysis and data-driven science	Takeo Hoshi	Plasma Quantum Processes Unit, Department of Research, National Institute for Fusion Science
23	2024-Cb-0034	密度汎関数理論を用いた表面／界面における分子の吸着と反応に関する研究	濱田　幾太郎	大阪大学大学院工学研究科　物理学系専攻　精密工学コース	Density functional theory study of adsorption and reaction of molecules on solid surfaces and interfaces	Ikutaro Hamada	Department of Precision Engineering, Graduate School of Engineering, Osaka University

24	2024-Ca-0028	合金の自由エネルギー評価	合田　義弘	東京科学大学物質理工学院材料系	Free-energy evaluation of alloys	Yoshihiro Gohda	Department of Materials Science and Engineering, Institute of Science Tokyo
25	2024-Ca-0037	マルチスケールモデリング及び第一原理計算による水素エネルギー材料の理解	李　昊	東北大学材料科学高等研究所	Understanding Hydrogen Energy Materials by Ab Initio Calculations and Multiscale Modeling and Simulations	Hao Li	Advanced Institute for Materials Research (WPI-AIMR), Tohoku University
26	2024-Ca-0135	材料の誘電特性予測手法と構造探索手法の高度化	常行　真司	東京大学大学院理学系研究科物理学専攻	Advancement of methods for predicting dielectric properties and structure exploration of materials	Shinji Tsuneyuki	Department of Physics, University of Tokyo
27	2024-Cb-0014	光による半導体輸送特性制御の第一原理計算	佐藤　駿丞	筑波大学計算科学研究センター	First-principles calculation of optical control on semiconductor transport properties	Shunsuke Sato	Center for Computational Sciences, University of Tsukuba
28	2024-Ca-0005	第一原理波動関数理論における構造最適化の精度検証	越智　正之	大阪大学	Accuracy verification of structural optimizaiton using first-principles wave function theory	Masayuki Ochi	Osaka University
29	2024-Cb-0013	燃料電池電極触媒とギ酸分解触媒の省貴金属化	坂口　紀史	北海道大学大学院工学研究院　附属エネルギー・マテリアル融合領域研究センター	Reduction of Rare Metals in Fuel Cell and Formic Acid Decomposition Catalysts	Norihito Sakaguchi	Center for Advanced Research of Energy and Materials, Faculty of Engineering, Hokkaido University
30	2024-Cb-0030	2次元ハニカムヘテロ構造における第一原理電子輸送特性研究	江上　喜幸	北海道大学大学院工学研究院	First-principles study on electron transport properties in heterostructures made of 2-dimensional materials with honeycomb lattice	Yoshiyuki Egami	Faculty of Engineering, Hokkaido University
31	2024-Cb-0039	GaN/SiO2界面に生じるホールトラップの起源解明とGaN-MOSFETの実現	白石　賢二	名古屋大学　未来材料・システム研究所	Clarification of Hole Trap at GaN/SiO2 Interfaces and Fabrication of GaN-MOSFET	Kenji Shiraishi	Institute of Materials and Systems for Sustainability, Nagoya University
32	2024-Cb-0012	密度汎関数法と溶液理論を用いた電気化学反応の解析 6-2	春山　潤	理化学研究所開拓研究本部	Electrochemical reaction analysis using density functional calculation + implicit solvation model 6-2	Jun Haruyama	RIKEN Cluster for Pioneering Research
33	2024-Ca-0078	機械学習された原子間ポテンシャルを用いた分子動力学計算による負熱膨張挙動の解析	望月　泰英	東京科学大学物質理工学院	Elucidation of negative thermal expansion behavior based on the first-principles molecular-dynamics calculations using machine-learning potential	Yasuhide Mochizuki	School of Materials and Chemical Technology, Tokyo Institute of Technology
34	2024-Ca-0086	触媒性能向上を目指したペロブスカイト半導体光触媒の第一原理物質設計	天能　精一郎	神戸大学	First-principles materials design of perovskite semiconductors toward improving photocatalytic performance	Seiichiro Ten-No	Kobe University
35	2024-Ca-0123	第一原理計算に基づいた固体酸化物／液相界面のマルチスケールシミュレーション	中山　哲	東京大学大学院工学系研究科化学システム工学専攻	Multiscale simulation for liquid/oxide interface based on first-principle calculations	Akira Nakayama	Department of Chemical System Engineering, The University of Tokyo
36	2024-Cb-0009	金属材料の水素脆化を抑制するセラミックス保護被膜の開発	國貞　雄治	北海道大学大学院工学研究院　附属エネルギー・マテリアル融合領域研究センター	Development of Ceramic Protective Coating for High Corrosion Resistance of Metallic Materials	Yuji Kunisada	Center for Advanced Research of Energy and Materials, Faculty of Engineering, Hokkaido University
37	2024-Cb-0011	第一原理GWΓの開発	野口　良史	静岡大学工学部	Development of first-principles GWΓ method	Yoshifumi Noguchi	Graduate School of Engineering, Shizuoka University
38	2024-Cb-0028	合金の力学特性に関する第一原理的研究	上村　直樹	京都先端科学大学ナガモリアクチュエータ研究所	First-principles study of mechanical properties on alloys	Naoki Uemura	The Nagamori Institute of Actuators, Kyoto University of Advanced Science
39	2024-Ca-0052	燃料電池電極触媒とギ酸分解触媒の省貴金属化	坂口　紀史	北海道大学大学院工学研究院　附属エネルギー・マテリアル融合領域研究センター	Reduction of Rare Metals in Fuel Cell and Formic Acid Decomposition Catalysts	Norihito Sakaguchi	Center for Advanced Research of Energy and Materials, Faculty of Engineering, Hokkaido University
40	2024-Cb-0025	プラズマ表面相互作用の動的解析	浜口　智志	大阪大学工学研究科	Dynamical analyses of plasma-surface interactions	Satoshi Hamaguchi	Graduate School of Engineering, Osaka University
41	2024-Cb-0042	二次元材料の高次フォノンデータベースと高性能熱スイッチ	ソン　ジ゛エ	東京大学 工学系研究科・総合研究機構	High-order phonon database and high-performance thermal switch of two-dimensional materials	Sun Jie	Department of Mechanical Engineering, The University of Tokyo
42	2024-Cb-0052	理論計算によるセラミックス界面の機能探索	井上　和俊	東北大学材料科学高等研究所	Theoretical exploring of the functionalities in ceramics interfaces	Kazutoshi Inoue	Advanced Institute for Materials Research, Tohoku University
43	2024-Ca-0132	大規模第一原理電気伝導計算法による量子伝導理論	小林　伸彦	筑波大学 数理物質系　物理工学域	Quantum transport theory by large scale first-principles electron transport calculations	Nobuhiko Kobayashi	Department of Applied Physics, University of Tsukuba
44	2024-Ca-0051	第一原理分子動力学法によるセメント水和過程における CO$_{2}$ 固定メカニズムの解明	大村　訓史	愛媛大学　先端研究院	Ab initio molecular-dynamics study of CO$_{2}$ adsorption mechanisms in cement hydration process	Satoshi Ohmura	Premier Institute for Advanced Studies, Ehime University
45	2024-Ca-0001	第一原理計算によるナノ物質の構造・機能の解明と予測	武次　徹也	北海道大学大学院理学研究院化学部門	Ab initio study on the structure and functions of nanomaterials	Tetsuya Taketsugu	Department of Chemistry, Faculty of Science, Hokkaido University
46	2024-Ca-0043	機械学習MDシミュレーションによるプラズマ物質表面相互作用解析	浜口　智志	大阪大学工学研究科	Analysis of plasma-material interactions by Machine-Learning-based MD simulation	Satoshi Hamaguchi	Graduate School of Engineering, Osaka University
47	2024-Ca-0027	高機能スピントニクス磁性材料の電子構造・磁気異方性解析および準粒子自己無撞着GW法の並列化開発・応用	小田　竜樹	金沢大学理工研究域数物科学系	Analyses on electronic structure and magnetic anisotropy in high-performance spintronics magnetic materials and parallelization development/application in quasi-particle self-consistent GW code	Tatsuki Oda	Faculty of Mathematics and Physics, Institute of Science and Engineering, Kanazawa University

48	2024-Cb-0045	有機半導体の電子-フォノン相互作用に関する第一原理的研究	柳澤　将	琉球大学理学部物質地球科学科物理系	First-principles study on the electron-phonon coupling in organic semiconductors	Susumu Yanagisawa	Department of Physics and Earth Sciences, Faculty of Science, University of the Ryukyus
49	2024-Ca-0014	第一原理計算による光熱変換原理の解明	江目　宏樹	山形大学	Study of the principle of photothermal conversion by ab initio calculations	Hiroki Gonome	Yamagata University
50	2024-Ca-0081	交換相互作用テンソルの非摂動論的計算	田中　友規	東京科学大学物質理工学院	Non-perturbative calculation of exchange coupling tensor	Tomonori Tanaka	School of Materials and Chemical Technology, Institute of Science Tokyo
51	2024-Ca-0094	メタンを用いた燃料電池の効率向上に向けた改質触媒の最適組成探索	藤崎　貴也	島根大学 材料エネルギー学部	Exploring the optimal composition of reforming catalysts for improving the efficiency of fuel cells using methane	Takaya Fujisaki	Faculty of materials for energy, Shimane university
52	2024-Ca-0113	第一原理計算による二次元物質の不純物ドーピングの設計	BAE　SOUNGMIN	東北大学金属材料研究所	Doping strategy design for two-dimensional materials from first principles	Soungmin Bae	Institute for Material Research, Tohoku University
53	2024-Eb-0001	第一原理計算を用いた非調和フォノン特性データベースの構築	大西　正人	統計数理研究所	Development of anharmonic phonon property database using first-principles calculations	Masato Ohnishi	The Institute of Statistical Mathematics
54	2024-Ea-0010	水素液化のための計算材料設計	トラン バ　フン	東北大学	Computational material design for hydrogen liquefaction	Hung Tran Ba	Tohoku University
55	2024-Ca-0009	交替磁性体におけるスピン分裂現象の理解	山内　邦彦	大阪大学基礎工学研究科	Understanding of spin-splitting phenomena in altermagnets	Kunihiko Yamauchi	Graduate School of Engineering Science, Osaka University
56	2024-Ca-0067	GW近似を超える試み:2次の交換項の開発	野口　良史	静岡大学工学部	Beyond GW: Development of second-order exchange term	Yoshifumi Noguchi	Graduate School of Engineering, Shizuoka University
57	2024-Ca-0127	モット絶縁体の不純物ドーピング	レービガー　ハンネス	横浜国立大学　大学院工学研究院　物理工学コース	Chemical doping of Mott insulators	Hannes Raebiger	Depertment Physics, Yokohama National University
58	2024-Cb-0026	高機能スピントロニクス磁性材料の電子構造・磁気異方性解析および準粒子自己無撞着GW法の並列化開発･応用	小田　竜樹	金沢大学理工研究域数物科学系	Analyses on electronic structure and magnetic anisotropy in high-performance spintronics magnetic materials and parallelization development/application in quasi-particle self-consistent GW	Tatsuki Oda	Faculty of Mathematics and Physics, Institute of Science and Engineering, Kanazawa University
59	2024-Ca-0136	新規機能性相転移材料の物性に関する理論的研究	大越　慎一	東京大学大学院理学系研究科化学専攻	Theoretical studies on the physical properties of novel functional phase transition materials	Shin-Ichi Ohkoshi	Department of Chemistry, School of Science, The University of Tokyo
60	2024-Ca-0105	密度汎関数法と溶液理論を用いた電気化学反応の解析 6	春山　潤	理化学研究所開拓研究本部	Electrochemical reaction analysis using density functional calcula- tion + implicit solvation model 6	Jun Haruyama	RIKEN Cluster for Pioneering Research
61	2024-Ca-0106	密度汎関数理論を用いた表面／界面における分子の吸着と反応に関する研究	濱田　幾太郎	大阪大学大学院工学研究科　物理学系専攻　精密工学コース	Density functional theory study of adsorption and reaction of molecules on solid surfaces and interfaces	Ikutaro Hamada	Department of Precision Engineering, Graduate School of Engineering, Osaka University
62	2024-Ca-0062	フラッシュメモリ応用を目指したa-SiN中の局在Floating Stateを起源とする新規電子トラップ欠陥の理論的研究	白石　賢二	名古屋大学　未来材料・システム研究所	Theoretical Studies on New Types of Electron Trap Defects Origninated from Localized Floating States in a-SiN towards Flash Memories Application	Kenji Shiraishi	Institute of Materials and Systems for Sustainability, Nagoya University
63	2024-Ca-0134	ナノ炭素材料デバイス構造の動的特性評価理論	草部　浩一	兵庫県立大学大学院理学研究科	Theoretical evaluation of mechanical properties of nano-carbon device structures	Koichi Kusakabe	Graduate School of Science, University of Hyogo
64	2024-Cb-0035	ナトリウムイオン電池に適用可能な有望な正極材料の研究	ルオン　フードック	東京工業大学	Investigation on positive electrodes applicable for Na-ion batteries	Huuduc Luong	Tokyo Institute of Technology
65	2024-Ca-0006	機械学習原子間ポテンシャルによる分子動力学計算の安定化の改善	島村　孝平	熊本大学大学院先端科学研究部	Improving Stability of Molecular Dynamics Simulation using Machine-Learning Interatomic Potentials	Kohei Shimamura	Faculty of Advanced Science and Technology, Kumamoto University
66	2024-Ca-0026	第一原理計算と分子動力学計算に基づく新規二次電池材料の探索	山田　淳夫	東京大学工学系研究科	Exploration of novel rechargeable battery materials using first-principles and molecular dynamics calculations	Atsuo Yamada	Faculty of Engineering, The University of Tokyo
67	2024-Ca-0053	金属材料の水素脆化を抑制するセラミックス保護被膜の開発	國貞　雄治	北海道大学大学院工学研究院　附属エネルギー・マテリアル融合領域研究センター	Development of Ceramic Protective Coating to suppress hydrogen embrittlement of metallic materials	Yuji Kunisada	Center for Advanced Research of Energy and Materials, Faculty of Engineering, Hokkaido University
68	2024-Ca-0128	有機半導体結晶における電子ーフォノン結合を考慮した第一原理バンド計算	柳澤　将	琉球大学理学部物質地球科学科物理系	First-principles bandstructure calculation with the electron-phonon interaction of organic semiconductor crystals	Susumu Yanagisawa	Department of Physics and Earth Sciences, Faculty of Science, University of the Ryukyus
69	2024-Cb-0050	超微細金属酸化物の構造歪とその電子状態に関する研究	横　哲	東北大学国際放射光イノベーション・スマート研究センター	Distortion of ultrasmall metal oxides and their electronic state	Akira Yoko	International Center for Synchrotron Radiation Innovation Smart, Tohoku University
70	2024-Ca-0011	2D遷移金属ハロゲン化物に生じる量子異常ホール効果	グエン　ティフォンタオ	大阪大学 産業科学研究所	Quantum anomalous Hall effect in 2D transition metal halides	Thi Phuong Thao Nguyen	Osaka University, Institute of Scientific and Industrial Research
71	2024-Ca-0002	機械学習を用いた環境発電用ストレッチャブル･エレクトレット材料の開発	鈴木　雄二	東京大学大学院工学系研究科機械工学専攻	Development of Stretchable Electret Materials for Energy Harvesting with the Aid of Machine Learning	Yuji Suzuki	Dept. of Mechanical Engineering, The University of Tokyo
72	2024-Cb-0015	階層的機械学習モデルによる化合粒半導体粒界の熱・電子特性の高精度予測	横井　達矢	名古屋大学大学院工学研究科　物質科学専攻	Hierarchical machine-learning model for accurately predicting thermal and electronic properties of grain boundaries in compound semiconductors	Tatsuya Yokoi	Department of Materials Physics, Nagoya University
73	2024-Cb-0029	ウルツァイト型強誘電体LiGaO2の分極反転における単一原子変位モデルの調査	安原　颯	東京科学大学	Investigation of atomic displacement mechanism during a polarization switching in LiGaO2	Sou Yasuhara	Institute of Science Tokyo

74	2024-Ca-0034	構造探索と第一原理計算による材料開発	山下　智樹	長岡技術科学大学技学研究院電気電子情報系	Materials Development by Crystal Structure Prediction and First-principles Calculations	Tomoki Yamashita	Nagaoka University of Technology
75	2024-Cb-0017	第一原理計算による光熱変換原理の解明	江目　宏樹	山形大学	Study of the principle of photothermal conversion by ab initio calculations	Hiroki Gonome	Yamagata University
76	2024-Ca-0033	第一原理分子動力学法に基づく分子性発光材料の静的構造の研究	高良　明英	熊本大学技術部	Ab Initio Study on Static Structure of White Light Generating Amorphous Molecular Materials	Akihide Koura	Technical Division, Kumamoto University
77	2024-Ca-0070	触媒表面基準エッチング法におけるSiのエッチング除去機構の解明	藤　大雪	大阪大学大学院工学研究科	Study on the etching mechanism of Si in catalyst-referred etching	Daisetsu Toh	Department of Precision Engineering Graduate School of Engineering
78	2024-Ca-0108	2次元層状物質におけるキャリア輸送特性の歪み依存性に関する第一原理研究	江上　喜幸	北海道大学大学院工学研究院	First-principles study on strain dependence of carrier transport properties in two-dimensional layered materials	Yoshiyuki Egami	Faculty of Engineering, Hokkaido University
79	2024-D-0016	中性子回折実験を反映したプロトン互変異性伝導経路のNEB計算	森　初果	東京大学物性研究所	First-principles NEB calculations of proton tautomeric conduction pathways based on Neutron diffraction	Hatsumi Mori	The Institute for Solid State Physics, The University of Tokyo
80	2024-Ca-0018	数理科学・MIと分子動力学計算を用いた界面反応の解明	佐藤　龍平	東京大学工学系研究科マテリアル工学専攻	Interfacial Reaction Study Driven by Mathematical Science, MI and Molecular Dynamics	Ryuhei Sato	Department of Materials Engineering, The University of Tokyo
81	2024-Ca-0074	第一原理フォノン計算によるK2NdTa5O15の安定構造探索	安原　颯	東京科学大学	Exploration of Stable Structure in K2NdTa5O15 using First-Principles Phonon Calculations	Sou Yasuhara	Institute of Science Tokyo
82	2024-Ca-0116	第一原理計算による白金ナノ粒子の被毒状態の研究	佐々木　岳彦	東京大学　大学院新領域創成科学研究科	Study on poisoning states of platinum nanoparticles	Takehiko Sasaki	Graduate School of Frontier Sciences, The University of Tokyo
83	2024-Ca-0083	ハイスループット計算による酸素発生反応のための低コストなヘテロ構造酸化物触媒の設計	JIA　XUE	東北大学材料科学高等研究所	Designing low-cost Metal Oxide Heterostructure catalysts for oxygen evolution reaction through High-Throughput Calculations	Xue Jia	Advanced Institute for Materials Research, Tohoku University
84	2024-D-0009	密度汎関数理論を用いた表面／界面における分子の吸着と反応に関する研究-二次元系物質を中心に	濱田　幾太郎	大阪大学大学院工学研究科　物理学系専攻　精密工学コース	Density functional theory study of adsorption and reaction of molecules on solid surfaces and interfaces: cases of two-dimensional materials	Ikutaro Hamada	Department of Precision Engineering, Graduate School of Engineering, Osaka University
85	2024-Ca-0013	ナノ粒子および永久磁石の安定性に関する第一原理的研究	立津　慶幸	名桜大学	First-principles study on stability of nano particles and permanent magnets	Yasutomi Tatetsu	Meio University
86	2024-Ca-0054	固体表面界面における構造的素励起の物性の研究	影島　博之	島根大学大学院自然科学研究科	Study on physical properties of structural elementary excitations at solid surfaces and interfaces	Hiroyuki Kageshima	Graduate School of Natural Science and Technology, Shimane University
87	2024-Ca-0126	燃料電池応用に向けたPt基ハイエントロピーの合金マルチスケールシミュレーションと機械学習による解析	ホ　ゴック　ナム	名古屋大学工学研究科　物質プロセス工学専攻	Pt-based high entropy alloys for fuel cell applications from multiscale simulations and machine learning method	Ngoc Nam Ho	Department of Materials Process Engineering, Graduate school of Engineering, Nagoya University
88	2024-Ca-0044	第一原理計算における高速ベリー位相計算コードの開発とエネルギー変換材料への応用	山口　直也	金沢大学ナノマテリアル研究所	Development of Fast Calculation Codes of Berry Phases in First-principles Calculations and its Application to Energy Conversion Materials	Naoya Yamaguchi	Nanomaterials Research Institute, Kanazawa University
89	2024-Ca-0075	有機分子薄膜の光電子強度計算手法の開発	二木　かおり	千葉大学	Development of photoelectron intensity calculation method for organic molecular thin films	Kaori Niki	Chiba University
90	2024-Cb-0027	第一原理計算を用いたセリア系複合触媒の理論的研究	辻　雄太	九州大学総合理工学研究院	Theoretical study of ceria-based composite catalysts using first-principles calculations	Yuta Tsuji	Faculty of Engineering Sciences, Kyushu University
91	2024-Ca-0021	閉じ込められた水の第一原理分子動力学シミュレーション	大戸　達彦	名古屋大学大学院工学研究科	First-principles molecular dynamics simulations for confined water	Tatsuhiko Ohto	Graduate School of Engineering, Nagoya University
92	2024-Ca-0050	第一原理計算による有機強誘電体・圧電体の物性予測	石橋　章司	産業技術総合研究所	Prediction of properties of organic ferroelectrics and piezoelectrics by first-principles calculations	Shoji Ishibashi	National Institute of Advanced Industrial Science and Technology
93	2024-Ca-0133	人工界面・多層膜におけるスピン軌道相互作用誘起物性と物質探索	中村　浩次	三重大学大学院工学研究科電気電子工学専攻	Material search and spin-orbit coupling induced properties at artificial interfaces and multilayers	Kohji Nakamura	Division of Electrical and Electronic Engineering, Graduate School of Engineering, Mie University
94	2024-Cb-0010	Sb系テラヘルツトランジスタのための歪バンド構造設計	藤代　博記	東京理科大学	Strained Band-Structure Engineering for Antimonide-Based Terahertz Transistors	Hiroki Fujishiro	Tokyo University of Science
95	2024-Cb-0038	第一原理計算によるパワー半導体材料の表面系および欠陥系の物性解明	制野　かおり	九州工業大学大学院工学研究院物質工学研究系	First-principles study of surface and defect systems for power-electronics materials	Kaori Seino	Department of Materials Science and Engineering, Kyushu Institute of Technology
96	2024-Ca-0059	第一原理計算を用いた二酸化炭素還元触媒の理論的研究	辻　雄太	九州大学総合理工学研究院	Theoretical study of carbon dioxide reduction catalysts using first-principles calculations	Yuta Tsuji	Faculty of Engineering Sciences, Kyushu University
97	2024-Ca-0004	合金の力学特性に関する第一原理的研究	上村　直樹	京都先端科学大学ナガモリアクチュエータ研究所	First-principles study of mechanical properties on alloys	Naoki Uemura	The Nagamori Institute of Actuators, Kyoto University of Advanced Science
98	2024-Ca-0017	2次元物質におけるフォノン流体力学の変調	許　斌	東京大学大学院機械工学専攻	Modulation of the phonon hydrodynamic in 2D materials	Xu Bin	Department of Mechanical Engineering, The University of Tokyo
99	2024-Ca-0068	第一原理計算によるパワー半導体材料の表面系および欠陥系の物性解明	制野　かおり	九州工業大学大学院工学研究院物質工学研究系	First-principles study of surface and defect systems for power-electronics materials	Kaori Seino	Department of Materials Science and Engineering, Kyushu Institute of Technology
100	2024-Ca-0072	第一原理計算を用いた反強磁性体の機能開拓と磁気トンネル接合への応用	田中　克大	東京大学大学院理学系研究科物理学専攻	First-principles exploration of physical properties of antiferromagnets and its application to magnetic tunnel junction	Katsuhiro Tanaka	Department of Physics, Graduate School of Science, University of Tokyo
101	2024-Ca-0031	DFTと高精度多重参照理論を用いたゼオライトによるC-H活性化の研究	フン　マイン クアン	名古屋大学理学部 化学科	Studying C-H bond activation in zeolite using DFT and highly accurate multi-reference theory	Manh Quan Phung	Department of Chemistry, School of Science, Nagoya University

102	2024-Ca-0032	大規模励起状態法による多重励起子生成機構の解析	藤田　貴敏	量子科学技術研究開発機構	Computational Investigation of Multi-Exciton Generation Mechanism by Large-Scale Excited-State Method	Takatoshi Fujita	National Institutes for Quantum Science and Technology
103	2024-Ca-0060	金属-窒素-炭素触媒上の酸素還元反応におけるスピンによる促進効果の探求	ジャン　デイ	東北大学材料高等研究所	Spin Promotion Effect in Magnetic Catalysis: Exploring High-Performance Metal-Nitrogen-Carbon Catalysts under External Magnetic Fields	Di Zhang	Advanced Institute for Material Research, Tohoku University
104	2024-Ca-0061	マテリアルズインフォマティクスによる材料探索ループの構築	原嶋　庸介	奈良先端科学技術大学院大学	Materials exploration loop with materials informatics.	Yosuke Harashima	Nara Institute of Science and Technology
105	2024-Ca-0121	第一原理計算によるMg合金系における力学特性の起源解明	圓谷　貴夫	熊本大学先進マグネシウム国際研究センター	First-Principles Study on the Origin of Mechanical Properties on Magnesium based Alloys	Takao Tsumuraya	Magnesium Research Center, Kumamoto University
106	2024-Ca-0046	進化的アルゴリズムによる水素化物高温超伝導の探索	石河　孝洋	東京大学大学院理学系研究科物理学専攻	Search for high temperature superconductivity in hydrides	Takahiro Ishikawa	Department of Physics, The University of Tokyo
107	2024-Eb-0002	不規則系におけるフォノン輸送特性解析	塩見　淳一郎	東京大学工学系研究科	Analysis of phonon transport properties in disordered systems	Junichiro Shiomi	School of Engineering, The University of Tokyo
108	2024-Ca-0016	極端非線形光電子スペクトルの第一原理シミュレーション	篠原　康	東京大学工学系研究科附属光量子科学研究センター	First-principles simulations for photoelectron spectra via extremely nonlinear processes	Yasushi Shinohara	Photon Science Center, School of Engineering, the University of Tokyo
109	2024-Ca-0035	Sb系テラヘルツトランジスタのための歪バンド構造設計	藤代　博記	東京理科大学	Strained Band-Structure Engineering for Antimonide-Based Terahertz Transistors	Hiroki Fujishiro	Tokyo University of Science
110	2024-Ca-0080	窒素還元反応のための遷移金属カーバイド触媒の磁気特性の探索	王　天一	東北大学 材料科学高等研究所	Explore magnetic properties of transition metal carbide catalysts for nitrogen reduction reaction	Tianyi Wang	Tohuku University
111	2024-Ca-0122	ガウス過程回帰による銀(111)薄膜上ゲルマネンの構造探索	濱本　雄治	岡山県立大学 情報工学部 情報通信工学科	Structure search for germanene on Ag(111) thin films by Gaussian process regression	Yuji Hamamoto	Department of Communication Engineering, Okayama Prefectural University
112	2024-Ca-0038	金属間化合物の表面原子構造と化学的特性に関する第一原理計算	野澤　和生	鹿児島大学理学部物理科学科	First-principles study of surface atomic structure and chemical properties of intermetallic compounds	Kazuki Nozawa	Department of Physics and Astronomy, Kagoshima University
113	2024-Ca-0041	金属表面におけるアンモニア分解反応および窒化のモデル化	李　敏赫	東京大学大学院工学系研究科機械工学専攻	Modeling of the Ammonia Decomposition Reaction and Nitriding on Metal Surfaces	Minhyeok Lee	Department of Mechanical Engineering, The University of Tokyo
114	2024-Ca-0036	酸化物系蛍光体における誘電率の第一原理計算	平田　研二	産業技術総合研究所	First-principles calculation of dielectric constant in oxide-based phosphor	Kenji Hirata	National Institute of Advanced Industrial Science and Technology
115	2024-Ca-0056	不純物ドープ型カーボンナノチューブの電子特性研究	藤本　義隆	九州大学工学研究院	First-principles study of Impurity-doped carbon nanotubes	Yoshitaka Fujimoto	Faculty of Engineering, Kyushu University
116	2024-Ca-0077	太陽光選択吸収材料の第一原理物質設計	中村　和磨	九州工業大学	Ab initio Material Design for Solar Absorption Films	Kazuma Nakamura	Kyushu Institute of Technology
117	2024-Cb-0053	Cu(100)表面上に吸着した銅フタロシアニンのFano共鳴の第一原理計算	濱本　雄治	岡山県立大学 情報工学部 情報通信工学科	First principles study of the Fano resonance in Copper phthalocyanine adsorbed on Cu(100)	Yuji Hamamoto	Department of Communication Engineering, Okayama Prefectural University
118	2024-Cb-0040	金属間化合物の表面原子構造と化学的特性に関する第一原理計算	野澤　和生	鹿児島大学理学部物理科学科	First-principles study of surface atomic structure and chemical properties of intermetallic compounds	Kazuki Nozawa	Department of Physics and Astronomy, Kagoshima University
119	2024-Ca-0071	照射損傷と格子欠陥との相互作用の研究	大澤　一人	九州大学応用力学研究所	Study of interaction between radiation damage and lattice defect	Kazuhito Ohsawa	Research Institute for Applied Mechanics, Kyushu University
120	2024-Ca-0110	完全フォトニックギャップハイパーマテリアルの探索	竹森　那由多	大阪大学　理学研究科	Exploration of photonic hypermaterials with complete-gap	Nayuta Takemori	Graduate School of Science, Osaka University
121	2024-Cb-0006	ドープ型カーボンナノチューブの電子構造研究	藤本　義隆	九州大学工学研究院	Electronic structures of doped carbon nanotubes	Yoshitaka Fujimoto	Faculty of Engineering, Kyushu University
122	2024-Cb-0019	次世代全固体電池、熱管理システム、水素貯蔵への応用を目指した理論シミュレーションによる先端水素化物材料開発	サウ　カーテイツク	東北大学 材料科学高等研究所 デバイス・システムグループ	Developing Advanced Hydride Materials using Theoretical Simulation Toward Next-Generation All-Solid-State-Battery, Heat/cooling Management Systems and Hydrogen Storage application.	Kartik Sau	Advanced Institute for Materials Research (WPI-AIMR), Tohoku University
123	2024-Ba-0054	常温高圧重合をおこす分子性結晶の反応機構と物性解析	島田　敏宏	北海道大学　大学院工学研究院	Analysis of reaction mechanism and physical properties of molecular crystals that undergoes polymerization under high pressure	Toshihiro Shimada	Faculty of Engineering, Hokkaido University
124	2024-Ba-0077	第一原理計算によるホイスラー合金型磁気トンネル接合の電子状態解析	海住　英生	慶應義塾大学	Electronic structure analysis of Heusler-alloy-based magnetic tunnel junctions using first-principles calculation	Hideo Kaiju	Keio University
125	2024-Ca-0008	立方晶系の原子層	小野　頌太	室蘭工業大学大学院工学研究科	Freestanding cubic crystals in the monolayer limit	Shota Ono	Muroran Institute of Technology
126	2024-Bb-0036	多層２次元材料における電子・フォノン局在・輸送に関する第一原理および古典分子動力学シミュレーション	鶴田　健二	岡山大学学術研究院環境生命自然科学学域	Ab-initio and classical molecular-dynamics simulation on electron/phonon localization and transport in multilayer 2D materials	Kenji Tsuruta	Faculty of Environmental, Life, Natural Science and Technology, Okayama University
127	2024-Ca-0025	パワーMOSFETのチャネル界面特性向上のための電子状態計算	吉岡　裕典	国立研究開発法人 産業技術総合研究所	Calculation of electronic states for improving characteristics at the channel interface of power MOSFETs	Hironori Yoshioka	National Institute of Advanced Industrial Science and Technology

128	2024-Bb-0033	バイオガス直接供給による燃料電池の高効率化に向けた硫化水素吸着材の研究	八代　圭司	島根大学	Study of hydrogen sulfide adsorbent for high efficiency of fuel cells with direct biogas supply	Yashiro Keiji	Shimane University
129	2024-Ca-0058	ダブルペロブスカイトの仕事関数とバンドギャップに関する理論的研究	西館　数芽	岩手大学理工学部	Theoretical study of work function and band gap of double-perovskite	Kazume Nishidate	Faculty of Science and Engineering, IWATE University
130	2024-Cb-0018	Ca2MnO4の酸素正八面体の回転の電子物性に対する影響の第一原理解析	中村　和磨	九州工業大学	Ab initio calculation of the rotation effect of oxygen octahedron in Ca2MnO4 on electronic properties	Kazuma Nakamura	Kyushu Institute of Technology
131	2024-Ba-0052	磁性形状記憶合金の第一原理計算	小幡　正雄	金沢大学理工研究域	First-principles investigation on magnetic shape memory	Masao Obata	Institute of Science and Engineering, Kanazawa University
132	2024-Ba-0024	新たなナノスケール表面界面の電子物性に関する理論的研究	小林　功佳	お茶の水女子大学理学部物理学科	Theoretical study on electronic properties of new nanoscale surfaces and interfaces	Katsuyoshi Kobayashi	Department of Physics, Faculty of Science, Ochanomizu University
133	2024-Bb-0004	金属原子ドープによる光触媒の活性化原理の解明	泉　康雄	千葉大学 大学院理学研究院	Clarification of the Activation Principle of Photocatalyts by Doping Metal Atom	Yasuo Izumi	Graduate School of Science, Chiba University
134	2024-Bb-0016	第一原理計算に基づく接着性高分子材料の接着機構の解明	住谷　陽輔	山口大学大学院創成科学研究科	Elucidation of adhesion mechanism of adhesive polymer materials based on first-principle calculations	Yosuke Sumiya	Graduate School of Sciences and Technology for Innovation, Yamaguchi University
135	2024-Bb-0017	反強磁性金属を用いたトンネル磁気抵抗効果の第一原理計算	田中　克大	東京大学大学院理学系研究科物理学専攻	First-principles study on tunnel magnetoresistance effect using antiferromagnetic metals	Katsuhiro Tanaka	Department of Physics, Graduate School of Science, University of Tokyo
136	2024-Bb-0020	ハイエントロピー合金の電子状態と相変態	御手洗　容子	東京大学新領域創成科学研究科	Phase transformation and electric state of high entropy alloys	Yoko Mitarai	Graduate School of Frontier Sciences, The University of Tokyo
137	2024-Bb-0026	第一原理計算によるハーフメタル型磁気トンネル接合の電子状態解析	海住　英生	慶應義塾大学	Electronic structure analysis of half-metal based magnetic tunnel junctions using first-principles calculation	Hideo Kaiju	Keio University
138	2024-Ba-0036	金属表面における酸化過程の理論的研究	萩原　聡	筑波大学計算科学研究センター	A theoretical study on an oxidation process at a metal surfaces	Satoshi Hagiwara	Center for Computational Sciences, University of Tsukuba
139	2024-Ba-0055	光による電流制御の第一原理計算	佐藤　駿丞	筑波大学計算科学研究センター	First-principles analysis on optical-control of current in solids	Shunsuke Sato	Center for Computational Sciences, University of Tsukuba
140	2024-Ba-0063	第一原理バンド計算を用いた多軌道多層化合物の研究	榊原　寛史	鳥取大学大学院工学研究科	First-principles study of multi-orbital and multi-layer compounds	Hirofumi Sakakibara	Graduate School of Engineering, Tottori University
141	2024-Ba-0043	ゴニオ極性熱電材料の第一原理計算による解析	臼井　秀知	島根大学総合理工学部	First principles study on the thermoelectric properties of goniopolar compounds	Hidetomo Usui	Department of Physics and Materials Science, Shimane University
142	2024-Bb-0023	酸化物準結晶超薄膜の構造解析	柚原　淳司	名古屋大学	Structural analysis of oxide quasicrystal thin films	Junji Yuhara	Nagoya University
143	2024-Bb-0032	イオン熱電材料の機械学習支援型計算設計	アン　モン	東京大学 機械工学科	Machine learning-assisted computational design of Ionic thermoelectric materials	Meng An	Department of Mechanical Engineering, The University of Tokyo
144	2024-Ba-0015	ジラジカル-界面相互作用の理論解析に立脚した双安定性機能物質の設計	多田　幸平	大阪大学　大学院基礎工学研究科　物質創成専攻化学工学領域	Theoretical design of bistable functional materials based on calculations for diradical-solid interaction	Kohei Tada	Devision of Chemical Engineering, Department of Materials Engineering Science, Graduate School of Engineering Science, Osaka University
145	2024-Ba-0020	従来型超伝導理論再考：ほとんど一様な電子系への展開	明石　遼介	量子科学技術研究開発機構	Revisiting the conventional superconducting theory: Toward nearly uniform electron systems	Ryosuke Akashi	National Institutes for Quantum Science and Technology
146	2024-Ba-0039	樹木由来ナノセルロース１本の構造解析	藤澤　秀次	東京大学農学生命科学研究科	Structural analysis of a single nanocellulose from wood	Shuji Fujisawa	Graduate School of Agricultural and Life Sciences, The University of Tokyo
147	2024-Ba-0061	カルコゲナイド半導体ナノ粒子の表面修飾による不純物準位制御	首藤　健一	横浜国立大学・工学部	Impurity control of chalcogenides by surface-modification	Ken-Ichi Shudo	Yokohama Nat'l Univ.
148	2024-Bb-0010	トポロジカル磁性体における異常ネルンスト効果の第一原理計算	見波　将	京都大学工学研究科機械理工学専攻	First-principles study for anomalous Nernst effect in topological magnets	Susumu Minami	Department of Mechanical Engineering and Science, Kyoto University
149	2024-Bb-0011	第一原理計算を用いた有機スピンバルブ素子における電子状態解析	海住　英生	慶應義塾大学	Electronic structure analysis of organic spin valve devices using first-principles calculation	Hideo Kaiju	Keio University
150	2024-Bb-0015	原子スケール磁性強誘電性創発に向けた格子欠陥機能の第一原理的設計	嶋田　隆広	京都大学 大学院工学研究科 機械理工学専攻	First-principles lattice defects engineering for atomic-scale multiferroics	Takahiro Shimada	Department of Mechanical Engineering and Science, Graduate School of Engineering, Kyoto University
151	2024-Ba-0010	ベーテサルペーター方程式によるデラフォサイト型銅酸化物の励起子物性	牧野　哲征	福井大学遠赤外領域開発研究センター	Excitonic properties of delafossite-type cuprates	Takayuki Makino	Research Center for Development of Far-Infrared Region, University of Fukui
152	2024-Ba-0011	RbAg$_{4}$I$_{5}$とRb$_{2}$AgI$_{3}$の比較によるAgイオンの伝導メカニズムの研究	田原　周太	中京大学教養教育研究院	Study on Ag conducting mechanism by comparison between RbAg$_{4}$I$_{5}$ and Rb$_{2}$AgI$_{3}$	Shuta Tahara	Faculty of Liberal Arts and Sciences, Chukyo University
153	2024-Ba-0053	局所密度量による物質表面のAFM像予測	福田　将大	東京大学物性研究所	Prediction of AFM images of material surfaces by local density quantities	Masahiro Fukuda	Institute for Solid State Physics, The University of Tokyo

154	2024-Ba-0075	グラフニューラールネットワーク力場を用いた振動スペクトル計算の検証	平塚　将起	工学院大学機械工学科	Calculation of vibrational spectra using graph neural network force field	Masaki Hiratsuka	Department of Mechanical Engineering, Kogakuin University
155	2024-Bb-0044	Ni表面上での単層ボロフェンおよびホウ化物の構造解析	中川　剛志	九州大学大学院総合理工学研究院	Structural analysis of single layer borophene and boride on Ni surfaces	Takeshi Nakagawa	Interdisciplinary Graduate School of Engineering Sciences, Kyushu University
156	2024-Ba-0027	機能性物質中の原子スケール構造に基づく表面・界面現象および機械的特性に関する研究	三澤　賢明	福岡工業大学工学部知能機械工学科	Computational study of surface and interface phenomena and mechanical properties of functional materials based on atomic-scale structures	Masaaki Misawa	Department of Intelligent Mechanical Engineering, Fukuoka Institute of Technology
157	2024-Ba-0045	ホウ化物ライブラリー構築に向けた第一原理計算	安藤　康伸	東京科学大学 総合研究院	First-principles calculation for building boron-compounds library	Yasunobu Ando	Institute of Integrated Research, Institute of Science Tokyo
158	2024-Ba-0049	ハイエントロピー合金の電子状態と相変態	御手洗　容子	東京大学新領域創成科学研究科	Phase transformation and electric state of high entropy alloys	Yoko Mitarai	Graduate School of Frontier Sciences, The University of Tokyo
159	2024-Ba-0059	動的骨格を持つHOFの溶媒吸脱着に伴う構造変化の第一原理的予測	出倉　駿	東北大学多元物質科学研究所	First-principles prediction of structural changes by vapor sorption in HOFs with dynamic skeleton	Shun Dekura	Institute of Multidisciplinary Research for Advanced Materials, Tohoku University
160	2024-Ba-0071	タングステン合金の第一原理計算	河野　翔也	九州工業大学	first-principles calculation of tungsten alloy	Shoya Kawano	Kyushu Institute of Technology
161	2024-Ba-0073	電磁場と物質の相互作用の数値計算モデル開発	加藤　洋生	東京大学光量子科学研究センター	Development of Numerical methods for Light-Matter Interaction	Hiroki Katow	Photon Science Center, the University of Tokyo
162	2024-Bb-0022	ホウ化物ライブラリー構築に向けた第一原理計算	安藤　康伸	東京科学大学 総合研究院	First-principles calculation for building boron-compounds library	Yasunobu Ando	Institute of Integrated Research, Institute of Science Tokyo
163	2024-Ca-0093	第一原理計算によるIn誘起Si(111)表面超構造の安定性の研究	福田　常男	大阪公立大学大学院工学研究科電子物理系専攻	First-principles Study of In-induced Superstructures on the Si(111) surface	Tuneo Fukuda	Depart. of Physics and Electronics, Graduate School of Eng., Osaka Metroolitan University
164	2024-Cb-0023	パワーMOSFETのチャネル界面特性向上のための電子状態計算	吉岡　裕典	国立研究開発法人 産業技術総合研究所	Calculation of electronic states for improving characteristics at the channel interface of power MOSFETs	Hironori Yoshioka	National Institute of Advanced Industrial Science and Technology
165	2024-Ba-0016	低環境負荷・高耐久を両立する新規Na-ion蓄電池材料の設計指針確立に向けた理論研究	多田　幸平	大阪大学　大学院基礎工学研究科　物質創成専攻化学工学領域	Theoretical investigation to design of novel Na-ion battery materials with low environmental impact and high durability	Kohei Tada	Devision of Chemical Engineering, Department of Materials Engineering Science, Graduate School of Engineering Science, Osaka University
166	2024-Ba-0003	Cu(111)表面上における有機金属構造体薄膜に捕獲された吸着分子に対するDFT計算	塚原　規志	群馬工業高等専門学校	DFT calculations of adsorbed molecules captured by metal-organic films on Cu(111)	Noriyuki Tsukahara	National Institute for Technology, Gunma College
167	2024-Ba-0023	固体表面･界面、ナノ構造体の新規電子物性の探索と実現	稲岡　毅	琉球大学理学部	Search and realization of novel electronic properties of surfaces and interfaces and of nanostructures	Takeshi Inaoka	Department of Physics and Earth Sciences, Faculty of Science, University of the Ryukyus
168	2024-Ba-0006	第一原理計算による、プラズマ処理したフッ素樹脂／酸化銅界面の接着メカニズムの解明	大久保　雄司	大阪大学大学院工学研究科	Clarification of adhesion mechanism at interface between plasma-treated fluoropolymer and copper oxide using first-principles calculations	Yuji Ohkubo	Graduate School of Engineering, Osaka University
169	2024-Ba-0035	無機高分子材料の第一原理分子動力学計算	本武　陽一	一橋大学大学院ソーシャル・データサイエンス研究科	Ab initio molecular dynamics study of inorganic polymer	Yoh-Ichi Mototake	Faculty of Social Data Science, Hitotsubashi university
170	2024-Ba-0038	Si、Ge、ダイヤモンド表面のスピン分割計算 材料	Kadarisman Hana	Kanazawa University	Spin-splitting calculation of Si, Ge, and Diamond materials	Hana Kadarisman	Nanomaterials Research Institute, Kanazawa University
171	2024-Ba-0076	機械学習ポテンシャルの生成とそれによる半導体表面プロセスの解析	稲垣　耕司	大阪大学大学院工学研究科	Analyses of semiconductor surface processes by machine-learning based potentials	Kouji Inagaki	Graduate Scool of Engineering, Osaka University
172	2024-Bb-0003	DFT+U法に基づく、プラズマ処理したフッ素樹脂／CuO界面の接着メカニズムの解明 —CuO層内での酸素欠陥の拡散の影響—	大久保　雄司	大阪大学大学院工学研究科	Clarification of adhesion mechanism at interface between plasma-treated fluoropolymer and CuO using DFT+U method -Influence of oxygen vacancy diffusion in CuO layer-	Yuji Ohkubo	Graduate School of Engineering, Osaka University
173	2024-Ba-0017	水和高分子の電子状態	高橋　修	広島大学大学院理学研究科	Electronic structure of aqueous polymers	Osamu Takahashi	Graduate School of Science, Hiroshima University
174	2024-Ba-0057	機能性グラフェンと接触した半導体表面のエッチング現象の解析	有馬　健太	大阪大学 大学院 工学研究科	Detailed analysis of etching at functional graphene/semiconductor interface	Kenta Arima	Graduate School of Engineering, Osaka University
175	2024-Bb-0030	クラフトリグニンの水熱液化におけるカーボンナノファイバー担持Ni/CeO2の触媒反応機構に関する検討	布浦　鉄兵	東京大学大学院新領域創成科学研究科	Study on catalytic hydrothermal liquefaction of kraft lignin with carbon-nanofiber-supported Ni/CeO2	Teppei Nunoura	Graduate School of Frontier Sciences, The University of Tokyo
176	2024-Ba-0040	WO$_{3}$の電子構造	眞榮平　孝裕	琉球大学　理学部	Electronic Structure of WO$_{3}$	Takahiro Maehira	Faculty of Science, University of the Ryukyus
177	2024-A-0003	金属触媒表面の分子吸着に関する理論的研究	巽　俊暢	九州大学総合理工学研究院	Theoretical study on molecular adsorption on metal catalyst surface	Toshinobu Tatsumi	Interdisciplinary Graduate School of Engineering Sciences, Kyushu University
178	2024-A-0004	新規炭素同素体の構造と安定性に関する理論研究	草野　茜	九州大学大学院総合理工学研究院	Theoretical study on the structure and stability of new carbon allotropes	Akane Kusano	Interdisciplinary Graduate School of Engineering Sciences, Kyushu University

179	2024-A-0006	第一原理計算に基づく接着メカニズムの解明	住谷　陽輔	山口大学大学院創成科学研究科	Elucidation of adhesion mechanism based on first principle calculations	Yosuke Sumiya	Graduate School of Sciences and Technology for Innovation, Yamaguchi University
180	2024-A-0007	酸化物準結晶超薄膜の構造解析	柚原　淳司	名古屋大学	Structural analysis of oxide quasicrystal thin films	Junji Yuhara	Nagoya University
181	2024-A-0011	有機薄膜太陽電池材料の電子状態計算	鬼頭　宏任	近畿大学理工学部	Electronic Structure Calculations of Organic Solar Cell Materials	Hirotaka Kitoh	Faculty of Science and Engineering, Kindai University
182	2024-A-0013	第一原理計算と機械学習による高機能新材料の探索	陳　迎	東北大学 グローバルラーニングセンター	Exploring new materials with noval properties using first-principles approaches combing machine learning	Chen Ying	Global Learning Center, Tohoku University
183	2024-A-0014	大型欠陥を含むGaN結晶に対する振動モード解析(準備)	小田　将人	和歌山大学システム工学学部	Vibrational mode analysis of GaN crystals containing a large size of defects	Masato Oda	Department of Systems Engineering, Wakayama University
184	2024-A-0016	ベリリウム銅合金の表面電子状態と分子吸着特性	長田　渉	産業技術総合研究所	The surface electronic state and adsorption property of the Be-Cu alloy	Wataru Osada	National Institute of Advanced Industrial Science and Thechnology
185	2024-A-0019	第一原理計算を用いたSn/Geダブルペロブスカイト型太陽電池の欠陥構造に関する理論的研究	村岡　梓	日本女子大学　理学部　数物情報科学科	Theoretical Study on Defect Structure of Sn/Ge Double Perovskite Solar Cells Using First-Principles Calculations	Azusa Muraoka	Dept. of Mathematics, Physics and Computer Science, Japan Women's University,
186	2024-A-0023	金属触媒表面の分子吸着に関する理論的研究	巽　俊暢	九州大学総合理工学研究院	Theoretical study on molecular adsorption on metal catalyst surface	Toshinobu Tatsumi	Interdisciplinary Graduate School of Engineering Sciences, Kyushu University
187	2024-A-0024	二元系物質群に関するマテリアルズインフォマティクス基盤研究	草野　茜	九州大学大学院総合理工学研究院	Fundamental Materials Informatics Research on Binary Systems of Materials	Akane Kusano	Interdisciplinary Graduate School of Engineering Sciences, Kyushu University
188	2024-A-0026	密度汎関数計算を用いたアクチノイド核の核壊変と電子軌道の相関	金子　政志	大阪大学大学院理学研究科	Correlation between nuclear decay and electronic orbitals in actinide compounds using density functional theory calculations	Masashi Kaneko	Graduate School of Science, Osaka University
189	2024-A-0031	第一原理計算によるリチウム硫黄電池の電極/電解液界面におけるフッ素含有溶媒の還元分解メカニズム	韓　智海	新潟大学自然科学系	Reductive decomposition mechanism of fluorine-containing solvent at the electrode/electrolyte interface of lithium sulfur batteries by first-principles calculations	Jihae Han	Graduate School of Science and Technology, Niigata University
190	2024-Bb-0028	大型欠陥を含むGaN結晶に対する振動モード解析	小田　将人	和歌山大学システム工学学部	Vibrational mode analysis of GaN crystals containing a large size of defects	Masato Oda	Department of Systems Engineering, Wakayama University

2. 強相関 / Strongly Correlated Quantum Systems

No.	課題番号	課題名	氏名	所属	Title	Name	Organization
1	2024-Ea-0004	強相関第一原理計算を用いた相関トポロジカル物質の研究	三澤　貴宏	東京大学物性研究所	Study of correlated topological insulators using the ab initio method for correlated electron systems	Takahiro Misawa	IInstitute for Solid State Physics, The University of Tokyo
2	2024-Ea-0003	量子多体系の機械学習を用いた研究	今田　正俊	上智大学	Studies on Quantum Many-Body Problem by Machine Learning	Masatoshi Imada	Faculty of Science and Engineering, Sophia University
3	2024-Ea-0007	トランスフォーマー型の変分波動関数の開発と応用	野村　悠祐	東北大学金属材料研究所	Variational Ansatz based on Vision Transformers	Yusuke Nomura	Institute for Materials Research, Tohoku University
4	2024-D-0007	擬フェルミ粒子汎関数繰り込み群法による3次元拡張キタエフ模型の数値的研究	求　幸年	東京大学大学院工学系研究科	Numerical study of extended Kitaev models in three dimensions by the pseudo-fermion functional renormalization group method	Yukitoshi Motome	Department of Applied Physics, The University of Tokyo
5	2024-D-0010	フェルミマシンによる量子多体計算手法の開発	今田　正俊	上智大学	Development of Fermi Machine for Quantum Many-Body Solver	Masatoshi Imada	Faculty of Science and Engineering, Sophia University
6	2024-Ea-0011	非マルコフモンテカルロ法と人工ニューラルネットワークを組み合わせた大規模並列変分モンテカルロ法	山地　洋平	物質・材料研究機構	Massively parallel variational Monte Carlo method augmented by non-Markovian Monte Carlo and artificial neural networks	Youhei Yamaji	National Institute for Materials Science
7	2024-Cb-0020	量子多体シミュレーションと情報科学を駆使した強相関電子系の研究	求　幸年	東京大学大学院工学系研究科	Theoretical study of strongly correlated electron systems using quantum many-body simulation and information science	Yukitoshi Motome	Department of Applied Physics, The University of Tokyo
8	2024-Ca-0124	第一原理計算による結晶構造及びフォノン解析に基づく新規ニッケル化合物高温超伝導体の理論探索	黒木　和彦	大阪大学	Theoretical search for new high T_c nickelate superconductors based on structural and phonon DFT analysis	Kazuhiko Kuroki	Osaka University
9	2024-Ca-0065	量子多体シミュレーションと情報科学を駆使した強相関電子系の研究	求　幸年	東京大学大学院工学系研究科	Theoretical study of strongly correlated electron systems using quantum many-body simulation and information science	Yukitoshi Motome	Department of Applied Physics, The University of Tokyo
10	2024-Ca-0069	多軌道強相関電子系における自発的乱れの形成とダイナミクス	堀田　知佐	東京大学総合文化研究科	Disorder and dynamics of strongly correlated elecron in a multi-orbital systems	Chisa Hotta	Department of Basic Science, The University of Tokyo
11	2024-Ca-0073	フラストレートスピン系と多自由度が絡み合う磁場誘起相	諏訪　秀麿	東京大学大学院理学系研究科物理学専攻	Magnetic field-induced phases emerging from frustrated spin systems coupled to multiple degrees of freedom	Hidemaro Suwa	Department of Physics, The University of Tokyo
12	2024-Ca-0085	パイロクロア格子上の創発量子スピン液体	ポーレ　リコ	静岡大学　学術院理学領域	Emergent Quantum Spin Liquids on the Pyrochlore lattice	Rico Pohle	Faculty of Science, Shizuoka University
13	2024-Ca-0020	電子相関に起因する電流・スピン流テクスチャを持つ新奇量子相	遠山　貴己	東京理科大学先進工学部物理工学科	Novel quantum phases with current and spin current textures due to electron correlation	Takami Tohyama	Department of Applied Physics, Tokyo University of Science
14	2024-Ca-0096	3チャンネル近藤相の周辺に出現する量子臨界点の研究	堀田　貴嗣	東京都立大学理学研究科物理学専攻	Research of quantum critical points in the vicinity of three-channel Kondo phase	Takashi Hotta	Department of Physics, Graduate School of Science, Tokyo Metropolitan University

15	2024-Ca-0012	強相関系における非平衡現象	ピータース　ロバート	京都大学	Nonequilibrium phenomena in strongly correlated systems	Robert Peters	Kyoto University
16	2024-Cb-0003	圧力下のf電子系化合物におけるスピンゆらぎと超伝導	清水　真	京都大学理学研究科	Spin fluctuations and superconductivity in f-electron compounds under pressure	Makoto Shimizu	Faculty of Science, Kyoto University
17	2024-Ca-0097	多成分フェルミ粒子系のDMFTによる強磁性秩序の解析	古賀　昌久	東京科学大学	Analyzing Ferromagnetic Order in Multi-Component Fermionic Systems using DMFT	Akihisa Koga	Institute of Science Tokyo
18	2024-Cb-0046	Ab-initio法を用いた分子性導体での圧力誘起量子相転移の解析	吉見　一慶	東京大学物性研究所	Ab-initio analysis of pressure-induced quantum phase transitions in molecular materials	Kazuyoshi Yoshimi	Institute for Solid State Physics, The University of Tokyo
19	2024-Cb-0007	非エルミートSU(N)ハバードモデルにおける散逸の誘起する超流動相の探索	古賀　昌久	東京科学大学	Numerical analysis of the dissipation-induced superfluidity in non-Hermitian SU(N) Hubbard model	Akihisa Koga	Institute of Science Tokyo
20	2024-Ca-0109	量子スピン液体における非可換エニオンの外場駆動	那須　譲治	東北大学	Driving non-Abelian anyons by external fields in quantum spin liquids	Joji Nasu	Tohoku University
21	2024-Ca-0003	機械学習を用いたスピン模型生成	速水　賢	北海道大学大学院理学研究院	Generation of spin model based on machine learning	Satoru Hayami	Department of Physics, Hokkaido University
22	2024-Ca-0030	ハバードモデルをもちいた強相関電子系の超伝導状態と磁性状態の研究。	山田　篤志	千葉大学理学研究科	A study of superconductivity and magnetism of strongly correrated electron systems using Hubbard model.	Atsushi Yamada	Department of Physics, Chiba University
23	2024-Ba-0067	磁気秩序系における高次高調波発生とサブサイクルダイナミクスの解明	小野　淳	東北大学大学院理学研究科	High harmonic generation and subcycle dynamics in magnetically ordered systems	Atsushi Ono	Department of Physics, Tohoku University
24	2024-Bb-0043	動的平均場法を用いた強相関化合物の多極子物性の研究	大槻　純也	岡山大学異分野基礎科学研究所	Study of multipolar properties in strongly correlated electron systems by dynamical mean-field theory	Junya Otsuki	Research Institute for Interdisciplinary Science, Okayama University
25	2024-Bb-0005	DFT+DMFT法による強相関交替磁性体のスピン分裂とX線分光応答の理論研究	播木　敦	大阪公立大学工学研究科	Computational study on spin splitting and x-ray spectroscopy responses in altermagnets using DFT+DMFT method	Atsushi Hariki	Department of Physics and Electronics, Osaka Metropolitan University
26	2024-Ba-0056	回路複雑性とテンソルネットワーク	小野　清志郎	理化学研究所	Circuit complexity and tensor network	Seishiro Ono	RIKEN
27	2024-Ba-0018	有機導体において電子相関が誘起する新奇な秩序とそれに関連した異常物性の解明	小林　晃人	名古屋大学　大学院理学研究科	Elucidation of novel order induced by electronic correlation in organic conductors and related anomalous properties	Akito Kobayashi	Graduate School of Science, Nagoya University
28	2024-Bb-0025	最適化量子変分モンテカルロ法による強相関多体問題の研究	柳沢　孝	産業技術総合研究所	Study of strongly correlated many-body problem based on the optimization quantum variational Monte Carlo method	Takashi Yanagisawa	National Institute of Advanced Industrial Science andTechnology
29	2024-Ba-0047	強相関電子系における高温超伝導機構の研究	柳沢　孝	産業技術総合研究所	Optimized variational Monte Carlo study of high-temperature superconductivity of strongly correlated electrons	Takashi Yanagisawa	National Institute of Advanced Industrial Science andTechnology
30	2024-Ba-0062	強相関電子系におけるBCS-BECクロスオーバーの理論的研究	渡部　洋	日本大学生産工学部	Theoretical study of BCS-BEC crossover in strongly-correlated electron systems	Hiroshi Watanabe	College of Industrial Technology, Nihon University
31	2024-Ba-0044	マグノンバンドトポロジーへの多体相関の効果とその光学的検出に関する理論研究	望月　維人	早稲田大学先進理工学部応用物理学科	Theoretical study on the correlation effects of magnon-band topology and their optical detections	Masahito Mochizuki	Waseda university
32	2024-Ba-0033	スピン揺らぎによる熱電性能の増強メカニズムの理論的研究：弱結合理論からのアプローチ	西口　和孝	神戸大学大学院システム情報学研究科	Theoretical study of enhancement mechanism of thermoelectric properties with spin fluctuations: A weak-coupling approach	Kazutaka Nishiguchi	Graduate School of System Informatics, Kobe University
33	2024-A-0018	有機伝導体のバンド計算	圷　広樹	大阪大学大学院理学研究科化学専攻	Band structural calculations of organic conductors	Hiroki Akutsu	Department of Chemistry, Graduate School of Science, Osaka University
34	2024-A-0029	量子ホール・超伝導接合系のトポロジカル相	工藤　耕司	九州大学	Topological phases in quantum Hall superconductor hybrids	Koji Kudo	Kyushu University

3. 巨視系の協同現象 / Cooperative Phenomena in Complex, Macroscopic Systems

No.	課題番号	課題名	氏名	所属	Title	Name	Organization
1	2024-Ea-0001	全原子及び粗視化モデルによるソフトマターの大規模分子シミュレーション	篠田　渉	岡山大学異分野基礎科学研究所	Large-scale Molecular Simulation of Soft Materials using All-Atom and Coarse-Grained Model	Wataru Shinoda	Okayama University, Research Institute for Interdisciplinary Science
2	2024-Eb-0011	テンソルリング分解による新しい低ランク近似法と臨界現象への応 用	川島　直輝	東京大学物性研究所	New low-rank approximation by tensor ring decomposition and its application to critical phenomena	Naoki Kawashima	Institute for Solid State Physics, University of Tokyo
3	2024-Eb-0003	全原子及び粗視化モデルによるソフトマターの大規模分子シミュレーション	篠田　渉	岡山大学異分野基礎科学研究所	Large-scale Molecular Simulation of Soft Materials using All-Atom and Coarse-Grained Model	Wataru Shinoda	Okayama University, Research Institute for Interdisciplinary Science
4	2024-Ea-0012	テンソルリング分解による新しい低ランク近似法と臨界現象への応用	川島　直輝	東京大学物性研究所	New low-rank approximation by tensor ring decomposition and its application to critical phenomena	Naoki Kawashima	Institute for Solid State Physics, University of Tokyo
5	2024-Ea-0009	流れの中における赤血球の多体効果の解析	渡辺　宙志	慶応義塾大学理工学部	Analysis of the many-body effect of red blood cells in flow	Hiroshi Watanabe	Faculty of Science and Technology, Keio University
6	2024-Eb-0007	揺らぐ流体力学の数値計算プログラムの開発とその応用	中野　裕義	東京大学物性研究所	Development of a numerical solver for fluctuating hydrodynamics and its applications	Hiroyoshi Nakano	The Institute for Solid State Physics, The University of Tokyo
7	2024-Ea-0005	分子動力学計算による超音波キャビテーションの解析	浅野　優太	医療創生大学国際看護学部	Molecular dynamics analysis on ultrasonic cavitation	Yuta Asano	Iryososei University Faculty of Global Nursing
8	2024-Eb-0008	超音波キャビテーションの分子動力学シミュレーション	浅野　優太	医療創生大学国際看護学部	Molecular dynamics simulation of ultrasonic cavitation	Yuta Asano	Iryososei University Faculty of Global Nursing

9	2024-D-0011	変分モンテカルロ法による多層型超伝導体の圧力下での基底状態探索	金子　隆威	上智大学 理工学部 機能創造理工学科	Variational Monte Carlo study of ground states of a multilayer superconductor under pressure	Ryui Kaneko	Department of Engineering and Applied Sciences, Faculty of Science and Technology, Sophia University
10	2024-Ca-0047	生体膜の構造形成	野口　博司	東京大学物性研究所	structure formation of biomembrane	Hiroshi Noguchi	Institute for Solid State Physics, University of Tokyo
11	2024-Cb-0047	フラストレート磁性体の有限温度物性の解明	大久保　毅	東京大学大学院理学系研究科知の物理学研究センター	Finite temperature property of frustrated spin systems	Tsuyoshi Okubo	Institute for Physics of Intelligence, The University of Tokyo
12	2024-Cb-0032	大規模計算による半結晶性高分子の破壊プロセス	樋口　祐次	九州大学情報基盤研究開発センター	Fracture process of semicrystalline polymers using large-scale simulation	Yuji Higuchi	Research Institute for Information Technology, Kyushu University
13	2024-Cb-0033	多層CNT糸複合材料の高機能化のための多層CNT糸構造設計	山本　剛	東北大学大学院工学研究科・航空宇宙工学専攻	Designing MWCNT Fiber Structures for High Mechanical Performance Composites	Go Yamamoto	Department of Aerospace Engineering, Tohoku University
14	2024-Ca-0119	テンソルネットワークマルコフ連鎖モンテカルロ法の開発と量子多体系への応用	藤堂　眞治	東京大学大学院理学系研究科物理学専攻	Development of tensor-network Markov-chain Monte Carlo and application to quantum many-body systems	Synge Todo	Department of Physics, University of Tokyo
15	2024-Ca-0125	テンソルネットワーク法によるハニカム格子量子スピン模型の研究	大久保　毅	東京大学大学院理学系研究科知の物理学研究センター	Tensor network study of quantum spin models on the honeycomb lattice	Tsuyoshi Okubo	Institute for Physics of Intelligence, The University of Tokyo
16	2024-Cb-0049	医療および産業応用のための新規タンパク質設計法の開発	新井　宗仁	東京大学大学院総合文化研究科	Development of a novel protein design method for medical and industrial applications	Munehito Arai	Graduate School of Arts and Sciences, The University of Tokyo
17	2024-Ca-0042	非エルミート系の準位統計と臨界現象	大槻　東巳	上智大学理工学部	Level statistics and critical phenomena in non-Hermitian systems	Tomi Ohtsuki	Faculty of Science and Technology, Sophia University
18	2024-Cb-0002	機械学習を用いた磁気スキルミオン結晶の効率的探索	速水　賢	北海道大学大学院理学研究院	Efficient search of magnetic skyrmion crystal by using machine learning	Satoru Hayami	Department of Physics, Hokkaido University
19	2024-Cb-0021	拡張近藤格子模型の基底状態相図	井戸　康太	東京大学物性研究所	Ground-state phase diagram of extended Kondo lattice models	Kota Ido	Institute for Solid State Physics, The University of Tokyo
20	2024-Cb-0024	蜂の巣格子上のS=1拡張キタエフ模型の基底状態相図	鈴木　隆史	兵庫県立大学　大学院工学研究科	Ground state phase diagram of an extended Kitaev model on a honeycomb lattice	Takafumi Suzuki	Graduate School of Engineering, University of Hyogo
21	2024-Ca-0029	フラストレーションのある遍歴磁性体の基底状態相図	井戸　康太	東京大学物性研究所	Ground-state phase diagram of frustrated itinerant magnets	Kota Ido	Institute for Solid State Physics, The University of Tokyo
22	2024-Ca-0111	高分子の伸長流動シミュレーション	村島　隆浩	東北大学大学院理学研究科	Elongational Flow Simulation of Polymers	Takahiro Murashima	東北大学大学院理学研究科
23	2024-Ca-0100	量子多体系のスクランブリングの理解と量子計算機による実現	手塚　真樹	京都大学大学院理学研究科物理学・宇宙物理学専攻	Understanding scrambling dynamics in quantum many-body systems and realizing the dynamics in quantum computers	Masaki Tezuka	Department of Physics, Kyoto University
24	2024-Cb-0041	拡張アンサンブル法とスピングラス模型の大規模計算	福島　孝治	東京大学大学院総合文化研究科	Large scale computation for spin glasses using extended ensemble methods	Koji Hukushima	Department of Basic Science, The University of Tokyo
25	2024-Ca-0066	複雑流動のマルチスケールシミュレーション	川勝　年洋	東北大学大学院理学研究科物理学専攻	Multiscale simulations for complex flows	Toshihiro Kawakatsu	epartment of Physics, Faculty of Science, Tohoku University
26	2024-Ca-0084	添加物によるNaCl晶相変化機構の大規模メタダイナミクス計算研究	灘　浩樹	鳥取大学	A Large-Scale Metadynamics Simulation Study on the Mechanism of Habit Change of NaCl Crystal by Additives	Hiroki Nada	Tottori University
27	2024-Ca-0138	センサー材料のための量子回路データベースの作成	水上　渉	大阪大学 量子情報・量子生命研究センター	Creating a quantum computing database for sensor materials	Wataru Mizukami	Center for Quantum Information and Quantum Biology
28	2024-Cb-0051	センサー材料のための量子回路データベースの作成	水上　渉	大阪大学 量子情報・量子生命研究センター	Creating a quantum computing database for sensor materials	Wataru Mizukami	Center for Quantum Information and Quantum Biology
29	2024-Ca-0010	過冷却液体・ガラスにおけるJohari-Goldstein緩和の普遍性	荒木　武昭	京都大学大学院理学研究科物理学・宇宙物理学専攻	Universaliry of Johari-Goldstein relaxation in supercooled liquids and glasses	Takeaki Araki	Department of Physics, Kyoto University
30	2024-Ca-0022	固体壁近傍における揺らぎ抑制の包括的数値計算	中野　裕義	東京大学物性研究所	A comprehensive numerical investigation of suppression of fluctuations near solid wall	Hiroyoshi Nakano	The Institute for Solid State Physics, The University of Tokyo
31	2024-Ca-0045	らせん構造をもつ高分子の結晶構造と力学特性	樋口　祐次	九州大学情報基盤研究開発センター	Crystal structure and mechanical properties of polymers with helical structure	Yuji Higuchi	Research Institute for Information Technology, Kyushu University
32	2024-Ca-0023	タンパク質凝集の分子動力学シミュレーション	奥村　久士	自然科学研究機構生命創成探究センター	Molecular dynamics simulation of protein aggregation	Hisashi Okumura	Exploratory Research Center on Life and Living Systems, Institute for Molecular Science
33	2024-Ca-0090	蛋白質物性に強く関与するソフトモードの効率的サンプリングシミュレー ション	北尾　彰朗	東京科学大学生命理工学院	Efficient sampling simulation of the soft modes significantly contribute to protein properties	Akio Kitao	School of Life Science and Technology, Institute of Science Tokyo
34	2024-Ca-0137	量子フラストレート磁性体における多体量子もつれ	下川　統久朗	沖縄科学技術大学院大学	Multipartite entanglement in quantum frustrated magnets	Tokuro Shimokawa	Okinawa Institute of Science and Technology Graduate University
35	2024-Cb-0004	機械学習ポテンシャルを用いたファンデルワールスヘテロ構造におけるフォノン熱輸送の変調	許　斌	東京大学大学院機械工学専攻	Modulation of Phonon Heat Transport in Van der Waals Heterostructures Utilizing Machine Learning Potentials	Xu Bin	Department of Mechanical Engineering, The University of Tokyo
36	2024-Ca-0129	ガラス転移付近での動的相転移の数値的研究	西川　宜彦	北里大学理学部物理学科	Numerical study of the dynamical transition near the glass transition in the s ensemble	Yoshihiko Nishikawa	Department of Physics, School of Science, Kitasato University
37	2024-D-0001	統計力学理論によるタンパク質のフォールディング反応機構の高精度予測	新井　宗仁	東京大学大学院総合文化研究科	Accurate prediction of protein folding mechanisms by statistical mechanical models	Munehito Arai	Graduate School of Arts and Sciences, The University of Tokyo

38	2024-Ca-0091	カルコゲナイド系熱電材料における欠陥構造と輸送特性	藤井　進	九州大学大学院工学研究院材料工学部門	Defect structures and their transport properties in thermoelectric chalcogenides	Susumu Fujii	Department of Materials, Faculty of Engineering, Kyushu University
39	2024-Ca-0099	機械学習を利用した多層カーボンナノチューブ紡績系の構造パラメータと力学的・破壊特性との関係性解明	山本　剛	東北大学大学院工学研究科・航空宇宙工学専攻	Machine learning-assisted high-throughput MD simulation on structure-mechanical property relationships in carbon nanotube yarns	Go Yamamoto	Department of Aerospace Engineering, Tohoku University
40	2024-Ca-0082	ナノ細孔からの高分子引き抜き過程の分子動力学シミュレーション	細野　暢彦	東京大学大学院工学系研究科応用化学専攻	Molecular Dynamics Simulation of Polymer Extraction Process from Nanopores	Nobuhiko Hosono	Department of Applied Chemistry, Graduate School of Engineering, The University of Tokyo
41	2024-Ca-0089	改良された揺らぎの緩和解析による臨界普遍性の検証	尾関　之康	電気通信大学情報理工学研究科	Confirmations of critical universality by improved analysis for relaxations of fluctuations	Yukiyasu Ozeki	Department of Applied Physics and Chemistry, The University of Electro-Communications
42	2024-Ca-0063	相共存状態境界条件依存性と自由エネルギー	中川　尚子	茨城大学理学部	Free energy and phase coexistence in various boundary conditions	Naoko Nakagawa	Department of Physics, Ibaraki University
43	2024-Ca-0088	ビトリマーに対する全原子分子動力学計算手法の開発	大矢　豊大	東京理科大学先進工学部	All-atomic molecular dynamics simulation for vitrimers	Yutaka Oya	Faculty of Advanced Engineering, Tokyo University of Science
44	2024-Ca-0102	摩擦の物理	松川　宏	青山学院大学理工学部	Physics of Friction	Hiroshi Matsukawa	Faculty of Science and Engineering, Aoyama Gakuin University
45	2024-Ca-0107	高伝導性オリゴマー型電荷移動錯体の示す二量化ゆらぎの起源の解明	藤野　智子	東京大学物性研究所	Elucidation of the Origin of Dimerization Fluctuations in Highly Conductive Oligomeric Charge Transfer Complexes	Tomoko Fujino	Institute for Solid State Physics, The University of Tokyo
46	2024-Cb-0043	量子フラストレート磁性体における多体量子もつれ	下川　統久朗	沖縄科学技術大学院大学	Thermal effects on quantum frustrated magnets	Tokuro Shimokawa	Okinawa Institute of Science and Technology Graduate University
47	2024-Ca-0040	Biquadratic相互作用のある量子スピン鎖における磁場誘起スピン液体相	坂井　徹	兵庫県立大学大学院理学研究科	Field-Induced Spin Liquid Phase of Quantum Spin Chain with Biquadratic Interaction	Toru Sakai	Graduate School of Science, University of Hyogo
48	2024-Ca-0048	κ型BEDT-TTF超伝導体の転移温度およびギャップ構造の同定	Jeschke　Harald	岡山大学異分野基礎科学研究所	Superconducting critical temperature and gap structure of kappa-type BEDT-TTF superconductors	Harald Jeschke	Research Institute for Interdisciplinary Science Okayama University
49	2024-Eb-0005	ガウス過程回帰を用いた揺らぎの緩和解析による臨界普遍性の高精度評価	尾関　之康	電気通信大学情報理工学研究科	High-precision evaluation of critical universality by relaxation analysis of fluctuations using Gaussian process regression	Yukiyasu Ozeki	Department of Applied Physics and Chemistry, The University of Electro-Communications
50	2024-Ca-0101	高分子架橋ネットワーク系のトポロジー構造解析による物性メカニズムの解明	萩田　克美	防衛大学校応用科学群応用物理学科	Physical properties of crosslinked polymer networks through network topology analysis	Katsumi Hagita	Department of Applied Physics, School of Applied Sciences, National Defense Academy
51	2024-Ca-0104	テンソルネットワーク形式を用いた情報量解析	原田　健自	京都大学大学院情報学研究科	Information analysis of complex system with a tensor network formalism	Kenji Harada	Graduate school of Informatics, Kyoto University
52	2024-Ca-0118	Tensor network study of an effective spin model for cuprates	ゴウケ　マティアス	沖縄科学技術大学院大学	Tensor network study of an effective spin model for cuprates	Matthias Gohlke	Okinawa Institute of Science and Technology Graduate University
53	2024-Ca-0087	CuO$_{2}$スピン鎖のRIXSスペクトル	大西　弘明	日本原子力研究開発機構 先端基礎研究センター	RIXS spectrum of CuO$_{2}$ spin chain	Hiroaki Onishi	Advanced Science Research Center, Japan Atomic Energy Agency
54	2024-Cb-0008	量子スピン系における欠損の効果	安田　千寿	琉球大学理学部	Effects of deficit on quantum spin systems	Chitoshi Yasuda	Department of Physics and Earth Sciences, University of the Ryukyus
55	2024-Cb-0036	量子スピン液体における非可換エニオンの生成機構の解明	那須　譲治	東北大学	Creation mechanism of non-Abelian anyons in quantum spin liquids	Joji Nasu	Tohoku University
56	2024-Ca-0092	電極との界面に電気二重層を形成するイオン液体電解液の電位応答ダイナミクスの解析	福井　賢一	大阪大学大学院基礎工学研究科	Analyses on the Potential-dependent Dynamics of Ionic Liquid Electrolytes Forming Electric Double Layers Facing the Electrodes	Ken-Ichi Fukui	Graduate School of Engineering Science, Osaka University
57	2024-Ca-0114	一般変分波動関数ランダム量子状態を用いた有限温度高次元系の計算	飯高　敏晃	理化学研究所	Calculation of high dimensional systems at finite temperature using random quantum sates of general variational wave functions	Toshiaki Iitaka	Riken
58	2024-Ca-0112	SU(N)対称DMRGの大規模フラックスインサーション計算	山田　昌彦	理学系研究科物理学専攻	Large-scale calculation with a flux insertion for SU(N)-symmetric DMRG	Masahiko Yamada	Department of Physics, Faculty of Science, The University of Tokyo
59	2024-Cb-0005	数理結晶化学	小正路　嶬太郎	東京大学物性研究所	Mathematical Crystal Chemistry	Ryotaro Koshoji	Institute for Solid State Physics, The University of Tokyo
60	2024-Cb-0016	相転移キネティクスとポリアモルフィズム	渕崎　員弘	愛媛大学理工学研究科	Kinetics of phase transition and polyamorphism	Kazuhiro Fuchizaki	Department of Physics, Ehime University
61	2024-D-0002	高強度テラヘルツ光によって誘起された量子スピン流の学理創出	玉谷　知裕	東京大学物性研究所	Research on quantum spin currents induced by high-intensity terahertz light	Tomohiro Tamaya	Institute for Solid State Physics, The University of Tokyo
62	2024-Ca-0064	量子スピン系の低エネルギー状態に関する数値的研究	中野　博生	兵庫県立大学大学院理学研究科	Numerical study on low-energy states of quantum spin systems	Hiroki Nakano	Graduate School of Science, University of Hyogo
63	2024-Ca-0019	ハイパーユニフォームガラスの機械および熱物性	ワン　インチャオ	東京大学 先端科学技術研究センター	Mechanical and thermal properties of hyperuniform glasses	Yinqiao Wang	University of Tokyo, RCAST
64	2024-Ca-0055	高分子電解質のコイル-小球転移における流体力学的相互作用の重要な役割	ユアン　ジャアシン	先端科学技術研究センター	Key roles of hydrodynamic interactions on coil-globule transition of polyelectrolytes	Jiaxing Yuan	Research Center for Advanced Science and Technology, The University of Tokyo
65	2024-Eb-0004	水滴の不均一核生成	モイド　モハマド	生産技術研究所	Heterogeneous nucleation of water droplet	Mohammad Moid	Institute of Industrial Science, University of Tokyo

66	2024-Ba-0065	強結合電子・格子・光子系のコヒーレントダイナミクス	石田　邦夫	宇都宮大学工学部	Coherent dynamics of strongly coupled electron-phonon-photon systems	Kunio Ishida	School of Engineering, Utsunomiya University
67	2024-Bb-0042	有機固体電解質の粒界イオン伝導機構の微視的解明	佐々木　遼馬	東京工業大学	Microscopic investigation of Li-ion conduction mechanism on grain boundary of organic solid electrolyte	Ryoma Sasaki	Tokyo Institute of Technology
68	2024-Ba-0064	対称性のある測定下の量子系における普遍性	藤　陽平	東京大学工学系研究科物理工学専攻	Universality in monitored systems with symmetry	Yohei Fuji	Department of Applied Physics, University of Tokyo
69	2024-Bb-0034	強結合電子・格子・光子系のコヒーレントダイナミクス	石田　邦夫	宇都宮大学工学部	Coherent dynamics of strongly coupled electron-phonon-photon systems	Kunio Ishida	School of Engineering, Utsunomiya University
70	2024-Ca-0039	フラストレート磁性体における新奇秩序	川村　光	神戸大学分子フォトサイエンス研究センター	Novel order in frustrated magnets	Hikaru Kawamura	Molecular Photoscience Research Center, Kobe University
71	2024-Ca-0049	相転移キネティクスとポリアモルフィズム	渕崎　員弘	愛媛大学理工学研究科	Kinetics of phase transition and polyamorphism	Kazuhiro Fuchizaki	Department of Physics, Ehime University
72	2024-Ba-0037	並列化された高次元テンソルネットワークくりこみ群による臨界現象の解明	押川　正毅	東京大学物性研究所	Elucidation of critical phenomena by parallelized higher-dimensional tensor network renormalization group	Masaki Oshikawa	Institute for Solid State Physics, University of Tokyo
73	2024-Ba-0046	分数量子ホール系におけるエニオンの輸送特性の数値計算	加藤　岳生	東京大学物性研究所	Numerical Simulation of Anyons in Fractional Quantum Hall Systems	Takeo Kato	Institute for Solid State Physics, The University of Tokyo
74	2024-Ba-0074	イジングマシン向けハイブリッドアルゴリズムの研究	田中　宗	慶應義塾大学理工学部物理情報工学科	Study on hybrid algorithms for Ising machines	Shu Tanaka	Dept. Applied Physics and Physico-Informatics, Keio University
75	2024-Ba-0002	ランダムサンプリングによる自由ボゾン系におけるエンタングルメントダイナミクスの計算	金子　隆威	上智大学 理工学部 機能創造理工学科	Calculating entanglement dynamics in free boson systems by random sampling	Ryui Kaneko	Department of Engineering and Applied Sciences, Faculty of Science and Technology, Sophia University
76	2024-Ba-0004	濃厚電解質系における遮蔽効果	寺尾　貴道	岐阜大学工学部	Screening in concentrated electrolytes	Takamichi Terao	Faculty of Engineering, Gifu University
77	2024-Ba-0009	強誘電性ネマチック液晶の発現に関する物理的起源	荒木　武昭	京都大学大学院理学研究科物理学・宇宙物理学専攻	The Physical Origin of the Emerging Ferroelectric Nematic Phase	Takeaki Araki	Department of Physics, Kyoto University
78	2024-Ba-0019	テンソルネットワークくりこみ群におけるボンド重み最適化	森田　悟史	慶應義塾大学大学院理工学研究科	Bond-weight optimization in tensor network renormalization groups	Satoshi Morita	Faculty of Science and Technology, Keio University
79	2024-Ba-0069	情報統計力学におけるイジングモデルの解析	関　優也	慶應義塾大学	Analysis of Ising model in statistical-mechanical infomatics	Yuya Seki	Keio University
80	2024-Ba-0070	Tensor learning approaches to computational physics	品岡　寛	埼玉大学理学部物理学科	Tensor learning approaches to computational physics	Hiroshi Shinaoka	Department of Physics, Saitama University
81	2024-Bb-0001	ボルツマン方程式に基づく非平衡電子動力学：カーボンナノチューブへの適用	小野　頌太	室蘭工業大学大学院工学研究科	Nonequilibrium electron dynamics based on Boltzmann equation: Application to carbon nanotubes	Shota Ono	Muroran Institute of Technology
82	2024-Bb-0008	非平衡Green関数法を用いた熱平衡および非平衡FFLO状態のダイナミクスの研究	河村　泰良	日本大学 理工学部 物理学科	A study of the dynamics of thermal equilibrium and nonequilibrium FFLO states using the nonequilibrium Green's function technique	Taira Kawamura	Department of Physics, College of Science and Technology, Nihon University
83	2024-Bb-0041	非相溶高分子ブレンドにおける分子動力学シミュレーション	佐藤　健	金沢大学設計製造技術研究所	A molecular dynamics simulation study for immiscible polymer blends	Takeshi Sato	Advanced Manufacturing Technology Institute, Kanazawa University
84	2024-Ba-0022	近藤ウオークの数値シミュレーション	羽田野　直道	東京大学生産技術研究所	Numerical Simulation of Kondo Walk	Naomichi Hatano	Institute of Industrial Science, The University of Tokyo
85	2024-Ba-0041	材料探索用ブラックボックス最適化手法の開発	田村　亮	国立研究開発法人 物質・材料研究機構	Development of black-box optimization method for materials exploration	Ryo Tamura	National Institute for Materials Science
86	2024-Bb-0024	高圧氷Ⅲの融液成長機構に関する大規模分子動力学シミュレーション研究	灘　浩樹	鳥取大学	A Large-scale Molecular Dynamics Simulation Study on the Melt Growth Mechanism of High-Pressure Ice III	Hiroki Nada	Tottori University
87	2024-Bb-0031	加振による粉体粒度偏析の発現機構：実効粒子間力に基づく解析	仲井　文明	大阪大学大学院理学研究科宇宙地球科学専攻	Mechanism of Size Segregation in Granular Media under Vibration: Analysis Based on Effective Interparticle Forces	Fumiaki Nakai	Department of Earth and Space Science, Osaka University
88	2024-Bb-0002	量子多体系のダイナミクスへの動的モード分解の適用	金子　隆威	上智大学 理工学部 機能創造理工学科	Dynamic mode decomposition of time-series data in quantum many-body systems	Ryui Kaneko	Department of Engineering and Applied Sciences, Faculty of Science and Technology, Sophia University
89	2024-Bb-0012	分子動力学シミュレーションを用いて、抗菌ペプチドLL-37とHNP1の分子レベルでの相乗効果のメカニズムに関する研究です	杉原　加織	生産技術研究所	Investigating the Molecular Mechanisms Behind the Synergistic Antibacterial Actions of LL-37 and HNP1 Peptides Through Molecular Dynamics Simulations	Kaori Sugihara	Institute of Industrial Science, The University of Tokyo
90	2024-Ba-0005	ソフトマテリアルの秩序構造とそのダイナミクス，光学的性質の計算	福田　順一	九州大学　大学院理学研究院	Calculation of ordered structures, dynamics and optical properties of soft materials	Jun-Ichi Fukuda	Faculty of Science, Kyushu University
91	2024-Ba-0072	グラフニューラルネットワークによるガラスの深層学習	芝　隼人	兵庫県立大学 大学院情報科学研究科	Deep learning glassy dynamics by graph neural networks	Hayato Shiba	Gracuate School of Information Science, University of Hyogo
92	2024-Ba-0012	１次元フラストレート量子スピン系の数値的研究	飛田　和男	埼玉大学大学院理工学研究科物質科学部門	Numerical Study of One Dimensional Frustrated Quantum Spin Systems	Kazuo Hida	Division of Material Science, Graduate School of Science and Engineering, Saitama University
93	2024-Ba-0021	自己駆動複雑分子系の局所構造解析と非平衡相転移	礒部　雅晴	名古屋工業大学	Local structure analysis and non-equilibrium phase transition in self-propelled hard polygon systems	Masaharu Isobe	Nagoya Institute of Technology
94	2024-Ba-0025	傾いたダイポール相互作用を持つボーズハバード模型における超固体状態	鈴木　隆史	兵庫県立大学　大学院工学研究科	Supersolid in Bose-Hubbard model with tilted dipole interactions	Takafumi Suzuki	Graduate School of Engineering, University of Hyogo

95	2024-Ba-0028	ハニカム格子多スピン交換模型における磁性	安田　千寿	琉球大学理学部	Magnetism in the multiple-spin exchange model on a honeycomb lattice	Chitoshi Yasuda	Department of Physics and Earth Sciences, University of the Ryukyus
96	2024-Ba-0029	原子層物質の磁気的性質の理論的研究	苅宿　俊風	物材機構	Theoretical study of magnetic properties in atomically thin materials	Toshikaze Kariyado	NIMS
97	2024-D-0006	連続量子測定下での散逸のある量子ビットにおける量子熱の流れ	山本　剛史	筑波大学数理物質系	Quantum heat flow in a dissipative qubit under continuous quantum measurement	Tsuyoshi Yamamoto	Faculty of Pure and Applied Sciences, University of Tsukuba
98	2024-Bb-0009	ソフトマテリアルの秩序構造とそのダイナミクス，光学的性質の計算	福田　順一	九州大学　大学院理学研究院	Calculation of ordered structures, dynamics and optical properties of soft materials	Jun-Ichi Fukuda	Faculty of Science, Kyushu University
99	2024-Ba-0032	S=1/2フラストレートスピン系におけるマグノン分散関係の級数展開法による研究	福元　好志	東京理科大学	A series expansion study of magnon dispersion relations in S=1/2 frustrated spin systems	Yoshiyuki Fukumoto	Tokyo University of Science
100	2024-Ba-0050	ANNポテンシャルを用いたシリカガラスの永久高密度化の大規模分子動力学シミュレーション	若林　大佑	高エネルギー加速器研究機構物質構造科学研究所	Large-scale molecular-dynamics simulation of permanent densification in silica glass with ANN potentials	Daisuke Wakabayashi	Institute of Materials Structure Science, High Energy Accelerator Research Organization (KEK)
101	2024-Ba-0051	散逸が量子アルゴリズムに与える影響の解析	白井　達彦	早稲田大学高等研究所	Dissipation effects on quantum algorithm	Tatsuhiko Shirai	Waseda Institute for Advanced Study, Waseda University
102	2024-Bb-0029	高分子バリア層を表面に有する鉄筋コンクリート構造物の長期信頼性評価	石田　崇人	名古屋大学高等研究院	Long-term Reliability Assessment of Reinforced Concrete Structures with Polymer Barrier Layers on the Surface	Takato Ishida	Institute for Advanced Research, Nagoya University
103	2024-Bb-0038	量子グラウバーダイナミクスによる臨界相の解析	堀田　知佐	東京大学総合文化研究科	Analysis on the critical phases using quantum Glauber dynamics	Chisa Hotta	Department of Basic Science, The University of Tokyo
104	2024-Cb-0037	細胞の集団運動秩序の極性の対称性依存性の解明	松下　勝義	広島大学統合生命科学研究科	The Investigation of Effects of Cell Polarity Symmetries on Motion Order of Cells	Katsuyoshi Matsushita	Graduate School of Integrated Sciences for Life, Hiroshima University
105	2024-Ba-0042	カゴメJ1-J3反強磁性体におけるスピンダイナミクス	青山　和司	大阪大学大学院理学研究科宇宙地球専攻	Spin dynamics in J1-J3 antiferromagnets on kagome lattices	Kazushi Aoyama	Department of Earth and Space Science, Graduate School of Science, Osaka University
106	2024-Ba-0066	傾斜磁場下における量子カイラルスピン模型のソリトンと相転移	正木　祐輔	東北大学	Solitons and phase transitions in quantum chiral spin model in tilted magnetic field	Yusuke Masaki	Tohoku University
107	2024-Bb-0007	濃厚電解質系における遮蔽効果	寺尾　貴道	岐阜大学工学部	Screening in concentrated electrolytes	Takamichi Terao	Faculty of Engineering, Gifu University
108	2024-Bb-0014	１次元フラストレート量子スピン系の数値的研究	飛田　和男	埼玉大学大学院理工学研究科物質科学部門	Numerical Study of One Dimensional Frustrated Quantum Spin Systems	Kazuo Hida	Division of Material Science, Graduate School of Science and Engineering, Saitama University
109	2024-Bb-0037	パターン形成をともなう気相反応と固体表面における相互作用の解明に向けた反応モデルの構築	秋葉　貴輝	工学系研究科　機械工学専攻	Modeling for interaction between gas-phase reaction with pattern formation and solid surface	Takaki Akiba	Department of Mechanical Engineering, School of Engineering
110	2024-Ba-0014	カーボンナノチューブに包摂されたイオウ鎖の構造	池本　弘之	富山大学	Structures of Sulphur Confined in Carbon Nanotubes	Hiroyuki Ikemoto	University of Toyama
111	2024-Bb-0006	ホタル生物発光基質類似体seMpaiの吸収・蛍光スペクトル解析	樋山　みやび	群馬大学	Analysis for absorption- and fluorescence-spectra of seMpai by quantum chemical calculations	Miyabi Hiyama	Gunma University
112	2024-Ca-0007	高速で駆動されたマクロな物体の摩擦法則	大槻　道夫	島根大学学術研究院理工学系	Friction law for macroscopic objects driven at high speed	Michio Otsuki	Institute of Science and Engineering
113	2024-Ca-0115	Impact of electrostatic interactions on colloidal gelation	Opdam　Joeri	Research center for advanced science and technology	Impact of electrostatic interactions on colloidal gelation	Joeri Opdam	Research center for advanced science and technology
114	2024-Ba-0008	空間構造をもつ一次元量子スピン系の数値的研究	利根川　孝	神戸大学大学院理学研究科	Numerical Study of the One-Dimensional Quantum Spin Systems	Takashi Tonegawa	Graduate School of Science, Kobe University
115	2024-Ba-0013	ホタル生物発光in situ吸収スペクトルの量子化学計算による解析	樋山　みやび	群馬大学	Analysis for in situ absorption spectra in firefly bioluminescence by quantum chemical calculations	Miyabi Hiyama	Gunma University
116	2024-Ba-0058	TRHEPDによるRashba型表面をもつ原子層合金の構造解析	高山　あかり	早稲田大学	Structure analysis of atomic layer alloy with Rashba effect studied by TRHEPD	Akari Takayama	Waseda University
117	2024-Ba-0068	過冷却状態における臨界媒介相互作用液体	ベンガイルクリシュナン　ヴィシュヌ	東京大学先端科学技術研究センター	Criticality mediated interactions in supercooled liquids	Vishnu Vengayil Krishnan	Research Center for Advanced Science and Technology, The University of Tokyo
118	2024-Bb-0019	クラスター展開法における長距離相互作用の導入に関する研究	福元　好志	東京理科大学	Investigation of efficient methods for introducing long-range interactions in the cluster expansion method	Yoshiyuki Fukumoto	Tokyo University of Science
119	2024-Bb-0021	超伝導接合における局所状態密度と輸送現象に関する理論	深谷　優梨	岡山大学学術研究院環境生命自然科学学域（工）	Theory of local density of states and transport properties in superconductor junctions	Yuri Fukaya	Faculty of Enviromental, Life, Natural Science and Technology, Okayama University
120	2024-Ba-0060	ハバード模型の多重Q秩序に関する分子スピン動力学的研究	内田　尚志	北海道科学大学	Molecular spin dynamics study on the multiple-Q orders in Hubbard models	Takashi Uchida	Hokkaido University of Science
121	2024-Ba-0030	高次磁気多極子や螺旋磁性と共存・競合する新奇超伝導状態の提案	角田　峻太郎	東京大学大学院総合文化研究科	Proposal of novel superconducting states coexisting/competing with higher-order magnetic multipole order or helical magnetism	Shuntaro Sumita	Department of Basic Science, The University of Tokyo

122	2024-Bb-0039	コロイドゲルの降伏と老化	ベンガイルクリシュナン　ヴィシュヌ	東京大学先端科学技術研究センター	Yielding and aging of colloidal gels	Vishnu Vengayil Krishnan	Research Center for Advanced Science and Technology, The University of Tokyo
123	2024-Ca-0024	極性の対称性の違いによる集団運動の安定性解析	松下　勝義	広島大学統合生命科学研究科	Stability Analysis of Collective Cell Movement due to Different Polarity Symmetry	Katsuyoshi Matsushita	Graduate School of Integrated Sciences for Life, Hiroshima University
124	2024-Ba-0007	固有値ソルバの統一的インターフェースRokkoの開発と量子スピン系への応用	坂下　達哉	東京大学　理学系研究科	Development of integrated interface of eigensolvers Rokko and application to quantum spin systems	Tatsuya Sakashita	Graduate School of Science, The University of Tokyo
125	2024-Bb-0027	グラフェン・ナノスペーサー積層構造の分子動力学	小林　慶裕	大阪大学大学院工学研究科	Molecular dynamics simulation of graphene-nanosapcer stacking structure	Yoshihiro Kobayashi	Graduate School of Engineering, Osaka University
126	2024-A-0002	分子シミュレーションによる高分子電解質溶液のダイナミクスの解析	佐藤　健	金沢大学設計製造技術研究所	A molecular simulation study for dynamics of polyelectrolyte solutions	Takeshi Sato	Advanced Manufacturing Technology Institute, Kanazawa University
127	2024-A-0005	数理結晶化学	小正路　峻太郎	東京大学物性研究所	Mathematical Crystal Chemistry	Ryotaro Koshoji	Institute for Solid State Physics, The University of Tokyo
128	2024-A-0009	MD-FEM連成解析手法の開発	村松　眞由	慶應義塾大学	Development of a MD-FEM Coupling Analysis Method	Mayu Muramatsu	Keio University
129	2024-A-0010	非平衡超伝導ワイヤーにおける超伝導秩序パラメータの時空間ダイナミクスの解明	河村　泰良	日本大学 理工学部 物理学科	Spatiotemporal dynamics of a superconducting order parameter in a nonequilibrium superconducting wire	Taira Kawamura	Department of Physics, College of Science and Technology, Nihon University
130	2024-A-0012	OpenMXによる光電子放出角度強度分布解析プログラムの開発	佐藤　祐輔	自然科学研究機構分子科学研究所極端紫外光研究施設	Development of the analysis programs for investigating the photoemission angular distribution	Yusuke Sato	UVSOR Synchrotron Facility, Institute for Molecular Science, National Institutes of Natural Sciences
131	2024-A-0015	イジングマシンの性能向上を目指した手法の解析	菊池　脩太	慶應義塾大学大学院理工学研究科	Analysis of the methods for improving the performance of Ising machines	Shuta Kikuchi	Graduate School of Science and Technology, Keio University
132	2024-A-0017	水素貯蔵材料の熱伝導率予測	三輪　和利	東北大学　材料科学高等研究所	Theoretical prediction of thermal conductivity of hydrogen storage materials	Kazutoshi Miwa	Advanced Institute for Materials Research, Tohoku University
133	2024-A-0021	外場下における量子スピン液体の研究	多田　靖啓	広島大学	Study of spin liquids under external fields	Yasuhiro Tada	Hiroshima University
134	2024-A-0022	MD-FEM連成解析手法の開発	村松　眞由	慶應義塾大学	Development of a MD-FEM Coupling Analysis Method	Mayu Muramatsu	Keio University
135	2024-A-0025	3D循環流動床フルループ解析のためのMP-PICベースのソルバーの開発	王　津新	大学院総合文化研究科	Development of an MP-PIC-based solver for 3D circulating fluidized bed full-loop analyses	Jinxin Wang	Graduate School of Arts and Sciences
136	2024-A-0027	促進輸送膜の気体分離機構に関する準備的研究	杵淵　郁也	東京大学 大学院工学系研究科 機械工学専攻	Preliminary study on gas separation mechanisms in facilitated transport membranes	Ikuya Kinefuchi	Department of Mechanical Engineering, The University of Tokyo
137	2024-A-0028	パイロクロア型化合物のX線散漫散乱データを用いた短距離秩序解析	鬼頭　俊介	東京大学大学院 新領域創成科学研究科 物質系専攻	Analysis of short-range order in pyrochlore-type compounds using X-ray diffuse scattering data	Shunsuke Kitou	Department of Advanced Materials Science, Graduate School of Frontier Sciences, The University of Tokyo
138	2024-A-0032	全原子分子動力学シミュレーションによるリチウム硫黄電池の正極およびリチウム金属負極と電解液の相互作用	梅林　泰宏	新潟大学自然科学系	All-atom molecular dynamics simulation of the interaction between the cathode and the lithium metal anode and electrolytes for lithium sulfur batteries	Yasuhiro Umebayashi	Graduate School of Science and Technology, Niigata University
139	2024-Ba-0034	グラフェン・ナノスペーサー積層構造の分子動力学	小林　慶裕	大阪大学大学院工学研究科	Molecular dynamics simulation of graphene-nanosapcer stacking structure	Yoshihiro Kobayashi	Graduate School of Engineering, Osaka University
140	2024-Bb-0018	固有値ソルバの統一的インターフェースRokkoの開発と量子スピン系への応用	坂下　達哉	東京大学　理学系研究科	Development of integrated interface of eigensolvers Rokko and application to quantum spin systems	Tatsuya Sakashita	Graduate School of Science, The University of Tokyo
141	2024-Ba-0026	文脈に依存する言語文法が生じる相転移の解析	鈴木　岳人	高千穂大学人間科学部	Analysis of phase transition generated by context-sensitive grammar	Takehito Suzuki	Department of Human Science, Takachiho University
142	2024-Bb-0013	組み合わせ範疇文法に基づく言語における相転移の解析	鈴木　岳人	高千穂大学人間科学部	Analysis of phase transition in languages based on Combinatory Categorial Grammar	Takehito Suzuki	Department of Human Science, Takachiho University

2024年度　CCMSスパコン共用事業枠課題一覧 / Supercomputing Consortium for Computational Materials Science Project List of Supercomputer System 2024

※共同利用ではなく共用事業の実施課題一覧。所属は申請時のデータ

前期課題

No.	課題名	氏名	所属	Title	Name	Organization
1	配置・構造不規則性を有する磁性材料を対象としたハイスループット計算	福島 鉄也	産業技術総合研究所	High-throughput calculations for magnetic materials with configurational and structural disorders	Tetsuya Fukushima	National Institute of Advanced Industrial Science and Technology
2	第一原理計算による磁性材料の研究	三宅　隆	産業技術総合研究所	First-principles study of magnetic materials	Takashi Miyake	National Institute of Advanced Industrial Science and Technology
3	人工ポリペプチドの溶媒溶解性の全原子モデル計算と溶解に重要な因子の解明	松林　伸幸	大阪大学	All-atom model calculations of the solubility of artificial polypeptides in solvents and factors important for their dissolution	Nobuyuki Matubayasi	Osaka University
4	核の量子効果を含む第一原理シミュレーションによる燃料電池材料中でのプロトン移動に関する研究	島崎　智実	横浜市立大学	Theoretical study on proton transfer in fuel cell material based on first-principles method with nuclear quantum effect	Tomomi Shimazaki	Yokohama City University
5	ベイズ最適化を用いた量子磁性体のハミルトニアン推定	三澤 貴宏	東京大学物性研究所	Estimation of Hamiltonians of quantum magnets using Bayes optimization	Takahiro Misawa	Institute for Solid State Physics, University of Tokyo
6	第一原理計算とデータ駆動アプローチによる機能性ホイスラー合金の開発	只野 央将	物質・材料研究機構	Development of functional Heusler alloys by first-principles calculations and data-driven approaches	Terumasa Tadano	National Institute for Materials Science

後期課題

No.	課題名	氏名	所属	Title	Name	Organization
1	第一原理シミュレーションによる燃料電池材料中でのプロトン挙動の解明	島崎　智実	横浜市立大学	Theoretical study on proton behavior in fuel cell material based on first-principles method	Tomomi Shimazaki	Yokohama City University
2	ベイズ最適化を用いた量子磁性体のハミルトニアン推定	三澤 貴宏	東京大学物性研究所	Estimation of Hamiltonians of quantum magnets using Bayes optimization	Takahiro Misawa	Institute for Solid State Physics, University of Tokyo

The Institute for Solid State Physics (ISSP), The University of Tokyo

Address	5-1-5 Kashiwanoha, Kashiwa, Chiba, 277-8581, Japan
Phone	+81-4-7136-3207
Home Page	https://www.issp.u-tokyo.ac.jp